

**PROCEEDINGS OF
UNIVERSITY SEMINAR ON
POLLUTION AND WATER RESOURCES**

Volume XI 1975-1978

PROCEEDINGS OF
UNIVERSITY SEMINAR ON
POLLUTION AND WATER RESOURCES

Volume XI 1975-1978

Edited by
George J. Halasi-Kun
and
Kemble Widmer

COLUMBIA UNIVERSITY
in cooperation with
U.S. DEPARTMENT OF THE INTERIOR
GEOLOGICAL SURVEY

The New Jersey Department of
Environmental Protection
Bureau of Geology & Topography

BULLETIN 75 - E

CONTENTS

	Page
Introduction by George J. Halasi-Kun.....	v
Gary D. Cobb Future Directions of the Program of the Office of Water Research and Technology (1978).....	A (1-4)
George J. Halasi-Kun Water Quality and Pollution - Issues Involved in the Development of a National Water Policy (1978).....	B (1-11)
Michael Hermel, Martin S. Tanzer and George Claus The Applicability of Ultraviolet Spectrophotometry for Water Quality Analyses: A Review (1977).....	C (1-58)
George Redey Efficiency of Slipforms in Reinforced Concrete Construction of Water Towers (1978).....	D (1-19)
Donald V. Dunlop Precipitation and Snowfall Over New Jersey (1978).....	E (1-15)
Thomas F. McKinney Regional Geomorphology of the Inner New Jersey Shelf (1975).....	F (1-18)
Milorad Miloradov Simulation of Unsteady Flow in Natural Compound Channels (1978)...	G (1-23)
Lucien Duckstein, Martin Fogel and Donald Davis Mountainous Winter Precipitation: A Stochastic Event Based Approach (1977).....	H (1-18)
Paul H. Roux and David Miller Ground Water Monitoring at Solid Waste Disposal Sites-Two Case Studies (1977).....	I (1-32)
Gerald W. Robin Some Effects of Noise Pollution on Bioacoustics in the Sea (1978).....	J (1-25)
Appendix: Members of the Seminar 1975-1978	

INTRODUCTION

In the past three academic years, the program of the Seminar has been concentrated, besides the international and interstate aspect of the water resources problem, on the basic data collection and geodetic survey, including its interrelation with hydrology. The ninth volume is dedicated not only to oceanography and saline water but also to water resources data collecting and to some pollution problems. The entire tenth volume is devoted to the various problems of the geodetic and land surveying in connection with mapping, tidal water, basic data collection and especially the needs of the New York City-Philadelphia area. The eleventh volume is again pollution oriented handling not only water quality but also research in water resources.

Since 1975, the "Annual Meeting in Washington, D.C." has been held in the Cosmos Club with the U. S. Geological Survey as host, where each year a review of the world situation in water resources planning is the topic.

The most important activities of the Seminar besides its regular meetings were as follows:

On Sept. 21-25, 1975 in Reston, Va. the International Symposium on Computer-assisted Cartography was held and one paper was delivered on the water resources oriented data bank.

In the Spring and Fall of 1976, two different teams of Scientists from Hungary, sponsored by the UN, visited the "Land Oriented Reference Data System" of N. J. Bureau of Geology and Topography to learn more about the water resources data bank. This system has been in operation since 1974 with the assistance of the Seminar. The visits were feasibility studies as to how to apply the system also in Hungary.

In the Summer of 1976, the members of the Seminar were asked to write entries for the international "Encyclopedia on Earth Sciences, Vol. XVIII - Geohydrology and Water Resources" as they did in 1972 by contributing 20% of the articles in the "Encyclopedia on Earth Sciences, Vol. IV-A - Geochemistry and Environmental Science." (See introduction to Proceedings, Vol. V.) To date, our members committed themselves or wrote over sixty entries (25% of the volume).

On February 14-15, 1977, a "Seminar on Issues before the United Nations Water Conference" was organized in New York City with the assistance of the Seminar to prepare fifty-five participants from fifty-four countries for the United Nations Water Conference in Mar del Plata, Argentina in March 14-25, 1977. Five of our members delivered lectures to assist the United Nations in their effort.

In June 1977, the representative of Arizona State University visited the N. J. Bureau of Geology and Topography to inspect the previously mentioned data bank and its applicability to Arizona.

On August 15-19, 1977 in Baden-Baden, F. R. Germany, three members at the Conference of the International Association for Hydraulic Research, and one member at the University, Ghent, Belgium delivered papers on water resources

oriented data bank systems. Researchers from Belgium and Netherland were especially interested in the presentation at Ghent University because they are working on a similar system after they had received information about the data bank in 1974, and they wanted further details on how the system improved since then. The paper has been delivered as a supplement to the report of 1974 at the request of the University Ghent.

On August 23-25, 1977, the Geodetic Survey and Cadastre Offices of the State of Lower Saxony and the Geodetic Institute of Techn. University, Brunswick, both in F. R. Germany, were visited to gain information about the water resources mapping based on geodetic survey.

From Sept. 14, 1977 to Nov. 22, 1977, the National Academy of Sciences initiated international research exchange programs between the United States and Yugoslavia and also between the United States and Hungary. The Chairman of the Seminar was nominated as a fellow of the National Academy of Sciences to exchange ideas about water resources oriented data bank including hydrology of smaller watersheds and karst hydrology. The program generated ten lectures in Yugoslavia and six presentations in Hungary at various universities and national Academies of Science. As a further result of the trip, there were eleven articles prepared in English by Hungarian and Yugoslavian scientists for publication. In the joint program, five articles were delivered in English, German, Hungarian and Yugoslavian by members of the Seminar for publication in scientific journals of those countries. During this visit, the Water Data Banks in Zagreb, Yugoslavia and that of VITUKI in Budapest, Hungary were visited. Both centers had been informed in 1975 about the environmental data bank (LORDS) of N. J. Bureau of Geology and Topography. Finally, an exchange of scholars with fellowships, publications, and a joint research program in soil mechanics and geohydrology was initiated with the involvement of three universities in the United States (Columbia, Rutgers and Fairleigh Dickinson) and the Hungarian Academy of Sciences, Yugoslavian Academy of Arts and Sciences including Techn. Universities in Budapest, Miskolc in Hungary, and the Universities Zagreb and Sarajevo in Yugoslavia.

In the spring of 1978, two teams again visited the operating data bank of New Jersey in Trenton to check operational procedure and details of the system in order to organize similar information centers. The first team came in May of 1978 from Techn. University Stuttgart, F. R. Germany and the second team came in June of 1978 from the Techn. University Lisbon, Portugal.

Finally, the editors of the Proceedings wish to express their appreciation to all members contributing articles and lectures for the past three years. The publications were made possible only by the generous help and cooperation of the U. S. Department of the Interior-Geological Survey and the State of New Jersey, Department of Environmental Protection.

George J. Halasi-Kun
Chairman of the University Seminar
on Pollution and Water Resources
Columbia University

FUTURE DIRECTIONS OF THE PROGRAM OF THE OFFICE OF
WATER RESEARCH AND TECHNOLOGY¹

by

GARY D. COBB, B.S.

U.S. Dept. of the Interior, Office of Water Research
and Technology

¹Remarks of Gary D. Cobb, Director, Office of Water Research and Technology, U.S. Department of the Interior, at the University Seminars on Pollution and Water Resources, Washington, D.C., January 25, 1978.

Thank you for the invitation to meet with the members of the University Seminars on Pollution and Water Resources. I am very pleased to be here to discuss the program of the Office of Water Research and Technology.

When I accepted my appointment as Director of the Office of Water Research and Technology on August 22, had someone indicated what we would try to accomplish by January of this year, I guess my honest opinion would have been that it could not be done.

In that time, we have developed and presented a comprehensive statement with respect to the OWRT programs before the Subcommittee on Water and Power Resources of the Interior and Insular Affairs Committee, House of Representatives, on September 29, 1977.

We have redirected the program for FY 1978 to be more responsive to the new goals and objectives identified in our testimony before the Congress. We have revised the FY 1979 proposed budget request then under consideration in the Executive Branch, which had been earlier formulated and submitted to the Office of Management and Budget. And, finally, we have drafted new organic legislation for the entire program, as a portion of the authorizing legislation is due to expire at the end of FY 1978.

We have initiated activities leading to improved staffing and organization to be more responsive to the new goals and objectives, which include placing greater emphasis on desalting research, development, and demonstration, and on technology transfer.

The OWRT was formed by combining the Office of Saline Water and the Office of Water Resources Research, which brought together two very broad authorities for water research and development.

The Water Resources Research Act of 1964, as amended, provides for fifty-four State water resources research programs at State universities, funds for water resources research, and transfer of research results, and the establishment of a water resources research scientific information center. The Saline Water Conversion Act of 1971, as amended, provides for research and development of processes to convert saline or other chemically contaminated water to a quality suitable for municipal, industrial, agricultural, and other beneficial uses; for conducting basic scientific research and fundamental studies; for pursuit of research findings and studies having potential application to matters other than water treatment; for conducting engineering and technical work, including design and construction and testing of pilot plants, test beds, and modules; and for investigation of the feasibility and practicability of large-scale prototype plants.

To a large extent, the potential of these acts has never been met and the past few years have been, at best, frustrating for the OWRT. The consolidation of OSW and OWRR into a single office did not produce the results that were hoped for. The two programs should complement each other in arriving at solutions to water problems, rather than compete with one another as has been the case.

Recently, objectives were unclear; users, industry, and the research community had lost confidence in the program; U.S. leadership in desalting technology and commercial export slipped; staff organization and funding became out of balance with research needs. And even more significant, the Congress lost confidence in the direction of the program, perceiving that merger of the two programs was an attempt to de-emphasize and phase out saline water technology development.

We do not believe that combining the two programs is the reason for these problems, but believe a lack of commitment to a strong and balanced program is.

In part, new goals and objectives for the program the Carter Administration intends to follow, include:

- It will be a primary objective of OWRT to specifically identify the most significant national needs in the area of water research and technology development and either provide or seek support to meet them; and to do so in a manner which balances short, medium and long-term needs, but which emphasizes those programs having the most practical and foreseeable application.

- It will be an objective of OWRT to be a leader in research and development regarding water supply, water reuse and recycling, water conservation, and water planning techniques and methodology.

- It will be a complementary objective to coordinate closely with water research efforts devoted mainly to water quality and those programs which seek to assist local government and industry to apply existing and very new technology.

- It will be an objective to do a better job of identifying and targeting the key areas for greater effort and dedication of resources. Potential examples include: water conservation; water for energy development; land/water problems of urbanization; floods and droughts; water reuse; and water resources planning and management.

- It will be an objective, once priorities for research and technology development are set, to firmly apply them to the entire program of OWRT, whether it be basic research, university research and grants, desalting or international assistance. We will, in other words, attempt to find the key areas of need, and use all of our various programs to accomplish our goals, rather than allowing each program to pursue separate and sometimes contradictory goals.

- It will be a clear objective of the Carter Administration to broaden and increase the commitment to desalting research and development, and to change and improve the approach of OWRT to the overall desalting issue. It will further be an objective to specifically set out a rationale for the desalting program, which includes the following primary purposes: To develop reliable, cost effective desalination process technologies for conservation and/or augmentation of water resources through multiple reuse of waste waters; augmentation of local water supply systems for quality improvement through blending with high purity desalted product water; maintenance or

improvement of water quality by concentrating and disposing of undesirable water constituents; water supply for locations where desalting of sea or brackish water is the most practical alternative; and initiation of an aggressive research program to improve and discover new technologies for the same purposes, consistent with the national energy conservation policies.

- It will be a complementary objective of the desalting program, the university program, and the other OWRT programs, to substantially improve the information systems for sharing research results and for facilitating applications of research successes.

Within the program of OWRT, we specifically plan a greater emphasis on saline water research and development.

In Fiscal Year 1978, we intend to:

- Give additional support to basic research to improve reverse osmosis (RO) membranes, and improved feed-water pretreatment systems, and the RO systems. We believe this is needed to make this process more cost effective, particularly for water reuse, sea water, and brackish water application.

- Continue the research and orderly development of new concepts in freezing technology, which shows promise for reuse of industrial water by concentrating wastes.

- Initiate planning for appropriate demonstration of the various technologies as a part of a practical water solution. We believe that it would be a reasonable goal to initiate over the next few years, as many as three or four well planned demonstration programs of various aspects (reuse, supply, water quality) of the desalting technology applications as a part of an on-going water management system. Further, cost sharing involving the Federal Government, state, local water management and/or private entities will be part of these demonstration activities.

In conclusion, it is our intent to have a positive program, carefully directed, to provide the research needed for solving existing and emerging water problems.

Thank you very much.

WATER QUALITY AND POLLUTION
ISSUES INVOLVED IN THE DEVELOPMENT OF A NATIONAL WATER POLICY*

by

Dr. GEORGE J. HALASI-KUN

Chairman, Columbia University Seminars on Pollution and Water
Resources

*Presented at the United Nations Water Conference Seminar as a general statement for members of Permanent Missions of UN Conference in New York City on February 14-15, 1978.

Introduction

Water, essential to human life, is our most important natural resource. The steep rise in water demand and water utilization which has recently begun is now in the process of generating global problems. The recent industrialization and an explosive population growth focus our attention on water quality and pollution. Floods, droughts and a long list of water-related diseases such as cholera, dysentery, hepatitis, typhoid fever, schistosomiasis, etc. have long played a significant role in population control and warfare, but it is only relatively recently that water quality has become a major concern to governments and planners. Population used to be most dense in water-abundant regions, but now many cities are water-poor and at an early stage began to show an interest in water quality and therefore in water pollution control. For arid areas near the sea, desalination plants can add to the supply of clean fresh water, but the expenses, especially with soaring fuel costs, makes this source impractical in most circumstances.

The continuous misuse of our water resources can cause irreparable damage to our environment if the consumption and the pollution of water is not regulated. An alarming indication of the mismanagement and improper regulation of water consumption or pollution in force is the shameful devastation of the Great Lakes in North America, the Lake Baykal area around Irkutsk in the Soviet Union, the Ligurian shore in Italy, the great metropolitan areas like Cairo, London, New York, Paris, or Tokyo, the highly developed industrial regions such as the Rhine valley around Strasbourg or in the Ruhr district, the recent oil leaks from drilling on the seabed in Santa Barbara, California or the desertification of the Sahel in Africa by excess consumption of water. These and similar phenomena are constant reminders that time is running out for the proper regulation of these problems. Efficient use and reuse of water including that of developing countries is the secret to cope with the ever increasing demand for water. The excess flood management without proper water storage may eliminate the danger of flood but increases the water shortage as it has been occurring in the Carpathian basin. 140 year effort in flood protection of Hungary increased not only the peak flow of the Danube by 15% but also the problem in water supply became more acute. On the other hand, any successful waste water management of an industrialized area could increase the drinking water capacity of the downstream adjacent region as it is evident in the Lower Rhine valley in West Germany and the Netherlands.

World Water Balance

Before we discuss any further problems of water quality and its control, let's make an account of the available water resources of the Earth. It means not only taking an inventory of facilities currently being used and of their modernization, but also reviewing possible ways to increase the quantity of clean water by further exploration for such resources as are near to the consumers. Water on earth is abundantly present and it is a reusable commodity. It is estimated to be 1,357,506,000 km³, of which 97.2% is salt water, 2.15% is frozen, and 0.65% is fresh water (Doxiades, 1967). If we could place this fresh water on the non-frozen land area of the Earth, it would reach a height of 73.16 m (8,506,000 km³). Of this, the water of lakes, rivers and streams would account for only 1.08 m in height (126,250

km³). On the other hand, 97.54% (8,300,000 km³) of the fresh water is ground water (71.40 m in height) and half of this amount is available at a depth of less than one km under the surface. Of the annual water cycle of 422,000 km³ of water, about 100,000 km³ falls on land and 30% of this feeds plants by infiltration, supplies ground water, or runs off directly to seas; the other 50% falls on frozen land or evaporates, and only 20% of this precipitation is controllable. Unfortunately, at present, no more than 1.3% (1,326 km³) is controlled and used for consumption. This is a clear indication that the available fresh water is neither properly organized for rational consumption nor is fully available at the needed area.

Pollution by Erosion (Physical Pollution)

It is obvious from the previously given account of available water resources that we must concentrate our attention primarily on the ground water, especially in developing countries, and secondarily on the surface water. Furthermore, the water quality control and improvement should be concentrated accordingly as it will be discussed later. Besides the industrial use of water, the agricultural use of large land areas increase pollution by sedimentation. As an example, only in the United States, nearly four billion tons of sediment reach receiving bodies of water (Brady, 1967). These originate from farm lands, stream banks, highways, and urban constructions. These types of pollution from eroded soil are always detrimental to the beneficial uses of water, not only in terms of water supply, recreational usage, flood control, and waterway, but also because they destroy reservoir storage capacities, silt up channels and harbors, and deflect streamflows. The degree of silt (i.e. suspended) load varies from river to river and in the upper range it might be as much as 200,000 mg/liter, whereas in the lower range it is only about 5 mg/liter. The average is between 10 and 30,000 mg/liter. Studies by the United States Department of Agriculture have shown that the clearing of forest and the continued use of land for row crops increased erosion 10,000 fold. Plowing of grassland for continuous row crop cultivation increased erosion twenty to a hundred times. Erosion rates in areas of urban construction projects are approximately three times the averages of those found in agricultural areas. This increased erosion becomes a permanent feature of urbanized communities because of the consistently large areas of disturbed surfaces and this augments the erosion-sediment production in the surface runoffs.

Pollution in Urbanized and Industrialized Areas (Biological and Chemical Pollution)

The character of pollution in urbanized and industrialized areas has a completely different pattern. The physical pollution by erosion and sedimentation is more characteristic of agricultural lands. High concentration of people in urbanized areas or of various industrial enterprises cause biological and chemical pollution.

Biological pollutants in water are usually parasitic to humans. One of the most common biological pollutants is the bacterium *Escherichia Coli* which enters into the waters through fecal matter, and is routinely used as an indicator for the presence of fecal contamination. All of the biological

pollutants are nonconservative, and if their source is eliminated their population numbers rapidly decline.

The chemical pollutants fall into two large categories: inorganic and organic materials. Inorganic materials may enter the waters as by-products of industrial and agricultural activities. Many of the industrial waste waters contain quantities of inorganic acids, salts, or particles (for example, acid water from inactive mines which denudes the environment). Intensive agricultural activities combined with fertilizers also produce considerable inorganic waste such as nitrate and phosphate fertilizers. These inorganic nutrients on a large scale can cause eutrophication of waters as it has occurred in Lake Erie. The biggest source of organic pollution is domestic sewage of the municipalities. Many industrial processes involve the discharge of large quantities of organic materials. Paper and sugar mills produce waste water loaded with carbohydrates; oil refineries discharge large quantities of hydrocarbons; slaughter houses, meat packing, and dairy companies add fatty acids and proteins. Agricultural land use increases organic pollution directly in two ways. Animal husbandry gives huge amounts of manure and the usage of pesticides are major contributors to organic pollution.

Efficient pollution control can be achieved by the systematic recording of the data and by treating each type of waste water separately in accordance with its waste composition: separately the municipal wastes and separately each type of the industrial wastes on an individual basis.

Recording the Available Water

For proper water quality and pollution control planning in accordance with rational usage of water, it is essential to collect basic water resources data to evaluate their quantity and quality, especially in smaller watersheds where the sources are limited. The basic data should consist of descriptive surveying of surface and ground water of the area in question. The survey must be based on and carried out from a broad view-point because gradual extension and completion of the record can be very expensive and many times not feasible. It is necessary that the water-resources planner together with the geologist collaborate very closely and carefully in their survey with other experts of disciplines which are interrelated to the problem. Questionnaires distributed and filled out in advance by local authorities give the surveying team a wealth of information, but its reliability depends on the professional background, educational level and local knowledge of the persons involved--not to mention the length of time spent for filling out the forms--therefore, their value is dubious. On the other hand, such a preliminary survey saves time for the surveying team and enables it to be more efficient in data collecting, also from a local view-point.

The listings and the geographical descriptions of the springs, wells, rivers, lakes, swamps, reservoirs, ponds, creeks, glaciers and ground water conditions are accompanied by the necessary geologic information, and above all with respect to the permeability of the subsurface. The meteorologic records should include not only the extreme and average rainfall data with the information of characteristic storms but also temperature, evapo-transpiration and peak point rainfall intensity data. The extent of the

wooded region and that of urbanized area with the type of the impervious land use surface is another essential piece of information, along with the mean elevation of the drainage basin, soil classification and slopes of terrain. The ground water data can be secured by available studies, if such exist, and by surveying existing wells of the area. Finally, constructions across a stream can reveal valuable information about the stream conditions.

The hydrographic description of a region has very limited value if it is not supported by numerical evaluation of runoff, precipitation, intensity, evapotranspiration, and dates of occurrence. This basic information should be supplemented with data about location and detailed description (area, layout, capacity, etc.) of water supply, sewage including treatment plants, sanitary landfills, and similar facilities. The registration of pollution generating areas and points are of utmost importance with their description. All these previously described basic data organized into a data bank are the essential basic information for a water quality and pollution control plan.

Categories of Water Usage and Their Quality Measurement

For systematic usage of the available water by control of water quality and pollution, the distribution of the planned water consumption can be grouped as follows: (1) potable water; (2) cooling water; (3) industrial water intake; (4) irrigation; (5) recreational water including waterways; (6) municipal waste water; (7) waste water from manure of husbandry; (8) industrial waste; and (9) the minimal discharge of all recipient streams where waste water is emptied.

The general characteristics by which the polluted or clean water is controlled are the following measurements:

(a) field determination for temperature, acidity-alkalinity, available quantity (discharge), and fecals (coliform and streptococci).

(b) common constituents (measured in laboratories)--hardness (separately dissolved carbonate and non-carbonate).

(c) major nutrients: Phosphorus, Nitrite and Nitrogen.

(d) trace elements for toxicity such as Arsenic, Cadmium, Copper, Chromium, Cobalt, Iron, Lead, Manganese, Mercury, Selenium and Zinc.

(e) organic or biological measurements for organic Carbon, Phytoplankton, Periphyton (Chlorophyll).

(f) suspended sediments (inorganic) measurements.

Highlights in Pollution Control

The basic principles in pollution control can be summarized as follows:

(1) Domestic and animal waste can be treated efficiently and economically at the local level where they are generated, rather than by attempting to handle polluted water for an entire region. Such wastes should be kept separate from industrial wastes, which--especially if toxic--ought to be handled by each plant individually. Combining all types of wastes makes proper treatment difficult and expensive. In general, there are three steps in treatment of waste water.

Primary treatment or mechanical treatment usually involves after screening a plain sedimentation process with removal efficiencies of 20% BOD (Biochemical Oxygen Demand), 60% SS (Suspended Solids), 15% N (Nitrogen) and 15% P (Phosphorus).

Secondary treatment or biological treatment results in increased removals of most all types of solids except many dissolved salts. This type of treatment is usually a biological process involving trickling filters, activated sludge, or stabilization ponds. Removals with such units will vary but all may be operated under certain conditions to obtain the following removals: 95% BOD, 95% SS, 40% N and 40% P. Soon all treatment plants will include a secondary (oxidation) process.

Tertiary treatment or chemical treatment employs tertiary processes for increasing further the degree of removal of solids. This treatment is usually preceded by the two previously mentioned treatments and may be used to remove a portion or all of the solids remaining after secondary treatment by creating harmless chemical compounds. Our technology today will permit us to have a closed water system for our municipalities; that is, we can process our waste water and reuse it directly as a water supply.

(2) Industrial waste water must be treated always separately from the municipal waste water because they contain special polluting or even toxic material in accordance with their processing program. These pollutants can be precious raw materials for that industry, but otherwise are unwanted wastes. Regardless of this uneconomic wasting, the individual industrial enterprise has the most reliable knowledge about the quantity, composition and time of occurrence of the waste water dumping, including its concentration. Therefore, any treatment of this waste can be done most efficiently and economically by the pollution causing facilities. They have the required expertise and the necessary information to handle the problem.

In planning the water consumption for industrial purposes, there are several considerations as to how to secure the necessary water and increased capacity of the facility by either reducing the demand or better utilizing the available water. To mention a few methods: (a) installing reservoirs, the water storage capacity increases; (b) recycling water for cooling purposes or re-use of waste water, decreasing the demand; (c) planning operation on a 355-day minimum streamflow generally doubles the yearly minimum available in the everyday routine operation of the facility; on the other hand, the management must be aware that 10 days of the year the planned quantity of water will not be on hand or must be secured by other means.

(3) Most recently, the agricultural activities have produced considerable inorganic wastes not only by erosion and sedimentation--mentioned perviously--but also by nitrate and phosphate fertilizers which are used in copious quantities in developed countries, frequently in unwarranted amounts. Parts of these inorganic salts which are not utilized by plants will eventually enter the ground water (subsurface) systems and pollute them together with the rivers, lakes, and oceans. Small quantities of fertilizers cannot be considered as detrimental to the environment, but after certain levels have been reached, further nutrients will result in eutrophication of the waters as it occurred in Lake Erie. Similarly, the indiscriminate use of fertilizers in certain areas where intensive farming is practiced, as for

example by the potato farms of eastern Long Island, phosphate fertilizers are used in concentration fifty times higher than the national average causing significant pollution problems in the adjacent estuaries.

With the advent of intensive animal husbandry, the practice of maintaining animals in confined areas, such as poultry houses, has generated huge quantities of organic wastes. Without solving the waste disposal problem, this practice has already caused almost irreparable damage by the disposal of untreated duck manure into estuarine waters along the southern shore of Long Island, eliminating the once flourishing oyster industry.

(4) Most of our big metropolitan areas are located along the shore of the oceans or seas. Until recent years, their waste water management consisted of partial secondary treatment of the sewage, letting the effluent empty into the ocean and their solid wastes deposited in the close offshore area. This practice can cause further irreparable damage; the ocean cannot be considered as an enormous garbage dumping ground where wastes can be disposed "ad infinitum". The New York City "waste disposal grounds"--twenty kilometers offshore--are already causing eutrophication of the New York Bight area. The whole Ligurian shore of the Mediterranean Sea in Italy is also heavily polluted and we should not forget that the waste lumber from the Caribbean Sea region shows up in no time on the shore of Iceland as it is carried away by the Gulf Stream. Ultimate disposal of wastes on a large scale can hardly be found in the ocean.

(5) Toxic Pollutants, because of their complexity, are not treated in this presentation. (For details, see Fabianek, J. and Sajenko, V. (1972), "Toxic Water Pollutants" in Columbia University Seminar Proceedings, Vol. V p. 192-198).

Standards of Water Quality

For review of the water quality and pollution control standards the following three tabulations are attached:

(1) Drinking Water Standards of the U. S. Public Health Service (1962), including those of World Health Organization (International 1958, European 1961) are listing the chemical requirements imposed on domestic and municipal water supply.

(2) Weinberger's analysis (1966) about the composition of municipal secondary effluent because most of the municipal wastes do not have yet a tertiary treatment.

(3) Clean Water Standards of Lake Constance, Switzerland (1961) present a practical review about the pollution control requirements of a lake or reservoir which is used for potable water purposes.

TABLE 1. DRINKING WATER STANDARDS

DETERMINATION		USPHS		WHO
<u>Bacterial:</u>				
Coliform bacteria, per 100 ml		1.0	a	0.05
			b	1.0
<u>Physical:</u>				
Turbidity, silica scale units		5		--
Color, cobalt scale units		15		--
Odor, maximum threshold number		3		--
<u>Chemical, mg/liter:</u>				
Alkyl benzene sulfonate		0.5		--
Ammonia		--	a	0.5
Arsenic	c	0.05	ab	0.2
Barium	c	1.0		--
Cadmium	c	0.01	a	0.05
Calcium		--	b	200
Carbon chloroform extract		0.2		--
Chloride		250	a	350
Chromium (hexavalent)	c	0.05	ab	0.05
Copper		1.0	a	3.0
Cyanide		0.2	ab	0.01
Fluoride	c	1.6-3.4	a	1.5
Iron		0.3	b	1.0
Lead	c	0.05	ab	0.1
Magnesium		--	a	125
Magnesium + sodium sulfate		--	b	1000
Manganese		0.05	a	0.1
Nitrate, as NO ₃		45	a	50
Phenolic compounds		0.001	a	0.001
Selenium	c	0.01	ab	0.05
Silver	c	0.05		--
Sulfate		250	a	250
Total Solids		500	b	1500
Zinc		5.0	a	5.0
<u>Radiological, pc/liter:</u>				
Radium-226	c	3		--
Alpha emitters		--	ab	1
Strontium-90	c	10		--
Beta Emitters	c	1000	ab	10

- a WHO European Standards of 1961.
 b WHO International Standards of 1958.
 c Mandatory. Others are recommended by USPHS.

TABLE 2. AVERAGE COMPOSITION OF MUNICIPAL SECONDARY EFFLUENT

Component	Average concentration in secondary effluent		Average increment added during water use [†]
	(mg./l.)	mg./l.	lb./day/ 1000 pop.
Gross organics	55	52	64
Bio-degradable organics (as BOD)	25	25	31
Methylene blue active substance (MBAS) *	6	6	7
Na+	135	70	86
K+	15	10	12
NH ₄ ⁺	20	20	25
Ca ⁺⁺	60	15	18
Mg ⁺⁺	25	7	9
Cl ⁻	130	75	92
NO ₃ ⁻	15	10	12
NO ₂ ⁻	1	1	1
HCO ₃ ⁻	300	100	120
CO ₃ ⁼	0	0	0
SO ₄ ⁼	100	30	37
SiO ₃ ⁼	50	15	18
PO ₄ ⁼	25	25	31
Hardness (CaCO ₃)	270	70	86
Alkalinity (CaCO ₃)	250	85	100
Total dissolved solids	730	320	390

*Apparent alkyl benzene sulphonate

†Concentration increase from tap water to secondary effluent

After Weinberger et al. (1966.)

TABLE 3. CLEAN WATER STANDARDS OF LAKE CONSTANCE, SWITZERLAND

To preserve clean water usable for drinking purposes in the lakes of densely populated areas the following limits in pollution are allowed in accordance with standards used on Lake Constance:

pH:	6.0-9.0
Settleable solids:	0.3 mg/l
Total suspended solids:	30 mg/l
5 day BOD:	20 mg/l
Oxygen consumed from potassium permanganate:	80 mg/l
Toxic substances:	not detectable
Sulfides:	not detectable
Fats, oils, mineral oils:	10 mg/l
Total phosphorus reduction:	90 %

Conclusion

As a case study, the water quality and pollution control of the Lower Rhine, F. R. Germany, shows how close cooperation on the national and international level in waste water treatment and recycling of water can help to solve problems of the multiple use and reuse of fresh water in a region where not only the population density is one of the highest in the world (close to 260-400 people per km²) but also the industry is heavily concentrated, as it is in the Ruhr district and in the Netherlands. Because of the water shortage all the municipalities have tertiary treatment plants in the Ruhr valley and their treated water is re-used for drinking purposes in the adjacent Emscher valley and in the Netherlands. The industrial waste water is treated individually in one hundred and six secondary treatment plants and in several dozen tertiary treatment plants before their effluent is dumped in five additional huge tertiary treatment plants. These last treatment plants handle the purification of waste to such an extent that the effluent can be discharged into the Rhine. The quality of the river water is improved under international control so efficiently that downstream in the Netherlands the Rhine water is used for drinking purposes after being properly filtered and controlled. The Netherlands takes 65% of their drinking water from the Rhine. If there can be close cooperation on the national and international level as in the International Commission for the Protection of the River Rhine against Pollution (since 1963) in the use, treatment, and recycling of water, then we can look ahead with confidence that we will have adequate water in the future.

References

- Brady, N. C. (editor), 1967, "Agriculture and the Quality of our Environment", Washington, D.C. Am. Assoc. Advance. Sci. (AAAS), 476 pp.
- Claus, G. and Halasi-Kun, G. J., (1972) "Environmental Pollution" in Encyclopedia on Geochemistry and Environmental Sciences (editor: Fairbridge, R. W.) New York: Van Nostrand-Reinhold, p. 309-337.
- Doxiadis, C.A., 1967, "Water and Environment", Water for Peace, Vol. I, International Conference on Water for Peace - May 23-31, 1967, Washington, D. C. pp. 33-60.
- Fabianek, J. and Sajenkov., "Toxic Water Pollutants", Proceedings of University Seminar on Pollution and Water Resources, Vol. V (1971-1972), New York-Trenton: Columbia Univ.-State of N.J. p. 192-198.
- Falkenmark, M. and Lindh, G., 1976, Water for a Starving World, Boulder, Col.: Westview Press, pp. 204.
- Halasi-Kun, G.J., 1971, "Aspects hydrologiques de la pollution et des ressources en eau, dans les domaines urbains et industriels," Actes du Congres: Sciences et Techniques An 2000, Paris: SICF, 1971, Vol. 11, p. 1-16.

- Halasi-Kun, G.J., 1972, "Computation of extreme flow and ground water capacity with inadequate hydrologic data in New Jersey," Proceedings of University Seminar on Pollution and Water Resources, Vol. V (1971-1972), New York-Trenton: Columbia Univ.-State of N.J., p. 29-63
- O'Malley, C.K., 1970, Proceedings of the Conference on International and Interstate Regulation of Water Pollution, March 1970, New York, Columbia University, School of Law, 1970, 321 pp.
- Weinberger, L.W., Stephan, D.G., and Middleton, F.M., 1966, "Solving our water problems-water renovation, and re-use", Ann. N.Y. Acad. Sci. 136(5), 131-154.

THE APPLICABILITY OF ULTRAVIOLET
SPECTROPHOTOMETRY FOR WATER
QUALITY ANALYSES. A REVIEW.

by

MICHAEL HERMEL Ph.D. MARTIN S. TANZER Ph.D.
and GEORGE CLAUS, M.D., Ph.D. (1)

The American Academy of Ocean Sciences
33 South Bay Avenue, Amityville, N.Y. 11701

(1) Broadway Medical Lab. NYC; E.G. & G., Waltham, Mass. and Rutgers
University, Medical School

Acknowledgment

The authors wish to express their sincere appreciation to Mr. Gerald Robin for his kind contribution of materials treated in Section A of this review.

Abbreviations Used

- TC = Total carbon. Includes inorganic and organic carbon, be it dissolved or particulate. Expressed as mg C/l.
- TOC = Total organic carbon. Includes dissolved (both oxidizable and refractory) and particulate organic matter. Sample treated with acidification to flush out inorganic carbon. Expressed as mg C/l.
- DOC = Dissolved organic carbon. Sample obtained after filtration, thus particulate organic carbon is not present. Includes both oxidizable and refractory organics. Expressed as mg C/l.
- POC = Particulate organic carbon. After a sample has been filtered, organic carbon determination is carried out on the filter residue. DOC and POC together yield the value of TOC. Expressed as mg C/l.
- COD = Chemical oxygen demand. Includes both dissolved and particulate organics. However, some of the organic matter will not be oxidized under the test conditions, therefore, the COD expresses only the amount of oxidizable organics to which the refractories should be added to get the total chemical oxygen demand. Expressed in terms of O_2 consumption, i.e., mg O_2 /l.
- TCOD = Total chemical oxygen demand. Contains particulate and dissolved organic matter, the latter of which is a composite of both oxidizable and refractory organics. Expressed as mg O_2 /l.
- DCOD = Chemical oxygen demand of dissolved organics. After filtration, wet oxidation is performed on the sample. The result will be the difference between the total dissolved organic matter minus the refractories. Expressed as mg O_2 /l.
- PCOD = Chemical oxygen demand of particulate organics. Result of regular COD determinations carried out on the filter residue. The value of PCOD added to DCOD not necessarily yields TCOD, since the latter is also supposed to contain the oxygen consumption of the refractory materials. Expressed as mg O_2 /l.
- DOM = Dissolved organic matter. The sample is filtered and the amount of organic matter is determined. Expressed as mg M (organic matter)/l.
- POM = Particulate organic matter. The organics content of the filter residue. It is customary to acidify the sample and take its weight loss after ignition. Expressed as mg M/l.

BOD₅ = Biological oxygen demand. The O₂ content of the sample is determined and after five days of incubation it is redetermined. The oxygen consumption which is due to microbial degradation of the organic matter present is an indication of the pollutional load represented by dissolved and decaying particulate organics. Several refractory organics, however, are immune to microbial degradation. Expressed as O₂ consumption, i.e., mg O₂/l.

WLI = Weight loss at ignition. After acidification the evaporated sample is supposed to contain both the dissolved and particulate organics. Ignition in an oxygen atmosphere will remove the organics in form of CO₂, water, sulfur oxides and nitrous oxides. The weight loss represents the organic contents of the sample. Expressed as mg M/l.

Tye = Tyrosine equivalent. After filtration the absorptivity of the sample is measured at 280 nm in 1 cm path. The value of absorption (E) is established and the corresponding amount of tyrosine is read off from a standard dilution curve of pure tyrosine. Expressed as mg Tye/l.

A. The Color of Water

One cannot separate the history of investigations on the color of water from a discussion of water transparency or absorption studies. The earliest work dates from 1818, when Jordan published a paper in the Science Journal describing his studies on water color. From this period on, a number of investigations have been carried out to elucidate the reasons for the different colorations occurring in natural waters and also to study their transparency as related to depth. DuPré and Dawson (1961) provide an excellent review of such early works. In 1865 Secchi initiated studies of light absorption or water transparency by direct observations and attempted to determine whether or not the bottom of the sea could indeed be seen at great depth, as has been claimed by some observers. He designed a series of discs varying in diameter from 40 cm to 3.73 m, made of iron rings and covered with canvas. A system of weights was distributed in such a way as to hold the plates in the horizontal plane, and a line was graduated to indicate the depth to which the object was lowered. Some of his discs were white; others were yellow or silvery to imitate the color of silt in the sea. By this technique Secchi was able to demonstrate that transparency is partially influenced by turbidity, but also that at greater depths absorption of the whole spectrum of the light is involved.

The spectral absorption characteristics of sunlight in sea water were first determined by Tyndall in 1872 and then by Aitken in 1882. These studies settled the controversy over the color of the sea. The investigations have shown that it is the orange-red region of the sunlight which is most rapidly absorbed, and the blue light which penetrates the deepest into the water. Thus, short wavelength penetration is basically the cause of the bluish hue of clean water.

In 1877 Forel conducted extensive studies on the variation in transparency of the waters of Lake Geneva, and he developed a color scale based upon his results which is still referred to as the "Forel Scale". Many years later this subjective scale was evaluated in the absolute terms of the

trichromatic percentages of red, green and blue by Czepa (1955), who also compiled the maximum penetration values in water of the different wavelengths.

As early as 1890 Izawa gave an alternative explanation of the color of the sea in terms of reflection theory. Even earlier Kotzebue (1818), as claimed by Stupishin (1955), constructed an apparatus for the quantitative assessment of observations on the penetrability of light in water. Other methods for the measurement of light penetration in water were published by Ewald (1910) and by Gruber (1924). The latter constructed a special apparatus for the quantitation of light intensities at different depths, while Murray and Hjort (1912) exposed photographic plates at various depths in the clean fjords of Norway to study the phenomenon of light absorption. Their results showed that the red and orange rays are more quickly absorbed than the blue and violet, thus confirming, with a different technique, the early works of Tyndall (1872) and Aitken (1882).

Light penetration in water is always accompanied by a certain amount of absorption, regardless of the color or wavelength of the radiation. Media which are commonly designated as transparent, if not deployed in too great thickness, transmit the range of wavelengths comprised within the region of the visible spectrum, without appreciable absorption. The same materials, however, may exercise powerful absorption in the infrared and ultraviolet regions; and if a great enough thickness is employed, absorption will occur even in the range of visible radiations. Pure water, one of the most transparent substances, appears distinctly blue in long columns, showing that it absorbs more or less completely the red end of the spectrum, while letting the blue or violet rays through. The same is true of most varieties of glass. The definition "transparent" is at most arbitrary, since there is no perfectly transparent (invisible) substance in nature. On the contrary, transparent objects are visible only by virtue of non-uniform illumination, as pointed out by Lord Rayleigh in his article on optics in the Encyclopaedia Britannica (1911).

B. The Absorption of Light in Water

The law of absorption has been attributed to both Bouguer (1698-1758), Royal Professor of Hydrography at Le Havre; and Lambert (1728-1777), a German physicist and mathematician (Encyclopaedia Britannica, 1911).

If any radiant energy is transformed into heat while passing through a medium, absorption occurs; the amplitude and intensity of the waves will not be constant but will decrease. For plane waves, the fraction $\frac{dI}{I}$ of the intensity (I) lost in traversing an infinitesimal thickness is proportional to dx, so that

$$\frac{dI}{I} = -k dx$$

where k is the absorption coefficient, since it is the measure of the rate of loss of light from the direct beam.

To obtain the decrease in traversing a finite thickness x the equation is integrated to give:

$$\int_0^x \frac{dI}{I} = -k \int_0^x dx$$

Solving this, we find:

$$I_x = I_0 e^{-kx}$$

This law is referred to as Bouguer's exponential law of absorption.

If light of intensity I_0 enters a medium, the intensity of the radiation emerging at depth x (I_x) will be less than I_0 . Therefore, for a given density of water, I_x depends on the depth x according to the exponential law of absorption. However, most of the decrease in the intensity of I_x is in this case not due to a real disappearance of the light (transformation to heat), but rather results from the fact that some light is scattered by particulates floating in the medium and thus is removed from the direct beam. For example, in even a very dilute mixture of sea water and floating particles (as may be found in bays near estuaries), a considerable intensity of scattered light may be easily detected by observing the medium from one side to the lee of a shadow of an object, causing an area to appear darker than the liquid through which the beam passes.

True absorption represents the actual disappearance of light, the energy of which is converted into heat, so that the name "absorption coefficient" for k is not appropriate. In general k can be regarded as being made up of two parts: k_a due to true absorption, and k_s due to scattering. The equation then becomes

$$I_x = I_0 e^{-(k_a + k_s) x}$$

Therefore, it is more appropriate to call the exponential factor k the attenuation or extinction coefficient, where

$$k = k_a + k_s$$

Light scattering should not be confused with diffusion. In the case of a beam, any scattering is considered a loss, whereas in diffusion, light scattering in any forward direction is still counted as part of the diffused flux. Thus, diffuse light shows less attenuation than does a beam or ray of light. Duntley (1957) states in his paper on the penetration of light into waters "... that it is, perhaps, a startling fact that diffused light penetrates further than does a beam of light."

Typically, then, the attenuation of natural waters is given in terms of the absorption coefficient or extinction coefficient (Sverdrup, et al., 1942), and if the intensity of the radiation at some point is I_0 , then for

a depth x the intensity is I_x according to Bouguer's law. Thus, if the intensity at a given depth is known, then it is possible to calculate the intensity at any other, since the extinction coefficient is constant over a wide range of depths for any particular wavelength.

The law of absorption as expressed by Bouguer and Lambert was further developed by Lambert and von Beer, who have shown independently that the amount of light absorbed is inversely proportional to the thickness of the medium and to the concentration of absorbing material, if present. This proportionality is dependent upon the extinction coefficient, a value which is characteristic for any chemical compound having light absorptive capacities. The formulation of this law permitted the rapid development of absorption meters (photometers) for analytical chemical techniques, in which concentrations of unknown solutions are compared to a blank of known concentration. Calibration curves can be produced by serial dilutions of known concentrations measured, versus their light absorption, from which curves, knowing the absorptive value of the unknown, its concentration can be read off.

The absorption of visible light in naturally occurring waters is usually due to a "pigment" which was first described by Kalle (1937) and named as "Gelbstoff". The chemical identity of this material is still not yet completely understood, but this "yellow pigment" of the English literature is probably a complex of carotenoids, lignins, and humic acids. It is presumed to originate from decaying plant materials and is washed into waters by rains from the terrain. Indeed, the upper regions of the Amazon River flowing through dense rain forest areas contain exceedingly large quantities of this yellow pigment, still discoloring the mouth of the river several hundred miles downstream. The typical absorption for this material is in the caroten range of from 420 to 560 nm. Because of its broad range and non-specific nature, spectral measurement of the yellow pigment in natural waters does not serve as a useful indicator for the presence of any specific organic contamination.

C. The Absorption of Ultraviolet Light in Water

The penetration and absorption of ultraviolet light in natural waters has become a subject of scientific interest only during the past two decades. It is noteworthy that the first investigation on UV penetration or absorption in natural waters was carried out in 1903 by Aufsess (Munich), in which study he took typical absorption spectra of several lakes in Bavaria and Tirol from 10 to 70 cm depths. His work, however, apparently was completely forgotten and is mentioned only by H. Stooff in the discussion of Demmering's paper (1938, p. 236, see later).

It has been pointed out earlier that the shorter the wavelengths, the greater is their penetration both in fresh and in saline waters. However, since pure distilled water does not exist in nature, the absorption of incident UV radiation will be greatly influenced by the absorption and scattering produced by the particulates in the water and also, according to Lambert and von Beer's law, by the concentration of the dissolved inorganic and organic materials. Many inorganics exhibit marked absorption in the far-ultraviolet range, while dissolved organics absorb in the middle region of the UV spectrum, tailing off towards the close UV end. The recognition

that different compounds have characteristic and usually sharp absorption bands in the ultraviolet led to the first compilation by Möhler (1937) of absorption curves for identification purposes in his handbook: Solute Absorption Spectra; however, Hess had conducted some investigations into the spectral characteristics of soluble cellulose derivatives and other polymer plant substances, such as lignin, as early as 1928. On the basis of these works, Demmering published the results of his very thorough investigations on the possibility of utilizing ultraviolet spectral analysis for the study and monitoring of polluted surface waters in 1938. He compared the permanganate values of a six year period of the Mulde River with the UV spectra of the water in the range of 200-400 nm and also with the spectra of several organic and inorganic pollutants known to be present in the water through chemical determinations such as phenol, sodium carbonate, and lignin sulfonates. In lack of a spectrophotometer, he used a modified Pulfrich photometer with quartz cuvettes and tungsten light source. He foresaw the possibility of modifying this instrument, through the deployment of a flow-through cell, for the continuous monitoring of dissolved organic and inorganic water pollutants.

Whereas Demmering's work dealt with ultraviolet absorption in fresh water, Tsukamoto showed in 1927 that UV radiation steeply decreases in sea water between 200 and 300 nm. Investigating coastal waters, Kalle (1937) found that the absorption of the blue end of the spectrum is increased, when compared to findings for the open ocean. He ascribed this to the presence of undetermined organic materials, similar to the "yellow pigment" he had described, which he supposed to be washed in from the shore. Joseph (1949) used the wavelengths of 367 nm to measure the absorption of UV radiation in the Baltic and North Sea. He found that the low salinity value of Baltic Sea water was inversely related to the attenuation of light. This decrease of transparency, however, could not be ascribed simply to salinity differences, and he had to conclude that the coastal waters of the Baltic Sea must contain higher quantities of UV absorbing matter than the open waters of the North Sea. Jerlov (1950) conducted measurements at 310 nm, comparing waters from different seas. He found that in the Eastern Mediterranean the absorptivity of the water was equal to that of the Sargasso Sea; whereas the Skagerak waters absorbed almost 90% of the incident radiation at 1 m depths. Unfortunately in his later experiments (Jerlov, 1951), scattering caused by particulate matter could not be distinguished from the attenuation of light due strictly to absorption. Nevertheless, on the basis of his results it was possible to classify sea waters according to their absorption spectra, the distinctions being the greatest in the absorption of the shortest wavelengths.

Lenoble (1956) conducted absorption measurements in the wavelength region of 250-400 nm in situ in the Mediterranean and compared these results with those obtained from solutions of salts used to make up artificial sea water. He could not find any difference between the artificial and the natural sea water. His experiments were repeated by Chanu (1959) and by Armstrong and Boalch (1961a). Chanu came to the conclusion that Lenoble's results were not completely satisfactory because the component spectra of the individual salts occurring in sea water are quite characteristic and differ from the complete spectrum of native sea water. By extending the range of measurements down to 200 nm Armstrong and Boalch found that at short wavelengths, natural sea water has at least double the absorbancy of artificial sea water. This difference was ascribed to the presence of organic matter, the "yellow pigment" of Kalle. They also showed that both regional variations and

seasonal effects will influence absorption. Coastal waters or open seas may show increased absorbancy during certain seasons or after heavy rainfall. Absorptions below 235 nm were related to nitrate concentrations. Some chemical tests corroborated their findings regarding the importance of inorganic materials in producing higher absorbancies in the short wavelength region. Shapiro (1957) showed that colored materials can be extracted from sea water with organic solvents and also, that if native sea water is passed through activated charcoal filters, the UV absorption of the effluent is decreased. Highly colored materials can be further extracted from the charcoal with organic solvents (Wilson and Armstrong, 1952; Johnston, 1955). Fogg and Boalch (1958) demonstrated that numerous colored and highly UV absorbent materials are excreted by a variety of marine algae.

In preparing their samples Armstrong and Boalch (1961a) paid careful attention to avoid the loss due to light scattering, caused by particulates in the water. Therefore, prior to their measurements, they filtered the samples on membrane filters or porcelain candles of 1 μ m average pore size. Unfortunately they do not state in their methodology section which kind of membrane filter they used and which samples were filtered through the porcelain candles. The importance of this distinction will become clear in the later part of this review when we will be dealing with methodologies.

In a further study, Armstrong and Boalch (1961b) compared salinity distribution measurements in a transect of the English Channel with those of UV absorption readings, taken at 220 nm. They found that whereas the salinity measurements did not detect appreciable differences in the water masses, there were considerable variations in absorptivities, indicating that high UV absorbing materials entered the Channel on the French coast, probably by land drainage, and were flowing towards the South. It is interesting to note that they considered the source of the high UV absorption to be organic matter related to the "yellow pigment"; although their measurements were carried out at 220 nm, while in their previous paper they had pointed out that below 235 nm high absorptive values are usually produced by nitrates.

Finally the studies of Strickland (1959) should be mentioned. He investigated the penetration of light in artificial sea water, as it varied according to the composition and characteristics of the bottom sediment. Sandy gravel bottoms, even in heavy turbulence, resulted in the deepest UV penetration, while muddy clays, even under stagnant conditions, gave high absorption readings, due to the presence of colloidal suspensions.

D. The Role and Importance of Particulate and Dissolved Organics in Water

Organic matter in natural water can occur either in the form of particulate material or dissolved organics. Particulates can again be divided into living and non-living matter. The living fraction of particulate organics is composed of the micro- and macro-organisms of the water, but in general one usually refers only to microscopic inhabitants, such as bacteria, some fungi, and small algae. The non-living organic particulates are aggregates of either dead micro-organisms or organic precipitates formed around condensation nuclei, or a mixture of both. Finally, the dissolved organics range from relatively simple compounds such as urea, or amino acids, to exceedingly complex polymers such as lignin sulfonates and proteins.

There are three sources of non-living particulates and dissolved organics in water. (1) In situ decomposition. Organisms dying in the water will rapidly decompose through microbial action, during the course of which considerable quantities of intact organic materials are liberated. (2) Higher organisms excrete organic matter as body waste into natural waters, while algae secrete certain organic substances. According to the estimation of Fogg, et al. (1965), half of the carbons assimilated in the oceans will be secreted by the algae during their life cycle into the surrounding water. This organic material amounts to 10^{10} tons per year. (3) Finally, large quantities of organic matter are either washed in from the shores through rainfalls or ground water seepage, or are transported by the air - either as volatile compounds which undergo partition absorption at the air-water interface, or as biogenic particles, or materials attached to dust, oil and water droplets which eventually end up in the water. Man-made organic wastes, both domestic and industrial, fall also in this category of allochthonous organics, and with the increase of industrial production and population growth their amount in natural waters is by now considerable.

The dissolved organic matter represents a wide range of compounds which can be roughly classified as simple nitrogenous chemicals (such as urea, amino acids); simple and complex carbohydrates, other aliphatics and aromatics; and complex polymers such as humic acid types (ligninsulfonates), polypeptides, proteins, and polymer alcohols. Since water is a universal solvent, minor quantities of such materials which are generally considered as only organic solvent solubles will also be present; for instance, certain vitamins (A and E), etc.

The role of the dissolved organic material in the waters is primarily in the nutrition of both osmotrophic and phagotrophic organisms. It has been known for a long time that bacteria, and even certain autotrophic micro-algae, can utilize simple preformed organic matter for their metabolism. In recent years the range of organisms with this ability has been expanded to include such higher forms as mollusks and even crustacea. Galtsoff (1958) and Provasoli (1957) have confirmed earlier speculations that macro-organisms are also capable of taking up dissolved organic matter from their surroundings, presumably through active transport.

It has also been demonstrated that dissolved organic materials play a considerable role in the nutrition of obligate phagotrophic organisms. Condensation nuclei for the precipitation of dissolved organics occur in water. Either silt particles or dead microorganisms may serve as surfaces onto which, through electrostatic or van der Waal forces, dissolved organic material may attach itself (Riley, 1963; Suitcliffe, et al., 1963). The surfaces of these organically coated particulates will serve as sufficient substrate for bacterial colonizations. When the bacteria exhaust the nutrients of their immediate surrounding and also that represented by the precipitated organic material, they die. Their bodies will, however, become condensation points for the precipitation of further organic matter, and a cyclic phenomenon results in the production of ever growing aggregates. These may be eaten by phagotrophic organisms or, in the seas, may sink to greater depths. During their slow submersion the organic aggregates grow in size, and at around 10,000 m some of them may have a diameter exceeding one meter. Japanese deep sea explorers described the slow downward sinking of organic aggregates to be similar to falling snow, and the term "organic snowflakes" became accepted in oceanographic literature.

The air-water interface also helps in the production of organic aggregates. Due to currents or wave action, small air bubbles are constantly incorporated into the water, the surfaces of which serve again as condensation layers for dissolved organics. The process is quite similar to that described earlier, leading to the production of aggregates of increasing size. In spite of the fact that most dissolved organic compounds occur in sea water in concentrations in the parts per billion range, and their totality rarely exceeds a few parts per million, extrapolations to the total volume of ocean water gives tonnages in the billion ranges. It is, therefore, quite evident that this huge quantity of dissolved organic material plays a rather important role in the biodynamics of waters (Wallace and Willson, 1969).

The second importance of dissolved organics in waters is related to the problems of pollution which they represent, directly or indirectly. The quality of water for human usage can be judged by the kinds and amounts of organic pollutants it contains. The source of dissolved organics of the pollutant types in waters are basically the same as those which we have already discussed. However, when focusing on pollutional studies it would seem to be more important to pay attention to certain specific organic chemicals such as phenols, detergents, pesticides, proteinaceous matter, etc., originating from household or industrial waste, than to try to establish levels for relatively innocuous and naturally occurring products, such as carbohydrates or lignin sulfonates. Obviously under certain special conditions presented by the effluent of a sugar mill, a paper factory, or a slaughter house, analysis of the carbohydrate, lignin, or protein components of the waste waters should be performed.

The significance of organic pollutants in natural waters or in sewage treatment plant effluents lies in the fact that the higher the quantity of the microbially decomposable matter, the more microbes will appear in these waters. Since most bacteria obtain their nourishment through heterotrophic nutrition, both known pathogenic and non-pathogenic microorganisms will thrive in organically enriched waters. The massive growth of non-pathogenic bacteria, such as the sulfate-reducing organisms Beggiatoa, Thiothrix, and Spherotilus, in the effluents of paper mills, may not be harmful per se, but they certainly represent an unpleasant sight, not to mention the noxious odors of liberated H₂S they produce.

The problem is more dangerous when pathogenic organisms get access into and survive in waters carrying high organic loads. Such organisms represent a direct hazard to humans or higher animals, when the latter get in contact with infested waters. The list of water-borne diseases is quite impressive and the fact that many of the causative organisms are able to survive in these waters is due to the amount of dissolved organic matter available in their surroundings (Jamieson, et al., 1976). The tests for certain of these pathogens are not simple; or they may be rather fastidious organisms and their culturing may not always be successful. Therefore, the concept of utilizing indicator organisms in bacteriological water quality determinations became an accepted routine. E. coli was selected as one of the pollution indicators, since its presence in surface waters is associated with fecal contamination. Although E. coli per se has a low pathogenicity, the likelihood of other, more dangerous parasites being present in the waters when the coliform counts are high is greatly enhanced. Again one must

emphasize, however, that for the survival of coliform organisms, both in fresh or in sea water, certain amounts of dissolved organic matter have to be present. Therefore, it is being increasingly emphasized that the determination of organics in water has basic significance for establishing water quality grades. Today, organic matter is daily tested in the effluents of many sewage treatment plants or in water supply facilities.

E. Methods for Measuring Organic Matter in Water

Depending upon the analysis employed, several designations are used for characterizing organic matter in water. One of the older terms is the chemical oxygen demand (COD) which is determined by an oxidation technique using either potassium permanganate or potassium dichromate as the oxidant. It was recognized for quite a while that COD does not represent the total organic content of the water because several compounds will not be completely oxidized by this method. Therefore, the term total organic carbon (TOC) has been introduced to cover these refractory organics. Another method to measure organic matter is the five day biochemical oxygen demand (BOD₅). This method measures the microbial oxygen consumption of the waters during a five day period. The oxygen is utilized through decomposition to oxidize the organics in the water. The relationships between TOC, COD and BOD are tenuous.

In order to overcome some of the inadequacies inherent in these determinations it has been proposed that after acidification, the sample should be evaporated, the residue weighed, and the weight loss at ignition determined. The latter is supposed to represent the amount of organic matter. While in TOC and COD determinations, particulate organics are included, if the sample is either filtered or centrifuged, only the dissolved organics (DOC) are determined in the filtrate. Supposedly the difference: TOC minus DOC, represents the particulate organic matter of the sample (POC). In all of these determinations care is taken to remove inorganic carbonates, either from particles or from solutions, by strongly acidifying the samples and bubbling out the liberated CO₂. When such a procedure is not employed one obtains the total carbon content (TC), which in many instances in fresh water or in waters after filtration is identical to the DOC.

The analytical techniques employed for the determination of the enumerated parameters can usually be grouped into the following categories: 1) conventional wet chemistry, 2) infrared absorption spectroscopy, and 3) UV spectrophotometry.

1. The conventional techniques utilizing either potassium permanganate or potassium dichromate will result in COD determinations where the consumed oxygen is expressed as mg/l of starting materials (or ppm).

In the European literature for water quality testing, the potassium permanganate method is preferred. The samples are acidified with sulfuric acid and, after heating with standard KMnO₄ solution, the reduction of the permanganate ion into a colorless compound is spectrophotometrically measured, or the whole sample is directly titrated with standard permanganate solution.

The Standard Methods for the Examination of Water and Waste Water (1976) prefers the dichromate reflux method, since in the presence of Ag_2SO_4 catalyst it seems to yield a more perfect oxidation of the organic matter than permanganate. The organics are destroyed in the sample by a boiling mixture of chromic and sulphuric acids, while the sample is refluxed with known amounts of $\text{K}_2\text{Cr}_2\text{O}_7$ and H_2SO_4 . The excess of the dichromate is back titrated with Mohr's salt in the presence of Ferroin indicator. The consumed dichromate is proportional to the amount of oxidizable organic matter. Chlorides, bromides, and iodides interfere, becoming completely oxidized in the procedure. Therefore, corrections have to be carried out. This becomes rather complicated in samples of sea water containing large quantities of chlorides. A newer method, eliminating chloride interference but not yet incorporated in the Standard Methods, has been proposed by Dobbs and Williams (1963). In this technique the chlorides are complexed with mercurous sulfate. The standard COD method is incomplete because straight-chain aliphatic compounds, aromatic hydrocarbons and pyridine are not oxidized to any appreciable extent, and attempts at working at higher temperatures to oxidize these refractory materials were not successful on account of the decomposition of the dichromate: several other techniques have therefore been put forth. A combination procedure using wet oxidation with dichromate, followed by a dry oxidation (combustion) of the refractories and measurement of the carbon dioxide thus liberated, gives a TOC value which is as complete as one can hope for. This method, however, is expensive and cumbersome and it requires at least three hours for completion (AWTR-Summary Report, 1964).

The five day BOD measurement determines principally organic compounds of biological origin, but also many compounds which are found in petroleum. By its nature it does not measure organics resistant to biological attack, such as many of the plastics, refractory detergents, pesticides, etc. Certain compounds like cellulose, which do not represent a true organic load since only a few specialized microorganisms can decompose them, will not be included in the BOD, whereas they are broken down in the dichromate system. Conversely, many aliphatic compounds, among them such simple ones as acetic acid, will not be substantially oxidized with dichromate, whereas they are acceptable as food sources for microbes and will be utilized by them in the BOD test.

Since in many cases it is not too important to determine the amount of particulate organic matter (POC) which is incorporated in the previously discussed techniques, in several recently proposed tests only the dissolved organic carbon (DOC) is measured. Relatively good correlations have been found in variously polluted waters between COD and DOC, therefore, attention has recently been focused on investigations of DOC. In sample preparation for DOC analysis either filtration or centrifugation is used to remove all the particulate matter. Since the advent of the membrane filters, it is convenient to filter the samples on a Millipore® .45 μm filter because one can be reasonably sure that such a filtrate is free even of bacteria. Filtration through porcelain candles is somewhat more cumbersome than employing a membrane, whereas centrifugation has to be conducted with relatively high speeds (3000-5000 rpm) in order to sediment small floating particles effectively. Therefore, it is not surprising that in large portions of the literature dealing with DOC determinations (to be reviewed later), Millipore® filtration is used to remove interfering particulate

matter. An inherent problem, apparently not recognized by most of the investigators working in this field, lies in the fact that nitrocellulose filters are excellent absorbers of proteinaceous materials. This latter discovery led to the actual use of membrane filters for concentrating virus particles from sewage plant effluents (Wallis and Melnick, 1967), and also to the development of micro-analytical techniques for in situ protein determinations on the filters. Bennett (1967) reported that this method is highly effective over a wide range of protein contents (40 -2000 μg) while Kihara and Kuno (1968) showed that 5-60 μg proteins can easily be determined. The membrane filters quantitatively bind proteins up to 150 μg , while polypeptides will bind less firmly. These authors showed that proteins of high molecular weight bind to the filters more effectively than those of smaller size. The starting concentration of the proteins had little effect on the efficiency of binding; even such dilute solutions as .003 $\mu\text{g}/\text{ml}$ became completely bound on the filter. In view of this, one wonders about the accuracy of the DOC determinations reported in the literature after the deployment of membrane filters.

2. Infrared spectrophotometry has been recently developed for the measurement of DOC or TOC. Some automatic instruments have been introduced which perform such analysis on batch samples. One of these employs a dry oxidation, with complete oxidation of the organic matter in a combustion chamber. A small amount of the sample (30-40 ml) is squirted onto the hot plate of the combustion cube, where it is quickly converted to steam and its organic content is burned to CO_2 in a continuous flow of oxygen. The oxygen stream passes by a nondispersive infrared CO_2 analyzer, which measures the sample's CO_2 pulse when it reaches the infrared cell as a peak height and displays the results on a chart recorder. From this peak height the original TOC content of the sample can be calculated. Carbonates are removed by acidification and flushing with oxygen before introduction to the combustion furnace. The sample size constitutes a serious limitation in the technique, since many waste waters contain large quantities of suspended solids which will interfere with the obtaining of a homogenous sample, a requirement for receiving a contained CO_2 pulse in the analyzer.

Several modifications of this method have been worked out in recent years, among which substitution of the oxygen-conveying system with nitrogen, or the filtering of the samples to remove particulates have been proposed. These instruments are rather sophisticated both mechanically and electronically, and their price range is \$8000-10,000.

A comprehensive report on the applications of infrared analysis has been recently presented by Fredericks and Sackett (1970), dealing with the organic carbon content of the Gulf of Mexico. The methodology employed was a slight modification of the original Menzel and Vacarro (1964) technique, which is as follows. The samples are filtered through a Gelman, Type A glass fiber filter and separate determinations are carried out on the DOC and POC contents. The DOC is measured after conversion in an oxygen stream to CO_2 at 175°C with a nondispersive infrared analyzer. The filters holding the particulate material are placed in glass ampules with a strong oxidant ($\text{K}_2\text{S}_2\text{O}_8$ and H_3PO_4). Subsequently, the samples are treated identically to those serving for the DOC determinations. The ranges and mean values for DOC and POC in the Gulf of Mexico obtained by the authors are shown in Table I.

TABLE I. RANGES AND MEANS FOR DISSOLVED (DOC) AND PARTICULATE (POC) ORGANIC CARBON IN THE GULF OF MEXICO (in mgC/liter) (After Fredericks and Sackett, 1970)

Sample Type	DOC			POC		
	No. of Sample	Range	Mean	No. of Sample	Range	Mean
SHELF depth 100 fms	79	0.58—2.35	1.08	78	0.022—1.911	0.214
OPEN GULF surface 0-90m	76	0.45—1.07	0.79	76	0.013—0.126	0.050
OPEN GULF deep 90-3600m	109	0.33—0.94	0.52	107	0.004—0.117	0.028

3. UV spectrophotometric techniques are also being applied for the determination of DOC because of their simplicity and specificity. After the pioneering work of Demmering in 1938, no special effort was made until 1959 to utilize UV spectra of organic compounds in natural waters or in sewage effluents for the measurement of their concentration. Hoather and Rackham (1959) published a paper proposing that nitrate and nitrite determinations be carried out with the aid of UV spectrophotometry. In this short but remarkable work the authors make several interesting statements regarding the possibility of using absorption spectrophotometry for the estimation of organic matters in waters. Since the main objective of the work was the development of a rapid method for nitrate determination, the assertions about the usefulness of UV techniques for organic analysis are incorporated in order to discuss interferences from these compounds rather than to apply the method for their quantification. The authors state that the 210 nm wavelength can be utilized with a reproducibility of better than 5% for quantitative measurement of less than 1 ppm nitrogen in nitrates, and also that interference from organic impurities at this wavelength is negligible: "... reasonable accuracy can be attained by applying a relatively small correction for organic matter in solution, on the empirical basis that the absorption at 2100 Å due to organic matter is approximately four times as great as that at 2750 Å. The latter wavelength is suitable for assessing organic content because the absorption due to nitrate is extremely low. The optical density at 2750 Å (4-cm cell) multiplied by 7 is approximately equal to the oxygen absorbed (permanganate value)" (*loc. cit.*, p. 594). No data are supplied to substantiate these statements and no statistical correlations are given.

For another four years the utilization of UV spectrophotometry in the assessment of organic materials of waters lay dormant. Then Dornbush and

Ryckman (1963), while investigating the effect of physical-chemical processes in removing organic contaminants from waters, used UV spectral analysis to ascertain the effectiveness of the removal procedures tested. They came to the conclusion that absorption by activated charcoal is the only physical-chemical method which effectively reduces odors in contaminated waters and at the same time removes substantial quantities of dissolved organic pollutants. Their samples of purified water, following the charcoal treatment, were subjected both to conventional COD determinations and to UV spectrophotometric analysis carried out at 250 nm. A relatively good correlation was found between the absorbancy values and COD. Their absorption curves between 200-290 nm showed a uniform decrease towards increasing wavelengths and they could not discern any definite peaks in the absorbances. Figure 1 illustrates this effect. The characteristics of the control samples used in evaluating the different reactants and in comparing their absorbancy values with COD are included in Table II. However, one has to point out that the authors used membrane filters before the absorption measurements in order to clarify their solutions; and this may account for the lack of discernable peaks in the absorption curve, through the removal from the samples of any proteinaceous matter which might have been present.

TABLE II. CHARACTERISTICS OF CONTROL SAMPLES FOR
EVALUATION OF REACTANTS
(After Dornbush and Ryckman, 1963)

Reactant	Determination			
	pH	Ultraviolet Absorbance at 250 nm	Chemical Oxygen Demand (mg/l)	Threshold Odor Number
Activated Carbon	8.0	0.240	51	172
Ferric Sulfate	8.0	0.258	48	178
Aluminum Sulfate	8.0	0.253	51	181
Bentonite and 100 mg/l Alum	8.2	0.255	47	178
Natural Silt	8.0	0.230	49	100*

*Threshold odor determination made after 24 hr.

An application for UV spectrophotometry in the analysis of phenolic waste waters was proposed in 1963 by Wexler. He recognized that alkaline solutions of phenolic substances in water or alcohol show differing absorption peaks of the same compounds in identical concentrations, dependent on whether they are measured in a neutral or a slightly acidified solvent. These difference spectra then could be utilized for the chemical identification of the substances, as well as for the cancelling out of interferences due to nonionizing, nonphenolic species. When the difference peaks of 288 and 236 nm were used, close adherence to von Beer's law was observed for the phenols tested in the 5-50 ppm range. One should note that the author took the ultraviolet spectra of 13 phenolic materials, some of which had already been precisely measured both by Möhler (1937) and Demmering (1938); however, no reference was made to these works.

In the same year Wexler published another important paper in collaboration with Brako (Wexler and Brako, 1963) on the determination of lignosulfonates. Since cement contains quantities of lignosulfonates used as grinding aids and, in lack of sufficiently precise analytical procedures for their quantitative determination, the authors presumed that UV spectrophotometry might serve as a means for quantitating this cement additive. Lignosulfonates, in common with many substituted phenols, exhibit a definite absorption maximum in the range of 225 to 285 nm (Brauns, 1952). Because of the presence of the phenolic hydroxyl groups, it seemed logical to extract the lignosulfonates from the cement with alkaline solutions as soluble phenolates, and then measure their concentration through their UV absorption maximum around 280 nm. Figure 2 illustrates the linearity of the extracted lignosulfonate percentages to their optical density as measured in a 0.5 cm cell at 280 nm. Apparently this successful technique of quantitating lignosulfonates in cements gave Wexler the impetus to conduct a through investigation of the direct, as well as the difference spectra of a multiplicity of lignosulfonate model substances (1964). He found that the direct spectrograms are useful for establishing the gross features of the compounds; whereas the differential spectra obtained through the comparison of alkaline and neutral or acidic solutions of the lignosulfonates are of great value in the determination of the aromatic hydroxyl content of the materials.

In Figure 3 the direct and the difference spectra of a softwood lignosulfonate are shown. Both the direct and the difference spectra (which displays a strong peak at about 250 nm, a weak peak at about 300 nm and two minima at 229 nm and 275 nm) follow von Beer's law.

Table III contains Wexler's data (1964) from tests to ascertain the validity of Beer's law for lignosulfonates. Since these compounds, or materials closely related to them, are common constituents of natural waters, the importance of Wexler's work lies in the fact that he convincingly demonstrated that absorption spectrophotometry can be used for the quantitation of highly complex organics.

Fährnich and Soukup (1964) took up the problem of characterizing organic contents of waste treatment effluents by the application of UV spectrophotometry. They collected samples from the Váh, Moldau, Elbe and Ohre Rivers and measured their extinction characteristics between 200 and 350 nm. They found that each of the rivers tested showed a distinct peak in the region

TABLE III. BEER'S LAW TESTS OF ULTRAVIOLET SPECTROGRAMS OF LIGNOSULFONATES USING 0.5-cm MATCHED CELLS (After Wexler, 1964)

Dilution, ppm	Absorptivity, $l \cdot g^{-1} \text{ cm}^{-1}$					
	Direct Spectra		Difference Spectra			
	280 nm	282 nm	$\Delta 250$ nm ^a	$\Delta 300$ nm ^b	$\Delta 300$ nm ^a	$\Delta 300$ nm ^b
20	9.00	9.90	7.50	7.50	3.40	2.53
40	9.40	9.70	7.20	7.15	3.30	2.48
100	9.40	9.77	7.26	7.08	3.48	2.58
150	9.42	10.02	6.76	6.94	3.18	2.70
200	9.88	10.72	7.55	7.09	3.49	2.80
Av. absorptivity	9.42	10.04	7.25	7.15	3.37	2.62
Std. dev.	0.31	0.41	0.31	0.21	0.13	0.12

a Peak height measured from solvent zero line.
b Peak height measured from base lines.

Data at 280 and 282 nm are peak maxima of 0.1N acid and 0.1N alkali solutions of same lignosulfonate. All other data are at maxima or minima in difference spectrogram.

of 280 nm, which they considered typical for the presence of humic acids, although they could not rule out the possibility that two different compounds produced this peak. Several inorganic materials, such as nitrates, heavy metal hydroxides, carbonates, and bicarbonates, although absorbing in the ultraviolet, did not seem to influence the appearance of the 280 nm peak. The minimum observed at 260 nm was ascribed to the presence of sulfite-extract solutions of lignins. A comparison between the UV spectra of the river waters and the potassium permanganate COD values showed a good correlation, as seen in Figures 4a and b. This permitted the calculation of the quantity of organic matter from the measurement of the extinction coefficient at 280 nm divided by 0.013.

Beginning in 1964 several Japanese workers interested themselves in the possible application of UV spectrophotometry for the examination of dissolved organic substances both in fresh and in sea water. In their first paper on the subject Hanya and Ogura (1964) collected samples from the highly polluted Tokyo Bay, but also from some fresh water sources, and used the wavelength range from 200-300 nm for their measurements. They eliminated the influence of suspended matter either by centrifugation or filtration. In the first

series they measured absorption at 220 and 250 nm, and by dividing the two values $\left(\frac{250}{220}\right)$, they constructed histograms which reflected the polluttional characteristics of the different waters. As a control they used regular COD determinations to establish the values of the organic load present. In their next series, measurements were made also at 230 nm and again the absorbancies were divided by those obtained at 220. When the $\frac{250}{220}$ values were plotted against those of $\frac{230}{220}$ a straight line was obtained, with the following equation:

$$E_{230}/E_{220} = \alpha (E_{250}/E_{220}) + \beta$$

The conclusion was reached that alpha is a universal constant with the value of 1.2 while beta is characteristic for different types of waters. Its values could be calculated from the histograms. One surprising fact was that the complete UV scans of the waters showed no marked peaks or minima (see Figure 5). In the same study the authors were able to establish a mathematical relationship between the absorption values at 220 and COD, which was found to be:

$$\text{COD} = \alpha (E_{220}) 1.47$$

where the value of α varied between 11 and 36, dependent on the source of the water.

In further studies Ogura (1965a) elaborated on the values of his procedure, coming to the following conclusions: The absorption of natural waters did not always obey von Beer's law, especially when the waters were highly polluted. Absorbancy increased with the degree of pollution but also with the passage of time while the sample was kept in storage. In his second paper of the year (1965b) he presented additional results on the relationship between absorbance at 220 nm and COD. Since the relations were found to be linear he suggested that the absorption was due mostly to organic matter. When he investigated the influence of pH and nitrates on absorption values he found that an increase in pH will result in an increase of absorption and also that instead of using the 220 nm wavelength it might be more useful to conduct the measurements at 250 nm, because nitrate ions strongly absorb around 220 nm. Obviously, on the basis of this latter finding, considerable doubt is thrown on the validity of the earlier reasoning that the linear relationship between absorption at 220 nm and COD is caused by organic matter.

Ishiwatari, et al. (1965) carried out investigations on the qualitative and quantitative distribution of amino acids occurring in natural waters and in the air. They collected samples of snow, rain, lake, river, and underground waters, including the sea and also the air. Glycine, alanine, aspartic acid, and glutamic acid were detected in all samples; while valine, leucine and serine were also frequently found. The concentration of total amino nitrogen in natural waters was somewhat less than 1/4th of the total organic nitrogen as detected by the Kjeldahl method. It is interesting that neither phenylalanine nor tyrosine, two important amino acids, were found. Both of these are essential protein components having a high absorption peak in the UV region.

The first work in the United States utilizing UV spectrophotometry for pollution monitoring dates from 1966. A paper by Jones and Heinke was

presented at the 9th Conference on Great Lakes Research, in March of 1966, at Chicago. The authors gave an account of experiments for which they adapted a Beckman UV Spectrophotometer for continuous recording of absorbancies of surface waters during several cruises on Lakes Ontario and Erie. Significantly higher levels of absorbancy were obtained in polluted than in relatively clean waters, and they suggested that the method could be used for the rapid detection of polluttional zones in the Lakes. Unfortunately, they do not seem to have published their results, and no further studies are known which deal with the possibility of relating absorbancy levels to types and concentrations of known pollutants in these waters.

A relatively simple, continuous UV monitor was constructed in 1966 by Bramer and his co-workers. Details of the instrument will be given later. Here it should only be mentioned that the authors successfully tested the device on the effluent of a chemical plant containing phenol, pyridine and benzene.

Ishiwatari and his collaborators (1966) extended their studies on the composition and optical characterization of humic substances extracted from lake sediments. They found by infrared spectroscopy that these compounds show no signs of aromatic character but may contain peptide and polysaccharide structures. This seems to be somewhat in contradiction with the accepted derivation of humic substances from lignins or lignosulfonates. If humates contain peptide bonds, such should also occur in the lignins. On the other hand, the phenols which supply the aromatic character to the lignins should also be present in the humates, unless we are dealing with two completely different compounds. Should this latter be the case, then the derivation of the "yellow pigment" from humates, and its subsequent identification with lignin substances, is in itself contradictory.

Investigating the absorption of UV radiation by sea water, Ogura and Hanya (1966) presented some evidence that the organic matter "... which is usually in the form of fulvic acid or related substances in sea water shows the following relation, E_{220} (absorbance)/organic carbon (mg/l) = 0.02." (p. 758.) Below 230 nm only nitrate and bromine show strong absorptions. Thus, the measured absorptions at 220 nm are the composite of organic matter, nitrate and bromine. These relationships are illustrated in Figure 6 for surface and deep water.

The theoretical aspects of the fate of organic matter in sea water, when subjected to UV irradiation, were investigated by Armstrong, et al. (1966). They came to the conclusion that most of the organic matter was completely oxidized within one hour exposure, as indicated by a decrease of absorptivity between 200-250 nm. More prolonged irradiation of the water caused the quantitative oxidation to nitrate of most of the organic nitrogen compounds, followed by a reduction to nitrite. Urea represented an exception, since only about 50% was oxidized even in the presence of H_2O_2 . UV irradiation-induced destruction of organic matter in sea water could probably account for the higher nitrate contents of the deep waters (see Figure 6), as shown by Ogura and Hanya (1966), and this phenomenon should also be taken into account when measuring the absorptivity of waters exposed to UV irradiation.

The need for automated measurements of the organic carbon contents of waters was clearly recognized by 1966. Although automated carbonaceous analyzers were available from different commercial sources, the facts that they processed batch samples and that their prices were very high excluded them from wide-spread applications, where inexpensive continuous monitors were required. Briggs and Melbourne (1966), in their study on the advances of water quality monitoring, describe their efforts to correlate UV absorption spectra obtained on six different rivers and three different sewage plant effluents with values yielded by a Beckman carbonaceous analyzer. Following Hoather and Rackham (1959), they selected the wavelength 275 nm and found that the absorption values, both in the rivers and in the sewage plant effluents, corresponded closely to the organic carbon contents as measured by the carbonaceous analyzer. Figure 7 shows these results. Encouraged by these findings, the authors set out to design a battery-operated instrument suitable for water quality monitoring in field applications.

At a symposium held in Holland in connection with international biological problems, Lee (1966) gave a review about the then currently available automatic methods for the analysis of natural waters. Although ultraviolet spectrophotometry was mentioned, apparently the author did not think it to be too useful, since only passing comments were made regarding this technique in his evaluation. On the other hand Ogura and Hanya (1967) continued their investigations on the chemical identification of the organic matter giving rise to UV absorptivity in sea water. They used the same techniques for the measurements which they had developed earlier (Hanya and Ogura, 1964; and Ogura, 1965a,b). The authors recovered the organic matter from sea water by dialysis and measured its absorbance at 220 nm and its organic carbon contents in mg/l. When they compared the relationship (absorbance/organic carbon = 0.02) with that obtained for lake water humus of planktonic origin (Ishiwatari, *et al.*, 1966), they found that the ratio was the same and concluded that most of the organic matter in sea water had similar optical properties to those of lake water humus. Determinations of nitrate nitrogen showed that approximately 60% of the absorbance of deep water at 220 nm can be attributed to nitrate ions, while the rest of the absorbance, which is not the result of organic matter or nitrate, is due to bromide.

In the following year Ogura and Hanya (1968) expanded their results to an investigation of the usefulness of measuring UV absorbance as an index of sea water pollution. Unfortunately, they filtered all of their samples through a Millipore HA® type filter (0.45 μ m) before taking the absorption spectra. The curves obtained were correlated with transparency readings taken by a Secchi disc, while COD variations were followed with the potassium permanganate method using Zimmermann-Reinhart solution at 100°C for 30 minutes. They found that the absorbance at 220 nm of the oceanic surface water in the North Pacific is nearly constant (mean 0.11) and that its value at 250 nm is virtually zero. On the other hand, the absorbance of coastal waters at these wavelengths is considerably higher than that of the open seas. When they investigated the effect of dilution of the sea water through inland drainage, which contained great amounts of ultraviolet absorbing material, they found that this alone could explain the discrepancy between measurements obtained earlier on open oceanic, as distinct from coastal waters. They concluded that in highly polluted coastal waters the absorption

at 250 nm may be almost entirely due to allochthonous organic matter derived from land or ships, because in this spectral region neither the autochthonous organics, nor bromide and nitrate, have any interfering absorption. A correlation with the transparency studies confirmed the known fact that absorption increases with a decrease of transparency. They stated: "The ultraviolet absorbance of surface sea water was proved to be a useful index of the degree of pollution, mainly that due to organic substances derived from inland drainage or ship waste" (p. 467). In 1969 Ogura summarized the results of his studies about the applicability of UV absorption measurements for the characterization of both natural fresh and sea water and also about the usefulness of this technique for pollution monitoring purposes. He showed that by employing different absorbancy ratios one can differentiate between the fulvic acid type materials in lake waters and the lignin type substances in rivers.

Saltzman (1968) developed a method for the continuous monitoring of aromatic compounds in industrial plant effluents. He found that because of the high absorptivity of natural waters, such as the Delaware River on which he concentrated his studies, the general background absorption is too high for the detection of individual aromatic compounds. He therefore proposed the application of differential photometry for the identification of such substances. Two possibilities are discussed by the author. One is to take a first sample above and a second below the effluent discharge. The upper sample may be used as the reference and its reading compared with the effluent sample. The other possibility is to make use of the peak height shift of phenolic compounds when they are either acidified or alkalinized. A dual beam spectrophotometer is described, in which a highly acidified sample is placed into one of the chambers and an alkalinized sample into the other one. The differential spectra is then used for the quantitative determination of the aromatic compound. Saltzman's curve demonstrating the background absorbancy of the Delaware River (Figure 8) shows a non-specific attenuation without any minima or maxima. This seems to be in contradiction with the spectra obtained by Fähnrich and Soukup (1964) and also to several of the curves of the Japanese workers (see earlier). To obtain his differential spectra, Saltzman used the 254 nm line of a low pressure mercury discharge lamp, with the following justification: "Analytically, the 254 nm measuring wavelength would appear to be a reasonable choice for monitoring total aromatic hydrocarbon (monocyclic) concentrations in water. These compounds have strong and reasonably similar specific absorptions at 254 nm. For example, benzene, toluene and mixed xylenes (technical grade) in water have specific absorptions within 10% of their average" (p. 84).

The most complete report on the utilization of UV spectrophotometry for defining the pollutional load of natural waters was presented by Mrkva (1969). He characterized rivers according to the degree and types of pollution present, establishing three categories. Group 1 contains very pure reaches of rivers which have low concentrations of humic substances. Figure 9 shows the absorption curve of such a river. It has a peak around 220 nm and a rapid decline without any maxima or minima. Group 2 includes rivers which contain some ligninsulfonates. Figure 10 is the curve for such a river. A distinguishing characteristic of these rivers is the appearance of a typical niveau or minimum at 260 nm and a maximum at 280 nm. Finally in Group 3 those rivers are classified which carry additional waste products such as phenols originating from industrial activities. Figure 11 illustrates

the absorption spectrum of such a river. Since organic pollution derived from both lignins and other waste products shows a typical peak in the 280 nm range, the author concludes that measurements of absorbancy should always be carried out at the 280 nm wavelength. Mrkva, by conducting COD determinations simultaneous with his absorption measurements, could calculate a conversion factor for absorbance to milligram concentrations of humic substances and another one for converting absorbance to 'N', the value of oxidizability (COD):

$$N = A \times k, \text{ where } k \text{ is } 13.1 \text{ to } 24.3$$

Figure 12 depicts his results on the close correlation between absorbance and COD for a Group I type river; and Figure 13 shows the same relationship for a Group III river. He carried out specific determinations of the humic substances using a "sensitive photometric method ... The principle of this method is based on the extraction of the acidified sample with isoamylalcohol and on the reversion into an alkaline solution which is evaluated photometrically" (p. 1929).

Mrkva's results on the relationship between absorbancies, humic substance contents, and COD for Group I river are compiled in Table IV. These investigations confirmed his theoretically derived values for the conversion coefficients, thus proving the feasibility of using absorbance values instead of COD measurements.

TABLE IV. RELATIONSHIP BETWEEN ABSORBANCE, HUMIC SUBSTANCE CONTENT, AND OXIDIZABILITY IN THE HEADWATER REGION

$A_{280 \text{ nm}}$ (d = 30 mm)	Humic Sub. (mg/l)	mg O ₂ /l (Kubel)	k_1	k_2
0.108	1.7	1.8	15.741	16.667
0.070	1.0	1.0	14.286	14.286
0.086	1.7	1.1	19.767	12.790
0.092	1.2	1.3	13.043	14.130
0.232	4.1	3.3	17.672	14.224
0.046	1.0	0.6	21.739	13.043
0.076	1.7	1.0	22.368	13.158
0.246	3.7	3.3	15.040	13.414
0.063	1.4	1.0	22.222	15.873
0.074	1.0	1.0	13.513	13.513
0.075	1.4	1.1	18.667	14.666
0.104	2.0	1.4	19.230	13.461
Average values			17.774	14.102

Since Mrkva centrifuged his samples at 3000 rpm to remove particulates, membrane filter-induced absorption of proteinaceous matter from the water did not invalidate his results. On the other hand, isoamylalcohol extractions of his acidified samples would obviously also remove all of the proteinaceous matter, together with the humates. Therefore one wonders whether the absorbance values measured at 280 nm were indeed wholly due to the humic substances or were partially caused by the presence of some proteinaceous moieties. In this respect one should remember the infrared studies of Ishiwatari, et al. (1966) on the humate composition of lake sediments showing the presence of peptide bonds. Were the Japanese authors also dealing with some proteins?

Khailov and Burlakova (1970) used UV spectrophotometry for the measurement of the release of dissolved organic matter by seaweeds. They selected 260 nm as the wavelength of choice, claiming that in this range a direct relationship exists between UV absorption and DOM. They presented the following equation to describe this relationship:

$$C = 100 \times E_{260} (5 \text{ cm})$$

where C is the concentration of DOM in mg/l and E is the corresponding extinction in a 5 cm cuvette, as measured against artificial sea water. They concluded that the input of dissolved organic matter by plant excretion to the surrounding sea water is about 70% of the total gross production, which is 20% higher than the earlier estimate of Fogg, et al. (1965).

F. Determination of Nitrates by UV Spectrophotometry

We have several times referred to the high nitrate interference observed in the lower range of the UV spectrum. Because of the sharp absorbance of nitrates near the 220 nm region, Hoather and Rackham (1959) proposed the utilization of UV spectrophotometry for the quantitative determination of nitrates. Especially in view of the fact that the Standard Method's procedure for the quantitation of nitrates is highly questionable, a simple and precise test for this ion seems to be needed.

Nitrate nitrogen concentrations in natural waters as low as 10-30 ppm may cause serious disease conditions in infants. As early as 1945 infant methemoglobinemia was ascribed to high concentrations of nitrates in well waters in Minnesota. In the 1947-48 epidemics, 139 cases were reported in Minnesota alone, out of which 14 were fatal. This epidemic was definitely shown to be caused by the high nitrate contents of the water, and Waring (1949) came to the conclusion that drinking waters containing 10-20 ppm or more nitrate nitrogen may give rise to methemoglobinemia in infants. Goldman and Jacobs (1961) proposed a method for spectrophotometric analysis of nitrates. They showed that interference is presented by dissolved organic matter, nitrite, hexavalent chromium and carbonates. Chloride, however, does not interfere. They used the 220 absorption wavelength for the measurement of sea water and found that it has 72.5% transmittance, the equivalent of 2.5 ppm nitrate. Their absorption measurements correlated well with total Kjeldahl nitrogen determinations, and Goldman and Jacobs came to the conclusion that none of the common ions found in drinking water or industrial waste waters would interfere with the sensitivity of the method, since sea water contains much higher quantities of ions in solution. The organic

interference was determined by first measuring absorption at 275 nm, where nitrate does not absorb. They found that organic matter absorbs about 2.5 times more at 220 nm than at 275 nm; therefore, the absorbancy value obtained at 275 nm has to be multiplied by 2.5 and subtracted from the gross nitrate value read at 220 nm. This method has been criticized by Armstrong (1963). He pointed out that in some natural waters or in sea water there is an unduly steep increase in absorption at wavelengths shorter than 235 nm, producing a higher nitrate value than is actually present. He therefore proposed the pretreatment of the sample with concentrated sulfuric acid, which will shift the nitrate absorption spectrum in the presence of chloride ions to exhibit a maximum at around 230 nm. This wavelength can then serve for the determination of nitrates.

Because of interferences presented by synthetic detergents, chromium ions, organic matter, etc., in the Goldman and Jacobs (1961) procedure, Navone (1964) proposed a new method for the UV measurement of nitrate. He used a double-beam spectrophotometer in which the blank was a duplicate sample containing no nitrate ion, having been reduced to ammonia by a zinc-copper coupler. Since the blank contained all the other interfering substances in quantities equal to those in the sample, their effects cancelled each other out and the nitrates could be directly determined at 210 nm. The author used a Beckman model DU spectrophotometer, the sensitivity of which is low, below 220 nm. His absorption curve for nitrates is therefore somewhat questionable. The very broad peak which he obtained between 205 and 215 nm might have been the result of this lowered sensitivity of the instrument. On the other hand, the low absorbancy (0.2) at 220 nm is in complete contradiction to the findings of Japanese investigators, who showed much higher absorptions at 220 nm than at 210 nm.

G. Measurements of Tyrosine Equivalents in Natural Waters

In all of the above-discussed papers UV spectrophotometry was utilized to characterize certain inorganic and organic compounds occurring in natural waters, including the sea. The earlier spectra were composites of the different solutes, and only from 1960 on has there been any effort made to define the individual components which might contribute to the absorbtivity of these waters. We have seen that among the inorganic constituents, only the absorptions of nitrates and bromine have been investigated, whereas the organic materials studied fall into the categories of humates (more specifically fulvic acids), lignins and lignosulfonates, phenols, and the broad category of aromatic compounds, including even benzene. No reference is made in the whole body of published literature to the possibility of utilizing UV spectrophotometry for the detection of certain amino acids, polypeptides, or proteinaceous matter. Such materials must be components of natural waters, since proteins make up about 40-60% of all living matter. The fact that peptide bondings appear in humates would suggest that proteins do not decompose and undergo such rapid utilization as is generally supposed.

The only paper in the literature (Ishiwatari, et al., 1965) which dealt with the general abundance of amino acids in natural waters and in the air failed to detect phenylalanine and tyrosine compounds, which have sharp UV absorption peaks at 260 nm and 280 nm, respectively. This is surprising in view of the fact that analyses of ancient sediments and even of some meteorites (Ponamperuma, 1970) have shown the presence of minor quantities of

these amino acids. Based upon these considerations, it seemed potentially fruitful to investigate natural waters for the presence of proteinaceous substances with UV spectrophotometric techniques, using the 280 nm peak of tyrosine, and to correlate the results with earlier findings in the same environment on both dissolved organic carbon and quantities of humic and lignin type substances. Since several of the measurements in the literature were carried out in the 260-280 nm wavelength range, one cannot escape the conclusion that many of the absorbancies reported may represent composite values due to the presence of proteinaceous matter as well as humic substances. Conversely, until the end of the 1960's, sample preparation for spectrophotometric analysis routinely involved membrane filtration techniques, most commonly using cellulose nitrate filters. Since these membranes absorb proteins almost quantitatively, as has been pointed out earlier, some of the lower values calculated from absorbancy measurements, in comparison to chemical COD determinations, might have been caused by the removal of a considerable fraction of the organic constituents (proteinaceous matter) from the samples.

The essential amino acid tyrosine comprises approximately 3.2% of proteins. Its percentage naturally varies from one type to another, being less than 2% in albumin and over 17% in certain globulins. Nevertheless, the 3 to 3.5% value can be accepted as an average. Since proteins are continually liberated into natural waters both through decomposition and through excretion/secretion, and, in addition, their breakdown products, polypeptides and their component amino acids, occur naturally in these environments, it is surprising to learn that no investigation has yet been carried out to identify the presence of these moieties. In a quasi anticipatory manner, Wallace and Wilson (1969) conducted foam separation analysis to concentrate organic matter from sea water. "We have chosen protein for our present studies, since it has not, to our knowledge, been reported unequivocally as a natural constituent of sea water. One would expect to find soluble protein in at least trace amounts, however, and its isolation and characterization would be of major significance in marine microbial ecology. This report deals with the quantitative recovery of protein added to an artificial sea water system..." (p. 2). On the basis of the earlier consideration that tyrosine represents an average of 3% of proteinaceous matter and that proteins make up about 40-60% of the dry weight of organisms, one may presume that a correlation exists between the amounts of tyrosine measurable in water and the dissolved organic content, or even the total organic carbon present. Several investigators were therefore encouraged by us to initiate studies to confirm or negate this possibility (Truglio, 1968; Whalen, et al., 1970; Hermel, 1971).

Truglio (1968) correlated absorption measurements carried out at 280 nm with primary production, E. coli counts, and other ecological parameters, on samples obtained from eight stations from Great South Bay, New York, for a period of one year. Altogether, 120 samples were collected. Her results showed that conditions which were favorable for the increase of primary productivity also generally encouraged the growth of coliform bacteria. Although the trend was one in which the coliform count trailed the productivity rate, the time of year when both productivity and coliform organisms reached their highest peaks was when the temperature of the water also increased.

An analysis of the data obtained on the temporal distribution of dissolved organics as measured by their UV absorption, seemed to indicate that a rise in productivity is in most cases preceded by an increase in the amounts of organic matter. Peaks of organic matter occurred prior to the attainment of maximal productivity for most stations. This could indicate that once the dissolved organic matter is available, and other factors such as temperature are favorable, productivity begins to increase and removes some of the organics from the water, causing a drop in subsequent readings of the dissolved organic matter.

Whalen, et al. (1970) correlated absorption measurements at 280 nm with chemically determined COD values and Candida albicans counts in Long Island Sound. Two hundred samples each of one gallon originating from 14 stations were collected on the North Shore of Long Island from Glen Cove to Northport Harbor on the East. The authors withdrew 100 ml of each sample for the determination of COD. Another 10 ml of each sample was filtered through a porcelain candle and used for UV absorption readings. The particulate material on the filters was further analyzed by wet oxidation for its PCOD values.

The rest of the samples were centrifuged and a known portion of the residue was used for the culturing of C. albicans. Later on, the samples were filtered through an 8 μ m pore size Millipore® filter, and the residue collected on the filter pad was washed into 20 ml of sterile saline. 0.1 ml of this concentrate was used to inoculate mycosel plates. The plates were incubated at 27°C for 3 weeks and the typical fungal colonies were counted. Final identification of Candida colonies was carried out by a slide agglutination technique using Difco Candida albicans antiserum.

The findings of the authors are shown in Table V. Although 200 samples were analyzed, in this table only two representative values are included from each station tested.

As is evident from this table, the values of DCOD calculated from absorptivities are considerably lower than the COD results. The chemical tests for PCOD showed quantities of particulate organic matter at almost every station, which was due probably to the presence of massive algal blooms at the time of sampling. The DCOD and PCOD values together resulted in TCOD's which were much closer to the COD as determined by wet oxidation, but a discrepancy of about 10% was still found between these values. The appearance of these 10% deviations in the two sets of measurements might be ascribed to the presence of chlorine interference. The numbers of Candida cells per liter showed a relatively good correlation with the COD values.

From the data presented, it becomes obvious that large numbers of fungi are directly associated with high quantities of organic matter. The authors reported that the actual use of those areas where the highest fungal cell numbers occurred were marinas, port facilities, and sewage outfalls; the bathing beaches exhibiting both the largest number of fungi and the highest levels of absorptivity or COD. Places extensively used for recreational purposes showed the highest fungal numbers per liter of water, together with a substantial increase in the organic load. Whereas the relationship between organic load and fungi per liter, in general, is a direct proportionality, this picture is modified in bathing areas, at least during the period of

TABLE V. CORRELATION OF COD MG/L WITH
C. ALBICANS NUMBERS/L
 (After Whalen, et al., 1970)

Station	Sample No.	COD _{Ch.}	E ₂₈₀	DCOD _{Abs.}	PCOD _{Ch.}	TCOD	Candida No.
1	1	48.4	0.968	38.72	5.42	43.14	5,200
	2	39.2	0.784	31.36	4.39	34.75	4,300
2	16	74.0	1.480	59.20	8.29	67.49	8,600
	17	96.0	1.920*	76.80	10.75	87.55	10,400
3	32	7.3	0.146	5.04	0.71	5.75	520
	33	7.5	0.150	6.00	0.84	6.84	500
4	50	23.3	0.466	18.64	2.09	20.73	2,500
	51	25.0	0.500	20.00	2.80	22.80	2,800
5	80	36.6	0.734	29.36	4.11	33.47	8,200!
	81	37.0	0.740	29.60	4.14	33.74	9,500!
6	92	70.4	1.408	56.32	7.88	64.20	6,800
	93	72.0	1.440	57.60	8.06	65.66	6,400
7	101	106.0	2.012*	80.48	11.27	91.75	12,000
	102	102.0	2.004*	80.16	11.23	91.39	14,600
8	112	34.0	0.680	27.20	3.81	31.01	3,600
	113	35.0	0.700	28.00	3.92	31.92	3,200
9	132	7.8	0.156	6.24	0.87	7.11	730
	133	8.2	0.164	6.56	0.89	7.45	700
10	140	190.0	3.800*	152.00	21.28	173.28	14,200
	141	194.0	3.880*	155.20	21.73	176.93	14,000
11	151	206.0	4.120*	164.80	23.07	187.87	14,900
	152	210.0	4.200*	168.00	23.52	191.52	15,400
12	158	187.0	3.740*	149.68	20.94	170.62	16,500
	159	189.0	3.780*	151.20	21.17	172.37	16,000
13	175	250.0	5.000*	200.00	28.00	228.00	23,000
	176	254.0	5.080*	203.20	28.45	231.65	24,600
14	199	210.0	4.200*	168.00	23.52	191.52	19,300
	200	212.0	4.240*	169.60	23.79	193.39	20,200

* Samples diluted for absorption measurements

! Discrepancy between COD and Candida numbers

summer when they are heavily frequented. They presented a rough estimate between COD values in mg O₂/l and numbers of fungi present in estuaries. The COD multiplied by 100 gives the number of fungi per liter of water or conversely, if the primary determination relies upon the quantitation of the

fungus cells, then their numbers divided by 100 gives the COD reading in mg O₂/l.

The most extensive investigations on the usefulness of UV absorbtivity measurements for water pollution studies were conducted by Hermel (1971). He carried out correlation studies of tyrosine absorptions with DCOD and COD on both fresh and sea water samples, the latter being either electrolytically desalted or in native state. He also deployed absorption measurements for the determination of bacterial utilization of dissolved organic matter in water. The author first prepared a dilution series of L-tyrosine from 0.1 mg/l to 0.04 mg/l and constructed a calibration curve, measuring the 280 nm peaks in a Beckman DK spectrophotometer at 1 cm path. His calibration curve is included as Figure 14.

Samples of 100 ml of natural fresh water were collected from a) a tap, b) Central Park Reservoir, c) four small rivers in the Catskill area, d) from a home aquarium. All of the samples were filtered through either a Gelman Type A glass filter with 0.5 μm pore size or a stainless steel filter (Feltmetal FM 204) in order to avoid the selective absorption of proteinaceous matter which occurs on cellulose membrane filters. The absorbancy values of the filtered samples were read in the spectrophotometer and were reported as tyrosine equivalents (Tye). DCOD determinations on the filtered samples were carried out according to the precise of the Standard Methods (12th ed., 1965) using the dichromate reflux system. Aliquots of the samples, before filtration, were also tested by the Standard Methods's COD procedure, in order to determine the contribution of the particulate organics to the DCOD values obtained earlier. The results of these determinations are shown in Table VI.

TABLE VI. CORRELATIONS AMONG ABSORPTION, DCOD AND COD ON FRESH WATER SAMPLES (After Hermel, 1971)

Sample	E ₂₈₀	Tye mg/l	DCOD _{Abs.} mg O ₂ /l	DCOD _{Chem.} mg O ₂ /l	COD mg O ₂ /l	PCOD _{Calc.} mg O ₂ /l
Tap	.025	.0037	1.00	0.91	1.02	0.11
Reservoir	.060	.0088	2.40	2.15	2.43	0.28
River No. 1	.024	.0035	0.96	0.88	0.96	0.08
River No. 2	.051	.0074	2.04	1.73	2.00	0.27
River No. 3	.030	.0043	1.20	1.07	1.22	0.15
River No. 4	.029	.0042	1.16	1.02	1.15	0.13
Aquarium	.172	.0251	6.88	6.22	6.82	0.60

The following considerations were employed in the calculation of some of the data. The absorbancies obtained on the sample were multiplied by the value of tangent alpha, read from the calibration curve. This value k equals 0.146. The resultant figures are the tyrosine equivalents (Tye) mg/l. Since tyrosine represents 3% of proteins, its equivalent values multiplied by $t = 33.0$ will yield the absorptions in terms of proteinaceous equivalents (Pe) mg/l. In order to calculate the values of DCOD from the absorption measurements the following reasoning was used. Proteins contain 50% of carbon per weight. This 50% of carbon corresponds to 30% of the dissolved organic carbon in water, the rest of which is made up of approximately 27% carbohydrate carbon and 43% carbon in other miscellaneous organic materials. If the protein carbon, which represents the 50% of the proteinaceous matter by weight, corresponds to 30% of the dissolved organic carbon, then by multiplying with $d = 1.65$ the value of the proteinaceous equivalent per liter, we will obtain the DOC in mg C/l. Since at an average the COD values are five times that of the DOC, ($c = 5$), i.e., for each carbon atom present 5 oxygen atoms are required to fully oxidize the compound, then a multiplication of the DOC readings by five will give COD in mg O₂/l. If one carries out these proportional multiplications the following equations can be written:

$$\text{COD} = c \times d \times t \times k \times e, \text{ or } 5 \times 1.65 \times 33.0 \times 0.146 \times E, \text{ or } 39.8 \times E, \text{ or } 40 \times E$$

$$\text{DOC} = d \times t \times k \times e, \text{ or } 1.65 \times 33.0 \times 0.146 \times E, \text{ or } 7.96 \times E, \text{ or } 8 \times E$$

$$\text{Pe} = t \times k \times e, \text{ or } 33.0 \times 0.146 \times e, \text{ or } 4.82 \times E$$

$$\text{Tye} = k \times E, \text{ or } 0.146 \times E$$

Both in the present experiments and in several other publications it has been shown that at an average POC represents 1/7.7 of DOC, that is $p = 0.14$, thus the values of DOC multiplied by p will give POC in mg C/l. If we want to express POC in terms of absorption values the following equation can be written:

$$\text{POC} = p \times d \times t \times k \times E, \text{ or } 0.14 \times 1.65 \times 33.0 \times 0.146 \times E, \text{ or } 1.11 \times E$$

Finally DOC and POC in sum would result in TOC. Thus, TOC = DOC plus POC in mg C/l.

The absorption values when expressed in terms of tyrosine equivalent (i.e., readings obtained from the standard curve) showed an excellent correlation with the DCOD's of the filtered and the COD's of the untreated samples. A conversion factor of 4.86 times absorption measured at 280 nm seemed to give the milligram protein per liter. By presuming a 40% dry weight as the proteinaceous matter of any organism, a multiplication of the absorptivity reading by 40 should result in the COD values. Unfortunately, no direct correlation exists between COD and PCOD, but according to the data of Fredericks and Sackett (1970) and also from analysis of the results of the present investigation, the particulate organic contents would appear to be

1/5 to 1/8 of the DOC measurements. Therefore, by adding 1/5 to the determined DOC values one may obtain the TOC of any of the waters tested.

From Table VI it can be seen that the calculated DCOD values are actually closer to the values of COD measurements resulting from the wet oxidation technique than to the DCOD values obtained by wet oxidation. The PCOD values as calculated together with the DCOD's (chemically determined) result in TCOD's which are almost identical to the COD's as measured by the chemical technique. This would indicate that the DCOD values, obtained through calculations based upon the absorption data, are basically expressions of TCOD's, or in this particular case COD's (apparently the refractory materials do not play a substantial role in these samples). The author concluded that DCOD, as calculated from absorption measurements, is a good expression of the general COD level of the waters.

When investigating sea water samples, Hermel collected twenty-five, 100 ml samples at Oyster Bay, Long Island, including a variety of habitats. The salinity of the water in this region varies considerably because of the entrance of a small fresh water creek and also because of the presence of some sewage discharge effluents. The range was established between 17 to 28 ppt. Immediately after their collection approximately 50 ml of each sample was filtered for spectrophotometric analysis while the rest was refrigerated for COD measurements. The filtered sea water was divided into two aliquots. One of them served to measure the absorption at 280 nm whereas the other one was electrolytically desalted with a Research Specialities Co. mercury cathode desalting apparatus. After zero conductivity was obtained in the desalting process the absorptions of these samples were also established. This procedure served to define the influence of ionic specimens in the sea water on the absorption readings at 280 nm.

The glass filter pads were thrown into the oxidizing fluid and were treated in all respects similar to the filtered samples in order to establish the PCOD values. Prior to the determinations the filters were washed with a dilute hydrochloric acid to remove carbonates.

The results of these experiments are shown in Table VII. It contains the absorption values obtained on the native and desalted sea water, DCOD as calculated from the absorption readings, both PCOD and COD determined chemically, and lastly the concurrently measured salinity reading and information about the general area of the individual sample location. If one adds the values obtained for DCOD and PCOD, theoretically one should obtain the amount of TCOD in mg O₂/l. If the quantities of refractory organics is low, TCOD should be approximately the same as COD. However, in the case of these samples the sums of DCOD plus PCOD are consistently 8-10% less than the value of COD. This phenomenon must be ascribed to chlorine or other inorganic materials in the samples, interfering with the chemical determinations, since both the native and desalted absorptivities of the sea water were found to be very close, eliminating the possibility that these inorganics interfered with the absorption readings. Since the chemical COD values were found to be 8-10% higher than those based on absorptiometry, and the author reported difficulties in carrying out the wet oxidation because of chloride interference, it seems that one may have greater confidence in the validity of the values obtained by calculations based on absorptivity than in the standard COD determinations. The inadequacies of the dichromate technique

TABLE VII. CORRELATIONS AMONG ABSORPTION, DCOD, AND COD
ON SEA WATER SAMPLES
(After Hermel, 1971)

Sample No.	E ₂₈₀ (native)	E ₂₈₀ (desalt)	DCOD _{Abs} mg O ₂ /l	PCOD _{Chem} mg O ₂ /l	COD mg O ₂ /l	Salinity ppt	Remark
1	0.750	0.736	30.00	3.77	37.6	21	Poll. inflow
2	0.742	0.728	29.68	3.31	37.0	23	Poll. inflow
3	0.748	0.746	29.92	3.50	37.5	27	Mud
4	0.746	0.746	29.84	3.12	37.2	28	Mud
5	0.739	0.735	29.56	3.00	37.0	25	Mud
6	0.740	0.725	29.60	3.81	37.0	22	Poll. inflow
7	0.734	0.729	29.36	3.62	36.8	24	Poll. inflow
8	0.753	0.748	30.12	3.73	37.5	26	Mud
9	0.736	0.732	29.44	3.45	37.0	20	Mud
10	0.664	0.662	26.56	3.10	33.1	17	Fresh water
11	0.745	0.741	29.80	3.40	37.1	21	Mud
12	0.753	0.752	30.12	3.15	37.5	26	Mud
13	0.728	0.717	29.12	3.81	36.5	27	Mud
14	0.700	0.688	28.00	3.62	35.2	28	Mud
15	0.730	0.727	29.20	3.22	36.8	28	Mud
16	0.740	0.736	29.60	3.53	37.2	28	Mud
17	0.678	0.677	27.12	3.06	34.2	25	Sand
18	0.659	0.659	26.36	3.18	33.2	23	Sand
19	0.661	0.660	26.44	3.41	33.0	19	Sand
20	0.627	0.627	25.08	3.32	31.0	17	Fresh water
21	0.637	0.635	25.48	3.15	32.1	18	Sand
22	0.653	0.653	26.12	3.07	33.0	19	Sand
23	0.715	0.710	28.60	3.21	36.1	21	Mud
24	0.751	0.745	30.04	3.72	37.5	25	Mud
25	0.710	0.702	28.40	3.56	35.0	27	Mud

for measuring oxidizable organics in sea water have been often pointed out. On this account Menzel and Vaccaro (1964) developed their technique for converting the organics into CO₂ and measuring its infrared absorption. The much simpler method of measuring the absorbancies at 280 nm resulted, in Hermel's (1971) series, in values which corresponded well to the data reported in the literature earlier (Armstrong and Boalch, 1961; Hanya and Ogura, 1964, etc.).

Although the composition of aquatic micro- or macro-organisms has not been fully investigated, Bordovskiy (1965) quotes certain figures which seem to substantiate the author's theoretical consideration about the possibility of utilizing tyrosine absorptivities for determining amounts of organic materials in water. He states that the organic matter of diatoms contains approximately 30% of carbohydrates while their protein content varies between 30 and 47%; copepods have 59% of dry weight proteins and oysters 46.8%; some bacteria may contain as high as 80% of protein.

In his last experimental series, Hermel determined the utilization of dissolved organic matter through bacterial inoculation of native sea water. The rationale for performing these experiments was the consideration that if the organic matter in water is chiefly composed of fulvic acids and lignins, both of which are highly resistant to microbial degradation, then the inoculation and incubation of the samples with marine bacteria should not result in any appreciable change of their organic content. On the other hand, if the organic matter is mainly composed of proteins, carbohydrates, lipids, and other organic compounds which are readily accessible for microbial decomposition, then after the elapse of the incubation period the absorbancies of the water should be substantially decreased.

Twenty samples of 100 ml each were collected in the Oyster Bay area of Long Island and were filtered to remove particulate matter in the same way as described earlier. The UV absorbancies of the samples were established, after which they were halved. Each half sample (50 ml) was inoculated with a 1 ml suspension of a marine Pseudomonas sp. of a count of approximately 100,000/ml and the other with a Flavobacterium sp. in the same concentration. The organisms had been isolated and cultured from the area of the samples' origin. They were enriched in a sea water nutrient broth medium. Before inoculations the test organisms were thoroughly washed through repeated centrifugation with and resuspension in filter-sterilized sea water in order to avoid possible nutrient carry over. After one week of incubation, the 40 samples were filtered and the filtrate measured for absorption values.

Since these samples originated from the same areas as those of the previous series, COD determinations were not carried out on them. In Table VIII the values of absorbancies are shown before inoculation with the Pseudomonas sp. and Flavobacterium sp. as well as those obtained after the one week incubation period. For the sake of easy comparison the means of each set of values were calculated and the absorbancies were also converted to DOC (mg C/l). As can be seen from this table, a drastic reduction in the absorbancy values occurred, indicating a considerable utilization of the organic matter by the microorganisms. This, however, also means that most of the organic substances must have been present in easily biodegradable forms such as proteins, carbohydrates, lipids, etc., rather than in forms of resistant humates or lignins.

TABLE VIII. BACTERIAL UTILIZATION OF DISSOLVED ORGANIC MATTER (After Hermel, 1971)

Sample No.	E ₂₈₀ (native)	E ₂₈₀ after Inoculation with		DOC _{Calc.} (native)	DOC _{Calc.} Utilization by	
		Species #1	Species #2		Species #1	Species #2
1	0.742	0.153	0.052	5.94	1.23	0.42
2	0.748	0.183	0.020	5.98	1.47	0.16
3	0.739	0.168	0.010	5.91	1.35	0.08
4	0.734	0.250	0.022	5.97	2.00	0.18
5	0.753	0.235	0.043	6.02	1.88	0.35
6	0.664	0.122	0.070	5.31	0.98	0.56
7	0.745	0.171	0.077	5.96	1.37	0.62
8	0.728	0.137	0.052	5.82	1.10	0.42
9	0.730	0.216	0.030	5.84	1.73	0.24
10	0.678	0.136	0.015	5.42	1.06	0.12
11	0.661	0.143	0.067	5.29	1.15	0.54
12	0.627	0.155	0.042	5.02	1.24	0.34
13	0.637	0.206	0.053	5.10	1.65	0.43
14	0.653	0.190	0.010	5.22	1.52	0.08
15	0.715	0.237	0.025	5.72	1.90	0.20
16	0.751	0.216	0.045	6.01	1.73	0.36
17	0.710	0.130	0.050	5.68	1.04	0.40
18	0.745	0.232	0.052	5.96	1.86	0.42
19	0.736	0.255	0.040	5.89	2.04	0.32
20	0.728	0.203	0.030	5.82	1.63	0.24
Mean	0.711	0.187	0.039	5.69	1.50	0.33

Species #1 = Pseudomonas sp.

Species #2 = Flavobacterium sp.

Under the experimental conditions it was obviously impossible to ascertain the absolute values of the utilization of organics by the bacteria. At the same time, an unknown minor increase in organic content could have taken place during the week of incubation as a result of the secretion of organic compounds into their surroundings by the microorganisms. Since, however, the changes in absorption were relatively large, the secretion of organics by the bacteria was probably insignificant. These experiments have demonstrated that UV spectrophotometry is a convenient and simple means to follow the utilization of unspecified organics by microbes from their environment. In the same way as Khailov and Burlakova (1970) used UV spectrophotometry for the determination of the secretory activities of sea weeds (by which they organically enrich their environment) and were able to point out the ecological importance of the dynamics of this process, a measurement of the utilization of dissolved organics by microorganisms could further enhance our understanding concerning the cycling of organic matter in the aqueous environment.

H. Instrumentation Used in UV Spectrophotometry for Water Quality Testing

Instrumentation used in UV spectrophotometry will be discussed next, but only such instruments will be mentioned which have a limited capability of wavelength detection in the sense that they are supplied neither with prisms nor gratings to scan the complete spectrum, but are designed to make measurements at predetermined wavelengths, or throughout the total spectrum. The instruments usually fall into two categories: single beam and double beam meters. The first design was supplied by Bramer, *et al.* (1966) in which a mercury discharge lamp with a peak output at 2537 Å was utilized: "The lamp is positioned above the water surface. The sensor consists of two photo-resistive vacuum tubes having an S-5 spectral response (2000-7000 Angstroms; maximum at 3400 Angstroms) arranged in a bridge circuit. One tube looks at the lamp through a Pollexiglass lens and thus sees only visible light passing through the water; the other tube looks at the lamp through a visible-light filter and substantially sees only the unabsorbed ultraviolet radiation. A small dc potential is applied across the bridge and a millivolt recorder is used to measure the current flowing when the bridge circuit is unbalanced. The net response of the two phototubes is a function of ultraviolet absorption by the water sample, compensated for water surface turbulence, lamp flicker, and moderate turbidity" (p. 275).

A somewhat more complicated single beam instrument incorporating a chopper was devised by Briggs and Melbourne (1966, p. 115): "A collimated light beam from a small mercury vapour ozone lamp (0.3 Å at 12 V) is interrupted by a rotating disc in which alternate sectors are visible and ultra-violet light filters. The light passing through the sample is received by a vacuum photodiode with a wide spectral response (2000 Å to 7000 Å). A voltage derived from the photodiode is directly coupled to a logarithmic amplifier, with the result that the alternating component of the output is a function of the difference of the logarithms (that is the logarithm of the ratio) of the optical densities of the samples at the two wavelengths.... It can be shown that compensation is provided for variations in lamp emission, and since only one photocell is used, variations in its characteristics will have little effect on the calibration. Provided the optical density of fouling is identical for visible and for ultra-violet light, compensation for

this will occur also, since both light beams pass through the same sample windows.... It can also be shown that the presence of substantial quantities of suspended matter will have little effect on the calibration."

A simplified "colorimeter" has been devised by Seward (1970, p. 1): "A simple quartz test tube functions as the sample container and the necessary lens system concentrating light from an ultraviolet 'ozone lamp' through the sample to an ultraviolet detector. Rectified line current provides power for the ultraviolet source resulting in pulses at 60 herz frequency. Pulses derived respectively from the ultraviolet detector and from a reference detector, are compared to yield an electrical current proportional to the absorbance of the sample, which is logarithmically related to the transmittance and the sample detector current."

In 1973, Claus described a portable, single beam UV photometer which employs a narrow bandwidth filter, transmitting only at wavelength of 280 nm. The sample, after filtering with a suitable glass or stainless steel filter, enters a 1 cm path cuvette and the absorption of the liquid is measured by a narrow bandwidth, saffire window photosensor having a peak sensitivity in the 289 nm range. The results, after appropriate amplification, can either be displayed as millivolts on a reader or can be graphed on a chart recorder. A 1 cm path seems to be adequate, because in this way dilution of highly contaminated samples can be avoided on the one hand, and on the other hand, through properly graded amplification, even dilute specimens will give recordable measurements. The simplicity and the precision of the method recommends its application for the testing of natural waters, including sea water, as well as sewage plant effluents. The author points out, however, that in certain special cases where large quantities of organic pollutants enter the water which do not have a signal in the 280 nm UV range, such as carbohydrates from sugar mills, the validity of the obtained readings is questionable. This limitation should not serve as a deterrent to the widespread utilization of UV spectrophotometry for the quantitation of organic matter in water quality analysis.

The double beam instruments consist of meters employing either split beams or dual beams. Where split beams are used there is only one sample cell, while in the dual beam instruments two sample cells are employed. Design of such instruments is somewhat complex, but they permit the recording of differential spectra which are important in the monitoring of plant effluents containing specific organic compounds. A design by Martin, *et al.* (1967) shows such a continuous monitoring system for phenols, utilizing the 286 nm peak of the basic phenol band. The sample chamber is alternately filled with acidified and basic or neutral solutions. Saltzman (1968) showed a design of a dual beam analyzer in which one sample chamber is filled with the incoming sample stream and the other with effluent. The difference spectrum between the two samples is characteristic for the phenolic compounds leaking from the plant.

The applicability of differential spectrophotometry for the determination of potassium permanganate values and measurement of tyrosine oxidizability was shown by Kelly (1968). He demonstrated that under rigidly controlled conditions $KMnO_4$ can be used with H_2SO_4 for the complete oxidation of tyrosine. The decolorization of the permanganate solution as measured in a Carey 14 spectrophotometer was proportional to the amount of tyrosine in the

sample. The difference spectrum between the blank (permanganate without added tyrosine) and the decolorized sample permitted the detection and quantitation of 1 ng of this amino acid. The study showed, therefore, that spectrophotometric determinations for tyrosine or other proteinaceous compounds containing this amino acid are much more sensitive than other types of chemical analysis. Lowry, et al. (1951), when investigating the spectral absorbance detection limits of proteins at 280 nm, stated that the limit is 2 µg, a claim contradicted by Kelly's findings. Lowery, et al., advocate the use of Folin phenol reagent for the determination of 0.2 µg proteins, but this is not essential if one uses differential spectrophotometric techniques.

The extreme sensitivity of UV spectrophotometric measuring techniques for tyrosine or proteins permits their utilization in water quality studies. Even if the direct detection limit at 280 nm were only 2 µg protein, as claimed by Lowery et al. (1951), this amount is well below the milligram levels of organic matter found in one liter of natural waters. The measured absorbancy readings can then be correlated with DOC or TOC values or, by employing conversion factors, can be immediately expressed in mg/l organic matter.

I. Conclusion

In tests conducted by The Federal Water Pollution Control Administration's Advanced Waste Treatment Group (AWTR Summary Report, 1968) it has been found that significant amounts of chloramines may interfere with UV monitoring of waste water effluents. Also, the presence of turbidity and of many heavy metal ions lead to erroneously high UV absorption values. Finally "... recent studies of the UV-TOC relationship for a municipal tap water, river water, and several primary and secondary sewage effluents have in no case yielded acceptable linear correlations even after reduction of any chloramines present. (p. 96)" Since the group used 253.7 nm for carrying out their measurements - at which wavelength there is, indeed, an interference from heavy metals - their surprisingly bleak outlook does not seem to be thoroughly justified as far as the applicability of UV monitoring technique is concerned. In the papers published in the literature since 1967 the linear relationship between TOC and UV absorptivity has been several times confirmed for both pristine natural waters (rivers and sea) and also for highly polluted waters, including sewage and treatment plant effluents. In view of these results, skepticism about the applicability of UV spectrophotometry for the monitoring of the organic pollutional load of waters would appear to be out of date.

From the results of the different studies reviewed it seems clear that measuring the ultraviolet absorbancy of either fresh or sea water at the wavelength of 280 nm can be used for the characterization of the organic contents of the waters. Good correlations among absorption values, DCOD, COD, coliform and Candida counts were established. When the absorbancies were treated in terms of tyrosine equivalents, it was possible to calculate in a meaningful manner the other organic constituents of the water. On the basis of these more recent findings, doubts can be raised as to the validity of the determinations of previous authors regarding the nature of the UV absorbing components of natural waters, since many of them were thinking in terms of lignins, lignosulfonates, or humates. It was pointed out earlier in this paper that: 1) The distribution of tyrosine in nature has not yet been

determined, although its natural occurrence in water could be expected. 2) Proteinaceous matter, which undoubtedly shows a high absorption peak in the region of 280 nm, was not taken into account in the works of previous investigators, who tried to identify other components as responsible for the UV absorption of the waters at 280 nm. 3) The techniques utilized for the selective removal of certain humic compounds, such as fulvic acids, will also quantitatively remove proteins and polypeptides. 4) The identification of the presence of peptide bonds in humates and the lack of aromatic compounds in these moieties throws considerable doubt on their supposed chemical structure; they might at least in part represent some highly modified or denatured protein derivatives. 5) The fact that the autochthonous organic matter does not seem to absorb in the region of 280 nm would indicate that the substances of which it consists are not proteinaceous and do not particularly contribute to the 280 nm peak, which absorption can therefore be assessed as representing the allochthonous organic matter, the most important component of the organic load carried by natural waters. 6) Finally, due either to instrumental insensitivity in the very short wavelength region or on account of sample preparation procedure using membrane filters, most of the earlier works reported in this field of investigation have to be assessed with extreme caution. A further difficulty in the evaluation of determinations of organic matter in sea water is represented by the fact that both the standard dichromate procedure and its modification with chloride complexing result in somewhat erratic readings.

In perusing the literature one finds that different authors use different calculations to substantiate correlations among UV absorbancies and COD values. Thus Mrkva (1969) calculates:

$$k = \frac{\text{COD mg O}_2/\text{l}}{E_{280} (3 \text{ cm})} \quad [1]$$

The values which he obtains are around 17; thus, when he represents his correlations (for instance in Figures 12 and 13) he uses a simple conversion factor of 50 without ever explaining why. The rationale behind this, however, is the following. Absorptivity in a 3 cm path is three times more than if measured at 1 cm. Thus 3 times 17 is 51 or 50, which means that:

$$E_{280} (1 \text{ cm}) \times 50 = \text{COD mg O}_2/\text{l} \quad [2]$$

Ogura and Hanya (1966), working with sea water, found the correlation:

$$\text{DOC mg C/l} = \frac{E_{220}}{0.02} \quad [3]$$

They also point out that absorptivity at $E_{220\text{nm}}$ is only about 20% of that at 280 nm. Thus:

$$E_{220} (1 \text{ cm}) = 0.2 E_{280} (1 \text{ cm}) \quad [4]$$

Now, if we substitute these values into equation 3 we get:

$$\text{DOC mg C/l} = \frac{0.2 E_{280} (1 \text{ cm})}{0.02} = 10 \times E_{280} (1 \text{ cm}) \quad [5]$$

If this equation is combined with that of Mrkva (equation 2), one finds that the relationship between DOC and COD is:

$$5 \times \text{DOC mg C/l} = \text{COD mg O}_2/\text{l} \quad [6]$$

Whalen, et al. (1970) found that:

$$E_{280} (1 \text{ cm}) = 40 \times \text{TCOD mg O}_2/\text{l} \quad [7]$$

and that:

$$\text{No. } \underline{\text{Candida albicans}}/\text{l} = 100 \times \text{COD mg/l} \quad [8]$$

Khailov and Burlakova (1970), working on sea water, established the following equation:

$$\text{DOM mg/l} = 100 \times E_{260} (5 \text{ cm}) \quad [9]$$

Now, if this measurement were carried out at 1 cm and at 280 nm instead of 260 nm one would find that:

$$\text{DOM mg/l} = 500 \times E_{280} (1 \text{ cm}) \quad [10]$$

Finally, Hermel (1971), worked out the following series of equations:

$$\text{COD mg/l} = 40 \times E_{280} (1 \text{ cm}) \quad [11]$$

$$\text{DOC mg C/l} = 8 \times E_{280} (1 \text{ cm}) \quad [12]$$

$$\text{POC mg C/l} = 1.1 \times E_{280} (1 \text{ cm}) \quad [13]$$

$$\text{DOC mg C/l} + \text{POC mg C/l} = \text{TOC mg C/l} \quad [14]$$

It should be noted that equation 11 is practically identical to equation 2. Furthermore, since the relationships among all of these equations, arrived at by different authors under completely different and independent investigative considerations, are simple linearities, one may conclude that conversion of one type of experimental results or measurements into another type can be easily performed.

Thus, the review has shown that contemporary applications of UV absorption measurements represent a feasible, accurate and rapid technique for the characterization of water quality.

J. Summary

The phenomenon of light absorption in water is discussed and its laws are delineated. UV light is, as any other electromagnetic radiation, uniformly and exponentially attenuated in clear water. Penetration is an inverse function of wavelength. Several naturally occurring ions or compounds dissolved in water will show special absorbancies in the UV range, among them bromides at 218, nitrates at 220, phenols (or lignites) at 260 and 280 nm. The amino acids, phenylalanine and tyrosine, as well as polypeptides and proteins containing them, will show strong absorptions at the 260 and 280 nm wavelength bands.

Recent work is reviewed in which absorption measurements in natural waters were carried out at 280 nm, based on the assumption that the amino acid tyrosine must occur in water, since it represents an average of 3% of proteins, which in turn constitute 40-60% of living matter. These measurements were performed in conjunction with conventional chemical tests, and the possibility of establishing simple conversion factors from UV absorbancies to different currently used organic water quality indicators was verified. The amounts of UV absorbent organic solutes are linearly proportional with the total quantity of dissolved organic matter in the water, which thus permits the definition of the organic load present from the UV measurements. Instruments developed for this purpose are described and it is concluded that for the quantitation of COD, either in fresh or in salt water, UV spectrophotometry is a sensitive, reliable and rapid technique.

K. References

- Aitken, J.: "On the Colour of the Mediterranean and Other Waters," Proc. R. Soc. (Edinburgh, 1882), 11: 472-483.
- American Public Health Association: Standard Methods for the Examination of Water and Wastewater Including Bottom Sediments and Sludges, 12th Ed., 1965, 769 pp.
- Armstrong, F.A.J.: "Determination of Nitrate in Water by Ultraviolet Spectrophotometry", Anal. Chem. (1963), 35: 1292-1294.
- Armstrong, F.A.J. and G.T. Boalch: "The Ultra-Violet Absorption of Sea Water", J. Mar. Biol. Assoc. U.K. (1961a), 41: 591-597.
- Armstrong, F.A.J. and G.T. Boalch: "Ultraviolet Absorption of Seawater", Nature (London, 1961b), 192: 858-859.
- Armstrong, F.A.J.; P.M. Williams and J.D.H. Strickland: "Photo-oxidation of Organic Matter in Sea Water by Ultraviolet Radiation, Analytical and Other Applications", Nature (London, 1966), 211: 481-483.
- Aufsess, O. (1903): As quoted by H. Stooff in discussion of W. Demmering, Vom Wasser (Germany, 1936), 11: 236.
- Bennet, F.P.: "Membrane Filtration for Determining Protein in the Presence of Interfering Substances", Nature (London, 1967), 213: 1131-1132

- Bordovskiy, O.K.: "Accumulation and Transformation of Organic Substances in Marine Sediments", Marine Geology (1965), 3: 1/2: 3-114.
- Bramer, H.C.; M.J. Walsh and S.C. Caruso: "Instrument for Monitoring Trace Organic Compounds in Water", Water and Sewage Works (Aug. 1966), 113: 275-278.
- Brauns, F.E.: The Chemistry of Lignin, New York, N.Y. Academic Press, 1952, 345 pp.
- Briggs, R. and K.V. Melbourne: "Recent Advances in Water Quality Monitoring", Water Treatment and Examination (1968), 17: 107-120.
- Chanu, J.: "Extraction de la Substance jaune dans les eaux cotières", Rev. Opt. (theor. instrum.), (1959), 38: 569-572.
- Claus, G.: "Method and Apparatus for Continuous Monitoring of Dissolved Organics", U.S. Patents, No. 3,751,167. Awarded Aug. 7, 1973, 5 pp.
- Czepa, O.: "Reference Values of the Forel Color Scale for Determining Sea Color", Acta Hydrophys., (1955), 2: 145-147.
- Demmering, W.: "Application of the Absorption-spectroanalysis for the Investigation and Control of Polluted Surface Waters", Vom Wasser (Germany, 1938), 11: 220-237.
- Dobbs, R.H. and R.T. Williams: "Elimination of Chloride Interference in the Chemical Oxygen Demand Test", Anal. Chem. (1963), 35: 1064-1067.
- Dornbush, J.H. and D.W. Ryckman: "The Effects of Physiochemical Processes in Removing Organic Contaminants", J. WPCF (1963), 35: 1325-1338.
- Duntley, S.Q.: "The Penetration of Light Into the Sea", Proc. Symp. Aspects Deep-Sea Res. (1957), Comm. on Undersea Warfare, N.A.S., N.R.C. Publ. # 472: 79-89.
- DuPré, E.F. and L.H. Dawson: "Transmission of Light in Water: An Annotated Bibliography", NRL Bibliography (1961), Wash., D.C., Naval Research Laboratory #20, 80 pp.
- Dynson, H.; H.R. Jitts and B.D. Scott: Techniques for Measuring Organic Primary Production Using Radioactive Carbon. (Division of Fisheries and Oceanography, CSIRO, Crenulla, N.S.W.), Melbourne, CSIRO, 1965.
- Ewald, W.F.: "A Method for the Measurement of Lights in Water", Intl. Rev. Ges. Hydrobiol. Hydrogr. (1910-1911), 3: 67-78.
- Fährnich, V. and M. Soukup: "UV-Spectrophotometric Determination of Organic Compounds in Water", Wasserwirtschaft-Wassertechnik (1964), 14: 205-208.
- Fogg, G.E. and G. T. Boalch: "Extracellular Products of Marine Algae", Nature (London, 1958), 181: 789-790.

- Fogg, G.E.; C. Nalewajko and W.D. Watt: "Extracellular Products of Phytoplankton Photosynthesis", Proc. Roy. Soc., Ser. B., Biol. Sci. (1965), 162: 517-521.
- Forel, F.A.: "Etude sur les Variations de la Transparence des Eaux du Lac Leman", Arch. Sci. Phys. Nat. (1877), 59: 137-153.
- Fredericks, A.D. and W.M. Sackett: "Organic Carbon in the Gulf of Mexico" Preprint of Paper, Submitted for Publication in J. Geophys. Res. (1970), 13 pp.
- Galtsoff, P.: "The American Oyster, Crassostrea virginica Gmelin.", Fish. Bull. (1964), 64: 1-480.
- Goldman, E. and R. Jacobs: "Determination of Nitrates by Ultraviolet Absorption", J. Amer. Water Works Asso. (1961), 53: 187-191.
- Gruber, M.: "A Method for Measuring the Incidence of Light in Water with the Help of the Eder-Hecht Neutral Wedge Photometer", Intl. Rev. Ges. Hydrobiol. Hydrogr. (1924), 12: 17-150.
- Hanya, R. and N. Ogura: "Application of Ultraviolet Spectroscopy to the Examination of Dissolved Organic Substances in Water", in Advances in Organic Geochemistry, ed. by U. Colombo and G.D. Hobson, Proc. Int'l. Meeting Org. Geochem., Milan, Pergamon Press, Oxford, 1964, pp. 447-456.
- Hermel, M.: "Studies on Ultraviolet Spectrophotometric Methods for Water Quality Analyses". Unpublished Ph.D. dissertation, International Free Protestant Episcopal University, London. (1971), pp. 115.
- Hess, K.: Die Chemie der Zellulose und ihre Begleiter, Leipzig, Akademische Verlagsgesellschaft, 1928, 432 pp.
- Hoather, R.C. and P.F. Rackham: "Oxidized Nitrogen and Sewage Effluents Observed by Ultraviolet Spectrometry", Analyst (1959), 84: 548-551
- Ishiwatari, R.; S. Ito and T. Hanya: "Amino Acids in Natural Waters", Nippon Kagaku Zasshi (J. Chem. Soc. Japan, 1965), 86: 2: 201-205.
- Ishiwatari, R.; M. Kosaka and T. Hanya: "Composition and Optical Characteristics of Humic Substances Extracted from Lake Sediments", Nippon Kagaku Zasshi, (J. Chem. Soc. Japan, 1966), 87: 6: 557-566.
- Izawa, I.: "On the Color of the Sea Water", J. Geography (Chigaku Zasshi, Japan, 1890), 2: 603-604.
- Jamieson, W.; P. Madri and G. Claus: "Survival of Certain Pathogenic Microorganisms in Sea Water", Hydrobiologia (1976), 50: 117-121.
- Jerlov, N.G.: "Ultraviolet Radiation in the Sea", Nature (London, 1950), 166: 111.
- Jerlov, N.G.: "Optical Studies of Ocean Waters", Reports of the Swedish Deep-Sea Expedition, Physics and Chemistry (1951), #1: 3-59

- Jerlov, N.G. "Optical Oceanography", in Oceanography and Marine Biology Ann. Rev. (1963), ed. by Harold Barnes, London, George Allen and Unwin, Ltd., 1: 89-114.
- Johnston, R.: "Biologically Active Compounds in the Sea", J. Mar. Biol. Asso. U.K. (1955), 34: 185-195.
- Jones, P.H. and G.W. Heinke: "Ultraviolet Spectroscopy for Pollution Monitoring in the Great Lakes", 9th Conference on Great Lakes Research (Chicago, March 1966), 32 pp., in Water Poll. Abs. (Brit., 1968), 41: 354.
- Jordan, G.W.: "On the Colour of Waters", Science and Arts, R. Inst. G.B. (1818), 5: 81-89
- Joseph, J.: "Durchsichtigkeitmessungen im Meere im ultravioletten Spektralbereich", Deutsch. hydrogr. Z. (1949), 2: 5: 212-218.
- Kalle, K.: "Meerskundliche chemische Untersuchungen mit Hilfe des Zeisschen Pulfrich Photometers", Ann. Hydrogr. (Berlin, 1937), 65: 276-282.
- Kelly, R.: (Fairchild Hiller Corp., Republic Aviation Division, Farmingdale, N.Y.) "Personal Communication" (1968).
- Khailov, K.M. and Z.P. Burlakova: "Release of Dissolved Organic Matter by Marine Seaweeds and Distribution of their Total Organic Production to Inshore Communities", Limnol. Oceanogr. (1970), 14: 4: 521-527.
- Kihara, H.K. and H. Kuno: Microassay of Protein with Micro Cellulose Membrane Filters", Anal. Biochem. (1968), 24: 96-105.
- Kotzebue (1818) cited in A.V. Stupishin, Priroda (Moscow, 1955), 44: 76-77.
- Lee, G.F.: "Automatic Methods for the Analysis of Natural Waters", Proc. Symp. Intl. Biol. Program, 1966, Netherlands (1967), p. ? - 169, in Water Poll. Abs. (Brit., 1969).
- Lenoble, J.: "Sur le role des principaux sels dans l'absorption ultraviolette de l'eau de mer", C.R. Acad. Sci. (Paris, 1956), 242: 806-808.
- Lowry, O.H.; N.J. Rosebrough; A.L. Farr and R.J. Randall: "Protein Measurement with the Folin Phenol Reagent", J. Biol. Chem. (1951), 193: 265-275.
- Martin, J.M., Jr.; C.R. Orr; C.B. Kincannon and J.L. Bishop: "Ultraviolet Determination of Total Phenols", J. WPCF (1967), 39: 1: 21-32.
- Menzel, D.W. and R.F. Vaccaro: "The Measurement of Dissolved Organic and Particulate Carbon in Sea Water", Limnol. Oceanog. (1964), 9: 138-142.
- Möhler, H.: Lösungsspektren, Jena, G. Fischer, 1937, 346 pp.
- Mrkva, M.: "Investigation of Organic Pollution of Surface Waters by Ultraviolet Spectrophotometry", J. WPCF (1969), 41: 1923-1934.

- Murray, Sir J. and J. Hjort: Depths of the Ocean, London, MacMillan and Co., 1912, 821 pp.
- Navone, R.: "Proposed Method for Nitrate in Potable Water", J. Amer. Water Works Asso. (1964), 56: 781-783.
- Ogura, N.: "Ultraviolet Absorption Spectra of Natural Water", Nippon Kagaku Zasshi (J. Chem. Soc. Japan, 1965a), 86: 1281-1285.
- Ogura, N.: "Relation Between Ultraviolet Absorbance of Natural Water and Some Water Qualities", Nippon Kagaku Zasshi (J. Chem. Soc. Japan, 1965b), 86: 1286-1288.
- Ogura, N.: "Ultraviolet Absorbing Materials in Natural Waters", Nippon Kagaku Zasshi (J. Chem. Soc. Japan, 1969), 90: 7: 601-611.
- Ogura, N. and T. Hanya: "Nature of Ultraviolet Absorption of Sea Water", Nature (London, 1966), 212: 758.
- Ogura, N. and T. Hanya: "Ultraviolet Absorption of Sea Water, In Relation to Organic and Inorganic Matter", Intl. J. Oceanol. Limnol. (1967), 1: 91-102.
- Ogura, N. and T. Hanya: "Ultraviolet Absorbance as an Index of the Pollution of Seawater", J. WPCF (1968), 40: 464-467.
- Ponamperuma, C.: As quoted by R.D. Lyons: "Meteorite Hints Space Life is Possible", New York Times, Dec. 2, 1970, pp. 1 and 24.
- Provasoli, L.: "Nutrition and Ecology of Protozoa and Algae", Ann. Rev. Microbiol. (1958), 12: 279-308.
- Rayleigh, Lord A.: "Diffraction of Light", Encyclopedia Britannica (1911), 8: 238-257.
- Riely, G.A., ed.: Marine Biology, Proc. 1st Intl. Interdisciplinary Conf., Am. Inst. Biological Sci., Baltimore, Md., Port City Press, 1963, 286 pp.
- Saltzman, R.S.: "Continuous Monitoring of Aromatic Compounds in Water by Differential Photometry", Analysis Instrumentation (1968), 6: 79-85.
- Secchi, A.: "Sur la transparence de la mer", C.R. Acad. Sci. (Paris, 1865), 61: 100-104.
- Seward, H.H.: "Total Organic Carbon Colorimeter", U.S. Patents, No. 3,535,044 awarded Oct. 20, 1970, 7 pp.
- Shapiro, J.: "Chemical and Biological Studies of the Yellow Organic Acids of Lake Water", Limnol. Oceanogr. (1957), 2: 161-179.
- Steeman-Nielsen, E.: "The Use of Radioactive Carbon (^{14}C) for Measuring Organic Production in the Sea", J. Cons. Intl. Explor. Mer. (1952), 43: 117-140.

- Strickland, J.: "Assessment of the Accuracy and Precision of Data", Proc. N.A.S. (1959), N.R.C. Publ. #600, pp. 98-100.
- Stupishin, A.V.: "Contributions of Russian Investigators to the Invention of Hydrologic Apparatus", (in Russian) Priroda (Moscow, 1955), 44: 76-77.
- Suitcliffe, W.J., Jr.; E.R. Baylor and D.W. Menzel: "Sea Surface Chemistry and Langmuir Circulation", Deep-Sea Res. (1963), 8: 372-381.
- Sverdrup, H.U.; M.W. Johnson and R.H. Fleming: The Oceans, N.Y., Prentice-Hall, 1942, 918 pp.
- Truglio, D.: "Studies on Primary Productivity, Bacterial Pollution and Dissolved Proteinaceous Matter in the Great South Bay, Long Island, N.Y." Unpublished M.S. thesis, Long Island University, Greenvale, N.Y. (1968), pp. 36.
- Tsukamoto, K.: "Transparence de l'eau de mer pour l'ultraviolet lointain", C.R. Acad. Sci. (Paris, 1926), 184: 221-223.
- Tyndall, J.: "On the Colour of Water and on the Scattering of Light in Water and Air", Proc. R. Inst. G.B. (1872), 6: 189-199.
- Wallace, G.T., Jr. and D.F. Wilson: Foam Separation as a Tool in Chemical Oceanography, Wash., D.C., Naval Research Laboratory, Nov. 6, 1969, NRL Report # 6958, 17 pp.
- Wallis, C. and J.L. Melnick: "Concentration of Viruses from Sewage by Adsorption on Millipore Membranes", Bull. World Health Organization (1967), 36: 219-228.
- Waring, F.H.: "Significance of Nitrates in Water Supply", J. Amer. Water Works Asso. (1949), 41: 147-150.
- Wexler, A.S.: "Determination of Phenolic Substances by Ultraviolet Difference Spectrometry", Analytical Chemistry (1963), 35: 12: 1936-1943.
- Wexler, A.S.: "Characterization of Ligninsulfonates by Ultraviolet Spectrometry", Analytical Chemistry (1964), 36: 213
- Wexler, A.S. and F.D. Brako: "Use of Ultraviolet Spectrophotometry in Determining Lignosulfonate Additions in Cement", Materials Res. Standards (1963), 3: 5: 364-368.
- Whalen, C.; D.W. Ehresman and G. Claus: "Distribution of Candida albicans on the North Shore of Long Island", 33rd Ann. Meet. Am. Soc. Limnol. Oceanogr., (1970), Abstracts: 107.
- Wilson, D.P. and F.A.J. Armstrong: "Further Experiments on Biological Differences Between Natural Sea Waters", J. Marine Biol. Asso. U.K. (1952), 31: 335-349.

U.S. Department of the Interior; Summary Report: Advanced Waste Treatment, July 1961 - July 1964, Federal Water Pollution Control Administration (1964), Publ. WP-16-AWTR-9, 110 pp.

U.S. Department of the Interior; Summary Report: Advanced Waste Treatment, July 1964 - July 1967, Federal Water Pollution Control Administration (1968), Publ. WP-20-AWTR-19, 96 pp.

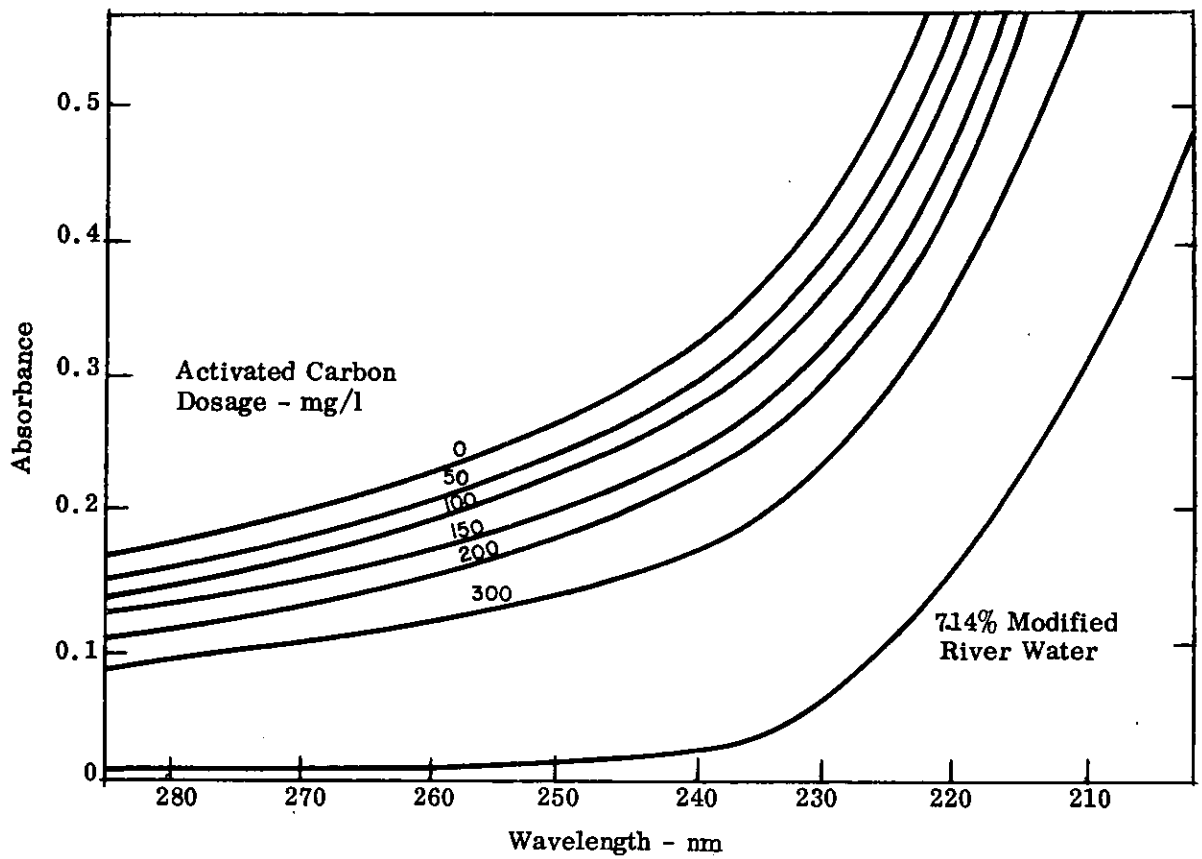


Figure 1. Ultraviolet spectra of organically fortified solutions reacted with activated carbon.
(After Dornbush and Ryckman, 1963)

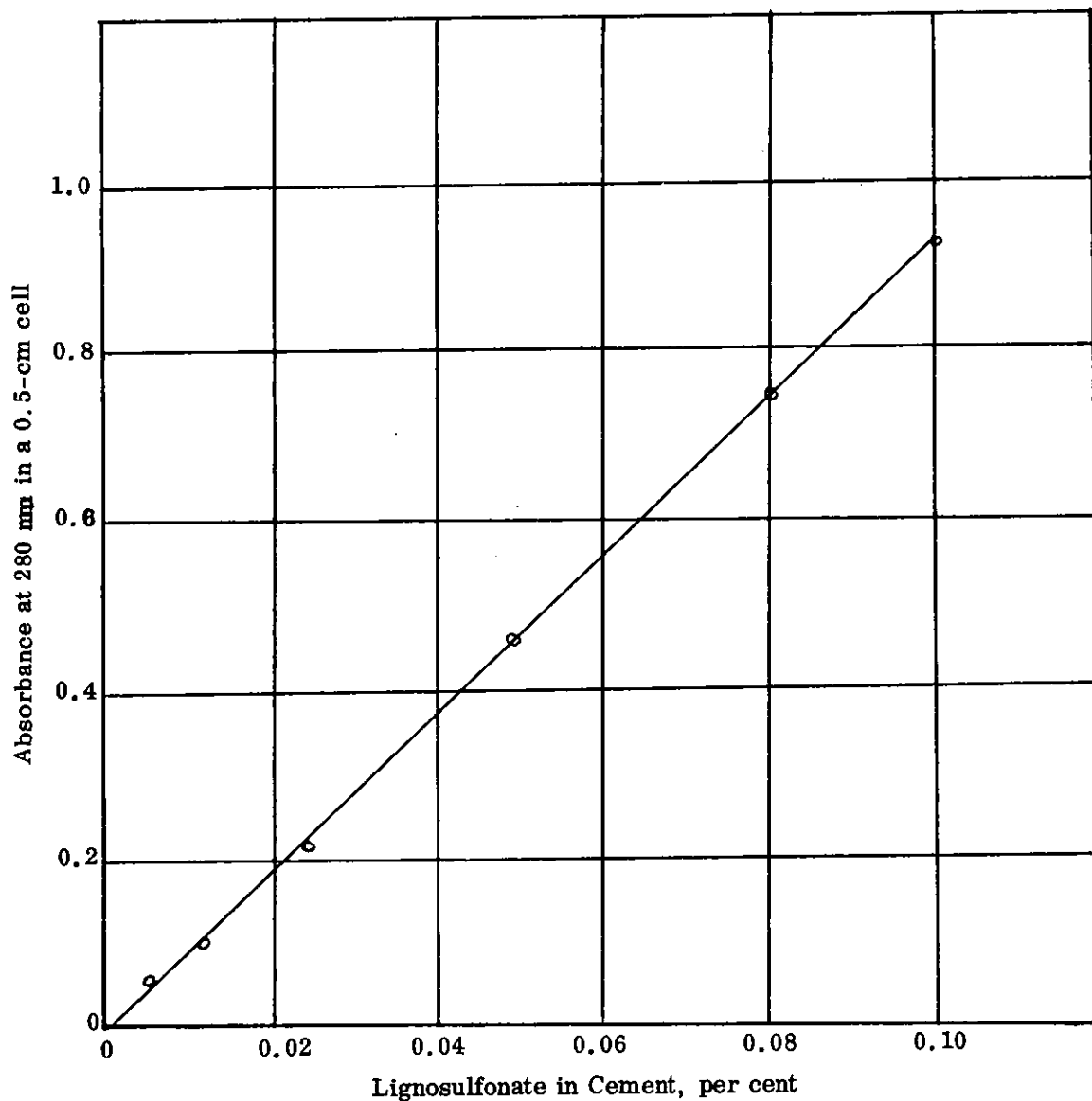
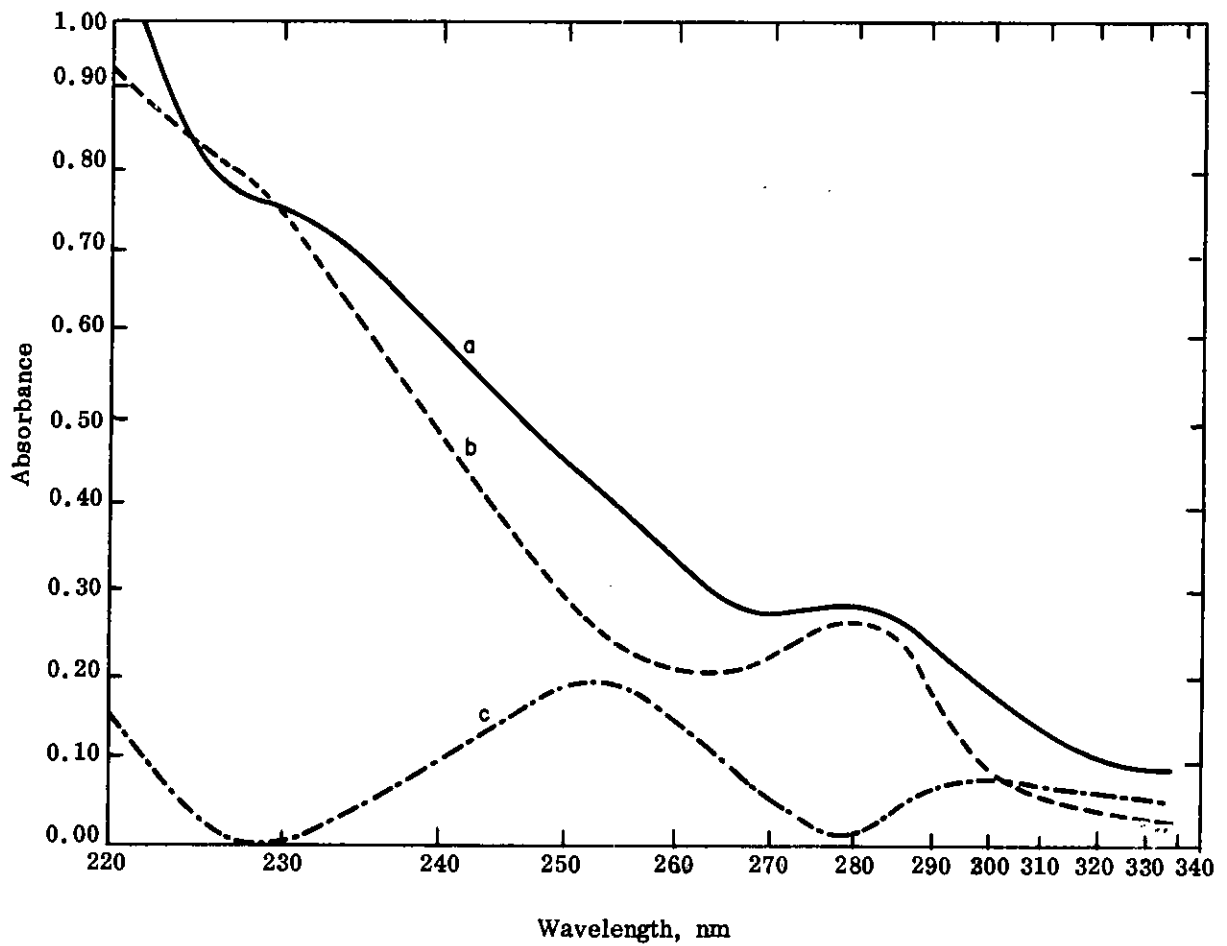


Figure 2. Absorbance of 10% Na_2CO_3 extracts of cement (5 g of cement extracted with 25 cm^3 of solution) at 280 nm in 0.5-cm cells. (After Wexler and Brako, 1963)



- a 33-1/8 ppm in 0.1 N KOH
- b 33-1/8 ppm in 0.1 N HCl
- c Difference spectrum with a in sample beam and b in reference beam

Figure 3. Direct and Difference Spectra of a Softwood Lignosulfonate
(After Wexler, 1964)

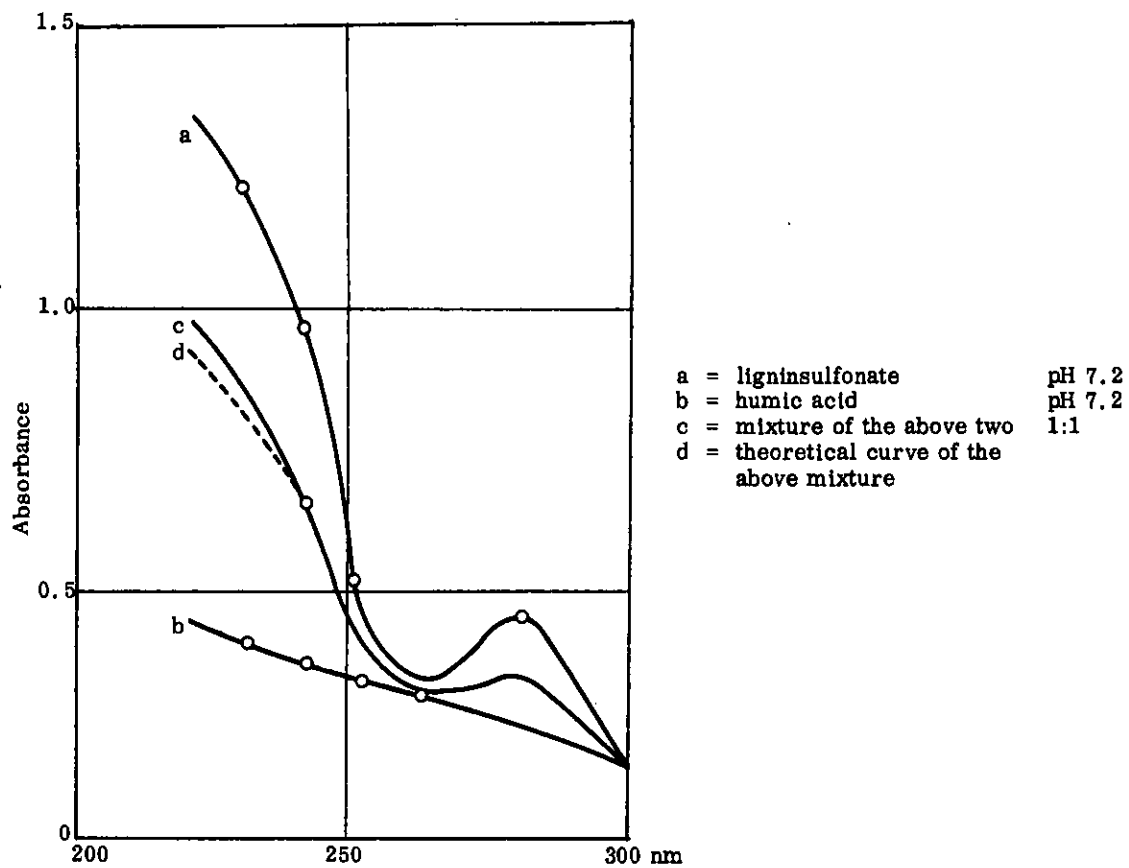


Figure 4a. Extinction characteristics of humic acid, ligninsulfonate and their mixtures.

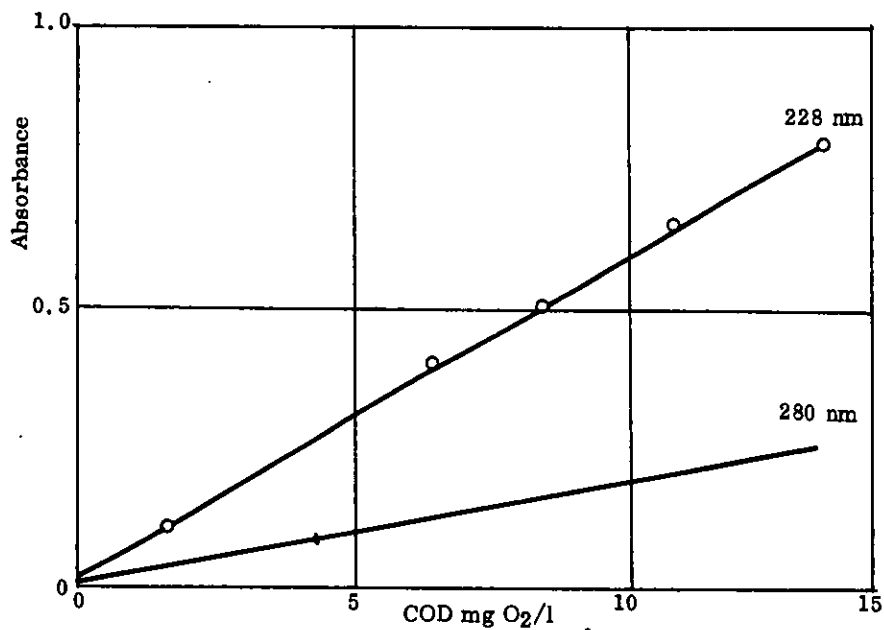


Figure 4b. Correlation between UV-absorption and permanganate COD.

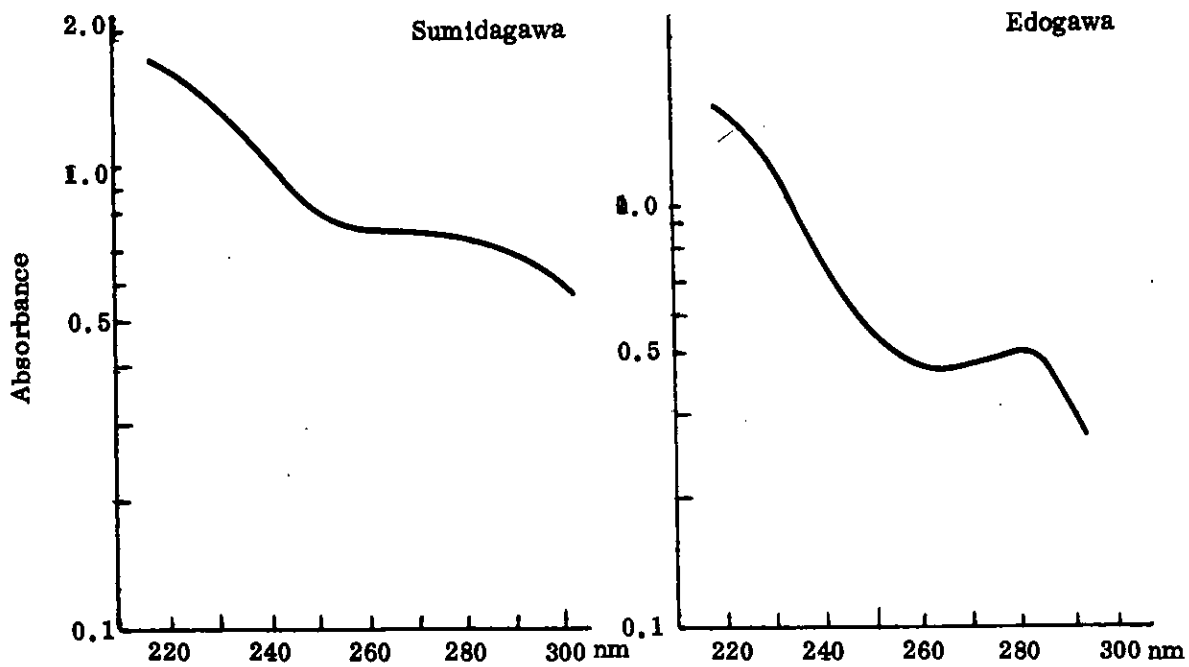
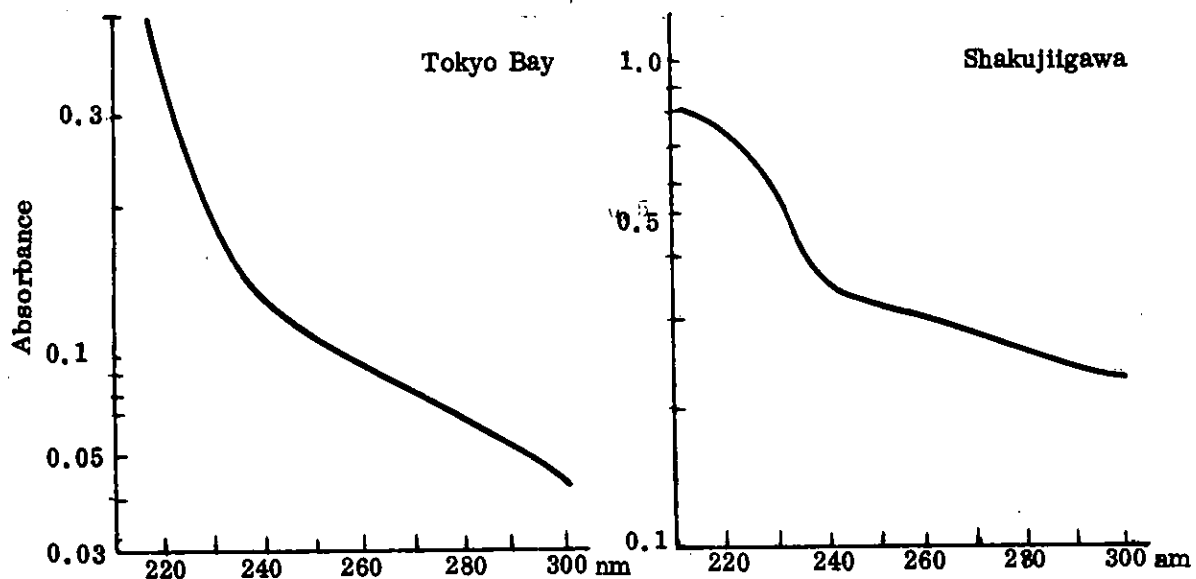


Figure 5. Examples of Ultraviolet Absorption Curves in Natural Waters (After Hanya and Ogura, 1964)

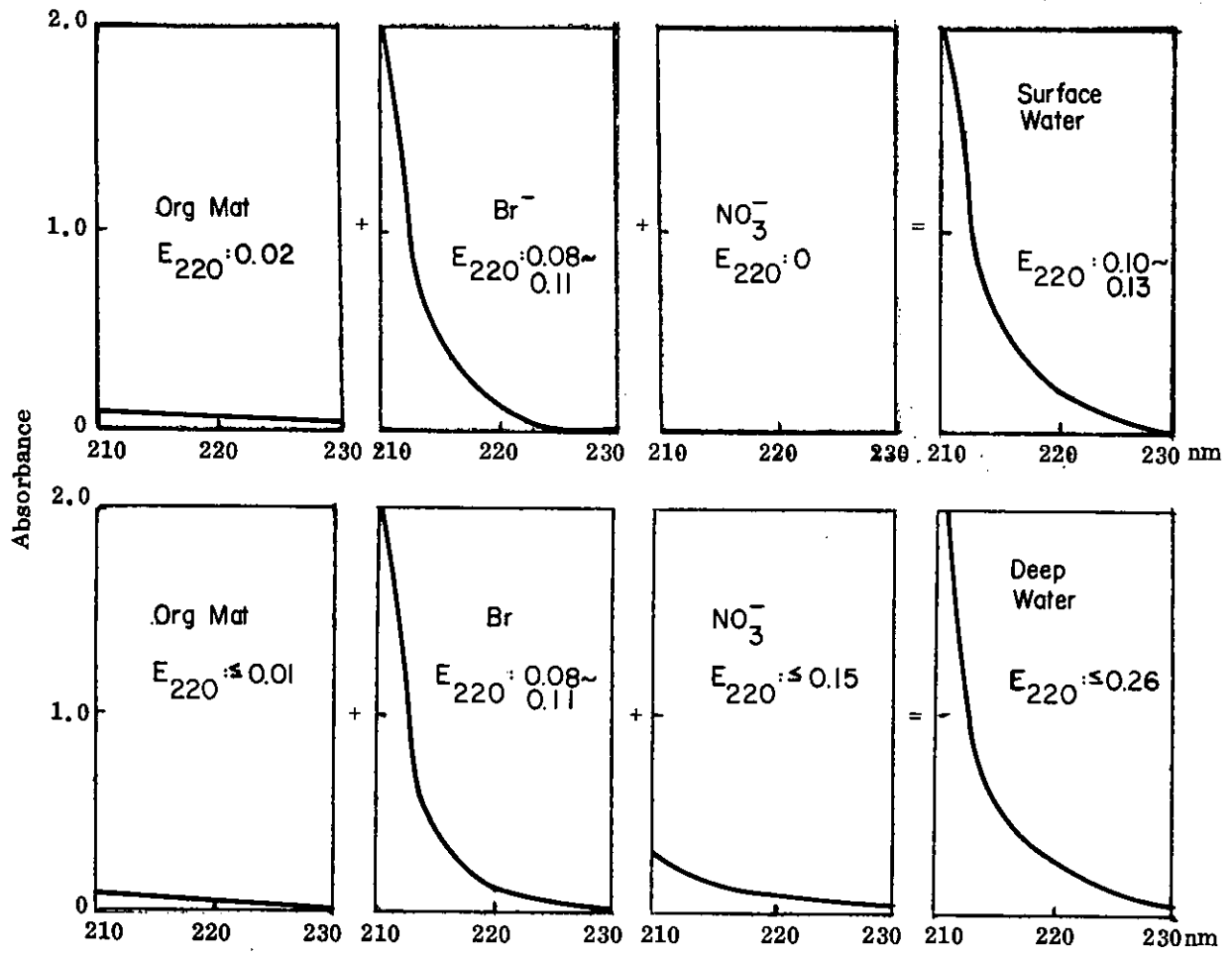


Figure 6. Model of ultraviolet light absorption by sea water.
 Ordinate, absorbance (E); abscissa, wavelength (nm).
 (After Ogura and Hanya, 1966)

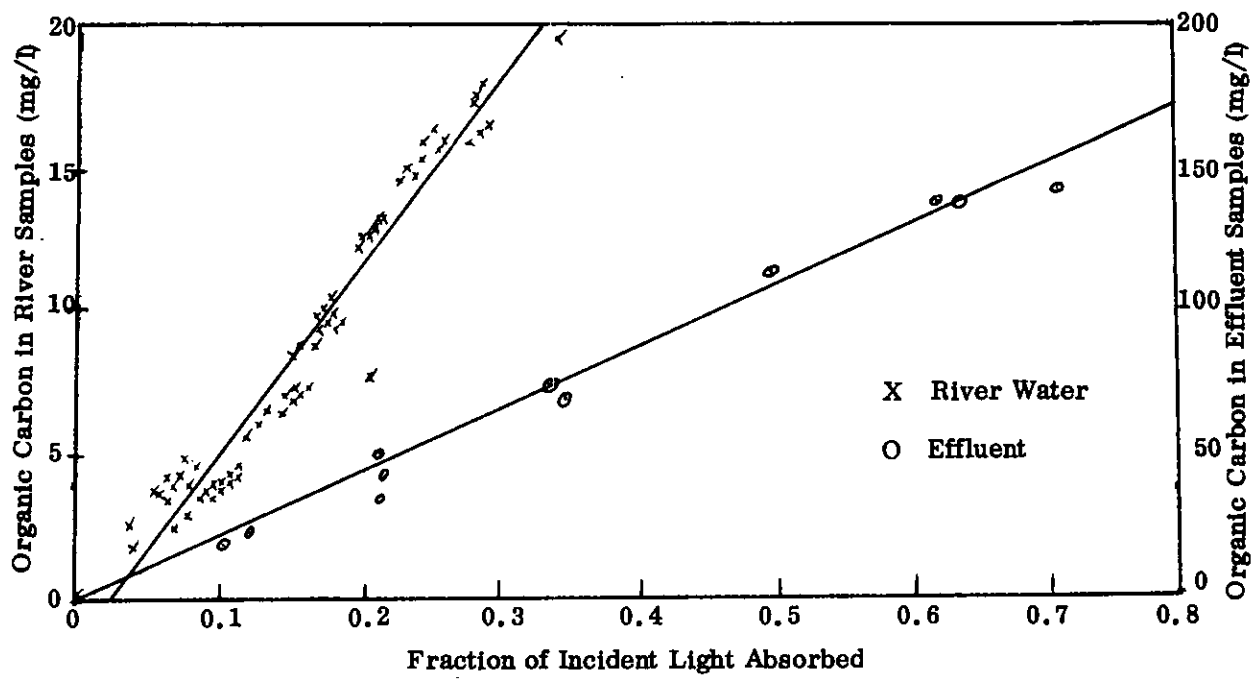


Figure 7. Relation between Absorption of Light at 2537 \AA and the Organic Carbon Content of Six River Waters and Three Sewage Effluents. (After Briggs and Melbourne, 1966)

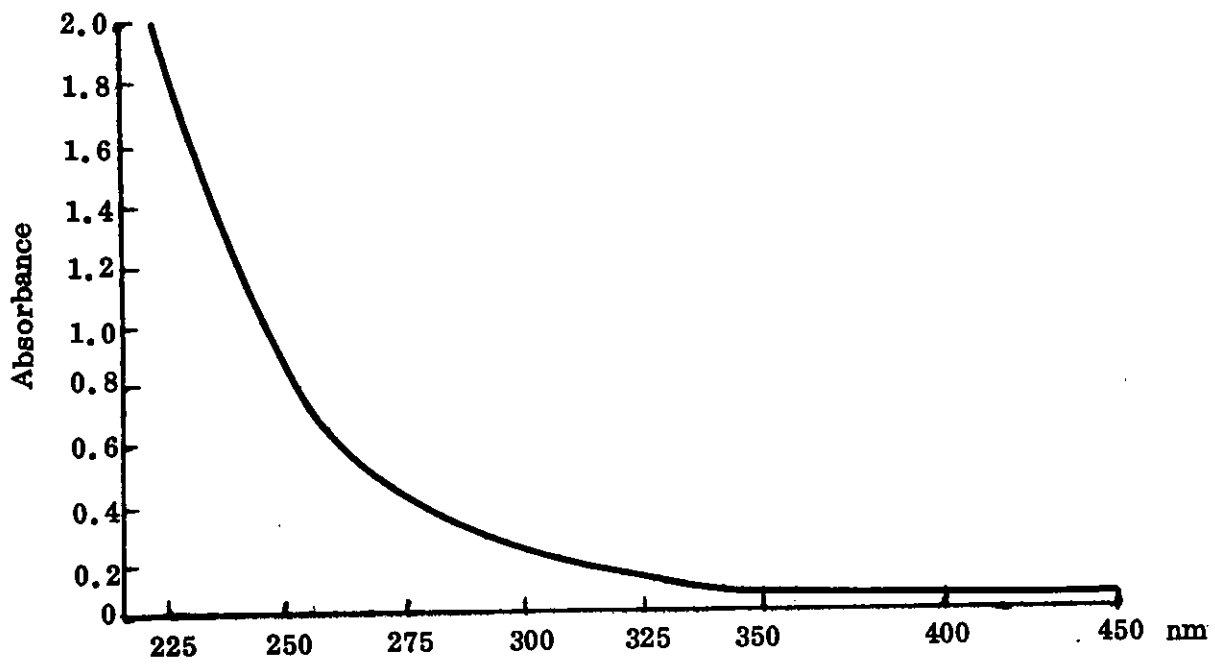
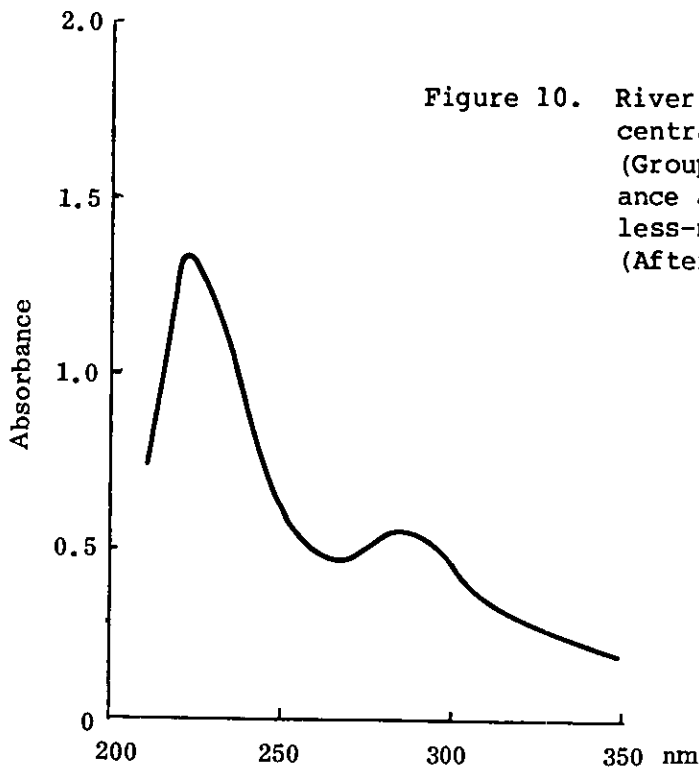
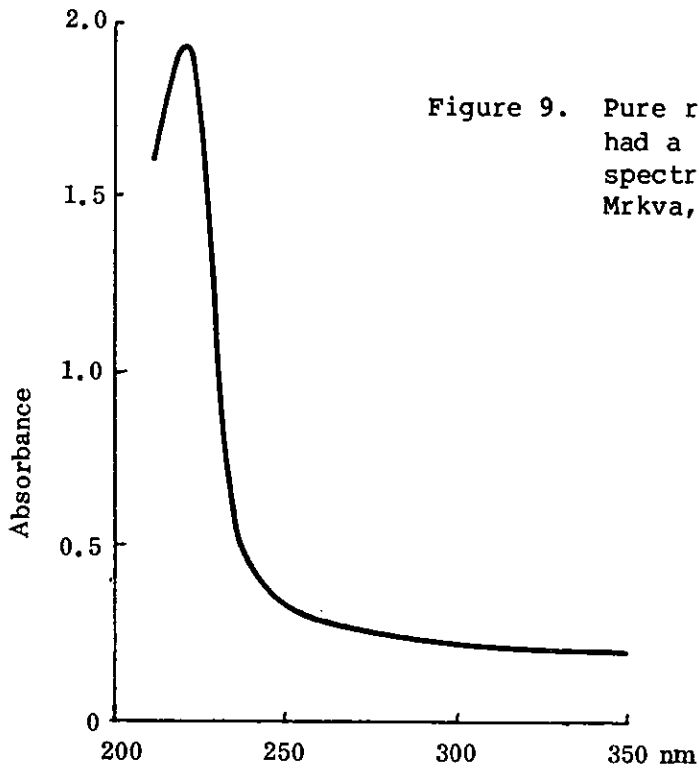


Figure 8. Delaware River Water (1 cm Cell)
(After Saltzman, 1968)



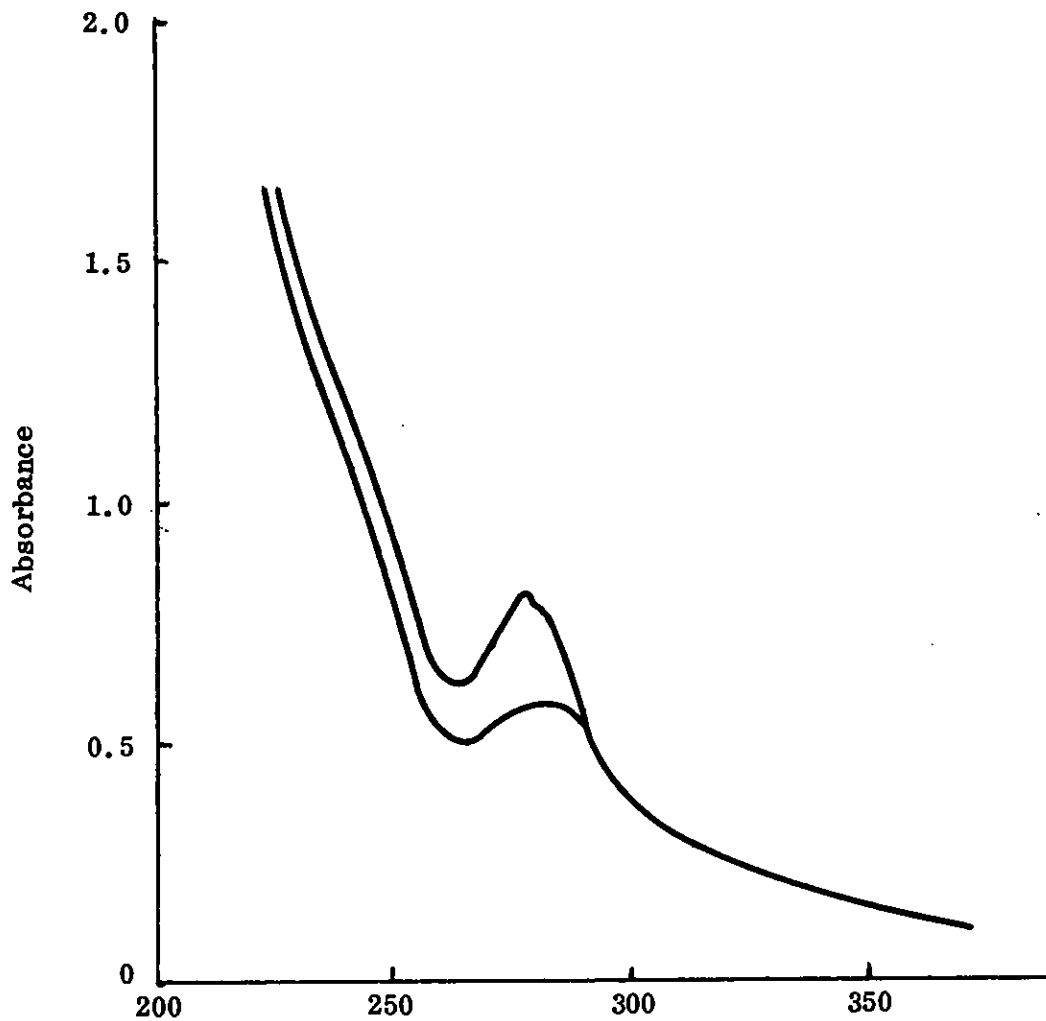


Figure 11. River stretches which receive, in addition to the pollutants present in those of Groups I and II, further waste products, may be classified as Group III. Absorbance measured at 280 nm to determine organic pollution. (After Mrkva, 1969)

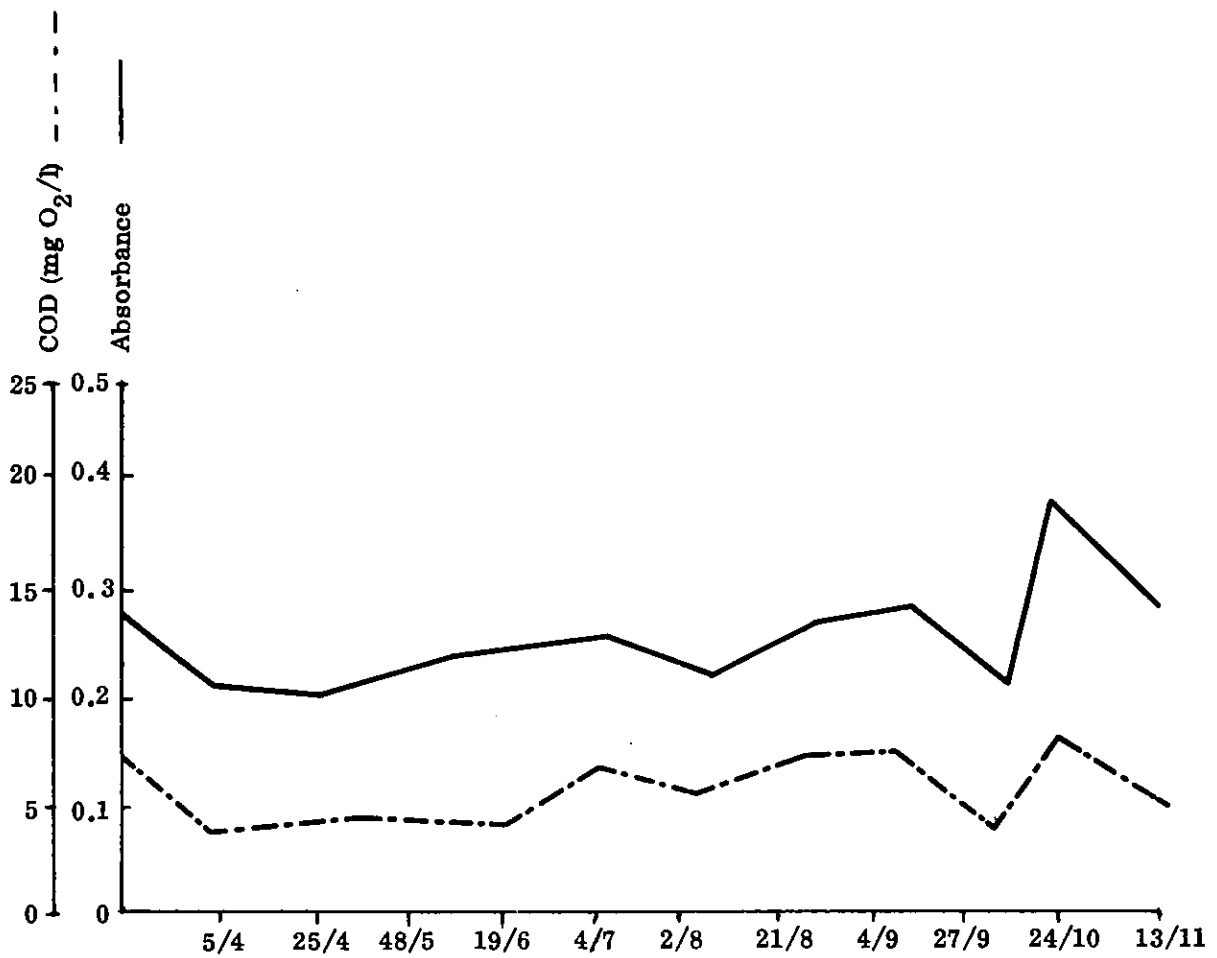


Figure 12. The interrelationship between absorbance and oxygen demand for Group I rivers was determined using the spectrophotometric method at 280 nm and using Kubel's technique. (The abscissa shows day/month for 1967.) (After Mrkva, 1969)

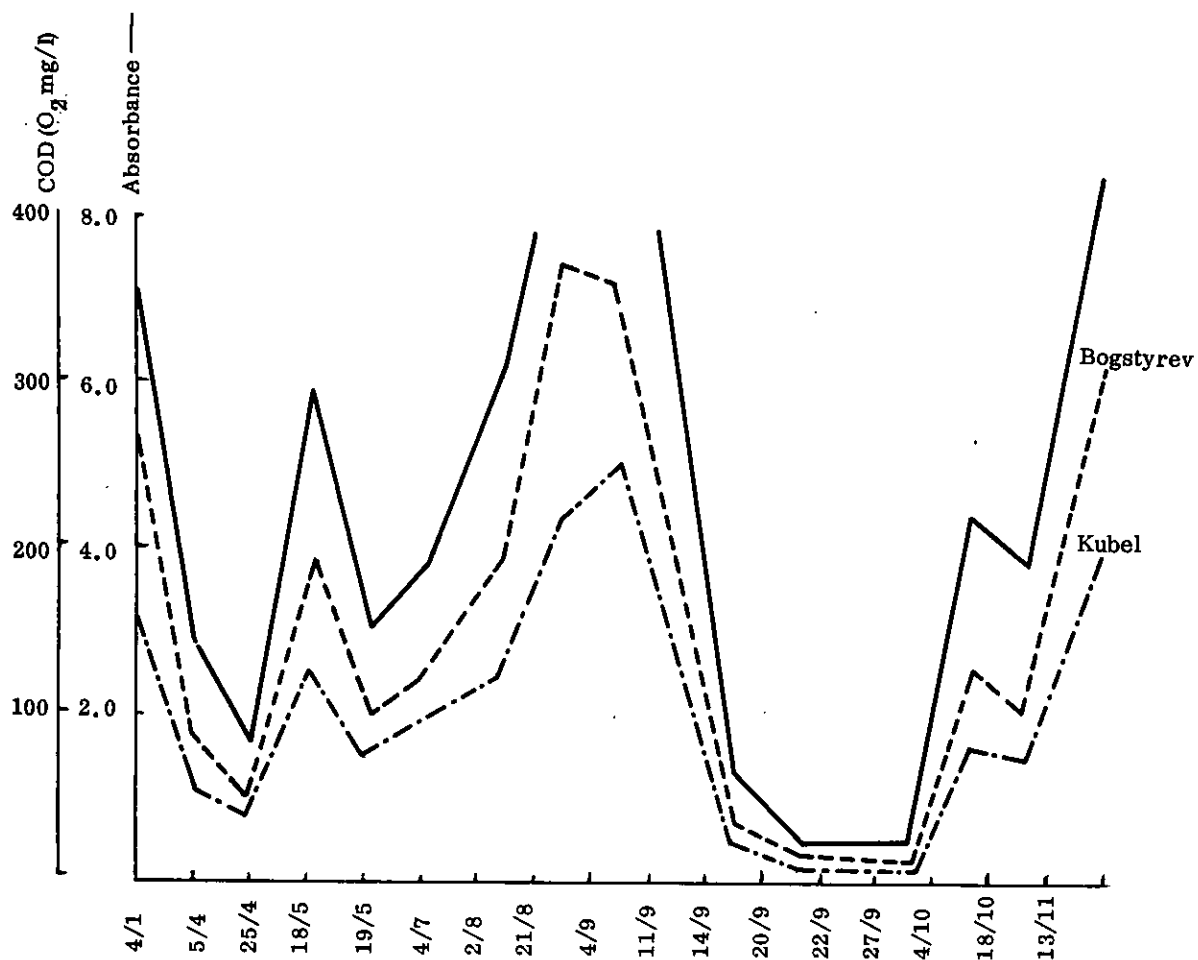


Figure 13. Group III river samples were diluted before being analyzed for oxygen demand determinations, using either the method of Kubel or Bogstyrev. (The abscissa shows day/month for 1967.) (After Mrkva, 1969)

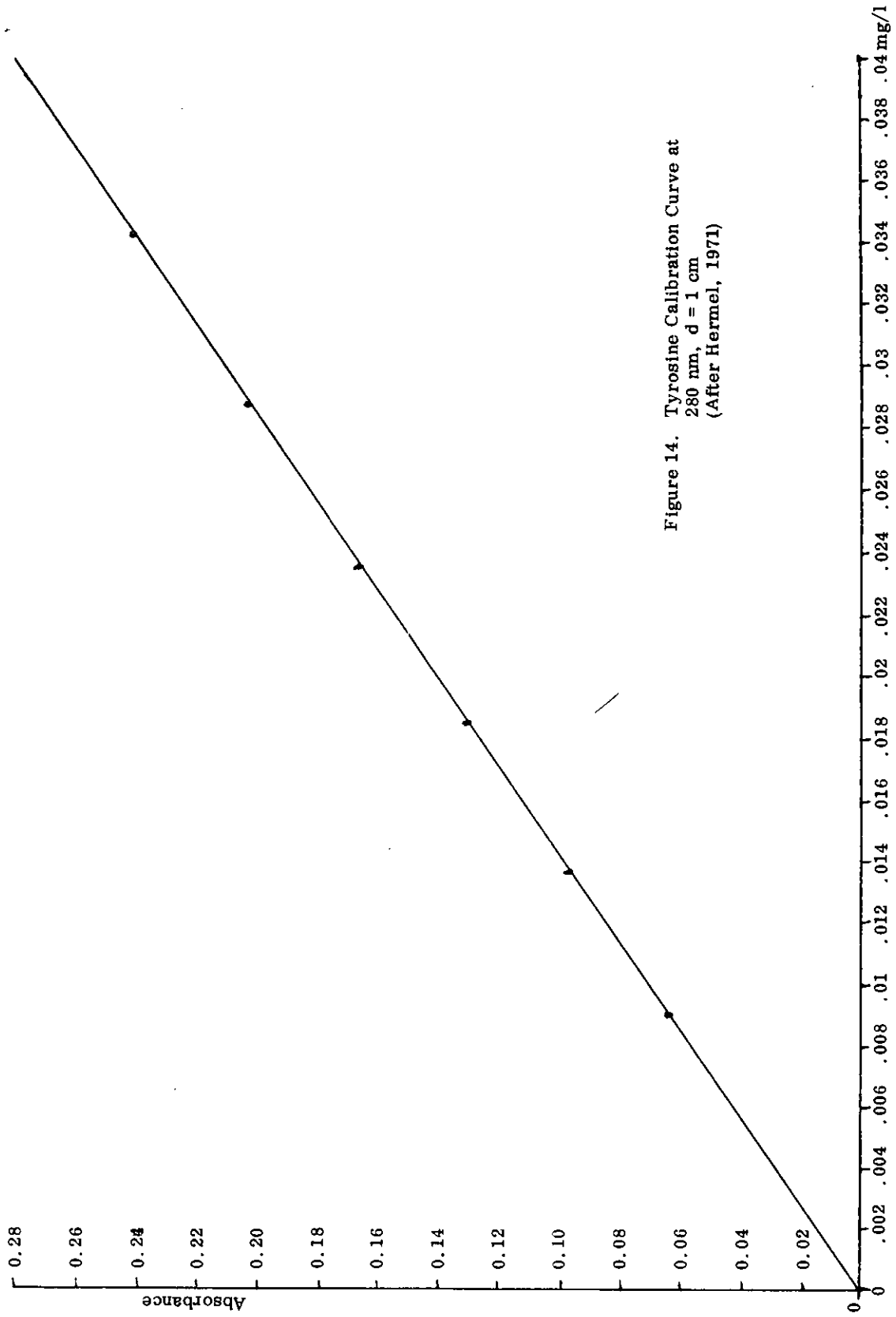


Figure 14. Tyrosine Calibration Curve at
280 nm, d = 1 cm
(After Hermel, 1971)

EFFICIENCY OF SLIP-FORMS IN REINFORCED CONCRETE
STRUCTURES OF WATER TOWERS*

by

GEORGE REDEY, C.E.

Civil Engineer
New York City Board of Water Supply

*Article is based on author's experience abroad and cited references.

The status of technology is very advanced for applying Slipforms to build concrete or reinforced concrete tall walls, towers and chimneys, particularly those without construction joints.

The principal value of the technology of the slipforms application is the rapid construction, and the monolithic structure. We can gain these advantages only with high organized, skillful, disciplined work.

Most of the problems arise on the construction site connection with the speed of lift of forms. Therefore, I would like to present a scheme to avoid these problems.

The concrete is in various state of hardening and strengthening between the forms during the continuous flow of the lift. See figure 1.

Generally we can differentiate three zones. The concrete in the first zone will be in a fresh and plastic condition, so-called "work in condition," as soft concrete, having $f_c = 0$. In the second zone it starts to bond or is more or less already bonded, and we can notice here the form - concrete separation. See point b location, figure 1. In the third zone, the concrete is strengthening, hardening and if it reaches the necessary strength, it should "step out" from the forms. See point c location, figure 1.

In order to gain "workable" concrete one should select the first zone or first layer of about eight (8) inches, considered as minimum pouring unit. Pouring the concrete fast involves rapid lift of forms, and the concrete will only in-bond and has not enough strength, so we have to decrease the speed of the formlift.

On the other hand the concrete tends to bond to the forms if we are slow in lifting it, causing horizontal cracks on the surface of the concrete during the lift operation.

One should find the right speed of lift, called the LIFT of OPTIMUM. The most favorable speed of form will be determined by the requirement of the strength of concrete at the bottom of forms.

The concrete should be able to bear the dead load of the new, fresh concrete layer, plus the weight load of the forms. This requirement will be especially important for tall towers, walls, and chimneys.

The recommended speed of Formslift is shown in figure 2 and table 1 as the function of time of concrete bond.

The time of bond should control the selected lift speed.

The concrete at the bottom of forms in passing upward will separate from the forms. Here the concrete strength should be enough. See figure 1, location b. For this reason setting the end of bond-time will be especially important, otherwise one should select the speed of formlift in accordance with the bondtime of the specified concrete.

The upper curve, the end of bond, shown in Figure 2, determines the speed of lift. The points on the curve marked below represent the fresh in-bond

concrete, and is prohibited for use in slipforms. The middle part of the "start of bond curve" represents the circumstance of optimum, when the new eight (8) inch layer should be poured on the same location. Because the uncertain time of the bond it will be better if we consider a zone around of curves, above and below, where the continuous line represents the optimum. The end-of-bond of concrete will determine the speed of lift, and for this we can read a value of start-of-bond at optimum. If the real start-of-bond time lays above the curve of optimum, we can consider the new portion of concrete at the pouring, (the layer of the concrete below) has not started to bond yet. Below the curve we consider it bonded already.

We are able to estimate the start and the end of time-of-bond if we investigate the applied concrete. The datas of the start time could be more accurately estimated as the end of bond time. For this reason it will be better to use the curve of specified strength to judge the speed of lift. The intensive investigation of bond time of concrete in laboratories or field gives an opportunity to estimate the speed of lift, and we are able to determine how useful it is to apply slipforms.

The effect the hardening of the concrete.

For determining of end time of bond it is difficult to determine the speed of lift. We can substitute it with the strength of specimens immediately after the mix of concrete when enough number of specimens are taken to determine the strength of concrete at 3, 6, 9, 12, and 24 hours; furthermore 7, 14, and 28 days age. With this data we are able to draw satisfactory "Time-Strength Curve."

The first twenty-four (24) hours are the most important time for the determination of the strength of concrete, and with this data the speed of life can be determined. Figures 3, 4, 5, and 6 show strengths of concrete with relation to hour days, temperature and water/cement ratio. The best time range to move the slipform is between 6 to 12 hours. At this time the strength of concrete varies above and below 68°F. Therefore, we can say, 68°F. is the best time to pour the concrete. Selection of those days is advisable. On figure 7 is shown the variance of relative strength of concrete at 1, 7, 14, and 28 days age, considering 100% strength at 28 days age. To satisfy the one-day strength requirement of about 25% of full strength, equivalent to $fc' = 1000$ lbs./sq. inch or $fc = 4000$ lbs./sq. inch after 28 days of pouring must be achieved. We can see the water/cement ratio of about 0.32 gives 24%-34% strength of fc' , but about 0.4 water/cement ratio already decreases the strength with the value about 15% of fc' . A soil-moisted, softly-plastic consistency of concrete gives the best result of strength at 24 hours. The first 24 hours gives the most important significance to determine the speed of Formlift. On figure 3 is shown the variance of the concrete strength at the first 24 hours. The application of the slipform method demands a 25% strength of 24 hours so the concrete already will free from the forms, moving up to the next higher position. We have to hold the time of the strengthening to secure the life of optimum on curve B, see figure 7 or we can say:

6 hour	concrete	strength	should	be	around	6%
12 hour	"	"	"	"	"	25%
18 hour	"	"	"	"	"	60%
24 hour	"	"	"	"	"	100%

Keeping the course of the strength on curve A, we gain the possibility of a more rapid speed of lift. We should keep in our mind the relative variance of strength of concrete beforehand, but finally we have to choose the speed of lift in accordance the real time of strengthening.

The determination of speed of Formlift by strengthening of the concrete.

- a/ The case of a given proportion of materials used in concrete.
 - b/ Given speed of lift.
 - c/ Specified strength of concrete.
 - d/ Determination of speed with mutual consideration of the start of bond and specified strength of concrete.
- a/ The case of a given proportion of materials used in concrete.

Determine the strength of concrete in the first 24 hours to know the variance of the strength.

Draw the gained values on a graph.

See figure 8. The upper part of figure 8 includes marked curves "A," "B," "C" and "D," which give information for the speed of lift. On the horizontal axis is marked the time in hours units. On the vertical axis is shown the strength of the concrete. If the data collected by testing drops below curve "A," the activity of the Formlift should stop, because the strengthening of the concrete is slow, and we cannot secure even the minimum speed.

The minimum speed should be at least 2 1/2 inch per hour or 5/6 inches for each 20 minutes, because if the speed is slower the concrete will bond to the forms.

Between curves "A" and "B" the concrete needs a slow speed of lift. Between "B" and "C" the lift will be the optimum, but between "C" and "D" rapid lift will be necessary. The lower part of figure 8 serves for the determination of speed. On the horizontal axis the speed in inch per hour is shown and the curves representing the distances moved by the forms upward for the considered speed and time.

Use the Figure as follows:

We know the history of the concrete strengthening in the first 24 hours by our testing. It is the real strengthening and is marked on figure 8 with the dashed line (see curves "E").

The job specifications will indicate the necessary strength where we will be able to free the forms from concrete and apply the lift.

The intersection between the curve "E" line and the specified strengths line, is selected as 355# per sq. inch giving us a proper time. In figure 8 we found 10 hours the time to obtain the necessary strength.

Select a 48-inch height form. Consider 5 inch a free zone on the top of forms, and an additional 8 inch zone for the new poured fresh concrete we found the distance the Form should travel for each cycle, here $48-2-20 = 38$ inches, to completely free the concrete from the forms. Because 10 hours is required to reach the specified strength we can see the proper speed will be 38 per 10 hours or 3.8 inch per hour.

Considering further, the concrete after 2-3 hours of separating from the forms, the real distance between forms and concrete will be less by the distance of the 2-3 hour way, equivalent to 12 inches, decreasing the total from 38 to $38-12 = 26$ inches (+). The real cycle will 26 inches with a 7-hour elapsing time to travel 26 inch with the above determined speed, the strength of the concrete is up to about 130# per sq. inch. Considering an 8-inch thick layer of concrete for each pour (it is a practical consideration to use a vibrator), we have a time of about 2.1 hour or 2 hours and 6 minutes time to pour each 8 inch zone with 3.8 inch per hour speed. See figure 9. We are in the slow speed zone.

We can choose 41 inch long forms and apply 6.25 inches per hour speed for example. The cycle will $41-2-8 = 31$ inches, and needs about 4.9 hour time to travel, but during this time the strength should reach the specified level, 355# per sq. inch (see figure 8). We can conclude, how important it is to determine accurately the course and history of the strength developments in the early hours.

at slow speed (2 1/4-4 inch per hour) at ages 9, 12, 18, 24 hours,

at lift of optimum (4-8 inch per hour) at ages 3, 6, 9, 12, 24 hours

at rapid lift (8-10 inch per hour) at ages 1, 2, 3, 6, 24 hours.

At the first test investigation of the concrete we can conclude which type of speed will be the most preferable to apply.

In every 24 hours we have to continue the testing of concrete in order to receive the values of strength of concrete. In other words we have to know the course of strengthening. Having this data we are able to change the speed from time-to-time as necessary.

b/ The case of given speed.

The applicable maximum speed could be determined on the jobsite by the following:

1/ The given technology of concrete work.

2/ The capacity of transportation, elevating machines, conveyors, etc.

3/ Quantities and qualities of tools.

4/ Number of laborers.

The concrete should reach the specified strength, 355# per sq. inch after -8 hours if we select the speed 5.1 inch per hour using a 40-inch high Formtable. See figure 8, with curve 30 inches. To satisfying the above selected example data, we should choose the right concrete mix or we should add chemicals so that the strength of concrete reaches the specified level at the right time considering the right time the time of concrete separation from the Formtable. If it is impossible to reach this time we can consider whether to apply chemicals (should be a careful consideration) or we can change the speed accordingly.

c/ The case of the specified strength of concrete.

A minimum strength of about 355# per sq. inch should secure the concrete at the separation time and location. It is about 2/3 the height of Form, measuring from the top and about 2-3 hour time after the concrete is poured. It is very important that the designer specify the strength of concrete and exercise control also. The designer should give to the field engineer or resident engineer a TIME-Strength LIMIT CURVES, detailed for the first 24 hours.

The field engineer should know the specified strength and should apply the right speed of Lift.

d/ The case of determination of the speed of lift considering the start time of bond and strength together.

We assumed previously the concrete would mix on the jobsite. But is possible the concrete mix plant is not close to the job site. The concrete, already in the place, should not have bonded at the time of arrival and pouring of the new portion of concrete delivered from the plant. If the course of bond already developed for the new layer of concrete will not "work-in" to the lower layer, because the head of the vibrator cannot merge deep enough in the concrete, a minimum about two (2) inches this headportion is necessary.

For this reason we have to determine not only the course of strengthening for the first 24 hours, but we have to determine the time of beginning of the hardening too.

We have to take into consideration the following to determine the speed of the Lift, if the concrete factory is far from the jobsite:

Build and mark a curve for time-strength, take the data from the tests. (See figure 10, curve "E.")

Measure time on the abscissa equivalent with the age of concrete if it was placed immediately after mix. Concrete "E" at 10-hour age reaches the specified, 355# per inch strength.

For example, consider a 44-inch high Formtable, 8 inch thick concrete layer, 2 inch free zone, the Formtable will slide up $44-8-2 = 34$ inch until the fresh poured concrete will free from the Formtable. In this case the speed will be 3.40 inch per hour (see point of "a" on figure 10). Let 3.50 hour be the start time of bond, which is marked on figure 10 with small circle. Between start to bond to reach the specified strength, the time interval will $10-3.5 = 6.5$ hours (See S_1 distance on the figure 10.) Move the S_1 distance on the curve 34-inch parallel with the abscissa until the starting point of it reaches the 8-inch curve. We found a speed about 4-inch per hour, see point "β." Actually we pushed the curve of strength "E" left with a 1.5 hours, and we apply the curve "E." An 8-inch thick layer will need about 2 hours time to pour a 3.5 hour bond start time, less 2-hour working time allows us only about 1.5 hour to wait to pour the next 8 inch layer.

We can see here, the maximum speed is 4 inch per hour with this high Formtable and given concrete. If we slide the Formtable faster, or increase the speed, the concrete has not yet the necessary strength to carry the load at time of freeing the Formtable.

If we moved the S_1 distance on the 34 inch curve further down, we gain speed as large as 4 inch per hour -- the bond should start before the placement of the concrete, which is obviously an impossible case.

With the above demonstrated procedure we are able to determine the minimum speed too. If the Formtable slides up exactly 8 inch, or one layer, it will be the minimum speed.

For 8-inch sliding with a 3.5 hour bond start time the curve "E" represent 2.17 inch per hour speed. For practical value we can select 2.5 inch per hour minimum and 4 inch per hour maximum speed if the Formtable height is 44 inch.

If the speed is slower the concrete is already in bond or we have to decrease the thickness of the 8-inch layer.

If we increase the thickness layer from 8 to 10 inch (for example), we receive new speed values of 2.75 inch per hour minimum and 3.5 inch maximum.

Generally speaking, one can decrease of layer by accelerating the speed and increase the layer by deaccelerating the speed and narrowing the zone of speed.

Examine another concrete, mixed with a changed proportion, designated by curve "F," (see figure 10).

We can consider another bond start time, of 1.5 hours (see small circle). The specified strength occurs at 5-hour age. S_2 distance represents the time interval for it, equivalent to $5-1.5 = 3.5$ hours.

Place the concrete immediately after mix and using a 44-inch high Formtable, 8-inch layer with a 34 inch sliding and 34 inch curve, we receive 6.5 inch per hour speed (see location of "γ" point, figure 10).

The minimum speed is 5.1 inch per hour (see location ψ .) We receive the maximum speed, if we push over the S_2 distance on curve 34 inch, equivalent 7.1 inch per hour (see location " σ ").

In a given case, we have to keep the speed of Lift between those two values with the same concrete, both higher form. For 48-inch height the minimum speed will be 5.1 and the maximum speed will be 8.1 inch per hours. Note that the increase of the height of Formtable in the zone of the rapid lift is significant. The same method could be applied if we select the speed of lift.

In this case we will have to change the sequence of the procedure to gain the curve of concrete with the predetermined speed requirement to satisfy the time and travel.

If we determine the thickness of the layer, the zone of speed should be calculated, applying the above technique.

CONCLUSION

We are able to predetermine the speed of SLIP-FORMS on the job-site, applying a rapid method using the graphic procedure. It is necessary to determine the variation of strength of concrete in the first 24 hours and the start time of the bond to satisfy the above mentioned and determine the speed of lift.

With the knowledge of course of strengthening of the concrete mixes, we are able to inspect the strength of concrete at the separation from the Formtable. Furthermore, the time when concrete just passes the forms could determine the time to pour the next, new layer.

Information about the strengthening in the first 24 hours is absolutely necessary.

With the knowledge of the bond time of mix it will be possible to determine the extreme values of speed of lift.

Reference Cited

Lanyi, J., Dr. Orosz, A.: Predetermination of Lifting Speed for Sliding Formworks. Mélyépítésitudoomány Szemle, Dec. 1973, Budapest.

American Concrete Institute: Building Code Requirements for Reinforced Concrete, ACI 318-63, ACI 318-71.

American Society for Testing and Materials/ASTM/: Book of ASTM Standard.

American Concrete Institute: Recommended Practice for Evaluation of Compression Test Results of Field Concrete, ACI 214-65.

Reference Recommended

American Concrete Institute: Causes, Mechanism and Control of Cracking In Concrete, ACI Publication SP-20.

- American Concrete Institute: Reinforced Concrete Design Handbook, ACI Publication SP-3.
- Rice and Hoffman: Structural Design Guide to the ACI Building Code, Van Nostrand Reinhold Company.
- Palotas, L.: Építőanyagok, I-II, Akadémiai Kiadó, Budapest, 1959-1961.
- Nenning, E.: Les coffragesglissants mode de construction rapide, Annales de l'Institut Technique du Batiment et des Travaux Publics, No. 111-112, 1957.
- Dinescu, T.-Sandru, A.-Radulescu, C.: Építés Csuszózsákkal, Műszaki Könyvkiadó, Budapest, 1967.
- Slipformed Tower Post - Tensioned to Record Height of 1805 Feet: Engineering News Record, May 23, 1974.
- Neel, J. Everard and Tanuer, J. L. III: Theory and Problems of Reinforced Concrete Design, Schoum Publication Company.
- Winter, G., Urquhart, L. C., O'Rourke, C. E., Nilson A. H.: Design of Concrete Structures, McGraw-Hill Book Co.

Table 1. - Speed of formslift and time of concrete bond

SLIDING SPEED OF FORM		TIME OF BOND IN HOURS	
INCH/HOUR	FEET/DAY	START	END
2.0	4.0	4-4.5	8-13
4.0	8.0	2-3.0	6-8
6.0	12.0	1.5-2.5	4-5
8.0	16.0	1-2	3-4.5
10.0	20.0	1-1.5	2.5-3.5

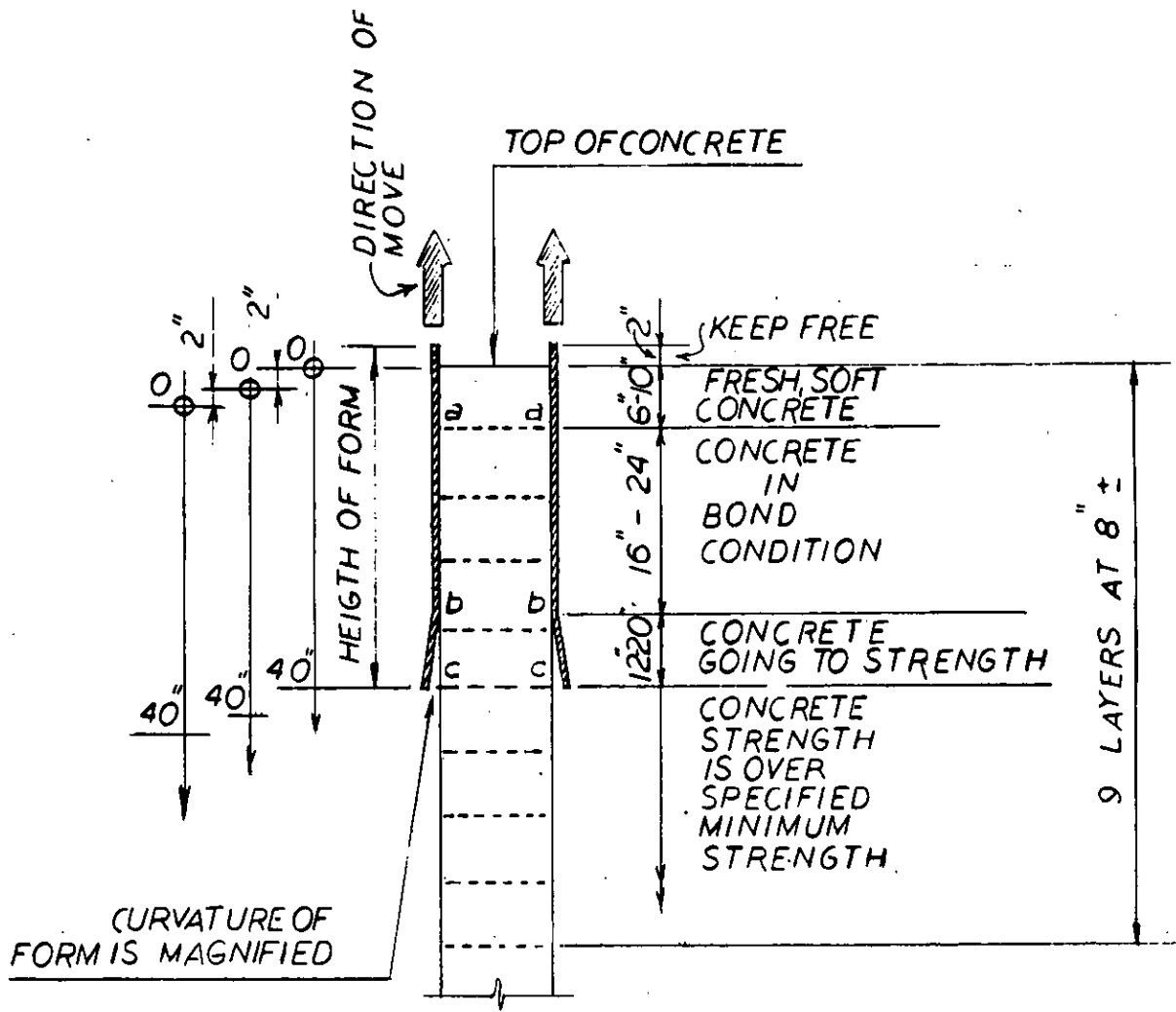


Figure 1. Zones of concrete in the flowlift.

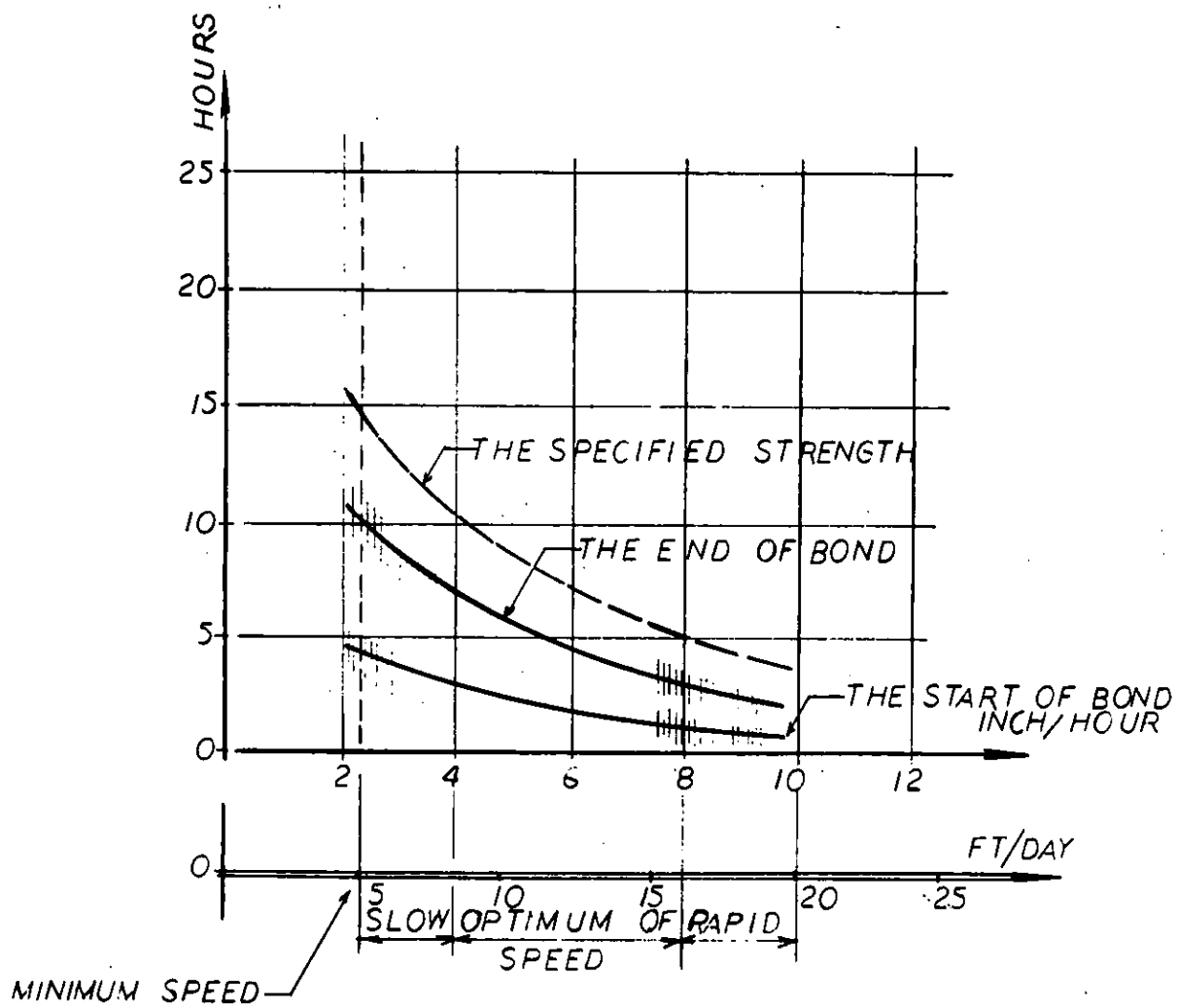


Figure 2. Speed of Formslift.

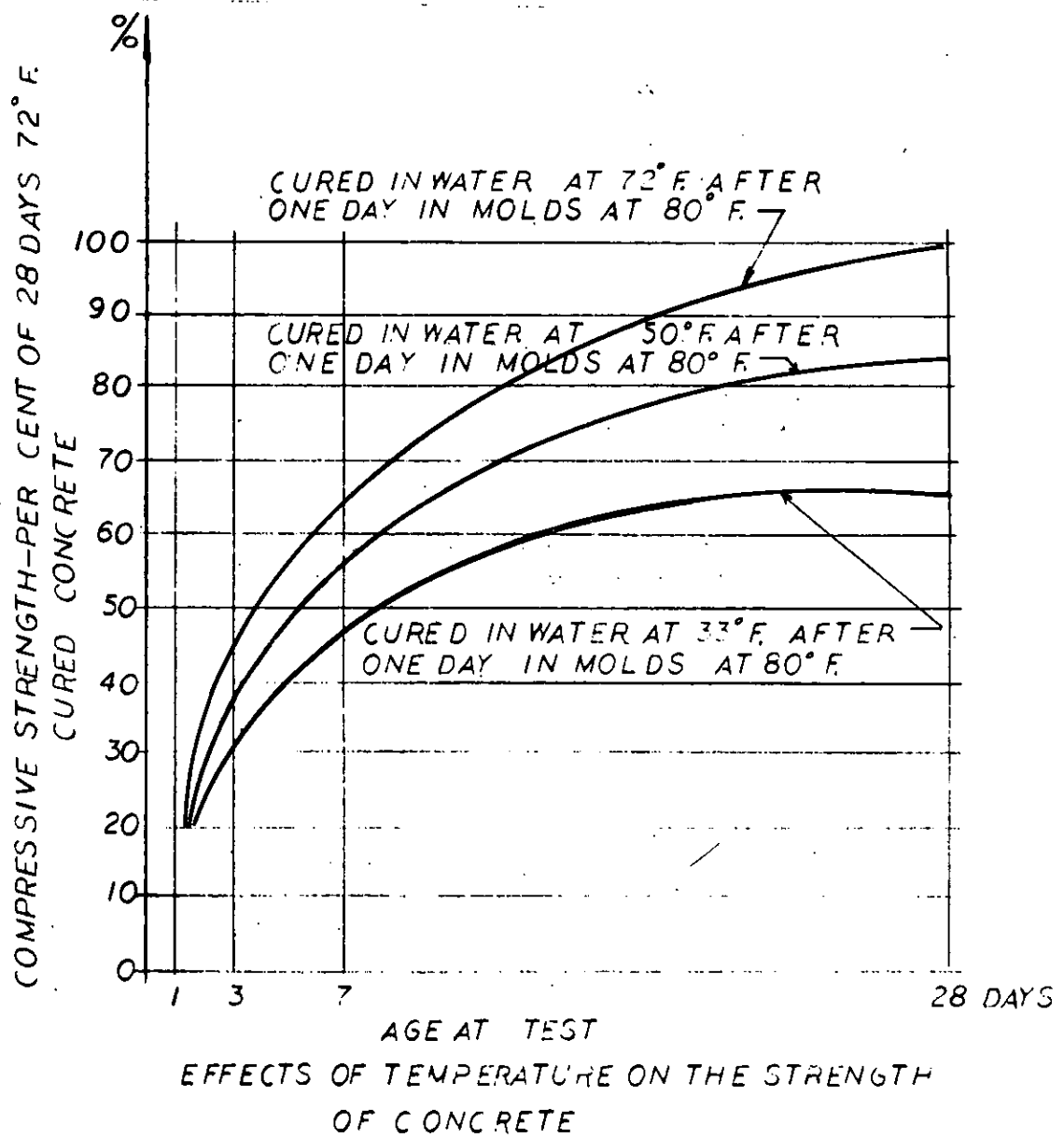
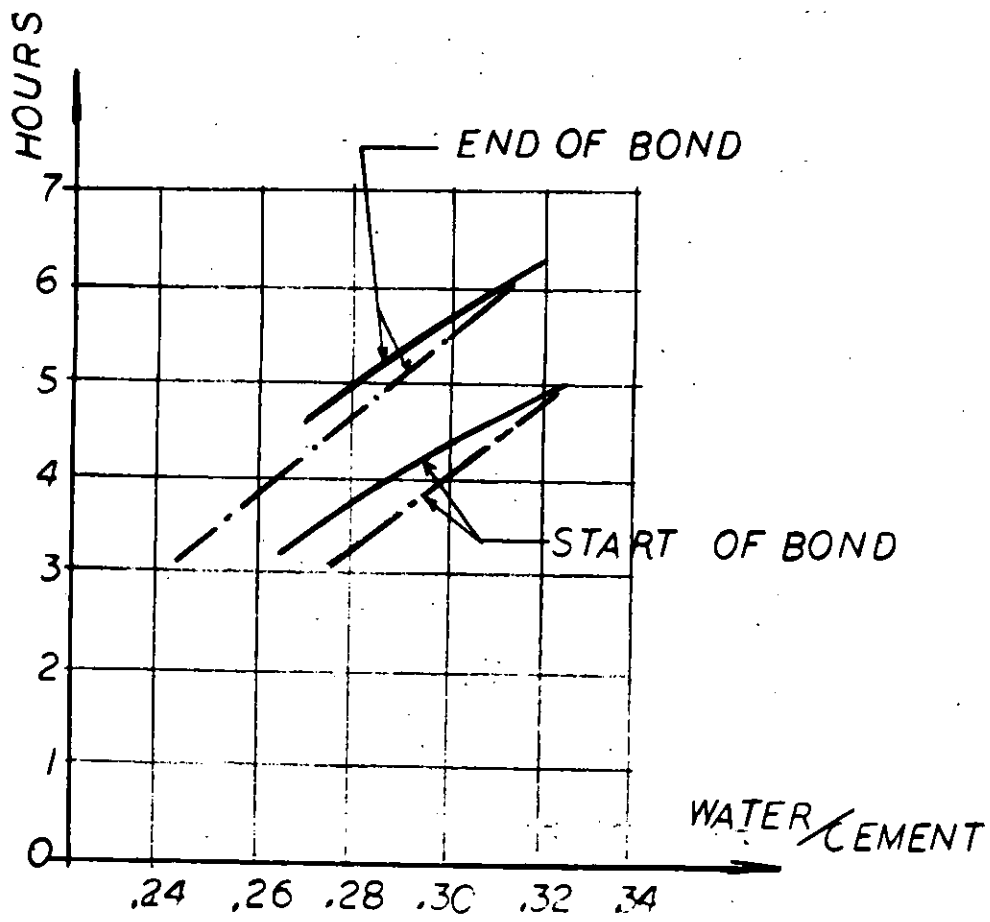


Figure 3



EFFECT OF RATIO OF WATER CEMENT
ON TIME OF BOND

Figure 4

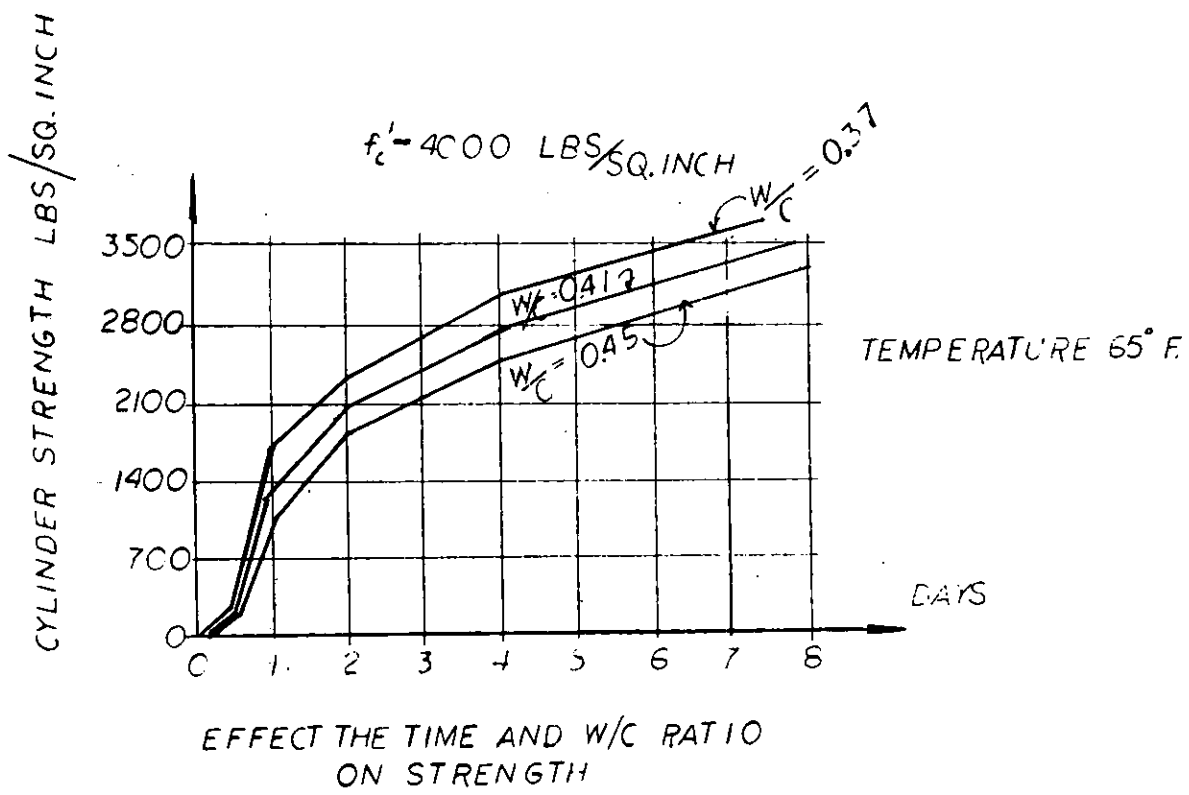


Figure 5

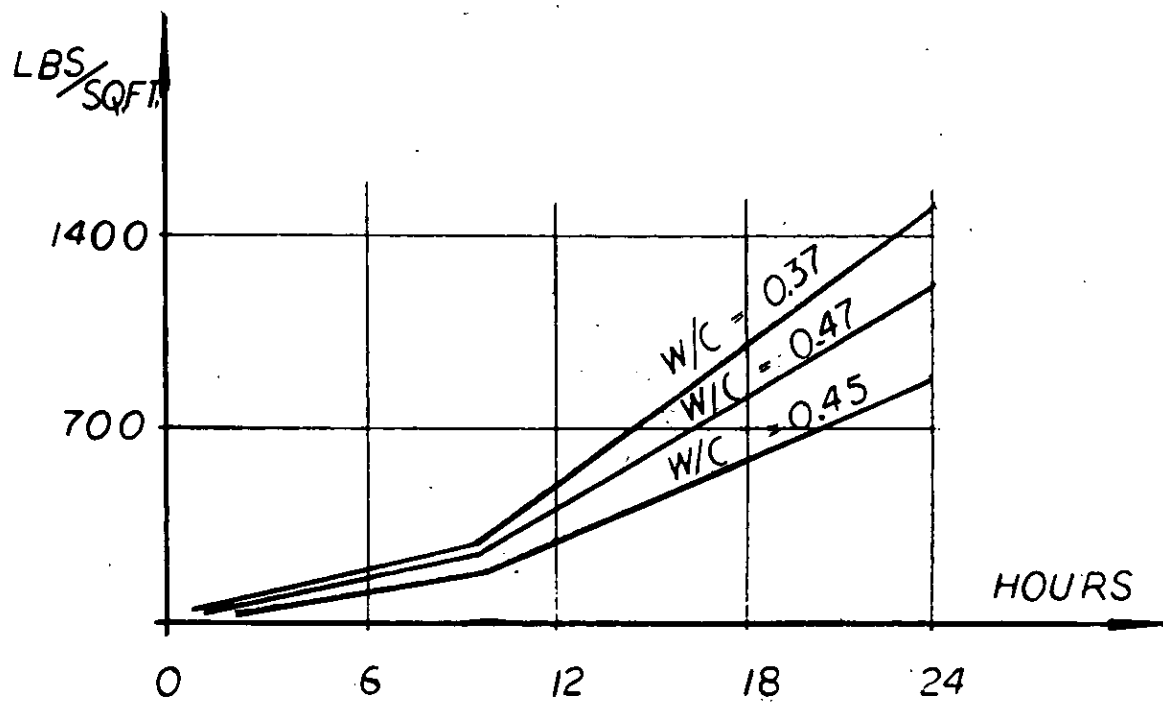


Figure 6

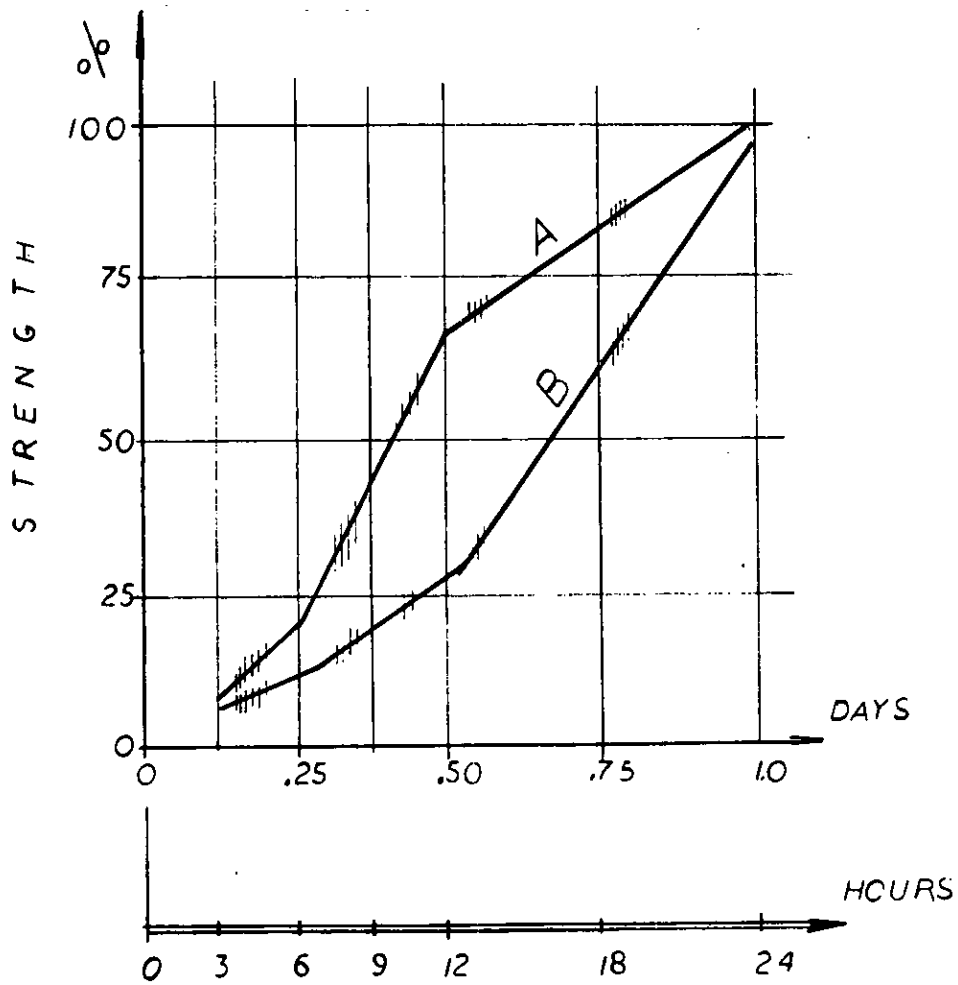


Figure 7. Variance of relative strength of concrete.

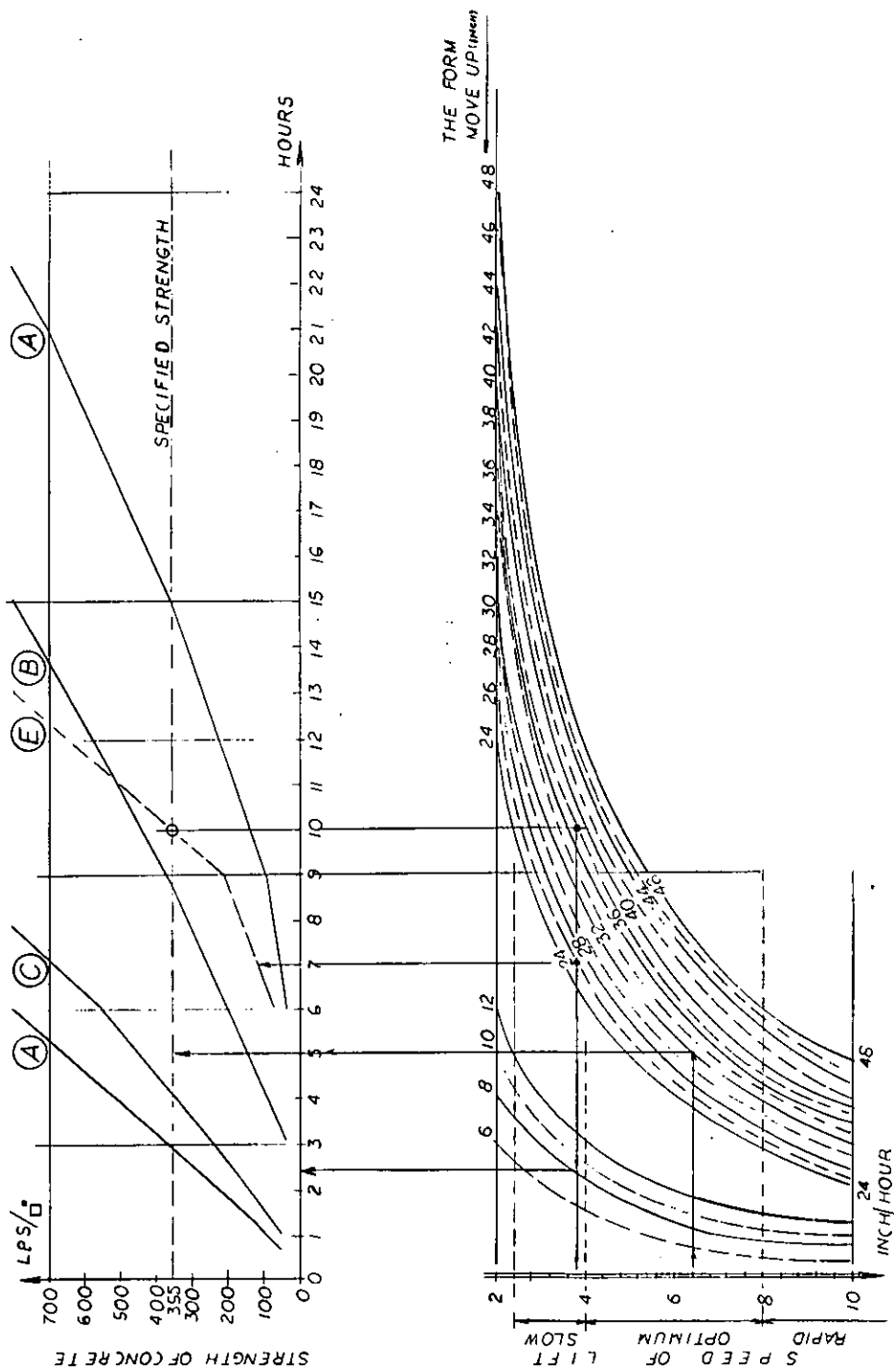


Figure 8. Speed of form and strength of concrete.

SLIDING FORM (EXAMPLE)
 (SPECIFIED STRENGTH 355 ψ)
 (THE FORM MOVE 3.8 INCH PER HOUR)
ELAPSED TIMES

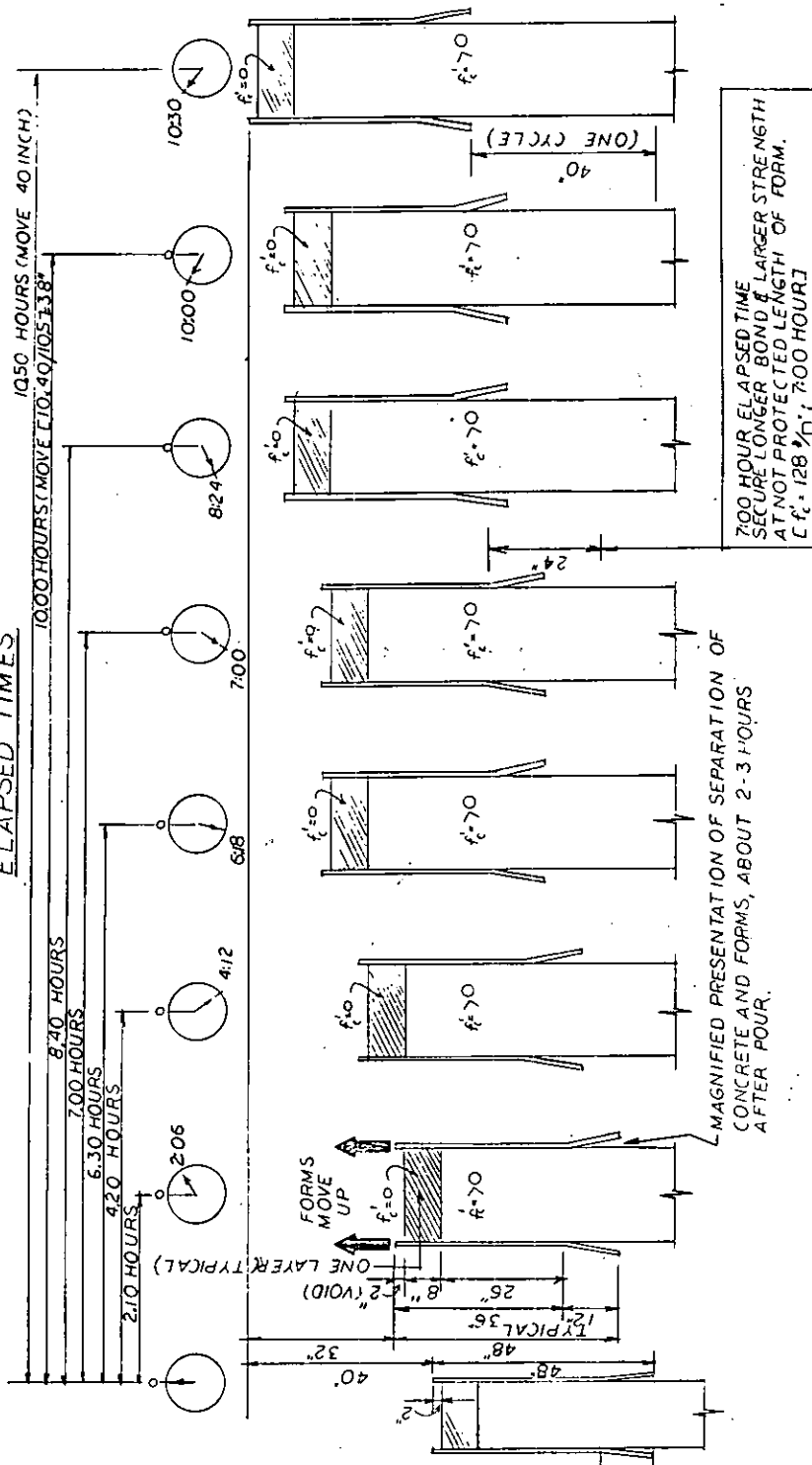


Figure 9. Sliding form elapsed times.

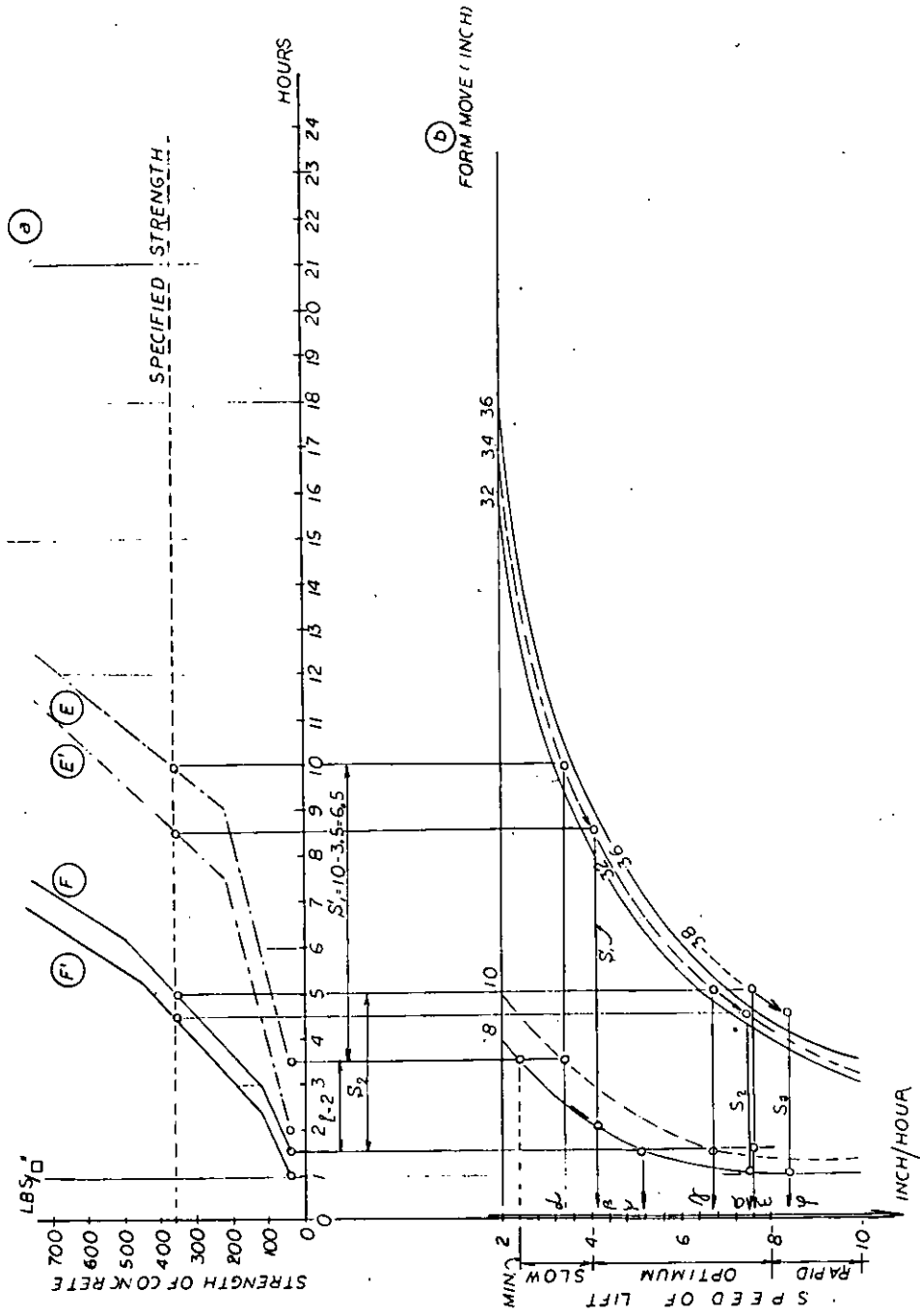


Figure 10. Speed of lift and strength of concrete.

PRECIPITATION AND SNOWFALL OVER NEW JERSEY

by

DONALD V. DUNLAP*, PH.D.

Rutgers University

*Formerly NOAA State Climatologist for New Jersey.
Currently Adjunct Professor of Meteorology at Rutgers University, and Lecturer
in Meteorology at Temple University.

Much interest has been generated over the past several years in climatic changes, whether they be real or imagined. The purpose of this paper is to examine the precipitation records for the three climatic divisions of New Jersey, from January 1929 through June 1978, in order to determine the magnitude of these changes. The starting point of 1929 was chosen because that is the first year for which official averages are available for individual climatic divisions.

Calculations of snowfall by climatic divisions were begun with the 1956-57 season, so that record is necessarily much shorter than the precipitation record.

Figure 1 shows the divisional boundaries within New Jersey, and indicates the weather reporting stations which were in operation in 1977. The northern division is that area lying north of Mercer and Middlesex counties. A strip about ten miles wide, extending from Sandy Hook to Cape May, comprises the coastal division. No point in the Cape May peninsula is more than ten miles from either the Delaware Bay or the Atlantic Ocean.

Long-term records of temperature and precipitation are frequently referred to as 'normal' values. Climatic 'normals' are calculated for 30-year periods, with the last year ending in zero. This is an international standard adopted around the turn of the century by the International Meteorological Organization, and continued by its successor, the World Meteorological Organization.

References are made in this paper to the normals for 1931-60 and for 1941-70. The 49-year record from January 1929 through December 1977 is compared with the two 30-year normals mentioned above.

Precipitation over northern New Jersey averaged 46.36 inches for the period 1929-77, while for the 1931-60 period the average was 46.96 inches, and for 1941-70 it amounted to 44.98 inches. The most significant difference, the drop in the figures for 1941-70, must be attributed to the prolonged drought of the early 1960's, which lasted from September 1961 through August 1966. This was the most severe drought, both in duration and in intensity, since weather records began in the early 1800's. Records from New York City and Philadelphia provide a good indication of the climate of New Jersey, prior to the establishment of weather stations in this State.

The drought of the early 1930's, responsible for the dust bowl of the southwestern United States, was much shorter and less intense in the middle Atlantic states than that of the 1960's. One exception was northern West Virginia, where the drought of the 1930's was more severe than that of the 1960's.

Decreases in precipitation for the 1941-70 period over the southern and coastal divisions of New Jersey occurred similarly to the decreases mentioned above over northern New Jersey.

The average precipitation over northern New Jersey for the period 1971-77 is 54.31 inches, which includes the record maximum annual total of 63.59 inches in 1975. The 1975 figure is 9 percent greater than the second highest value, 58.39 inches in 1952.

A look at the seasonal analyses of precipitation over New Jersey provides some interesting insights into the problem of rainfall distribution during the agricultural growing season. A review of precipitation records for southern New Jersey shows that the period from April through September 1957 was the driest growing season on record, while the same period in 1958 set a new record as the wettest growing season on record. The 13.29 inches in 1957 still stands as the driest growing season in southern New Jersey, notwithstanding the drought of the 1960's, while the 31.00 inches in 1958 was exceeded by the 34.19 inches from April through September 1975.

Over northern New Jersey, April-September precipitation has ranged from a minimum of 14.46 inches in 1965 to a maximum of 39.15 inches in 1975. The 1975 amount was 62 per cent of the annual total of 63.59 inches. The 14.46 inches in 1965 was 47 per cent of that year's total of 30.46 inches.

Similar comparisons may readily be made by using data from the coastal division. For those who have a special need, the year may be divided into three-month seasonal periods. Only a few samples of data handling are provided here; the monthly tabulations are to be found in Tables 1-3, for those who wish to make their own analyses.

Snowfall is exceedingly variable over New Jersey, with the northern division having seasonal totals ranging from 74.0 inches in 1960-61 to 7.6 inches in the 1972-73 season. The southern divisional totals have ranged from 52.0 inches in 1957-58 to 0.7 inch in 1972-73. The coastal division ranged from 45.6 inches in 1960-61 to 0.8 inch in 1972-73. The 22-season averages for these divisions are 35.2 inches in the north, 22.3 inches in the south, and 22.4 inches along the coast.

Monthly snowfall totals have ranged as high as 25.1 inches in the north, and 23.3 inches in the south, both in February 1967. The greatest monthly snowfall along the coast was 26.5 inches in January 1965. Tabulations of monthly and seasonal snowfall values are shown in Tables 4-6.

This paper brings together, probably for the first time, the monthly values of precipitation by climatic divisions in New Jersey, covering nearly half a century. Summaries of both precipitation and snowfall data are to be found in Table 7. Most of the data were extracted from publications of the U.S. Department of Commerce's National Climatic Center, Asheville, North Carolina. The precipitation data for 1929 and 1930 were extracted from an unpublished manuscript copy of Palmer Drought Index values, furnished by the National Climatic Center.

An examination of storm totals, both for rainfall and for snowfall, should be the subject of a future paper, with the inclusion of a statistical analysis of return periods for various intensities of precipitation or snowfall.

REFERENCES

U. S. Department of Commerce, NOAA, National Climatic Center, Climatological Data, New Jersey, 1931-1978.

_____, Decennial Census of United States Climate-Monthly Averages for State Climatic Divisions, 1931-1960, New Jersey, Climatography of the United States No. 85-24, 1963.

_____, Monthly Averages of Temperature and Precipitation for State Climatic Divisions, 1941-1970, New Jersey, Climatography of the United States No. 85 (By State), 1973.

_____, Climates of the States, New Jersey, Climatography of the United States, No. 60-28, 1967.

_____, Palmer Drought Index, unpublished tabulations for New Jersey, 1929-1978.

Figure 1

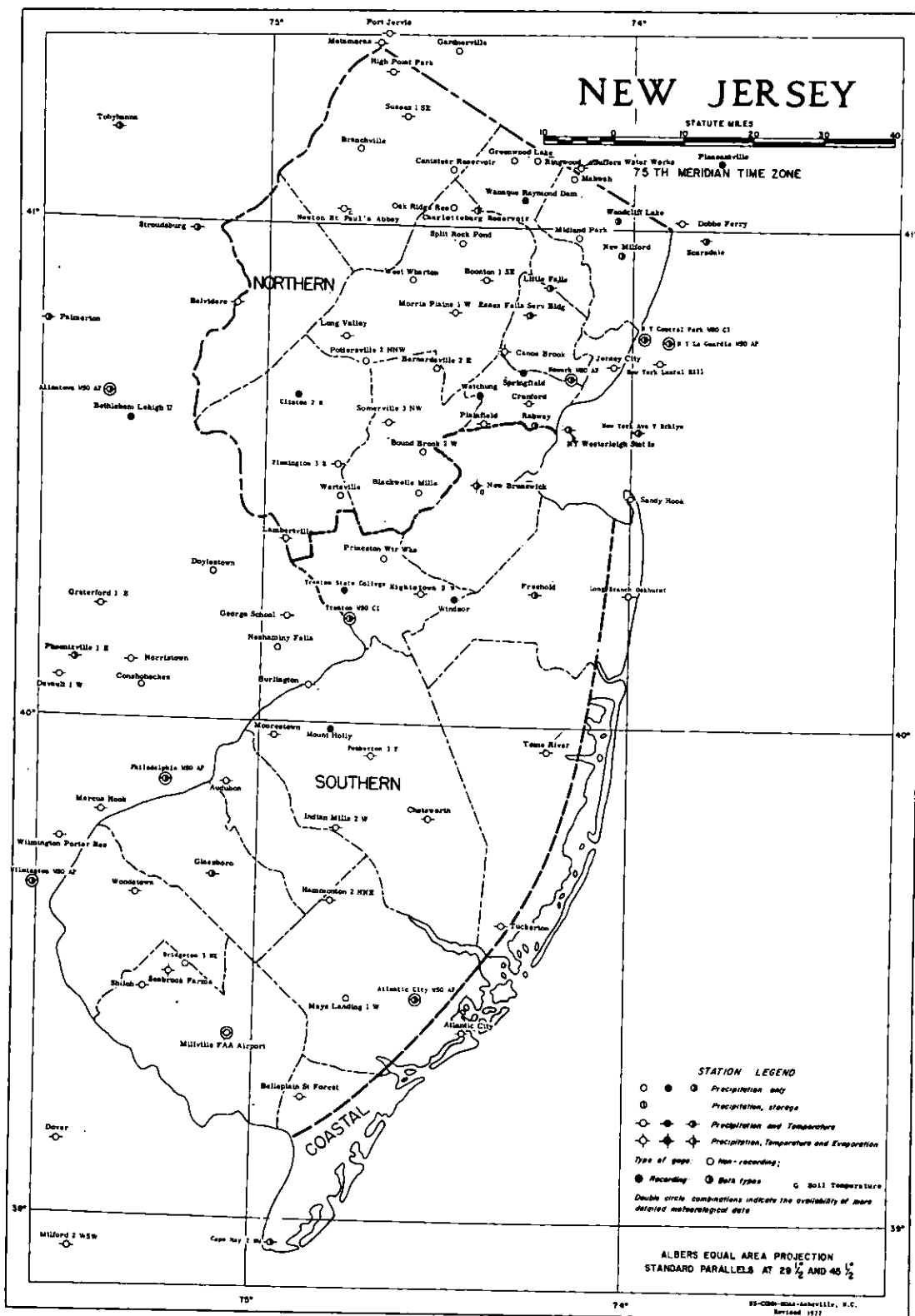


Table 1a

NORTHERN NEW JERSEY PRECIPITATION
(Inches)

Year	Jan.	Feb.	Mar.	Apr.	May	June	July
1929	3.59	4.03	3.25	6.57	3.88	3.05	1.62
1930	2.63	2.47	2.83	2.75	3.02	4.10	3.87
1931	2.09	2.34	3.69	2.99	4.50	5.30	5.18
1932	4.17	2.40	4.86	2.33	2.55	3.52	2.45
1933	1.82	3.17	5.07	5.11	4.67	2.79	3.66
1934	3.15	2.26	3.48	4.31	4.73	4.15	3.68
1935	3.49	2.55	2.48	1.81	1.20	4.34	6.28
1936	6.66	2.83	6.05	3.78	3.12	5.85	1.95
1937	6.29	2.47	2.80	4.67	3.34	5.11	3.59
1938	3.93	2.21	2.42	3.21	3.46	7.74	9.01
1939	3.63	5.21	4.47	5.06	1.51	3.65	2.21
1940	2.27	2.86	5.73	5.87	6.39	4.04	3.08
1941	3.04	2.44	2.69	2.23	1.90	4.82	6.07
1942	2.92	2.73	5.63	1.44	3.19	3.91	7.61
1943	3.06	2.09	2.85	2.67	5.71	3.56	4.50
1944	3.37	2.43	5.71	5.36	1.83	4.53	1.83
1945	3.53	3.19	2.73	3.87	6.11	4.93	10.23
1946	1.57	2.22	3.09	1.35	7.53	5.24	6.23
1947	3.48	2.06	3.19	5.02	7.67	4.55	4.94
1948	4.19	2.34	3.73	3.92	7.80	6.02	4.09
1949	6.28	3.05	2.16	4.38	4.86	0.24	4.49
1950	2.80	4.45	4.52	2.34	3.77	3.09	5.38
1951	3.67	4.47	6.41	3.33	4.28	4.13	6.47
1952	4.95	2.38	5.39	7.36	5.98	5.11	5.52
1953	5.97	2.34	7.43	6.26	4.92	2.49	4.13
1954	1.98	2.10	3.75	3.09	4.53	1.06	1.69
1955	0.93	3.23	4.39	2.65	1.60	3.76	1.10
1956	1.86	4.76	5.06	3.78	2.69	4.10	5.61
1957	2.10	2.49	2.72	5.81	2.71	2.21	1.92
1958	5.07	4.23	4.25	6.59	3.94	2.71	4.78
1959	2.51	2.02	3.78	3.02	1.45	5.10	4.00
1960	3.29	4.24	2.36	3.72	4.22	2.35	7.92
1961	2.88	3.40	4.91	5.68	3.58	2.58	6.44
1962	2.79	4.14	3.10	4.21	1.49	3.63	2.56
1963	2.53	2.35	3.45	0.86	2.91	2.59	3.23
1964	4.65	2.83	2.24	5.74	1.19	3.33	4.40
1965	2.64	3.08	2.83	2.43	1.54	1.34	2.37
1966	3.05	3.72	2.43	2.75	3.88	1.04	1.47
1967	1.47	2.04	6.17	2.68	3.90	3.55	6.45
1968	2.28	0.98	4.48	2.76	7.29	5.52	1.51
1969	1.69	2.17	3.30	3.52	2.87	3.75	8.56
1970	0.81	3.47	3.58	4.05	3.29	2.73	3.45
1971	2.73	5.10	3.45	2.55	4.54	1.56	5.36
1972	2.45	4.55	3.68	3.37	6.63	10.87	4.01
1973	4.60	3.67	3.69	7.09	5.43	6.49	4.31
1974	3.48	1.81	5.45	3.99	4.02	4.32	2.16
1975	5.43	3.67	4.21	2.95	4.75	6.99	10.83
1976	5.32	2.66	2.30	2.80	4.08	4.70	3.81
1977	1.62	2.76	7.22	4.69	1.83	4.70	2.31
1978	8.12	1.69	3.95	2.24	7.32	4.43	

Table 1b.

NORTHERN NEW JERSEY PRECIPITATION
(Inches)

Year	Aug.	Sept.	Oct.	Nov.	Dec.	Annual Total
1929	2.81	4.82	4.74	2.70	3.19	44.25
1930	3.63	2.45	1.67	4.65	2.83	36.90
1931	3.69	2.22	2.71	0.82	2.28	37.81
1932	2.96	2.16	6.52	8.70	2.32	44.94
1933	9.96	7.59	2.35	0.62	2.89	49.70
1934	3.23	10.14	2.63	3.14	2.79	47.69
1935	2.07	4.60	4.55	4.41	1.43	39.21
1936	4.50	2.88	3.83	1.41	6.36	49.22
1937	7.38	2.78	4.41	4.63	2.18	49.65
1938	2.77	8.99	2.26	3.27	3.49	52.75
1939	4.54	1.76	3.98	1.79	1.93	39.74
1940	5.30	4.12	2.41	4.57	3.48	50.12
1941	4.85	0.46	2.00	3.27	3.98	37.75
1942	9.49	6.13	3.27	4.66	5.05	56.03
1943	3.32	1.60	7.58	3.37	1.18	41.49
1944	2.48	7.17	1.75	6.24	3.32	46.02
1945	4.76	5.65	2.46	5.94	4.39	57.79
1946	4.92	3.94	1.79	1.32	2.10	41.30
1947	3.60	3.22	2.15	7.21	3.36	50.45
1948	4.71	1.03	1.89	4.00	6.73	50.45
1949	3.43	4.29	1.92	1.31	3.43	39.84
1950	4.84	2.29	1.87	5.73	5.07	46.15
1951	3.56	1.99	4.59	7.09	5.21	55.20
1952	6.15	5.20	0.89	5.06	4.40	58.39
1953	2.18	2.06	3.64	2.12	5.11	48.65
1954	7.47	5.73	2.21	5.94	3.70	43.25
1955	14.36	2.79	8.88	3.02	0.37	47.08
1956	3.61	4.16	3.02	3.77	4.36	46.78
1957	2.18	2.83	3.18	3.72	6.97	38.84
1958	3.32	4.51	5.95	3.13	1.36	49.84
1959	5.77	2.43	5.86	3.90	4.66	44.50
1960	5.92	7.17	2.10	2.31	2.86	48.46
1961	4.42	1.96	1.92	3.22	3.36	44.35
1962	5.58	3.52	3.58	4.43	2.65	41.68
1963	2.21	4.40	0.37	6.94	2.11	33.95
1964	0.64	1.59	1.21	2.43	4.40	34.65
1965	3.96	2.82	3.41	2.03	2.01	30.46
1966	2.59	7.24	4.21	3.80	3.91	40.09
1967	7.11	2.11	2.78	2.43	5.53	46.22
1968	3.20	2.32	2.51	4.99	3.86	41.70
1969	4.54	5.39	1.81	3.54	5.75	46.89
1970	4.45	2.29	4.54	5.65	2.74	41.05
1971	10.28	6.52	4.23	5.39	1.88	53.59
1972	1.89	2.38	4.67	9.70	6.16	60.36
1973	4.96	3.88	4.62	1.84	8.93	59.51
1974	6.78	7.62	2.15	1.86	5.03	48.67
1975	4.37	9.26	4.33	3.96	2.84	63.59
1976	4.14	3.40	6.22	0.64	2.41	42.48
1977	4.29	5.21	4.50	7.30	5.51	51.94
1978						

Table 2a

SOUTHERN NEW JERSEY PRECIPITATION
(Inches)

Year	Jan.	Feb.	Mar.	Apr.	May	June	July
1929	3.39	4.22	2.70	6.55	2.95	3.35	1.74
1930	3.18	3.35	2.35	1.88	2.56	4.31	4.09
1931	2.15	1.85	4.47	2.53	3.01	4.46	3.80
1932	4.77	1.72	6.39	2.88	3.33	3.94	3.28
1933	2.88	3.30	4.79	4.47	5.21	2.86	4.01
1934	2.60	3.16	3.13	3.45	4.38	3.48	3.31
1935	4.34	3.01	2.54	2.84	2.39	4.91	3.60
1936	6.20	3.23	4.57	2.60	2.31	4.20	3.14
1937	6.32	2.13	2.76	4.77	3.07	4.37	1.97
1938	3.17	2.49	1.90	2.38	3.48	7.95	8.59
1939	4.19	5.79	5.25	5.28	1.35	3.84	2.71
1940	1.60	3.25	4.54	5.47	6.30	2.48	2.13
1941	3.76	2.39	2.75	2.37	1.86	5.47	7.43
1942	3.01	2.60	5.77	1.34	1.91	2.74	6.44
1943	2.87	1.89	3.10	2.88	4.61	3.38	4.16
1944	3.52	2.17	5.85	5.47	1.54	3.85	1.24
1945	2.61	3.26	2.15	3.00	3.79	3.59	9.33
1946	1.97	2.14	3.57	1.57	5.96	5.50	5.67
1947	3.93	1.88	2.31	3.62	7.21	3.23	4.13
1948	5.35	2.68	3.52	3.54	8.19	4.76	3.98
1949	5.79	4.15	3.05	3.16	4.84	0.25	3.42
1950	2.11	3.44	4.32	2.05	3.74	2.47	5.03
1951	2.95	4.04	4.52	2.86	4.17	3.45	2.54
1952	5.27	2.18	5.52	6.21	5.46	2.82	4.69
1953	4.82	2.83	6.64	5.01	6.46	3.26	3.80
1954	2.18	1.65	3.75	3.80	3.59	1.23	1.71
1955	0.52	2.92	4.71	2.55	1.34	4.37	1.16
1956	2.80	5.15	4.90	2.89	2.70	4.83	5.88
1957	1.82	2.84	3.45	4.01	1.03	2.25	1.00
1958	4.77	5.06	5.96	5.16	4.61	3.44	6.68
1959	2.18	2.03	4.05	2.78	2.10	3.46	9.01
1960	3.16	4.53	2.38	2.61	3.56	1.76	7.17
1961	3.32	3.77	5.75	4.68	3.54	3.47	6.00
1962	2.88	3.88	3.98	3.84	1.79	4.84	3.19
1963	2.43	2.39	4.68	0.92	2.41	2.86	2.37
1964	4.63	3.74	1.91	6.07	0.82	1.46	5.32
1965	3.24	2.26	3.56	2.52	1.66	1.99	3.62
1966	3.28	4.27	1.29	3.01	3.93	1.06	2.55
1967	1.30	2.56	4.64	2.88	3.81	2.17	6.08
1968	2.76	1.12	5.48	1.66	5.59	5.17	2.53
1969	2.36	2.84	2.85	2.70	2.32	3.97	10.44
1970	1.01	2.70	3.93	6.07	2.36	4.45	3.34
1971	2.44	5.62	2.78	2.67	4.02	1.32	3.72
1972	2.93	4.98	3.22	4.05	4.75	7.00	3.96
1973	4.11	3.78	3.69	6.48	4.61	5.60	2.63
1974	3.70	2.26	5.12	2.78	3.51	3.20	2.20
1975	5.31	3.04	4.40	3.64	4.76	6.15	8.30
1976	5.52	2.34	1.91	1.69	3.49	1.82	3.94
1977	2.64	1.72	3.50	3.26	1.08	3.67	2.76
1978	7.13	1.25	4.47	1.83	7.08	2.64	

Table 2b

SOUTHERN NEW JERSEY PRECIPITATION
(Inches)

Year	Aug.	Sept.	Oct.	Nov.	Dec.	Annual Total
1929	2.44	5.00	4.62	2.84	2.85	42.65
1930	2.96	1.66	2.26	2.45	2.54	33.59
1931	6.67	1.56	2.97	0.87	2.10	36.44
1932	2.68	2.59	5.30	6.84	3.29	47.01
1933	11.27	4.33	1.49	1.34	3.46	49.41
1934	4.28	7.77	2.36	2.71	2.91	43.54
1935	3.23	7.67	4.95	5.61	2.01	47.10
1936	3.87	5.68	2.87	0.91	5.99	45.57
1937	6.42	2.28	6.14	4.39	1.26	45.88
1938	3.09	10.06	2.72	3.68	2.20	51.71
1939	8.92	1.24	4.31	1.92	1.16	45.96
1940	6.80	5.29	2.36	4.81	2.70	47.73
1941	3.13	0.17	1.79	2.75	3.36	37.23
1942	6.73	3.37	3.64	3.83	4.22	45.60
1943	1.30	1.54	7.45	2.67	1.59	37.44
1944	3.06	8.78	2.97	6.44	2.86	47.75
1945	4.14	3.99	2.63	5.24	5.43	49.16
1946	3.80	2.61	1.41	1.61	2.60	38.41
1947	4.72	2.14	1.94	5.51	2.30	42.92
1948	6.82	1.33	2.42	5.14	6.20	53.93
1949	3.77	4.23	2.87	1.77	2.70	40.00
1950	4.85	4.24	2.04	5.48	3.02	42.79
1951	2.65	1.67	4.33	6.43	5.71	45.32
1952	7.98	2.99	0.81	4.95	4.01	52.89
1953	3.86	1.05	3.91	3.40	3.92	48.96
1954	6.30	5.54	2.28	4.74	3.69	40.46
1955	9.98	2.28	5.95	1.62	0.37	37.77
1956	3.44	3.00	4.84	4.03	4.22	48.68
1957	2.13	2.87	2.44	4.22	5.92	33.98
1958	7.75	3.36	5.02	2.54	1.59	55.94
1959	4.50	1.69	3.73	4.55	3.82	43.90
1960	3.77	8.29	2.47	2.21	3.09	45.00
1961	4.04	2.99	3.23	2.09	3.51	46.39
1962	6.26	3.74	2.03	5.10	2.78	44.31
1963	3.43	5.04	0.32	7.08	2.10	36.03
1964	1.04	4.10	2.33	1.73	4.69	37.84
1965	2.99	2.26	1.44	1.11	1.75	28.40
1966	2.28	8.32	5.17	2.13	3.94	41.23
1967	10.18	2.23	2.21	1.78	5.95	45.79
1968	2.83	1.05	2.86	4.84	2.93	38.82
1969	3.04	3.95	1.79	2.88	8.15	47.29
1970	2.67	1.20	3.34	5.28	2.90	39.25
1971	10.83	5.52	4.93	5.42	1.98	51.25
1972	2.16	2.25	6.01	8.75	6.15	56.21
1973	1.80	3.37	3.61	1.17	6.38	47.23
1974	6.18	4.40	2.08	1.31	5.10	41.84
1975	3.62	7.72	3.70	3.68	2.73	57.05
1976	4.64	1.98	6.42	0.53	2.44	36.72
1977	6.30	3.74	4.11	7.80	6.30	46.88
1978						

Table 3a

COASTAL NEW JERSEY PRECIPITATION
(Inches)

Year	Jan.	Feb.	Mar.	Apr.	May	June	July
1929	3.29	4.08	3.17	5.70	3.01	2.47	1.85
1930	3.45	3.08	1.63	1.63	2.10	3.93	4.45
1931	2.26	1.54	4.92	2.35	2.94	3.14	1.74
1932	4.39	2.18	5.80	3.76	3.26	3.74	2.29
1933	2.43	3.59	4.84	4.15	4.85	2.97	2.54
1934	2.37	3.67	3.62	2.88	4.14	3.03	3.44
1935	4.70	3.29	2.10	2.51	1.82	4.47	2.71
1936	6.33	3.87	3.73	2.82	2.14	4.05	2.54
1937	6.04	2.51	2.84	4.13	1.80	3.77	1.73
1938	3.47	2.64	1.88	2.48	3.60	6.00	10.17
1939	4.68	6.07	5.22	4.51	0.81	2.80	1.07
1940	1.89	3.07	4.20	4.86	5.02	2.77	3.91
1941	4.20	3.19	2.74	2.31	1.81	3.95	5.14
1942	2.82	2.33	5.63	1.48	1.78	2.09	7.33
1943	3.13	2.13	3.23	3.13	2.29	2.50	2.07
1944	3.99	2.50	4.81	5.38	1.17	3.19	0.98
1945	2.88	2.90	1.60	2.51	3.72	3.97	8.00
1946	2.12	2.06	2.74	1.84	5.22	4.60	3.73
1947	3.78	2.14	2.12	4.18	4.81	1.73	2.72
1948	7.15	2.82	3.74	3.14	7.82	4.97	5.23
1949	5.66	4.65	3.06	3.05	3.86	0.22	2.72
1950	2.19	3.55	3.92	1.87	2.66	2.36	4.75
1951	2.79	4.44	4.18	2.10	3.47	3.44	2.59
1952	5.48	1.97	5.32	5.56	6.40	2.85	1.42
1953	4.15	2.69	6.41	4.17	4.99	2.20	3.41
1954	2.34	1.33	3.41	3.56	2.61	0.58	1.81
1955	0.63	2.84	4.55	2.63	1.21	3.77	1.12
1956	2.83	4.77	4.35	2.85	2.89	3.83	5.06
1957	1.96	3.13	3.93	4.18	0.78	2.11	1.03
1958	4.46	5.34	5.90	5.67	5.40	3.06	7.15
1959	1.59	1.95	4.40	3.16	2.03	2.18	11.42
1960	2.98	4.52	2.76	2.23	2.47	1.84	6.59
1961	3.08	4.42	5.68	3.70	3.95	2.94	5.28
1962	3.79	3.97	4.19	3.30	1.46	4.41	3.05
1963	2.86	2.38	5.80	0.98	3.07	1.63	2.95
1964	5.11	4.17	2.92	6.62	0.66	1.66	3.26
1965	4.38	2.71	3.85	2.53	1.66	2.18	5.09
1966	3.39	4.87	1.16	3.14	4.75	2.36	1.50
1967	1.18	3.19	3.75	2.87	4.97	3.70	3.72
1968	2.39	1.14	5.10	1.42	4.72	5.59	1.43
1969	2.46	2.99	2.94	3.26	1.87	2.76	8.46
1970	1.53	3.30	4.27	4.44	2.03	4.58	2.00
1971	2.63	4.75	2.46	2.47	3.69	0.70	3.91
1972	2.69	4.50	3.33	3.59	5.51	6.88	3.67
1973	3.62	3.34	3.20	5.58	4.03	5.49	2.82
1974	3.23	2.86	4.46	2.31	3.17	2.93	1.57
1975	5.00	3.24	3.42	4.07	3.71	5.04	5.97
1976	4.19	2.92	2.03	1.55	3.16	1.74	2.52
1977	3.01	2.09	3.31	2.53	1.26	2.50	2.49
1978	6.34	2.00	4.34	2.13	6.21	2.10	

Table 3b

COASTAL NEW JERSEY PRECIPITATION
(Inches)

Year	Aug.	Sept.	Oct.	Nov.	Dec.	Annual Total
1929	1.47	3.31	4.26	2.66	2.36	37.63
1930	2.46	1.89	2.21	3.59	2.17	32.59
1931	6.43	2.02	2.45	0.59	2.33	32.71
1932	1.62	1.98	4.60	5.91	3.39	42.92
1933	10.19	5.22	1.57	1.42	3.19	46.96
1934	3.34	7.40	2.06	2.60	2.69	41.24
1935	2.39	8.45	3.38	5.15	1.99	42.96
1936	3.05	5.90	3.11	0.99	7.83	46.36
1937	6.85	2.97	5.96	4.47	1.38	44.45
1938	4.12	11.57	2.64	4.01	2.07	54.65
1939	8.28	1.51	4.97	1.84	1.19	42.95
1940	5.41	2.14	2.13	4.87	2.43	42.70
1941	2.70	0.03	1.89	1.95	3.42	33.33
1942	6.97	3.60	3.68	3.09	3.83	44.63
1943	1.03	2.73	7.15	2.04	1.63	33.06
1944	2.77	8.16	3.17	7.03	2.44	45.59
1945	3.37	3.15	2.61	5.08	6.39	46.18
1946	4.60	2.95	1.15	1.15	2.32	34.48
1947	2.28	2.83	2.61	6.01	3.29	38.50
1948	6.74	0.93	3.43	5.81	6.12	57.90
1949	3.81	3.42	2.88	2.31	1.66	37.30
1950	6.48	4.12	1.25	4.46	3.04	40.65
1951	1.68	1.41	3.78	7.34	5.16	42.38
1952	8.24	1.70	0.87	3.03	4.54	47.38
1953	5.80	1.25	2.76	3.23	3.75	44.81
1954	6.69	6.01	2.31	4.49	3.50	38.64
1955	7.90	2.10	5.10	2.46	0.65	34.96
1956	3.27	3.12	6.20	2.52	4.34	46.03
1957	2.49	3.22	2.75	4.83	6.23	36.64
1958	8.87	3.30	5.66	2.32	2.42	59.55
1959	5.58	0.66	4.27	4.69	3.38	45.31
1960	5.26	6.25	2.58	1.86	3.63	42.97
1961	2.66	3.34	3.71	2.56	3.76	45.08
1962	4.35	3.50	2.04	5.28	3.17	42.51
1963	2.09	4.45	0.13	5.94	2.41	34.69
1964	1.13	4.68	2.23	1.50	3.39	37.33
1965	4.26	1.72	0.69	0.76	1.18	31.01
1966	2.95	6.92	3.86	1.81	4.00	40.71
1967	11.01	1.70	1.93	1.32	5.47	44.81
1968	3.12	1.53	2.46	5.13	3.47	37.50
1969	4.12	2.85	1.37	3.82	7.31	44.21
1970	3.32	1.23	2.75	5.05	2.94	37.44
1971	7.26	5.09	5.41	4.29	2.42	45.08
1972	1.34	3.28	5.13	8.27	5.79	53.98
1973	2.33	3.15	3.09	1.30	7.22	45.17
1974	5.42	3.81	2.14	0.98	6.10	38.98
1975	3.03	6.05	3.00	3.21	2.94	48.68
1976	6.40	3.32	5.65	0.76	2.43	36.67
1977	4.89	3.43	3.91	7.42	6.28	43.12
1978						

Table 4

NORTHERN NEW JERSEY SNOWFALL
(Inches)

Season	Oct.	Nov.	Dec.	Jan.	Feb.	Mar.	Apr.	May	Total
1956-57	T	0.4	1.2	8.6	8.2	2.9	4.6	0	25.9
1957-58	T	0.1	12.4	5.8	17.7	22.4	0.3	0	58.7
1958-59	T	0.2	4.3	2.4	0.9	9.1	1.3	0	18.2
1959-60	T	0.3	10.1	3.2	4.7	20.5	0.4	0	39.2
1960-61	T	T	21.1	24.5	20.7	5.2	2.5	0	74.0
1961-62	0	2.7	12.5	0.8	13.5	2.9	T	0	32.4
1962-63	0.5	1.3	11.5	8.5	7.1	4.1	0.1	T	33.1
1963-64	T	0.1	10.9	13.8	15.4	4.0	T	0	44.2
1964-65	0	T	4.1	13.2	2.1	6.4	1.1	0	26.9
1965-66	T	T	T	18.5	14.0	0.2	T	T	32.7
1966-67	0	T	21.3	1.6	25.1	22.0	1.0	T	71.0
1967-68	0	2.2	7.3	8.0	0.4	1.8	0	0	19.7
1968-69	T	4.3	6.9	1.7	16.9	9.0	T	0	38.8
1969-70	T	0.3	13.6	8.1	4.9	10.3	0.6	0	37.8
1970-71	T	T	6.6	15.4	3.4	6.5	2.0	0	33.9
1971-72	0	2.8	0.7	3.5	17.1	3.0	0.1	0	27.2
1972-73	0.6	0.1	1.2	4.1	1.2	0.4	T	0	7.6
1973-74	0	T	4.8	7.4	6.0	2.7	0.2	0	21.1
1974-75	0	T	0.3	6.6	12.0	1.9	T	0	20.8
1975-76	T	T	2.2	8.3	6.1	6.4	T	T	23.0
1976-77	T	0.3	6.8	12.0	7.1	2.6	T	T	28.8
1977-78	0	1.4	2.5	23.6	22.9	9.6	T	0	60.0
22-Season Average	0.1	0.7	7.4	9.1	10.3	7.0	0.6	T	35.2

Table 5

SOUTHERN NEW JERSEY SNOWFALL
(Inches)

Season	Oct.	Nov.	Dec.	Jan.	Feb.	Mar.	Apr.	May	Total
1956-57	0	T	0.2	6.4	5.6	0.8	0.6	0	13.6
1957-58	T	0.3	11.0	5.6	18.6	16.5	T	0	52.0
1958-59	0	T	1.9	2.9	0.2	2.3	0.4	0	7.7
1959-60	0	T	4.7	1.0	3.5	13.6	T	0	22.8
1960-61	T	T	15.5	17.2	10.9	0.1	T	0	43.7
1961-62	0	0.5	6.4	2.2	8.4	4.9	T	0	22.4
1962-63	0.4	0.1	5.2	4.8	2.9	0.3	T	T	13.7
1963-64	0	T	7.1	11.4	13.9	3.3	T	0	35.7
1964-65	0	T	1.6	13.1	2.6	6.0	1.3	0	24.6
1965-66	T	T	T	13.3	9.4	T	T	0	22.7
1966-67	0	T	11.1	0.7	23.3	7.1	T	0	42.2
1967-68	0	3.8	6.1	3.1	1.6	3.4	0	0	18.0
1968-69	0	T	5.4	1.8	8.9	13.5	0	0	29.6
1969-70	0	T	4.9	9.4	3.7	1.5	T	0	19.5
1970-71	T	0	1.1	6.4	0.6	1.6	1.3	0	11.0
1971-72	0	T	0.3	3.3	10.2	0.2	0.1	0	14.1
1972-73	0.3	T	T	0.1	0.3	T	T	0	0.7
1973-74	0	T	1.6	2.8	11.1	0.3	0.1	0	15.9
1974-75	0	T	0.1	3.4	4.9	0.6	T	0	9.0
1975-76	0	T	1.9	5.3	2.9	4.7	T	0	14.8
1976-77	0	0.2	3.9	11.8	0.8	T	T	T	16.7
1977-78	T	0.2	0.2	12.2	17.6	9.9	T	0	40.1
22-Season Average	T	0.2	4.1	6.3	7.4	4.1	0.2	T	22.3

Table 6

COASTAL NEW JERSEY SNOWFALL
(Inches)

Season	Oct.	Nov.	Dec.	Jan.	Feb.	Mar.	Apr.	May	Total
1956-57	0	0	0.1	6.4	4.7	1.2	0.7	0	13.1
1957-58	0	0.1	5.1	10.6	15.1	5.2	0	0	36.1
1958-59	0	0	4.0	0.6	0.1	5.5	T	0	10.2
1959-60	0	0.1	8.0	2.0	3.9	22.7	0	0	36.7
1960-61	0	0	16.4	20.7	8.5	T	T	0	45.6
1961-62	0	T	8.0	2.4	10.7	2.8	T	0	23.9
1962-63	0.4	T	4.5	7.5	2.0	0.3	0	T	14.7
1963-64	0	T	9.5	14.0	17.8	1.2	T	0	42.5
1964-65	0	T	3.0	26.5	5.2	8.5	1.0	0	44.2
1965-66	0	0	0	9.8	5.1	T	T	0	14.9
1966-67	0	0	7.9	1.4	22.5	9.8	T	0	41.6
1967-68	0	2.9	4.5	3.3	1.0	5.3	0	0	17.0
1968-69	0	T	6.8	0.7	8.1	11.6	0	0	27.2
1969-70	0	T	0.9	12.5	5.3	2.3	0	0	21.0
1970-71	0	0	0.7	4.3	0.5	1.6	0.1	0	7.2
1971-72	0	T	0.5	1.8	6.6	0.1	0.3	0	9.3
1972-73	T	T	T	0.1	0.7	T	T	0	0.8
1973-74	0	0	0.3	3.9	13.6	0.5	0.1	0	18.4
1974-75	0	0.1	T	2.2	2.7	1.1	T	0	6.1
1975-76	0	0	2.2	3.9	4.6	3.4	0	0	14.1
1976-77	0	0.5	3.8	10.7	0.3	T	0	T	15.3
1977-78	0	T	T	2.0	21.5	10.2	T	0	33.7
22-Season Average	T	0.2	3.9	6.7	7.3	4.2	0.1	T	22.4

Table 7

NORTHERN NEW JERSEY PRECIPITATION AND SNOWFALL

	Average Precip. 1941-70	Maximum Precip. & Year	Minimum Precip. & Year	: Average Snowfall 1956-78	Maximum Snowfall & Year	Minimum Snowfall & Year
Jan.	3.05	6.66 1936	0.81 1970	9.1	24.5 1961	0.8 1962
Feb.	2.91	5.21 1939	0.98 1968	10.3	25.1 1967	0.4 1968
Mar.	3.94	7.43 1953	2.16 1949	7.0	22.4 1958	0.2 1966
Apr.	3.76	7.09 1973	0.86 1963	0.6	4.6 1957	0 1968
May	3.95	7.80 1948	1.19 1964	T	T 1977+	0 1978+
June	3.47	10.87 1972	0.24 1949	0	0 ----	0 ----
July	4.63	10.83 1975	1.10 1955	0	0 ----	0 ----
Aug.	4.65	14.36 1955	0.64 1964	0	0 ----	0 ----
Sept.	3.61	10.14 1934	0.46 1941	0	0 ----	0 ----
Oct.	3.11	8.88 1955	0.37 1963	0.1	0.6 1972	0 1977+
Nov.	4.09	9.70 1972	0.62 1933	0.7	4.3 1968	T 1975+
Dec.	3.80	8.93 1973	0.37 1955	7.4	21.3 1966	T 1965
Year:	44.98	63.59 1975	30.46 1965	35.2	74.0 1960- 1961	7.6 1972- 1973

SOUTHERN NEW JERSEY PRECIPITATION AND SNOWFALL

Jan.	3.09	7.13 1978	0.52 1955	6.3	17.2 1961	0.1 1973
Feb.	2.98	5.79 1939	1.12 1968	7.4	23.3 1967	0.2 1959
Mar.	4.01	6.39 1932	1.29 1966	4.1	16.5 1958	T 1977+
Apr.	3.37	6.55 1929	0.92 1963	0.2	1.3 1971+	0 1969+
May	3.56	7.08 1978	0.82 1964	T	T 1977+	0 1978+
June	3.25	7.95 1938	0.25 1949	0	0 ----	0 ----
July	4.66	10.44 1969	1.00 1957	0	0 ----	0 ----
Aug.	4.45	11.27 1933	1.04 1964	0	0 ----	0 ----
Sept.	3.33	10.06 1938	0.17 1941	0	0 ----	0 ----
Oct.	2.99	7.45 1943	0.32 1963	T	0.4 1962	0 1976+
Nov.	3.77	8.75 1972	0.53 1976	0.2	3.8 1967	0 1970
Dec.	3.64	8.15 1969	0.37 1955	4.1	15.5 1960	T 1972+
Year:	43.12	57.05 1975	28.40 1965	22.3	52.0 1957- 1958	0.7 1972- 1973

COASTAL NEW JERSEY PRECIPITATION AND SNOWFALL

Jan.	3.24	7.15 1948	0.63 1955	6.7	26.5 1965	0.1 1973
Feb.	3.15	6.07 1939	1.14 1968	7.3	22.5 1967	0.1 1959
Mar.	3.95	6.41 1953	1.16 1966	4.2	22.7 1960	T 1977+
Apr.	3.24	6.62 1964	0.98 1963	0.1	1.0 1965	0 1977+
May	3.22	7.82 1948	0.66 1964	T	T 1977+	0 1978+
June	2.91	6.88 1972	0.22 1949	0	0 ----	0 ----
July	4.03	11.42 1959	0.98 1944	0	0 ----	0 ----
Aug.	4.52	11.01 1967	1.03 1943	0	0 ----	0 ----
Sept.	3.10	11.57 1938	0.03 1941	0	0 ----	0 ----
Oct.	2.91	7.15 1943	0.13 1963	T	0.4 1962	0 1977+
Nov.	3.63	7.42 1977	0.59 1931	0.2	2.9 1967	0 1975+
Dec.	3.63	7.83 1936	0.65 1955	3.9	16.4 1960	0 1965
Year:	41.52	59.55 1958	31.01 1965	22.4	45.6 1960- 1961	0.8 1972- 1973

Measurements in inches, T = Trace,
+ = Also earlier years.

REGIONAL GEOMORPHOLOGY OF THE INNER NEW JERSEY
SHELF

by

THOMAS F. MCKINNEY, Ph.D.

Dames & Moore Consultants

Introduction

The geomorphic analysis of the shelf surface attempts to provide a fuller understanding of the cumulative processes of erosion and deposition that have been operative in this region.

The geomorphology of the Middle Atlantic Bight has been reviewed recently by Swift and others, (1972) Duane and others, (1972) and Swift and others (1973). The present analysis describes the detailed aspects of the morphology of the inner New Jersey Shelf within the framework of these earlier works and supplements them by additional bathymetric analysis and recent data from cores and sub-bottom geophysical surveys. These earlier works establish the presence of various orders of morphology on the shelf surface. The first order morphologic elements are transverse features which subdivide the shelf surface into large-scale units. The major elements of transverse forms are shelf valleys. These features represent remnants of Pleistocene sub-aerial drainage systems which flowed across the shelf when sea level was at lower levels. These shelf valleys have been modified in varying degrees by tidal currents produced in association with the conversion of the sub-aerial valleys into estuaries by the advancing front of the Holocene transgressive sea. Depending on their original size and the degree of subsequent modification and infilling, variations exist in the degree to which the valleys are expressed as transverse lows across the shelf. Transverse valleys, which, due to their small size and subsequent infillings, do not have surface expression in the shelf bathymetry can only be identified and located by geophysical profiling and coring operations on the shelf.

The transverse valley lows are separated by broad higher influves which comprise the major extent of the shelf surface. The interfluve surface of the shelf is not of uniform slope but is characterized by a series of subtle terrace-like modifications. Analysis of the one-fathom bathymetric charts (ESSA, 1967) of the New Jersey Shelf by McClennen and McMaster (1971) in the ten- to one-hundred fathom range, reveals the presence of eight distinct erosional-depositional surfaces at 13, 20, 25, 30, 35, 38, 43, and 59 fathoms. The surfaces are inferred to have been developed as products of the Holocene transgressive shoreline. The terraced surfaces are marked on their landward edges by scarps. A prominent scarp associated with the 20-fathom terrace on the New Jersey Central Shelf represents the equivalent to the Block Island Shore of Emery and Uchupi (1972). The Block Island Shore as recognized in the bathymetric charts in the Middle Atlantic Bight appears to represent a Mid-Holocene shoreline development of considerable extent.

Superimposed on the terraced surfaces and representing the most prominent aspect of the shelf geomorphology, are sand ridges which represent second-order geomorphic forms. The origin and evolution of the sand ridge fields on the continental shelf of Eastern United States has been the subject of debate for some time. Recent analysis and reviews of the problem are given by Duane and others, (1972) Swift and others, (1972), and Swift and others, (1973). Duane and others, (1972) conducted geologic investigations of the linear sand shoals on the inner continental shelf of the East Coast. Their work indicates that the sand ridges are plano-convex bodies of sand trending northeast and resting on a nearly flat acoustic horizon. This acoustic horizon was formed by erosional retreat of the shoreface during the Holocene transgression. The underlying stratum consists of Holocene lagoonal

cohesive units for the most part. Locally, to the north, the acoustic reflector corresponds to very coarse gravelly sand. This erosion surface, "the billiard-table surface," is locally exposed at the sea floor in the troughs and in many locations is capped by a lag concentrate of coarse shell debris. Although the hydrologic details are lacking, the shoreface-connected shoals appear to be generated in response to south trending currents associated with major storms on the inner shelf while the isolated shoals on the inner shelf have been abandoned as the shore retreated in response to sea level rise. (Duane and others, 1972.) Stahl and others, 1972, describe the subsurface geologic framework for the Beach Haven Ridge off of the Little Egg-Beach Haven Inlet in a similar context.

Geomorphic Subdivisions

The inner New Jersey shelf can be divided into geomorphic zones based on the position of transverse elements and variations in the ridge fields and the associated terrace-like surfaces. Figure 1 illustrates the distribution of the zones for this region. These geomorphic zones are plotted from ESSA one-fathom bathymetric charts of the area as presented in Figure 2.

The zones are delineated by the boundaries between two transverse elements, the Great Egg Shelf Valley and the Little Egg Shelf Valley and three shelf-parallel zones A, B and C, delineated by topographic fabric and terrace levels. The outer boundaries of the study area are delimited by the position of the Block Island Shore of Emery and Uchupi (1972) as indicated in Figure 1. The regional and local geomorphic aspects of the ridge and trough topography on the Central New Jersey shelf beyond the Block Island Shore is discussed by McKinney and others (1974) and Swift and others, (1972).

Transverse Features

The Great Egg Transverse Valley

The most clearly defined transverse aspect of the inner New Jersey shelf is the Great Egg Transverse Valley. The valley appears as a broad transverse topographic low, trending across the shelf surface. Swift and others, (1972) traced the topographic expression of the Great Egg Shelf Valley across the shelf surface to the Baltimore canyon.

Geophysical investigations of the outer portion of New Jersey shelf indicates the presence of a buried channel of the Great Egg Shelf Valley (McClennen, 1973). The channel is a southerly-trending, flat-bottomed valley, four to six km wide, at least 74 km long and has been filled in with 10 to 15 m of sediments. Extrapolation of the valley floor by McClennen landward to the Northwest suggests that the Great Egg Harbor River and the Schuylkill River Valley in Pennsylvania are the modern ancestors to this older drainage. McClennen traces the Great Egg Channel seaward to the vicinity of the Wilmington Canyon.

On the inner shelf, the Great Egg Shelf Valley is well displayed in the region between the 20 and 12 fathom contours (Figure 2). Shoreward of this, the valley is represented by a broad transverse zone of smooth topography contrasting with the complex topographic fabric of the ridge and trough topography to the north and south. In the vicinity of the 10-fathom contour

within the valley, a general flattening and a slight seaward convexity of the contours is noticeable.

Little Egg Transverse Valley

Another transverse valley, the Little Egg Valley is located to the North of Great Egg Valley and traverses the inner shelf surface in a southeasterly direction from the vicinity of the double inlet system of Beach Haven and Little Egg Inlets. The Little Egg Valley, as here presented, has been designated through a combination of bathymetric and subsurface data. Subsurface information from geophysical surveys and geologic coring program conducted in the vicinity of the Atlantic Generating Station reveal a well developed buried channel trending 10 degrees west of north (Alpine Geophysical Assoc., 1973). Farther out on the shelf surface, bathymetric contours in the vicinity of the 15-fathom contour exhibit a transverse aspect which aligns with the projected direction of the buried channel on the inner shelf. Extensive reworking of the shelf surface beyond the Block Island Shore in the vicinity of the 20-fathom terrace has completely obliterated any surficial trace of the suggested Little Egg Valley in this vicinity (McKinney and others, 1974).

Preliminary analysis of bathymetric contours south of the Great Egg Transverse Valley in the vicinity immediately South of the Avalon Shoal and Five Fathom Shoals region, reveals a similar transverse topographic fabric which may present an equivalent to the Little Egg Transverse Valley on the north. This southerly transverse valley is approximately equal distance south of the Great Egg Valley that the Little Egg Transverse Valley is to the north.

Coast Parallel Zones

Three roughly coast parallel zones of morphology can be recognized on the inner New Jersey Continental Shelf: zones A, B and C (Fig. 1). Zone A is the most shoreward zone and is delineated by the distinctive aspect of the topographic fabric of the innermost ridge fields. Zones B and C are delineated by their terraced nature and the distinctive aspects of their associated ridges. The zones are further sub-divided into sub zones 1 and 2, related to the position of the Little Egg Transverse Valley.

Zone A

The distribution of zone A is indicated in Figure 1. For the purposes of discussion, Zone A can be subdivided into A-1, the portion of the A zone between the Great Egg Valley and the Little Egg Valley, and zone A-2, the portion of zone A to the north of Little Egg Valley. The distribution of zone A as outlined in Figure 1 shows that this zone is characterized by a series of ridges on the inner shelf and is not recognized to the north of Barnegat Inlet where the shoreline makes a pronounced bend from a northeasterly course.

The northern margin of zone A is narrow, approximately two nautical miles wide in the vicinity of the Barnegat Inlet. To the south, the zone widens gradually to the vicinity immediately north of the Little Egg-Beach Haven system where it widens abruptly to approximately 3 nautical miles offshore.

To the south of the Little Egg-Beach Haven Inlet system (zone A-1), zone A is represented by the well developed ridge and trough morphology of Brigantine Shoals. Here the zone is of comparable width and parallels the bending coastline. To the south of Great Egg Valley, zone A-type topography is represented by a very broad zone (to 11 nautical miles offshore) and includes the Avalon and Five Fathoms Bank.

In general, the A zone is characterized by a series of well developed ridges which have ridge crests which are accordant at about 3 to 5 fathoms. The outer margin of the zone is characterized by a sharp drop off to the general level of the 10-fathom terrace which marks the inner edge of the zone B. This outer scarp is also characterized by a series of ridges which plunge down the surface to the B zone. For the purposes of discussion, we can distinguish the nearly horizontal ridges as H-ridges and the plunging or slope ridges as S-ridges.

The A-1 zone is characterized by the well developed H-ridges which comprise the Brigantine Shoals. These shoals are characterized by having accordant crestal highs at 3 to 5 fathoms. While the general crestal highs on the ridges are nearly horizontal, the ridge crests are not actually continuous horizontal lines, but are divided into crestal highs and lows or saddles, producing a serrated longitudinal profile. This serrated aspect of the ridge crest is represented by the beaded aspect of the closed contours representing the crestal highs along the ridge axis (Figure 3). Orientations of these ridges are generally to the northeast in the northern part of the A-1 zone and curve to a more easterly trend near the southerly margins in the vicinity of the Great Egg Shelf Valley.

A separate geomorphic sub-division, the ebb-tidal delta of the Little Egg-Beach Haven Inlet System, is recognized in the northern portion of the A-1 zone. The delta forms a seaward bulge in the nearshore bathymetry as outlined by the two to four fathom contours. This large ebb-tidal delta appears to be over-lapping and displacing the ridge and trough morphology of the A zone in this zone area. Another bathymetric fabric is presented within the A-1 zone. It is represented by the poorly developed S ridges which occur between the H ridges of the Brigantine Shoals offshore and the shoreline, in the vicinity of the Brigantine Inlet, south of the delta. This fabric is represented by small ridges which plunge down the shoreface in an east by northeasterly direction, intersecting the northeasterly trend of the larger H ridges at the base of the sloping shoreface.

Beach Haven Ridge occurs along the border between the A-1 zone and the A-2 zone to the north. It has characteristics which are comparable to the H ridges of the A-1 zone. It is not as long as the H ridges to the south, however, apparently because the progradation of the Beach Haven-Little Egg Ebb Tidal Delta on its shoreward end.

In the A-2 zone, the H ridges are not nearly as well developed as in the A-1 zone. They are shorter and more widely spaced than the comparable H ridges to the south. They are tied to the steep shoreface at very shallow depths. The S ridges are better developed especially in the southern portion of the A-2 zone. In general, the S ridges have a trend distinctly more to the east than their shoreward equivalent H ridges, which have a uniform northeasterly trend (Fig. 3).

The A-1 zone can be characterized as a wide zone with better developed ridges and a generally sloping shoreface and nearshore zone. The A-2 zone is narrow and steep with ridges not as well developed.

Zone B

The B Zone is characterized by a terraced surface at about 10 fathoms, and ridges which are of lower relief and of wider spacing than the ridges of the A zone. The B zone can be divided into two zones (B-1 and B-2) based on distinctive bathymetric patterns. As with the other subzones, the Little Egg Transverse Valley is the dividing line between the B-1 and B-2 zone.

The terraced aspect of the B zone is best displayed in the southern half of the B-2 zone. The terrace forms a nearly featureless horizon up to three nautical miles wide in this area. The terrace is bounded on its seaward edge by a sloping zone between the 10 and 13 fathom contours. This sloping area marks the outer edge of the B zone and has been molded into a family of widely spaced S ridges of low relief.

The B-2 zone is widest in the south and narrows to the north and cannot be traced to the north of the Barnegat Inlet.

The B-1 zone to the south of Little Egg Valley shows a better developed system of closer spaced ridges than the B-2 zone. It is a narrower zone parallel to the A-1 zone and the present shoreline. The H ridges of the B-1 zone are built on the general 10-fathom surface as indicated by the closed 10-fathom depression contours marking the troughs near the central part of the zone. As discussed by Swift and others, (1972) there is a tendency for the ridge crests along the margins of the Great Egg Valley to increase in elevation in a southwesterly direction.

Zone C

Zone C is characterized by a terraced level at about 13 fathoms and corresponds in general to the 13-fathom terrace as indicated by McClennen and McMaster (1971). They were able to trace the 13-fathom terrace slightly further to the north than is indicated by the boundary of Zone C presented in Figure 1. The C-2 zone to the north, is comparable to the B-2 zone in that the terrace aspect is well displayed while the ridges are poorly developed and scattered. The C-1 zone to the south of Little Egg Valley is characterized by large well developed ridges which are distinctly different from those of the B-1 zone.

Other Features

In addition to the transverse elements and the terrace-like coast parallel zones discussed above, cuesta-like highs are present in the northern portion of the inner New Jersey shelf (figures 1 and 2). Swift and others (1972) have previously discussed these features (page 552 and figure 225).

These are cuesta-like features in their overall morphology in that they are elongate, asymmetrical high areas in the shelf bathymetry. The innermost high feature is well developed and forms a distinctive and abrupt rise on the seaward margin of the 13-fathom terrace of the B-2 zone. A well defined

lineation marks the seaward rising scarp (Griffiths Scarp of Veatch and Smith, 1938). A series of closed depressions occur in a linear pattern along the western boundary of the high. These depressions are two to three fathoms below the general level of the B-2 terrace which is truncated by the cuesta-like features on its northern margin. The sea floor rises in a seaward direction from depths of 16 to 17 fathoms in these depressions to the highs at 9 to 10 fathoms within a distance of less than two nautical miles. The high displays a subordinate ridge and trough pattern oriented to the northeast, especially on its lower seaward flank. The seaward margin of this flank displays a seaward facing scarp which correlates with the Block Island Shore.

The other cuesta-like feature does not have the well developed scarp on its landward flank. The upper surface of this high has been greatly modified into well developed ridges and trough system associated with the development of the 20-fathom surface comparable to the modification of bathymetry associated with the 20-fathom surface further to the south on the New Jersey shelf. (McKinney and others, 1974). The north-trending landward lows have been referred to as the Northern New Jersey Valley by Swift and others (1972).

Regional Distribution of Shelf Sediments

Fluvial Sediments

A number of previous workers have delineated a large area of gravel deposits on the inner and central northern New Jersey shelf (Shepard and Cohee, 1936; German Navy, 1943; and Schlee and Platt, 1970). Schlee and Platt, 1970, suggest that the gravel deposit of this portion of the New Jersey shelf originated as a fluvial terrace gravel deposit based on the following aspects of this material:

1. its bimodal size distribution
2. its moderately good roundness and
3. Limonite staining which characterizes the surface of the pebbles.

Schlee and Platt, 1970, have suggested that the bulging of the 40 meter contour on the inner and central portions of the New Jersey shelf (reference Fig. 1) can be explained as a result of the distribution of this resistant gravel unit which appears to be holding up the topography for this portion of the shelf. Recently Frank and Friedman (1973) have identified gravelly deposits from closely spaced samples across the southern portions of zones B-1 and C-1 offshore of Beach Haven, New Jersey and have correlated this deposit with the southern portions of the gravel deposit outlined by Schlee and Platt (1970). Detailed sampling in and around the Beach Haven ridge area have also identified the presence of the very southern terminus of this same gravelly deposit.

Frank and Friedman (1973) present heavy mineral data and review earlier regional heavy mineral studies to support the idea that the source of the New Jersey shelf deposits was glacial material transported out on to the shelf surface from the Hudson River during the last low stand of sea level. Alexander (1934) and Shepard and Cohee, (1938) noted in particular the

presence of angular salmon-colored garnets on the New Jersey shelf which had close affinity to garnets supplied from the Adirondacks by way of the Hudson River. Schlee and Platt (1970) also imply a dispersal source for these gravel deposits from the vicinity of the Hudson River. Recent coring and geophysical studies by CERC (Williams and Duane, 1974) in the New York Bight Apex off of Sandy Hook, New Jersey, revealed cross-bedded sandy gravel deposits below Holocene sediments which would fit the picture of such fluvial derived gravels during the last low stand of sea level.

Cores and geophysical data from the inner continental shelf off Harvey Cedars, New Jersey revealed the presence of similar regressive fluvial gravel deposits between 58 and 70 feet below sea level. These gravel deposits overlie earlier Pleistocene lagoonal clay units and are in turn overlain by a thin Holocene organic clay unit of lagoonal origin (Alpine Geophysical Associates, 1972). The gravel deposits are not present in stratigraphic sequence at the Atlantic Generating Station site off Beach Haven-Little Egg Inlet where Holocene lagoonal sediments overlie the Pleistocene clay units directly. There thus appears to be a thinning out to the south and southwest of this gravel depo-center away from its source area.

The close association of the presence of surficial gravelly deposits on B-2 and C-2 zones and the presence of this regressive gravel unit in subsurface suggest that the bulging effect of the shelf contours noted by Schlee and Platt (1970) may in fact be related to the distribution of the fluvial gravel deposit. South of the Beach Haven-Little Egg Inlet and the Little Egg Shelf Valley, zones A-1, B-1 and C-1 begin to converge again with the coastline. Here the gravel deposits are lacking in surface and subsurface. (Frank and Friedman, 1973; Stubblefield and others, 1974) These southern zones are characterized by finer sand sizes than the corresponding zones to the north. In particular zone A-1 is characterized by an abundance of fine to very fine sands composing the Brigantine Shoals. Thus there appears to be a marked subdivision of surficial and subsurface sediment composition north and south of the Little Egg Shelf Valley corresponding to the geomorphic subdivisions of these zones as indicated in figure 3.

A similar variation in grain sizes and heavy mineral composition can be delineated for the beach materials both north and south of the Beach Haven-Little Egg Inlet (McMaster, 1954). The beaches north of Beach Haven-Little Egg Inlet are characterized by coarse to medium sand sizes and an opaque heavy mineral assemblage while the beaches to the south are characterized by fine sands and a hornblende heavy mineral assemblage. The variations in the morphological aspects of the ridge systems for each of the zones may also be a reflection of this regional variation in available sizes to construct the ridges. In general, the ridge systems in the northern sub-zones are characterized by poorly defined ridge systems of lower relief and wider spacing, apparently reflecting the availability of the coarser grain sizes for ridge construction. The ridges to the south especially those of the A-1 zone, are characterized by well developed closely spaced ridge systems which are constructed from finer sand sizes.

Holocene Coastal Sediments

Additional insight into origin and evolution of these terrace like surfaces comes from recent geological studies on the shelf which indicate the

relationships between stratigraphic units, especially the lagoonal clay units which characterize the upper shelf surface, and the surface morphology. McClennan (1973) cited the presence of horizontal layering from shallow geophysical surveys of the 20-fathom surface in the central New Jersey shelf and suggested that these strata represent the fluvial terrace gravel deposits of Schlee and Platt (1970). Recent geophysical and coring studies by NOAA on the shelf surface to the north of the Great Egg Shelf Valley reveals that the horizontal bedding in this part of the 20-fathom surface is related to a layering of Holocene clay, Pleistocene sand and a lower Pleistocene clay horizon (Stubblefield and others, 1975, in press; (Stubblefield and Swift, 1974). The upper Holocene clay is a thin lagoonal clay unit and forms the basal framework which supports the terraced aspects of the morphology in this area at about 22 fathoms. Duane and others (1971) have indicated from studies on the inner shelf that the shoals here are underlain by a similar Holocene clay unit. The shallow stratigraphic framework of the inner 10- and 13-fathom surfaces of zones B and C is not known in detail. Clay material has been found underlying a thin sandy cover on the 10-fathom terrace from diver observations in this area. In addition, clay lumps have been reported from samples from these areas in the studies of Frank and Friedman (1973). There thus appears to be a common occurrence of a thin blanket of Holocene lagoonal clay coating these surfaces over much of the inner and central shelf.

Additional insight into the evolution of the inner shelf surface comes from the geological studies conducted at the Atlantic Generating Site Station (PSE&G NJ, 1972; Alpine Geophysical Associates, 1972; and Stahl and others, 1972). A summary profile across the area outlining the major stratigraphic sequences is presented in Figure 4. Of particular significance in this profile is the fact that the offshore ridge, the Beach Haven Ridge, rests on a foundation which is composed of a back-barrier sandy unit. This unit forms the leg or spur which flanks the northwest side of the ridge. This unit is in turn underlain by the Holocene lagoonal clay unit which rises in the shoreward direction and is exposed locally in the landward trough. Carbon-14 dating of material from within the backbarrier sand unit below the ridge at 12 meters below sea level (40 feet) indicates a radiocarbon age 6685 + 170 (Stahl and others, 1972).

If we picture this sequence during lower sea level, when these units were newly exposed to shoreface erosion as the barrier migrated over this area, some interesting features are noted. We note that the upper backbarrier sand unit is differentially preserved only under the reworked sandy sediments of the Beach Haven ridge. We also note that the relationship between the underlying Holocene lagoonal clay unit and the overlying backbarrier sand unit and their projection toward the nearshore zone suggest that little erosion of the Holocene clay unit has occurred. We can picture this upper shoreface erosion as one which removed the exposed backbarrier sand units down to the general horizon of the lagoonal clay.

It seems likely that this erosion in the upper shoreface environment reworked portions of the upper backbarrier sand unit and deposited them as a cleaner reworked unit on adjacent areas of the shoreface, covering and preserving segments of the back barrier sand faces from further shoreface erosion. It is postulated that the Beach Haven Ridge formed at a lower sea level due to this differential erosion in the upper shoreface environment. Continued southwest or downcoast migration of the ridge system, once formed,

appears unlikely since such migration would have exposed the underlying backbarrier sand faces to additional continued shoreface erosion and would have resulted in their reworking. The fact that the backbarrier facies is preserved below the ridge sands suggests that, having formed, the ridge system did not migrate and has been stabilized in relative position for some time.

Lying above this complex there occurs a zone characterized by brown coarse to medium sands locally occurring in thicknesses of up to 5 to 6 feet. Overlying this coarser sand basis is the lens shaped deposit of very fine silty sands which characterize the shoreface. Cleaner fine to medium sand comprise the distal portions of the ebb tidal delta. The coarser sand facies below the shoreface can perhaps be correlated with the reworked shelf sand facies which comprise the Beach Haven Ridge. These sands are brown in color, clean in texture and contain considerable amounts of shell debris. If this is correct, it would appear that the sea has transgressed this area depositing shelf sand unit during its passage. Subsequently progradation associated with the ebb tidal delta and shoreface deposits have covered this transgressing shelf sand unit. At the thin distal edge of the shoreface, these two facies are mixed as indicated by the bimodal aspect of the sediment texture (McKinney, in preparation). This would suggest that in this area due to higher rates of sediment input into the offshore zone there has been a progradation over the earlier-developed transgressive sand sheet. Progradation began probably shortly after sea level reached the approximate position of present sea level, approximately 3,000 years ago (Milliman and Emery, 1971). This suggestion of a progradational draping over an earlier shelf sand sheet is indicated also by the bathymetric bulge which has obliterated the pattern of ridges and swales which characterize the shallow shelf portions of Zone A to the north and south of this area. Urien and Ewing (1974) describe a similar seaward accretion and progradation over the Holocene transgress sand facies on the Argentine Shelf due to recent stabilization of sea level.

Two additional profile sections are added to the Beach Haven section for morphological comparisons and extrapolations of stratigraphic horizons of control (Figure 4). The Brigantine Shoal section represents a profile south of the Beach Haven Section through the outer ridges of the A zone and into the B zone horizon characterized by a 10-fathom contour terrace-like surface. The Five Fathom Bank Section represents a portion of the shelf surface south of the Great Egg Shelf Valley where in an offshore direction, ridge families comprising the A Zone reoccur as isolated remnants further out on the shelf surface with intervening B-zone morphology.

This schematic profile and the distribution of the A and B zones in figure 3-2 suggest that, by in large, the A zone ridges to the south of Great Egg Shelf Valley may represent isolated erosional remnants. Although geologic data is lacking, the geomorphic aspect suggests that the A and B zones may represent the erosion and reworking of a nearly flat suite of an underlying lagoonal clay and backbarrier sand units.

It can also be noted that the terrace-like B and C zones are not present in the shelf morphology in the inner portions of the northern New Jersey shelf surface. Here the shelf surface displays an erosional fabric revealing the northeast striking trend of the underlying coastal plain strata (Williams

and Duane, 1974). This erosional fabric however, does not indicate the presence of the terraced surfaces. To the south, south of Barnegat Inlet, the terrace-like surfaces appear. Especially well developed is the 10-fathom surface of the B zone.

In this area the presence of clay material indicates the formation of a lagoon behind an earlier barrier system, probably corresponding to the south trending barrier spit of the present coastal morphology. It is suggested that the terrace-like surfaces may correlate with the capping of thin Holocene clay units over the fluvial gravels as discussed earlier. This capping is probably discontinuous and in many places coarser gravels are exposed and have been reworked by the transgressing sea across this zone.

Thus the coast parallel zones may be related to stratigraphic units which developed in the advancing Holocene sea and their subsequent partial reworking by differential erosion by the over-riding shoreface zone. Sanders and Kumar, (1975) have recently suggested the possibility that barriers have skipped or jumped from the 13-fathom to the 10-fathom depth zone off of Fire Island. This jumping aspect of barrier migration is based on stratigraphic data from the inner shelf and modeled after Gilbert's earlier suggestion of in-place drowning (1884). The limited data and analysis presented here suggested a possibility that broad portions of the shelf surface are molded from nearly flat lying sequence lagoonal and backbarrier units on the New Jersey Continental Shelf. Their distribution and their apparent inefficient reworking by the advancing Holocene transgression may also reflect a similar rapid relative rise of sea level and rapid translation of the eroding zone.

Cuesta Like Features

No clear-cut explanation for the cuesta-like features discussed above is readily available. These features cannot be related to an erosional fabric of the underlying coastal plain sediments which strike to the northeast. Schlee and Platt (1970) indicate that these features occur within the regional boundaries of the wide fluvial gravel deposits discussed above. Swift and others (1972) reports the outcropping of clay from submersible dives on the northwest flank of the inner high.

The possibility exists that fairly recent faulting may have displaced the shelf surface along the linament marking the inner boundary of this inner feature, with an upward relative displacement of the seaward segment.

However, geophysical profiling across the northerly trace of this linament near the New York Bight apex has not revealed the presence of a fault. (Williams and Daune, 1974).

Another possible origin for these features is that they may represent differential deposition of gravelly deposits in elongate zones. Williams and Duane (1974) present geophysical data across the inner portions of the Hudson Shelf Valley which indicates a broad U-shaped valley floor, suggestive of glacial scouring. If tongues of ice did extend further on to the shelf surface, the north-trending highs may reflect an inversion of topography related to gravel deposition confined between ice labes.

However, the overall morphologic aspect of these features are more suggestive of a structural origin.

Recommendations

This synopsis indicates that geomorphic analysis can be utilized as a tool in regional geologic evaluation of the Shelf surface. Many questions remain concerning the detailed aspects of the shelf geomorphic surface. Detailed studies of the shallow stratigraphic framework are needed as well as studies of the responses of the shelf surface to the modern shelf regime. Such studies should be located and evaluated within the context of the existing knowledge of the regional geomorphic framework in order to address the myriad of questions which must be answered to evaluate the impact of potential development on the shelf.

In particular, the shelf valley systems require detailed studies in the nature and history of their infilling. The implications of the structural origin of the cuesta-like high on the Northern New Jersey Shelf also requires further detailed study.

Acknowledgements

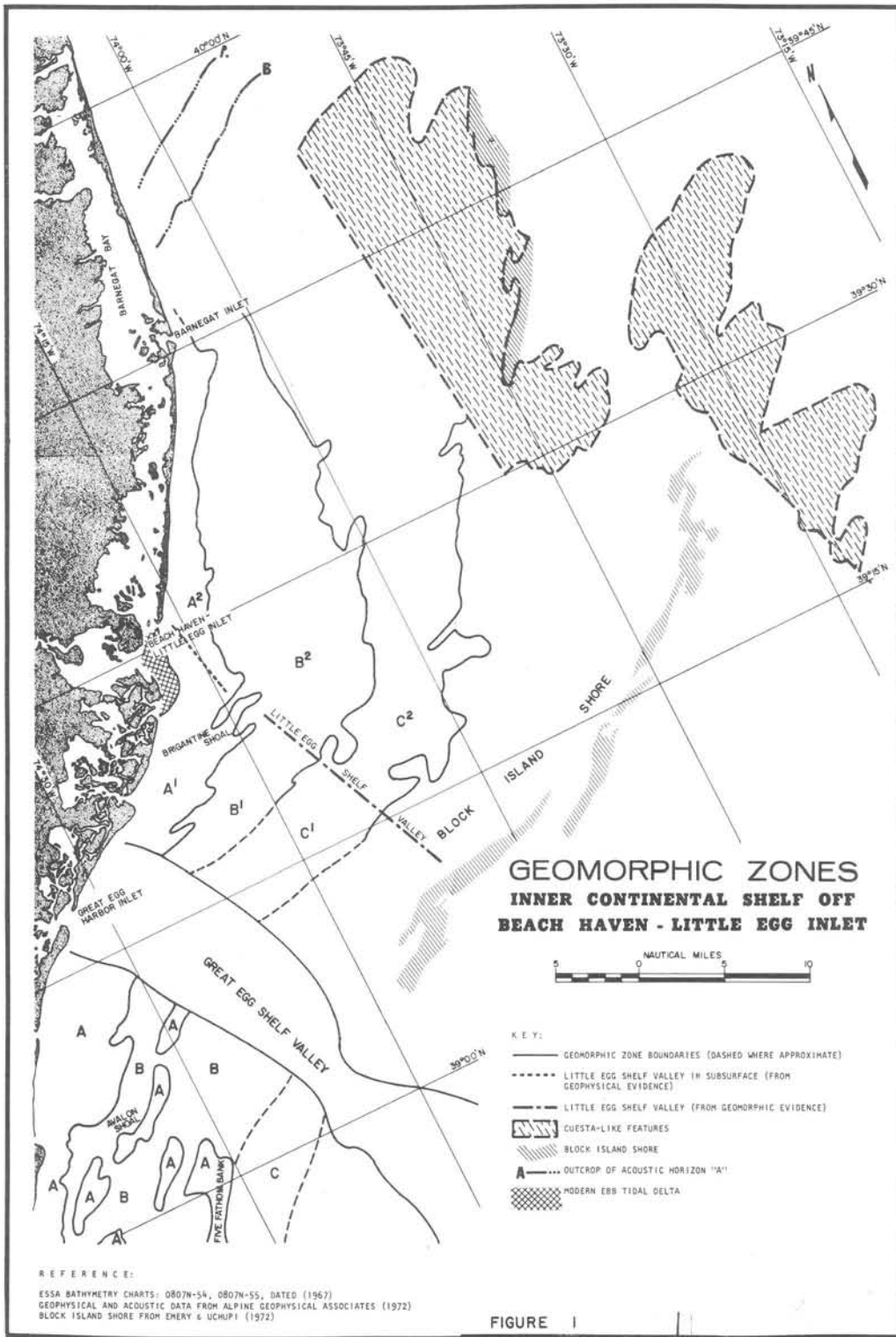
I would like to thank Donald J. Swift and Dave Duane for their comments on this paper and Public Service Electric and Gas Co. for their permission to publish this analysis. The efforts of colleagues at Dames and Moore, Roger Moose and Lloyd Stahl are also acknowledged.

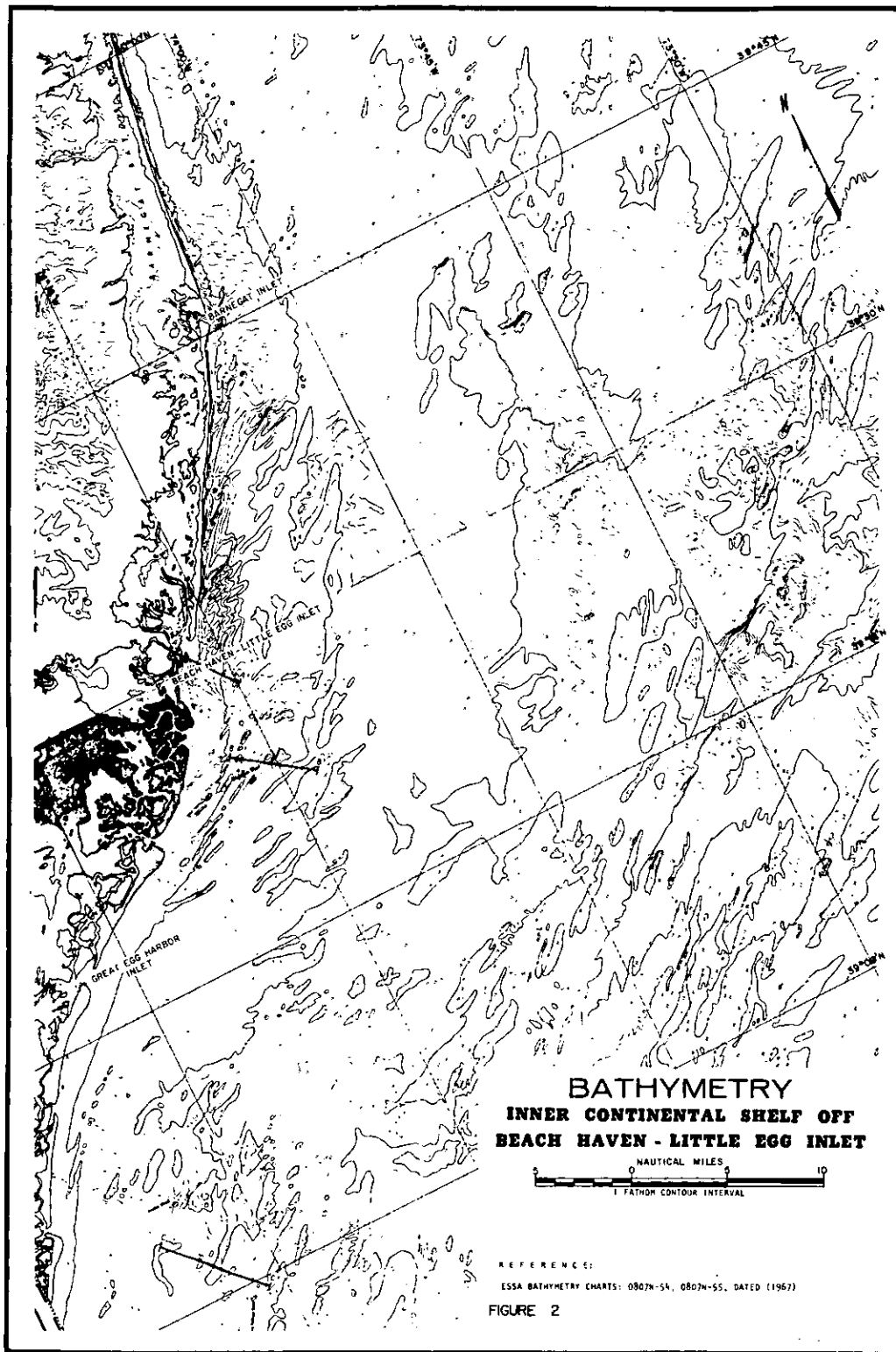
References

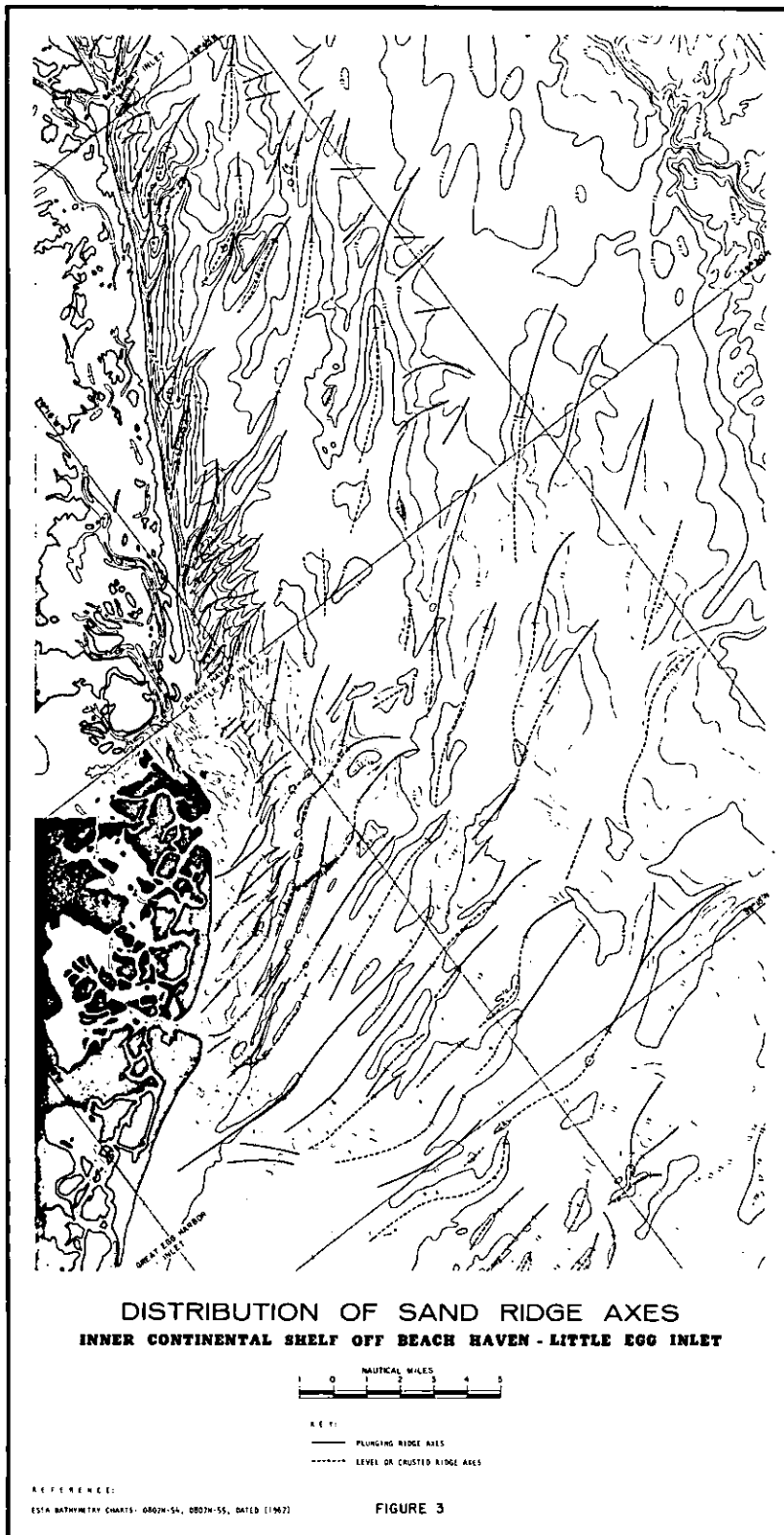
- Alexander, A.E., 1934, A petrographic and petrologic study of some continental shelf sediments: Jour. Sed. Petrology, 4: 12-22.
- Alpine Geophysical Associates, 1972, Geophysical Investigation of Atlantic Generating Station Site and Offshore Region for Public Service Electric and Gas Company.
- Duane, D.B., Field, M.E., Meisburger, E.R., Swift, D.J.P. and Williams, J.S., 1972, Linear shoals on the Atlantic inner continental shelf, Florida to Long Island, in: D.J.P. Swift, D.B. Duane and O.H. Pilkey, (Editors), Shelf Sediment Transport: Process and Pattern, Dowden, Hutchinson and Ross, Stroudsburg, Pa., pp. 447-498.
- Emery, K.O. and Uchupi, E., 1972, Western North Atlantic Ocean. American Association of Petroleum Geologists, Tulsa, Okla., 532 pp.
- Essa (1967), Bathymetric maps of the New York Bight, Atlantic Continental Shelf of the United States, Scale 1:125,000. National Ocean Survey, National Oceanic and Atmospheric Administration, Rockville, Md.
- Fisher, J.J. 1969, Coastal compartments of the Middle Atlantic Bight - unpublished work in Swift, J.P.D., 1969, Lecture: The new concepts of continental margin sedimentation, A.G.I. Short Course, Philadelphia, 7-9 Nov.

- Frank, W.M., and Friedman, G.M., 1973, Continental shelf sediments off New Jersey, Jour. Sedimentary Petrology, 43:224-237.
- German Navy, 1943, Oberkommand der Kreigsmarine; Uboat Handbuch der Ostkuste der Vereinigten Staaten van Nordamerica nordlicher Teil (Atlas): Berlin, 124 charts.
- Gilbert, G.K., 1885, The topographic features of lake shores: U.S. Geol. Survey Am. Rept., p. 69-123.
- McClennen, C.E., 1973, Nature and origin of the New Jersey continental shelf topographic ridges and depressions, Ph.D. dissertation, Univ. of Rhode Island, 93 p.
- McClennen, C.E., and McMaster, R.L. 1971, Probable Holocene transgressive effects on the geomorphic features of the continental shelf off New Jersey, United States, Maritime Sediments 7: 69-72.
- McKinney, T.F., Stubblefield, W., and Swift, D.J.P., 1974, Large-scale current lineations in the central New Jersey shelf: investigations by side-scan senser, Marine Geology, 17: 79-102.
- McMaster, R.L., 1954, Petrography and gneiss of the New Jersey beach sands: State of New Jersey Dept. of Conservation and Economic Development, Geol. Ser. Bull. G3; 239 p.
- Milliman, J.D., and Emery, K.O., 1968, Sea level during the past 35,000 years. Science 162: 1121-1123.
- Public Service Electric and Gas Co., 1972, Preliminary Safety Analysis Report, Atlantic Generating Station.
- Sanders, J.E., and Kumar, N., 1975, Evidence of shoreface, retreat and in-place "drowning" during Holocene submergence of barriers, shelf off Fire Island, New York, Geol. Soc. Amer. Bull. 86: 65-76.
- Schlee, J. and Platt, R.M., 1970, Atlantic continental shelf and slope of the United States - Gravels of the Northern Part., Geol. Survey Professional Paper 529-H.
- Shepard, F.P. and Cohie, G.V., 1936, Continental shelf sediments off the Mid-Atlantic States; Geol. Soc. American Bull., 47: 441-458.
- Stahl, L., Koczan, J., and Swift, D.J.P., 1972, Anatomy of a shoreface-connected ridge system on the New Jersey Shelf: Implications for the gneiss of the shelf surficial sand sheet, Geology, 2: 117-120.
- Stubblefield, W.L., Dicken, M., and Swift, J.P.D., 1974, Reconnaissance of bottom sediments on the inner and central New Jersey shelf, MESA Report No. 1, NOAA, 39 p.
- Stubblefield, W.L. and Swift, J.P.D., 1974, Influence of subsurface structure during submarine construction of ridge and swale topography, central New Jersey shelf, abs. Geol. Soc. of America, Annual Meeting, Miami Beach, p. 976.

- Stubblefield, W.L., Lavellé, J.W., McKinney, T.F., and Swift, D.J.P., 1975, Sediment response to the present hydraulic regime on the central New Jersey shelf (in press) Jour. Sedimentary Petrology.
- Swift, D.J.P., Kofoed, J.W., Saulsburg, F.P., and Sears, P., 1972, Holocene evaluation of the shelf surface, central and southern Atlantic shelf of North America. In: D.J.P. Swift, D.B. Duane, and O.H. Pilkey (Editors), Shelf Sediment Transport Process and Pattern. Dowden, Hutchinson and Ross, Stroudsburg, Pa. pp. 499-573.
- Swift, D.J.P., Duane, D.B., and McKinney, T.F., 1973, Ridge and swale topography of the Middle Atlantic Bight: secular response to the Holocene hydraulic regime, Marine Geology, 15: 227-247.
- Urein and Ewing, 1974, Recent sediments and Environments of Southern Brazil, Uruguay, Buenos Aires, and Rio Negro Continental Shelf in The Geology of Continental Margins, edited by C.A. Burk and C.L. Drake, Springer-Verlag, 1009 pp.
- Veatch, A.C. and Smith, P.A., 1939, Atlantic submarine valleys of the United States and the Congo submarine valley. Geol. Soc. Am. Spec. Paper. 7, 101 pp.
- Williams, S.J. and Duane, D.B., 1974, Geomorphology and sediments of the inner New York Bight continental shelf. U.S. Army Coast Eng. Res. Center Tech. Memo., 45.







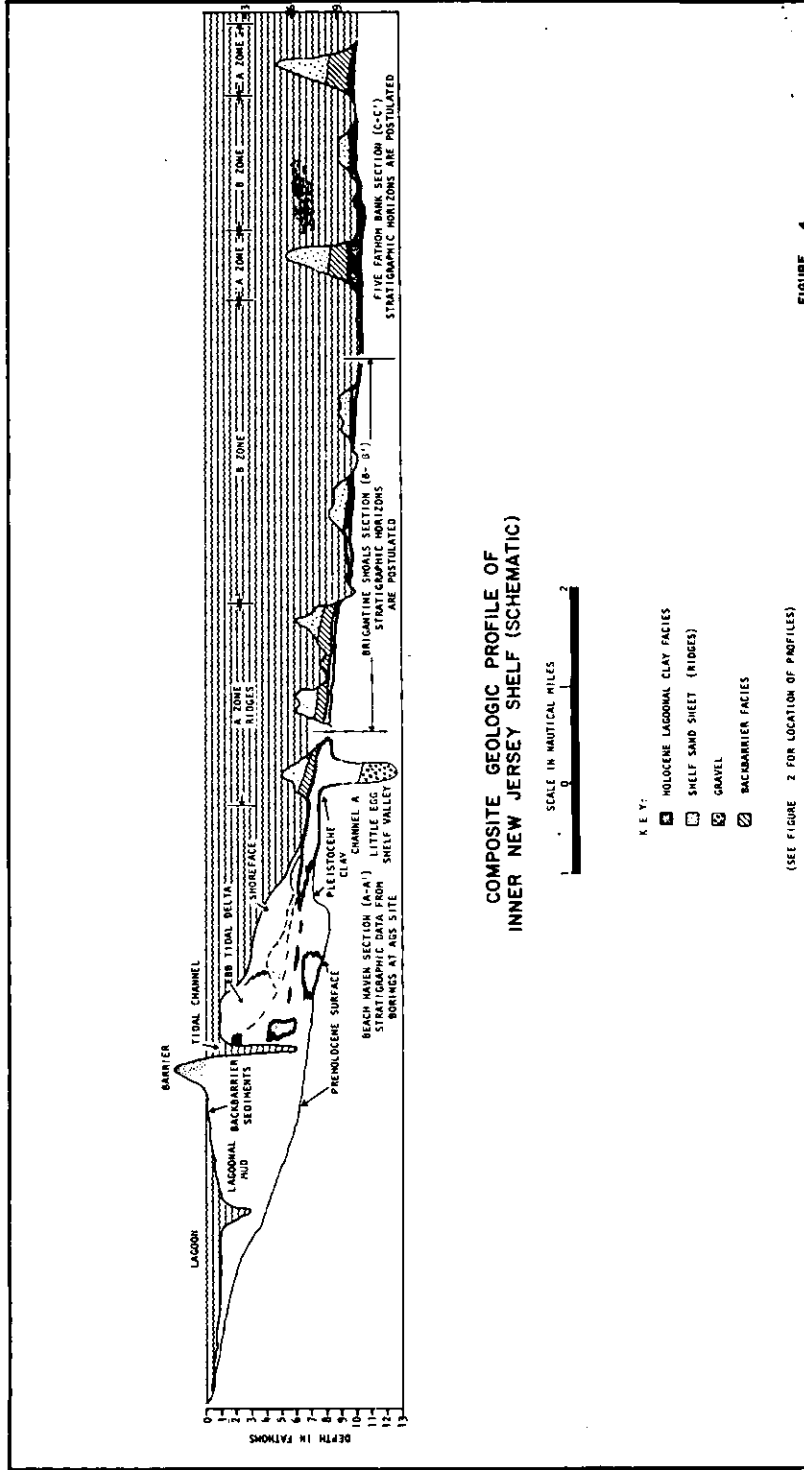


FIGURE 4

COMPOSITE GEOLOGIC PROFILE OF INNER NEW JERSEY SHELF (SCHEMATIC)

(SEE FIGURE 2 FOR LOCATION OF PROFILES)

SIMULATION OF UNSTEADY FLOW IN NATURAL COMPOUND CHANNELS

by

MILORAD MILORADOV, Ph.D.

Scientific Associate and Director "Jaroslav Černi" Institute for
Development of Water Resources, Belgrade

Natural watercourses generally have irregular compound beds (Fig 1) with different resistances and flow conditions in the main channel and the floodplain. During initial stages of the flood, the flow is confined between the river banks; with increasing discharge, flow on the flood-plain begins. The design of river training works and forecasting of bed evolution require an analysis of the influence of the different parts of the channel on flood routing.

In the present paper, a mathematical model developed at the Institute for Development of Water Resources, Belgrade (6, 8) for simulating unsteady flow in compound nonprismatic channels, will be described, together with its verification on a physical model.

Because of the complexity of flow, the following assumptions and simplifications were introduced:

(a) A natural meandering streambed can be schematically represented as consisting of two parts: the main channel and the floodplain (Fig. 1) (7);

(b) Resistance to flow or roughness is different in the two parts of the bed and varies with depth, i.e. with discharge: $n = f(Q)$, and along the stream: $n = f(X)$. Roughness is calculated in the usual way using the Manning formula.

(c) Flow is described by St. Venant's equations for one-dimensional flow.

(d) Lateral inflow, if any, only influences flow in the floodplain.

1. The mathematical model

With these assumptions St. Venant's equations can be written in the following form:

(a) Equation of continuity

for the main channel:

$$\frac{\partial Q_{gl}}{\partial X_{gl}} + B_{gl} \frac{\partial Z}{\partial t} + q_b = 0 \quad (1)$$

for the floodplain

$$\frac{\partial Q_{ai}}{\partial X_{ai}} + (B_{ai} + B_{mi}) \frac{\partial Z}{\partial t} - q_b + q = 0 \quad (2)$$

(b) Dynamic equation

for the main channel:

$$\begin{aligned} & \frac{1}{gA_{gl}} \frac{\partial Q_{gl}}{\partial t} + \frac{2}{g} \frac{Q_{gl}^2}{A_{gl}^3} \frac{\partial Q_{gl}}{\partial X_{gl}} + \frac{\partial Z}{\partial X_{gl}} \\ & = \frac{Q_{gl}^2}{gA_{gl}^3} \frac{\partial A_{gl}}{\partial X_{gl}} - S_{t,rgl} \end{aligned} \quad (3)$$

for the floodplain

$$\begin{aligned} & \frac{1}{gA_{ai}} \frac{\partial Q_{ai}}{\partial X_{ai}} + \frac{2}{g} \frac{Q_{ai}}{A_{ai}^2} \frac{\partial Q_{ai}}{\partial X_{ai}} + \frac{\partial Z}{\partial X_{ai}} + \frac{Q_{ai}}{gA_{ai}^2} \frac{\partial Z}{\partial t} = \\ & = \frac{Q_{ai}^2}{gA_{ai}^3} \frac{\partial Q_{ai}}{\partial X_{ai}} - S_{tra_i} + D - \frac{Q_{ai} \cdot g}{gA_{ai}^2} \end{aligned} \quad (4)$$

The equations for the compound bed are formally derived by adding equations (1) and (2), and (3) and (4), yielding:

Equation of continuity

$$\frac{\partial Q_{gl}}{\partial X_{gl}} + \frac{\partial Q_{ai}}{\partial X_{ai}} + B_{gl} \frac{\partial Z}{\partial t} + (B_{ai} + B_{mi}) \frac{\partial Z}{\partial t} + q = 0 \quad (5)$$

Dynamic equation

$$\begin{aligned} & \frac{1}{gA_{gl}} \frac{\partial Q_{gl}}{\partial t} + \frac{1}{gA_{ai}} \frac{\partial Q_{ai}}{\partial t} + \frac{2}{g} \frac{Q_{gl}}{A_{gl}^2} \frac{\partial Q_{gl}}{\partial X_{gl}} + \\ & + \frac{2}{g} \frac{Q_{ai}}{A_{ai}^2} \frac{\partial Q_{ai}}{\partial X_{ai}} + \frac{\partial Z}{\partial X_{gl}} + \frac{\partial Z}{\partial X_{ai}} + \frac{Q_{ai}}{gA_{ai}^2} \frac{\partial Z}{\partial t} \\ & = \frac{Q_{gl}^2}{gA_{gl}^3} \frac{\partial A_{gl}}{\partial X_{gl}} + \frac{Q_{ai}^2}{gA_{ai}^3} \frac{\partial A_{ai}}{\partial X_{ai}} \\ & - S_{t_{gl}} - S_{t_{ai}} + D_{lm} - \frac{Q_{ai} \cdot g}{gA_{ai}^2} \end{aligned} \quad (6)$$

Equations (5) and (6) describe unsteady flow in a compound channel, but they contain one more dependent variable than there are equations: apart from the unknown stage z , we also have the two unknown discharges Q_{gl} and Q_{ai} . A further equation must be introduced to enable solution. This supplementary equation is derived from the assumption that in every cross section, at right angles to the current, the water surface is horizontal, and that the ratio of the discharge in the main channel and the floodplain can be expressed by the Chézy relation. This yields the following equations:

$$\begin{aligned} Q &= Q_{gl} + Q_{ai}; \quad Q_{gl} = \frac{Q}{1+K} \quad Q_{ai} = \frac{K \cdot Q}{1+K} \\ \frac{Q_{ai}}{Q_{gl}} &= K = \frac{n_{gl}}{n_{ai}} \frac{A_{ai}}{A_{gl}} \left(\frac{R_{ai}}{R_{gl}} \right)^{2/3} \left(\frac{X_{gl}}{X_{ai}} \right)^{1/2} \end{aligned} \quad (7)$$

Substituting for Q_{gl} and Q_{ai} from (7) into (5) and (6) and carrying out the necessary differentiations yields:

Equation of continuity

$$\frac{1}{1+K} \frac{\partial Q}{\partial X_{gl}} + \frac{K}{1+K} \frac{\partial Q}{\partial X_{ai}} - \frac{K}{(1+K)^2} \frac{\partial K}{\partial X_{gl}} + \frac{Q}{(1+K)^2} \frac{\partial K}{\partial X_{ai}} + (B_{gl} + B_{ai} + B_{ml}) \frac{\partial Z}{\partial t} + q = 0 \quad (8)$$

Dynamic equation:

$$\begin{aligned} & \left(\frac{1}{1+K} \right) \left(\frac{1}{gA_{gl}} + \frac{K}{gA_{ai}} \right) \left| \frac{\partial Q}{\partial t} - \frac{Q}{(1+K)^2} \right. \\ & \left. \left(\frac{1}{gA_{ai}} \right) \left| \frac{1}{gA_{ai}} \frac{\partial K}{\partial t} + \frac{2}{9} \frac{Q}{A_{gl}^2} \cdot \frac{1}{(1+K)^2} \frac{\partial Q}{\partial X_{gl}} \right. \right. \\ & \left. \left. + \frac{2Q}{gA_{ai}^2} \frac{K^2}{(1-K)^2} \frac{\partial Q}{\partial X_{ai}} - \frac{2}{9} \frac{Q^2}{A_{gl}^2} \frac{1}{(1+K)^3} \right. \right. \\ & \left. \left. \frac{\partial K}{\partial X_{gl}} + \frac{2Q^2}{gA_{ai}^2} \frac{K}{(1+K)^3} \frac{\partial K}{\partial X_{ai}} + \frac{\partial Z}{\partial X_{gl}} \right. \right. \\ & \left. \left. \frac{\partial Z}{\partial X_{ai}} - \frac{Q}{gA_{ai}^2} \frac{K}{1+K} B_{ml} \frac{\partial Z}{\partial t} = \right. \right. \\ & \left. \left. \frac{Q^2}{gA_{gl}^3} \frac{1}{(1+K)^2} \frac{\partial A_{gl}}{\partial X_{gl}} + \frac{Q^2}{gA_{ai}^3} \frac{K^2}{(1+K)^2} \frac{\partial A_{ai}}{\partial X_{ai}} - \right. \right. \\ & \left. \left. - S_{trgl} - S_{trai} + D_{lm} - \frac{Qg}{gA_{ai}^2} \left(\frac{K}{1+K} \right) \right. \right. \end{aligned} \quad (9)$$

These equations contain both partial derivatives of the dependent variables Q and Z and derivatives of the variables A and K which are functions of X, t and Z

$$A = A(X,Z) = \int_{Z_0(x,t)}^{Z(x,t)} B(X,Z) dz \quad (10)$$

$$K = \left(\frac{n_{gl}}{n_{ai}} \right) \left(\frac{R_{ai}}{R_{gl}} \right)^{2/3} \left(\frac{A_{ai}}{A_{gl}} \right) \left(\frac{\Delta X_{gl}}{\Delta X_{ai}} \right)^{1/2}$$

The partial derivative of A is

$$\frac{\partial A}{\partial X} = \frac{\partial}{\partial X} \int_{Z_0(x,t)}^{Z(x,t)} B(X,Z) dZ = \int_{Z_0(x,t)}^{Z(x,t)} \frac{\partial}{\partial X}$$

$$B(X,Z) dZ + B(X,Z) \frac{\partial Z}{\partial X} - B(X,Z_0) \frac{\partial Z_0}{\partial X}$$

$$\int_{Z_0(x,t)}^{Z(x,t)} \frac{\partial B}{\partial X} dZ = \frac{\partial A}{\partial X} \Big|_{Z=\text{const}}$$

$$B(X,Z_0) \frac{\partial Z_0}{\partial X} = 0 \quad \begin{array}{l} \text{since by definition} \\ \text{the channel width at} \\ \text{the bottom is zero} \end{array} \quad (11)$$

$$\frac{\partial A}{\partial X} = \left(\frac{\partial A}{\partial X} \right)_{Z=\text{const}} + B \frac{\partial Z}{\partial X}$$

This equation shows that the overall change of the cross sectional area along the stream consists of two components, one which is due to the nonprismatic channel configuration with $Z = \text{constant}$, and the other which represents the change in A due to changes in stage in unsteady flow. The first term $(\partial A / \partial x)_{Z = \text{const}}$ may be positive or negative depending on whether the channel widens or narrows. The second term always has the same sign within a certain time interval. In very irregular channels the influence of the first term is greater than that of the second.

The expression for K is more complicated, since apart from A this variable also depends on the roughness and the hydraulic radius. The complete expansion of this expression in all parameters complicates the equation considerably, but the changes in the ratio between roughness and hydraulic radius are not usually great, and it can be assumed that they do not contribute much to the derivative $\partial K / \partial X$.

Analyzing the expression for K to see which factors have most influence on its variation reveals that A is the dominant parameter, so K is expressed as a function of two variables in the form

$$K = f_1(X) \cdot f_2(A) \quad (12)$$

Then the partial derivatives of K with respect to X have the form

$$\frac{\partial K}{\partial X} = \frac{\partial f_1}{\partial X} \cdot f_2 + f_1 \cdot \frac{\partial f_2}{\partial A} \cdot \frac{\partial A}{\partial X} \quad (13)$$

i.e. for the main channel

$$\begin{aligned}
 f_1(x) &= f_{g1}(X) = K \cdot A_{g1} \\
 f_2(A) &= \frac{1}{A_{g1}} ; \quad \frac{\partial f_2}{\partial A_{g1}} = -\frac{1}{A_{g1}^2} \\
 \frac{\partial K}{\partial X_{g1}} &= \frac{\partial f_{g1}}{\partial X_{g1}} \cdot \frac{1}{A_{g1}} - \frac{1}{A_{g1}^2} \cdot f_{g1} \cdot \frac{\partial A_{g1}}{\partial X_{g1}} = \\
 &\frac{1}{A_{g1}} \left(\frac{\partial f_{g1}}{\partial X_{g1}} - \frac{1}{A_{g1}} \cdot f_{g1} \cdot \frac{\partial A_{g1}}{\partial X_{g1}} \right)
 \end{aligned} \tag{14}$$

and for the floodplain

$$\begin{aligned}
 f_1(X) &= f_{ai}(X) = \frac{K}{A_{ai}} \\
 f_2(A) &= A_{ai} ; \quad \frac{\partial f_2}{\partial A_{ai}} = 1 \\
 \frac{\partial K}{\partial X_{ai}} &= \frac{\partial f_{ai}}{\partial X_{ai}} \cdot A_{ai} + f_{ai} \cdot 1 \cdot \frac{\partial A_{ai}}{\partial X_{ai}} = \\
 &\frac{\partial f_{ai}}{\partial X_{ai}} + f_{ai} \frac{\partial A_{ai}}{\partial X_{ai}}
 \end{aligned} \tag{15}$$

The calculation results prove satisfactorily accurate, which confirms that it is not necessary to expand K in all its variables, especially in the numerical procedure used for solving the system of equations here.

Hyperbolic partial differential equations like (8) and (9) cannot be generally solved by direct integration. The differential equations obtained for a simple channel are solved by the method of characteristics or by the method of finite increments with various schemes for replacing the partial derivatives. In the present case the equations are much more complicated and the number of terms changes during the process of solution. At first the flood wave is usually contained for a time by the main, simple channel, after which it overflows into the floodplain. Therefore many terms in the dynamic equation are zero during this initial period, but become nonzero when overflowing takes place. Furthermore the characteristics of flow in main channel and the floodplain are different, and change with distance downstream.

After analysis of a number of methods which have been used for solving the equations for simple channels and a survey of an extensive literature (1, 2, 3, 4, 5, 10, 12) dealing with the stability and accuracy of the solutions it was concluded that only an implicit finite increment method would be feasible. The method of characteristics, which is reliable and accurate for a simple prismatic channel, is not practical here because of the irregularity and composite nature of the channel, for which the characteristics have

different slopes and where, particularly in the compound case, solutions cannot be obtained in the same ΔX and Δt intervals.

On the other hand, various explicit methods were ruled out because of the large amount of computation necessitated by the limitations that are imposed by Courant's condition on the ratio of ΔX and Δt ($t \leq X/I_V + c_1$). Therefore two implicit schemes were tried, one with a six-point and one with a four-point quantization of the partial derivatives.

The expansion of the equations according to the six-point scheme was carried out according to the procedure proposed by Liggett and Woolhiser (9) in developing a model for a simple nonprismatic channel. In this procedure the equations are linearized by calculating the coefficients for a given time interval, and the linear equations solved by an elimination method. Since the results yielded by this scheme were not fully satisfactory for a compound non-prismatic channel, it will not be expounded here.

The model using the four-point scheme was developed using the quantization procedure proposed by Preissman / 11 /. However, the complete solution of the system of equations was here carried out for the first time (8) and proved satisfactory.

The basis of the solution is an iterative procedure for calculating the nonlinear coefficients and independent terms in the equations. Elsewhere the nonlinear coefficients have usually been calculated by two procedures: either by linearization, or by prediction from the preceding time interval. In the present work the relationship of eq. (22) was used in conjunction with an iteration procedure which will be described below.

From stability analyses of the computation scheme and the order of magnitude of the coefficients, especially in the range of overflow into the floodplain, it was concluded that the procedure applied was one of the crucial factors for stability.

Apart from the iterative procedure for calculating the coefficients and nonlinear terms, the complete system of equations was also solved by an iteration procedure using the usual method of direct elimination.

The computer program* retains the weighting parameter in the equations to enable subsequent testing of its stability under variation of θ . This proved to be a very important point since stability tests showed that the center-weighted scheme with $\theta = 0,5$ was not stable, which was also one of the reasons for the instability of the six-point scheme.

*Program worked out by P. Tanasković M.Sc., head of the Computing Center at the Mathematical Institute, Belgrade University Faculty of Mathematics and Natural Sciences, in consultation with S. Opricović, M.Sc., also of the Mathematical Institute.

The complete solution procedure is given in concise form below.

In equations (8) and (9) introduce the following symbols:

$$a = \frac{1}{1+K}, \quad b = \frac{K}{1+K}, \quad c_1 = \frac{1}{(1+K)^2}$$

$$c = c_1 \cdot \left(\frac{\partial K}{\partial X_a} - \frac{\partial K}{\partial X_g} \right)$$

$$B_u = B_{gl} + B_{ai} + B_{mi}$$

$$d = \frac{2Q}{A_{gl}^2} \frac{1}{(1+K)^2}, \quad e = \frac{2Q}{A_{ai}^2} \frac{K^2}{(1+K)^2}$$

$$h = \frac{1}{1+K} \left(\frac{1}{A_{gl}} + \frac{K}{A_{ai}} \right), \quad l = \frac{Q}{A_{ai}^2} \cdot \frac{K \cdot B_{mi}}{1+K}$$

$$f_0 = f_1 \frac{\partial K}{\partial t} - f_2 \frac{\partial K}{\partial X_{gl}} + f_3 \frac{\partial K}{\partial X_{ai}} - f_4 \frac{\partial A_{gl}}{\partial X_{gl}} -$$

$$f_5 \frac{\partial A_{ai}}{\partial X_{ai}} + f_6 + g (S'_{t_{gl}} + S'_{t_{ai}}) \tag{16}$$

$$f_1 = \frac{1}{(1+K)^2} \left(\frac{1}{A_{ai}} - \frac{1}{A_{gl}} \right), \quad f_2 = \frac{2Q}{A_{gl}^2} \frac{1}{(1+K)^3}$$

$$f_3 = \frac{2Q}{A_{ai}^2} \frac{K}{(1+K)^3}$$

$$f_4 = \frac{Q}{A_{gl}^3} \frac{1}{(1+K)^2}, \quad f_5 = \frac{Q}{A_{ai}^3} \frac{K^2}{(1+K)^2}, \quad f_6 = \frac{q}{A_{ai}^2} \frac{K}{1+K}$$

$$S'_{t_{gl}} = \frac{S_{tr_{gl}}}{Q} = \frac{1}{(1+K)^2} \frac{Q}{\left(\frac{1}{n_{gl}} A_{gl} R_{gl}^{2/3} \right)^2}$$

$$S'_{t_{ai}} = \frac{S_{tr_{ai}}}{Q} = \frac{1}{(1+K)^2} \frac{Q}{\left(\frac{1}{n_{ai}} A_{ai} R_{ai}^{2/3} \right)^2}$$

Multiplying (8) and (9) by g and introducing the above symbols yields

$$a \frac{\partial Q}{\partial A_{gl}} + b \frac{\partial Q}{\partial X_{ai}} + cQ + Bu \frac{\partial Z}{\partial t} + q = 0 \tag{17}$$

$$d \frac{\partial Q}{\partial X_{gl}} + e \frac{\partial Q}{\partial X_{ai}} + fQ + h \frac{\partial Q}{\partial t} + g \frac{\partial Z}{\partial X_{gl}} +$$

$$g \frac{\partial Z}{\partial X_{ai}} + l \cdot \frac{\partial Z}{\partial t} - gDIm = 0 \tag{18}$$

introduce the differential operator

$$D(f, S) = A \frac{\partial f}{\partial X_{g_i}} + B \frac{\partial f}{\partial X_{a_i}} + C \cdot f + D \frac{\partial f}{\partial t} + E \quad (19)$$

where S - is the set of coefficients A, B, C, D, E.

The partial differential equations then take the form:

$$\begin{aligned} D(Q, S_{Q1}) + D(Z, S_{Z1}) &= 0 \\ D(Q, S_{Q2}) + D(Z, S_{Z2}) &= 0 \end{aligned} \quad (20)$$

with

$$\begin{aligned} S_{Q1} &= \{a, b, c, 0, 0\} \\ S_{Z1} &= \{0, 0, 0, Bu, q\} \\ S_{Q2} &= \{d, e, f_o, h, 0\} \\ S_{Z2} &= \{g, g, 0, 1, -g D_{1m}\} \end{aligned} \quad (21)$$

Quantize the equations by the four-point scheme using the weighting factor (as proposed by Preissman).

Let \bar{f} be any dependent variable of coefficient. It can be quantized (see Fig. 2) by means of the following expressions:

$$f(x, t) = \frac{\theta}{2} (f_{i+1}^{j+1} + f_i^{j+1}) + \frac{1-\theta}{2} (f_{i+1}^j + f_i^j) \quad (22)$$

$$\frac{\partial f}{\partial X} = \frac{\theta}{\Delta x} (f_{i+1}^{j+1} - f_i^{j+1}) + \frac{1-\theta}{\Delta x} (f_{i+1}^j - f_i^j) \quad (23)$$

$$\frac{\partial f}{\partial t} = \frac{1}{2\Delta t} (f_{i+1}^{j+1} + f_i^{j+1}) - \frac{1}{2\Delta t} (f_{i+1}^j + f_i^j)$$

o - known

x - unknowns

Apply formula (22) to quantize the partial derivatives of operator D (eq. (19)), taking the coefficients to be constant for the time being:

$$\begin{aligned}
 D(f,S) &= A \frac{\partial f}{\partial X_{gi}} + B \frac{\partial f}{\partial X_{ai}} + Cf + D \frac{\partial f}{\partial t} + E = \\
 &= \frac{A}{\Delta X_{gi}} [\theta (f_{i+1}^{j+1} - f_i^{j+1}) + (1-\theta)(f_{i+1}^j - f_i^j)] \\
 &+ \frac{B}{\Delta X_{ai}} [\theta (f_{i+1}^{j+1} - f_i^{j+1}) + (1-\theta)(f_{i+1}^j - f_i^j)] \\
 &+ \frac{C}{2} [\theta (f_{i+1}^{j+1} + f_i^{j+1}) + (1-\theta)(f_{i+1}^j + f_i^j)] \\
 &+ \frac{D}{2\Delta t} [(f_{i+1}^{j+1} + f_i^{j+1}) - (f_{i+1}^j + f_i^j)] + E \\
 &= f_i^{j+1} [-\theta (\frac{A}{\Delta X_{gi}} + \frac{B}{\Delta X_{ai}}) + \theta \frac{C}{2} + \frac{D}{2\Delta t}] \\
 &+ f_{i+1}^{j+1} [\theta (\frac{A}{\Delta X_{gi}} + \frac{B}{\Delta X_{ai}}) + \theta \frac{C}{2} + \frac{D}{2\Delta t}] \\
 &+ f_{i+1}^j [(1-\theta)(\frac{A}{\Delta X_{gi}} + \frac{B}{\Delta X_{ai}}) + (1-\theta) \frac{C}{2} - \frac{D}{2\Delta t}] \\
 &+ f_i^j [-(1-\theta)(\frac{A}{\Delta X_{gi}} + \frac{B}{\Delta X_{ai}}) + (1-\theta) \frac{C}{2} - \\
 &\frac{D}{2\Delta t}] + E
 \end{aligned} \tag{24}$$

Introducing the notation:

$$\begin{aligned}
 r &= \frac{A}{\Delta X_{gi}} + \frac{B}{\Delta X_{ai}}, \quad s = \frac{C}{2}, \quad t = \frac{D}{2\Delta t}, \\
 V_i &= \theta (s - r) + t, \quad V_{i+1} = \theta (s + r) + t, \\
 W_i &= (f_{i+1}^j - f_i^j)(1 - \theta) r + (f_{i+1}^{j+1} - f_i^{j+1})[(1 - \theta) s - t] + E
 \end{aligned} \tag{25}$$

in expression (24) yields the system of equations

$$D(f,s) = V_i f_i^{j+1} + V_{i+1} f_{i+1}^{j+1} + W_i \tag{26}$$

Calculate the nonlinear coefficients and independent terms in eqs. (26) from expressions (16) making use of formula (22, 23) by the following iteration procedure

$$\begin{aligned} \text{for } r = 1 \quad f_{i+1}^{j+1} &= f_{i+1}^j, \quad f_i^{j+1} = f_i^j \\ \text{for } r = 1 \quad &\text{use equation (22)} \end{aligned} \tag{27}$$

r - serial number of the iteration step

In the first iteration of the $(j + 1)$ time interval the coefficients are taken to be the same as in the j th interval. After solution of the complete system of equations yielding interim values of Z and Q for $t = j + 1$ the coefficients are recalculated according to formula (27) as the second iteration, and put back into the system of equations. The cycle is repeated until the desired accuracy is achieved. This procedure avoids simplification of the complicated non-linear coefficients of the equations and the carry-over of inaccurate coefficients from the preceding time interval. The iteration converges fast and relatively few steps are necessary.

The expression in eq. (26), with the interpretations defined by previous expressions, is used to calculate the coefficients of the linear equations. For n cross sections of the stream, the expansion is carried out over $n - 1$ points. This yields the coefficients and a system of $2n - 2$ linear equations with $2n$ unknowns. Closure of the system is achieved by determining one unknown from the upper boundary condition ($x = 0$) and one from the lower ($x = x_n$). Substituting these two values in the above system yields a system identifiable with a $(2n - 2) \times (2n - 2)$ matrix of the form

```

xxx
xxx
xxxx
xxxx
----
----
---
xxxx
xxxx
xxx
xxx

```

It is solved by a modification of the elimination procedure in which the even and odd equations are treated in different ways. The computation operations are applied only to the non-zero elements of the matrix.

Direct elimination reduces the matrix to a triangular matrix with unity on the principle diagonal.

When an odd equation has three coefficients its first unknown is eliminated from the next equation which has the same distribution of coefficients. If the coefficient in the next equation is larger in magnitude, then the two equations are first interchanged.

When an even equation has two coefficients, its first unknown is eliminated from the next two equations except in the case of the last equation.

Inverse elimination reduces the matrix to unity, the solution of the system being yielded by the vector containing the right-hand sides of the equations.

When an even equation has one coefficient, the last unknown from the preceding equation is eliminated.

When an odd equation has one coefficient the last unknown of the two preceding equations is eliminated, except in the case of the first equation.

Since this is a direct procedure, the accuracy of the solution is not known. The correction is found by the following iterative procedure:

Introduce the notation

y^T exact solution

y^D solution yielded by the direct procedure

$y = y^T - y^D$ error

Then the following matrix relations hold:

$$A \cdot y^T = b$$

$$A(y^D - \Delta y) = b$$

$$A \Delta y = b - Ay^D = b$$

Solution of the system $A \Delta y = \Delta b$ by the same direct procedure yields the correction.

The program has been implemented in Fortran IV.

2. The hydraulic model*

To enable calibration of the mathematical model, hydraulic model tests were carried out as well as field measurements. The model represents a stretch of river with a non-prismatic channel, a wide floodplain and a highly meandering main channel. Unsteady flow was simulated with varying hydraulic parameters and streambed geometry, yielding data defining the flow for each test case, i.e. each set of chosen initial and boundary conditions.

*Model tests was carried out Mr. Jelisaveta Muškatirović. Head of the Hydraulic laboratory at the Jaroslav Černi Institute.

2.1 Description of the hydraulic model

A stretch of the Velika Morava 20 km long* (measured along the main channel) was chosen for modelling. It is in a certain sense representative in that it features all the morphological elements responsible for the most important influences, as: influence of floodplains (stagnant and flowing), influence of meanders in the main channel, influence of roughness changes, etc.

The relatively large length and width of the stretch of valley to be modelled (the channel width including the floodplain varies between 2 and 4 km) dictated in itself to a certain extent the choice of a 1:200 scale for length and width. The height scale of 1:40 was chosen in consideration of the type of tests to be carried out, the stream hydraulic characteristics, and earlier experience with similar models.

The main channel and floodplain were modelled with a fixed bed. At the upstream and downstream ends devices were set up enabling simulation of the desired characteristics flood hydrograms.

In order to obtain hydraulic similarity on this geometrically similar model, it had to be calibrated. Particular attention was paid to the roughening of the floodplain, making reference to all available data on the type of vegetation, its density and distribution. Calibration for chosen characteristic discharges under steady flow conditions yielded satisfactory similarity to nature as regards stage. The appearance of the model may be seen in Fig. 3.

2.2 Model tests and results

The model tests were carried out for three characteristic floods for which records of stage and discharge at Bagrdan and Ljubičevski Most were available. They differ in peak discharge and total volume. One of them (the flood wave of May 1974) was mostly contained by the main channel, while the other two inundated the floodplain.

To obtain data necessary for describing and defining the hydraulic characteristics of the stream, and especially certain local influences, measurements were made on the model at various characteristic points, viz.: bends (at the beginning, middle and end of the bend), on a straight stretch, on inflections, etc.

The influence of river training works (cutting off bends, exclusion of the floodplain, removal of levees, etc.) was also investigated by making measurements at these and other relevant cross sections.

The measurements covered stage, lateral gradient, velocity distribution and current pattern. From these data, for the three different flood waves

*Immediately upstream of Ljubičevski Most

and given states of the channel (straightening of bends), the following were derived:

- stage-time graphs of the flood waves at characteristic cross sections
- level lines along axis of the main channel at various times
- surface gradients in characteristic cross sections at various times
- diagrams of the velocity distribution in characteristic cross sections
- diagrams of the distribution of discharge between the main channel and the floodplain at characteristic cross sections
- hydrograms of the flood waves (in the main channel and the floodplain).

Current patterns were also registered. Figure 4 shows the surface streamlines in the case of straightening of a curve.

The results of these tests will not be separately presented here, but some will be given in the comparison between the physical and mathematical models.

3. Comparison and analysis of the simulation results

The routing of the flood waves with which the physical model tests were run was also worked out with the mathematical model, only a longer stretch of the stream was covered. In these computations the bed roughness was changed as a function of discharge ($n = f(Q)$), and roughness along the floodplain was varied in accordance with vegetation characteristic and data obtained from the physical model.

Figures 5, 6 and 7 compare the flood routing simulation results for several characteristic cross sections. It may be seen that the agreement is good, both as regards the flood routing as a whole and the distribution of discharge between the main channel and the floodplain. These results also provide a confirmation that the mathematical model provides good simulation of flow in a compound meandering natural channel despite the schematization it involves.

The stability of the mathematical model under variation of the weighting parameter and of the time and distance intervals Δt and Δx was also tested (Figs. 8, 9, 10, 11).

Its sensitivity to changes of the boundary conditions was also investigated. The model is so formulated that the boundary conditions can be changed at will, as for example by a dam at the upstream or downstream end whose outlet works can provide arbitrary control of the discharge. Figures 18 and 19 show the flood routing and the distribution of discharge between the main channel and the floodplain when the given lower boundary condition simulates discharge from pondage in the Velika Morava as if there were a run-of-river hydro plant with 24-hour carry-over. It may be seen that the model is quite stable.

From the results in Figs. 8, 9, 10 and 11 it may be seen that the model is stable for $1 \leq \theta \leq 0.6$, and for all time steps $\Delta t < 12$ h, which indicates a wide range of stability.

4. Applicability of the model

The model described here can find wide application in many hydraulic engineering projects on open channels. Since it is able to simulate various flow conditions in the main channel and floodplain it permits:

- variation of roughness in both parts of the channel as a function of x and t
- rapid changes of the boundary conditions during computation
- analysis of the influence of stagnant (non-flowing) floodplains on flood routing.

It may therefore be concluded that the model can be applied to analyze the influence of various river training works (regulation or leveling of the floodplain, straightening of the main channel, changes in roughness of the main channel and the floodplain, etc.), and the influence of the construction of dams on upstream and downstream flood routing, and in predicting the evolution of bed configuration under conditions of unsteady flow in natural alluvial streams.

List of Symbols

- A_{ai} - cross sectional area of active floodplain
- A_{g1} - cross sectional area of main channel
- B_{ai} - water surface width of active inundation
- B_{g1} - water surface width of main channel
- B_{di} - water surface width of dead inundation
- D_{ai}^1 - term which takes account of lateral inflow
- FR_{ai} - Froude number (active inundation)
- FR_{g1} - Froude number (main channel)
- g - gravity
- n_{ai} - Manning's coefficient of roughness (active inundation)
- n_{g1} - Manning's coefficient of roughness (main channel)
- Q_{ai} - water discharge rate in active inundation
- Q_{g1} - water discharge rate in main channel

- Q - total discharge
- R_{ai} - hydraulic radius (active inundation)
- R_{gl} - hydraulic radius (main channel)
- Sfr_{ai} - resistance slope (active inundation)
- Sfr_{gl} - resistance slope (main channel)
- z - water level

References

1. Amein M. and Hsiao - Ling Chu: "Implicit numerical modelling of unsteady flows," Proceedings ASCE, 1975.
2. Amein M. and Fang Ching: "Implicit flood routing in natural channels," Proceedings ASCE, 1970
3. Chaudhry Y. and Contractor D.: "Application of the implicit method to surgers in open channels," Water Resources Research, 1973.
4. Liggett J., J. Cunge: "Numerical Methods of Solution of the Unsteady Flow in Open Channels," Vol. 1 WPR Fort Collins, 1975.
5. Liggett J. and Woolhiser D.: "Difference solutions of the shallow-water equation," Proceedings ASCE, 1967.
6. Miloradov M., J. Muškatirović: "Modelling of Unsteady Flow in Natural Watersources," XVII Congress International Association for Hydraulic Research, Baden-Baden, 1977.
7. Miloradov V.: "The effect of the schematic representation of a natural river profile on calculated back up levels and bed deformation," Transactions No. 39, 1966, Institute "J. Černi," Belgrade.
8. Miloradov M.: "Contribution to the study of bed deformation of alluvial channels."
9. Preissman A., Cunge J.: "Calcul des intumescences sur machines électroniques," AIRH - Neuvieme Assemblee Generale, Dubrovnik, 1961
10. Price R.: "Comparison of numerical methods for flood routing," Proceedings ASCE, 1974.
11. Preissman A.: "Propagation des intumescences dans les canaux et rivières," I Congres de l'Association Francaise de Calcul, Grenoble, 1961.
12. Quinn F. and Wylie B.: "Transient analysis of the Detroit river by the implicit method," Water Resources Research, 1972.

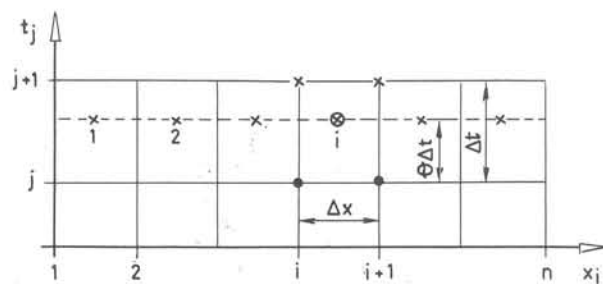
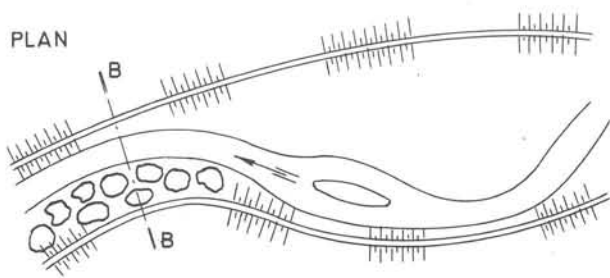


Figure 2

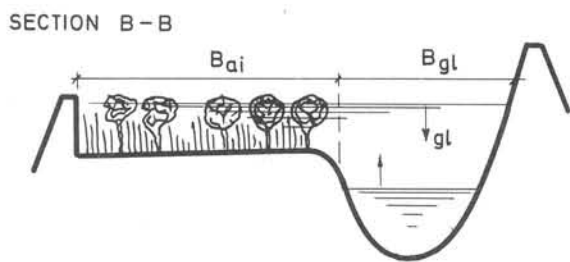


Figure 1

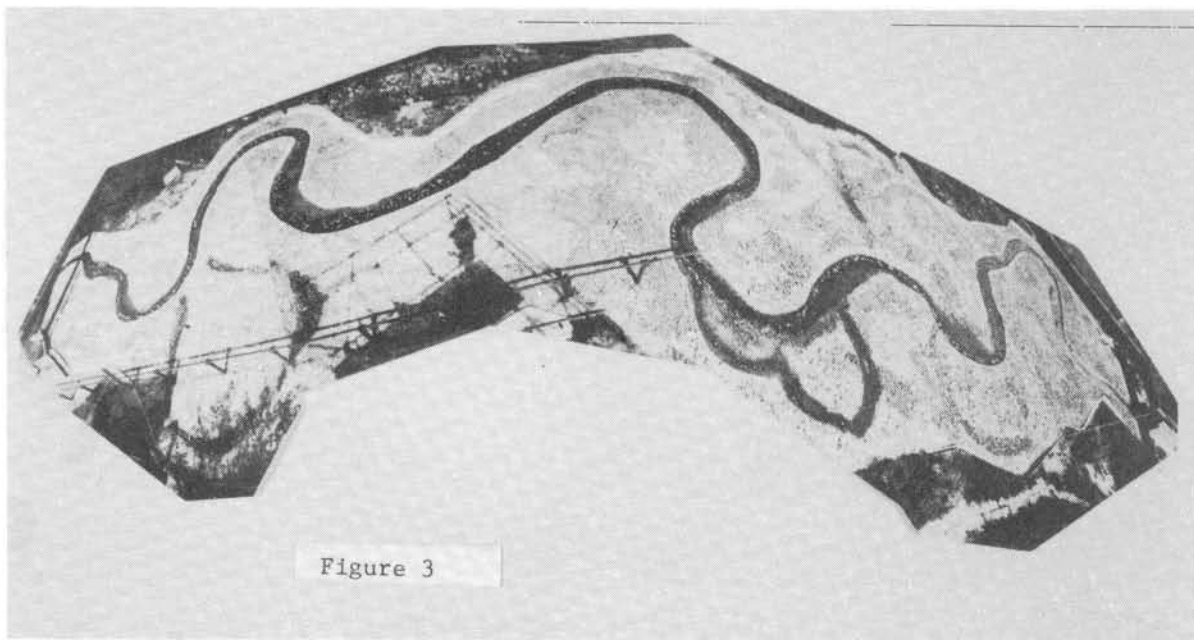


Figure 3



Figure 4

Figure 5

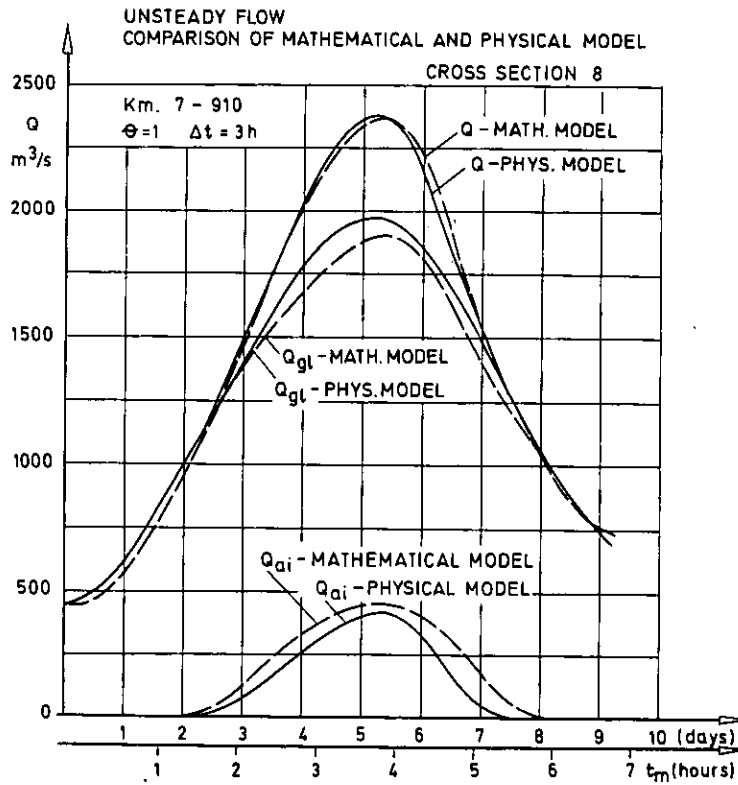
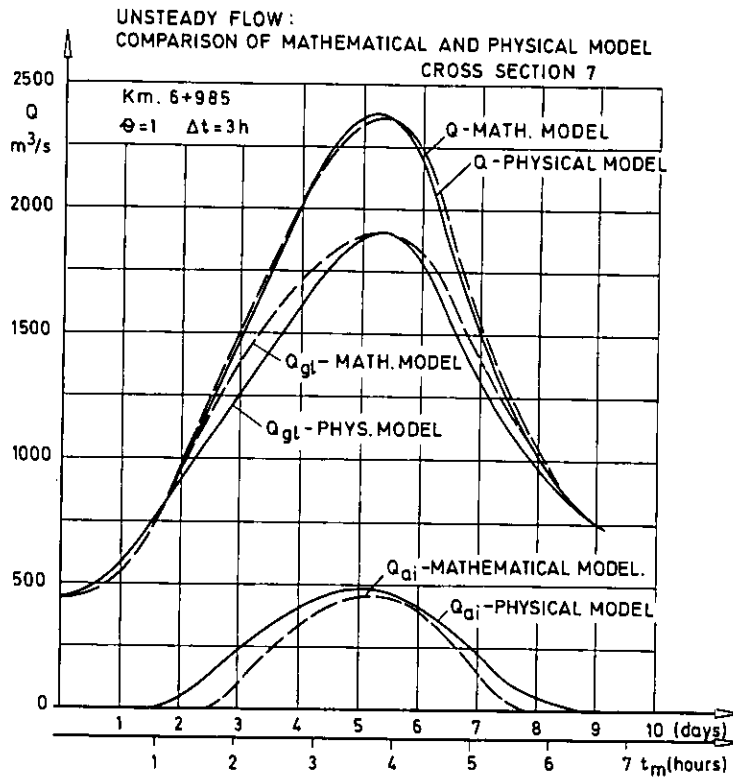


Figure 6

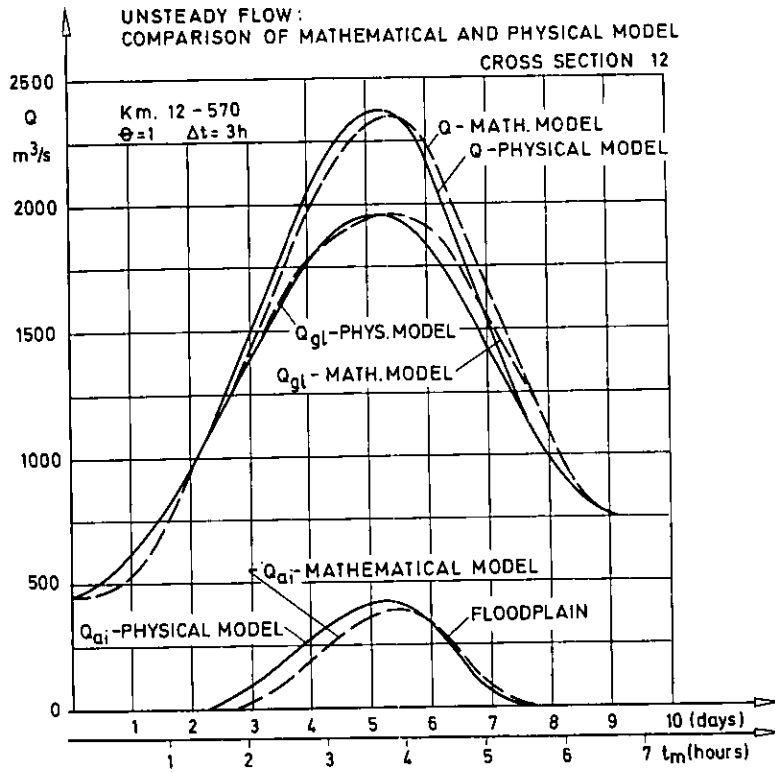


Figure 7

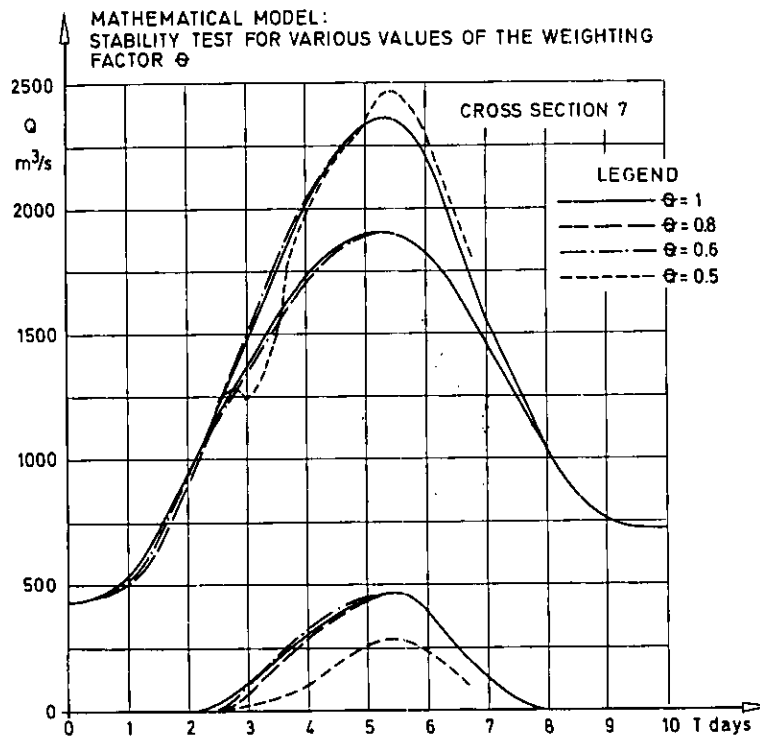


Figure 8

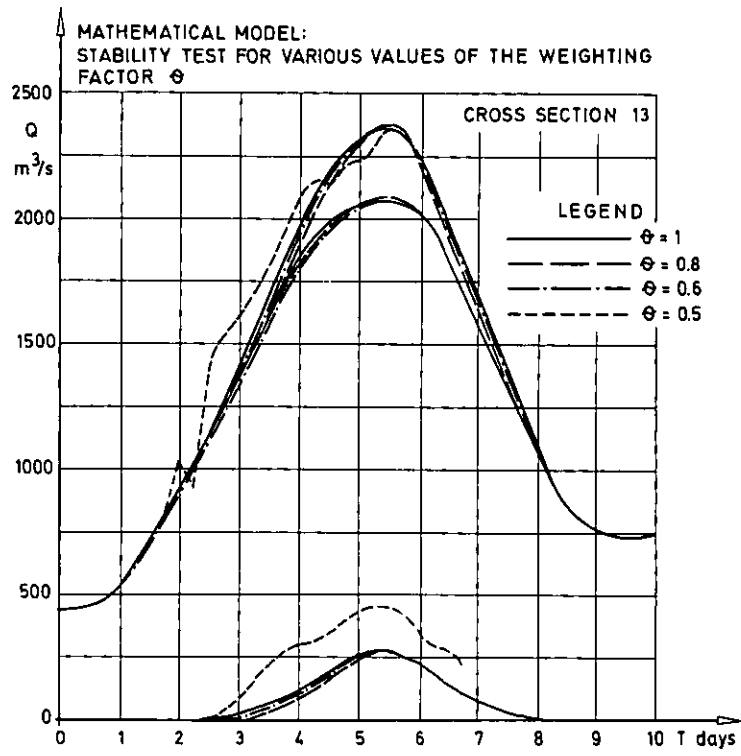


Figure 9

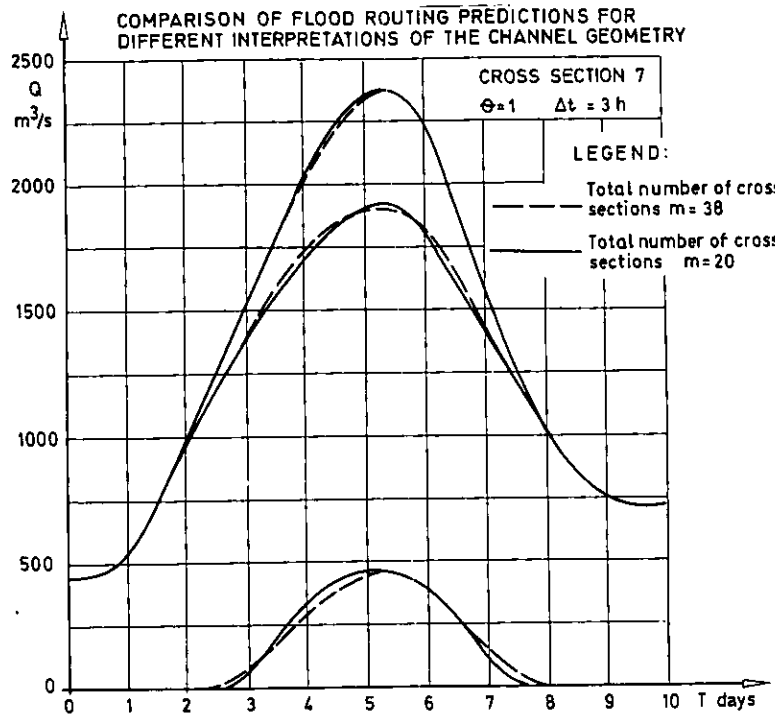


Figure 10

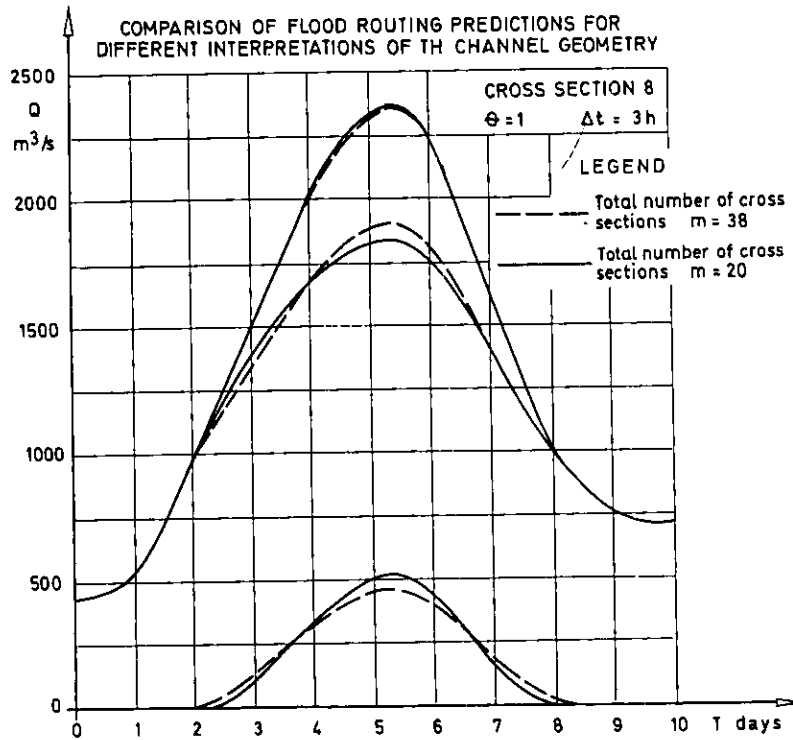


Figure 11

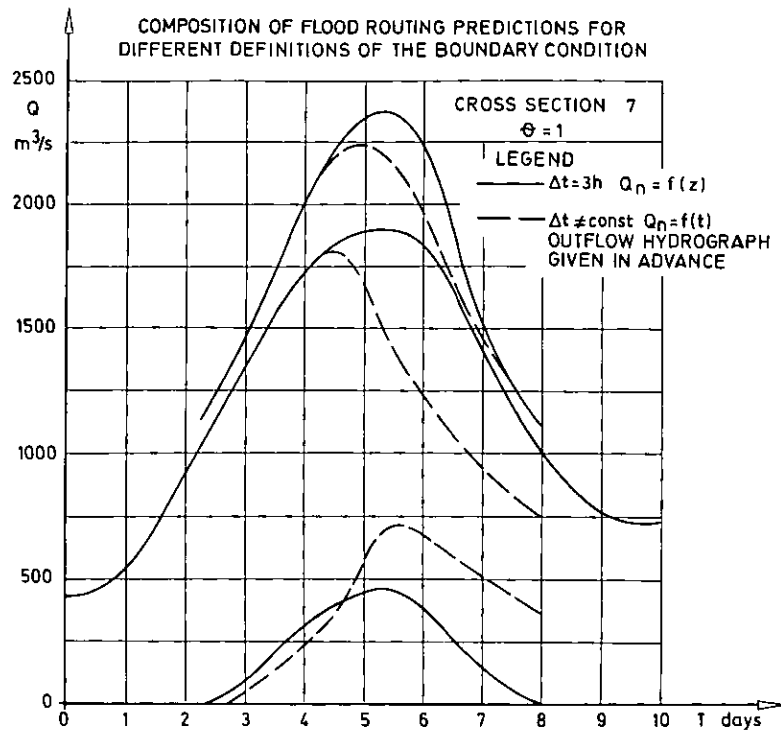


Figure 12

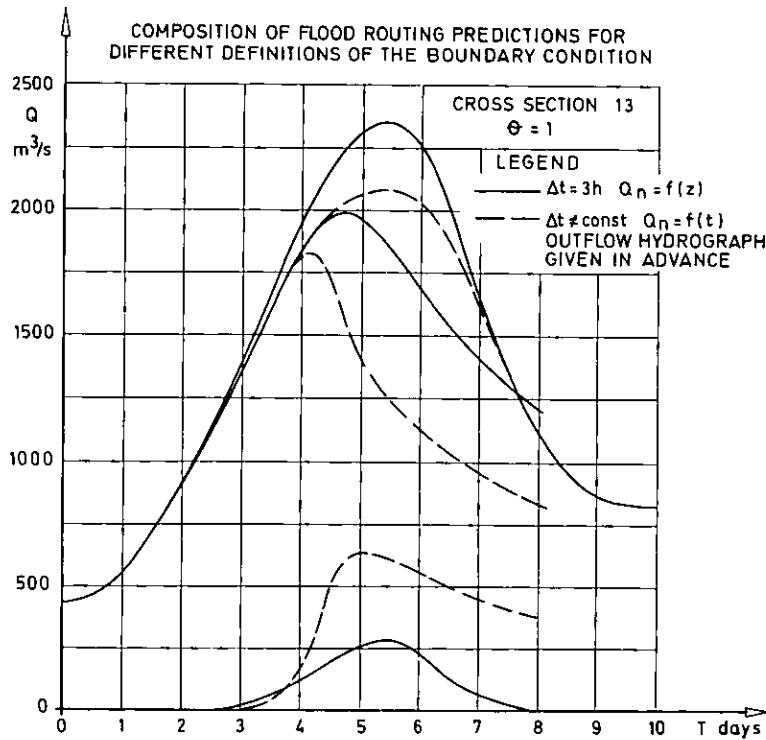


Figure 13

MOUNTAINOUS WINTER PRECIPITATION:
A STOCHASTIC EVENT-BASED APPROACH*

by

LUCIEN DUCKSTEIN, Ph.D., MARTIN FOGEL, Ph.D., and DONALD DAVIS, Ph.D.

The University of Arizona, Tucson, Arizona 85721

*Presented in the Seminar on June 1, 1977.

INTRODUCTION

In the western United States, much of the water available for regulation and use is directly related to the precipitation that falls during the cold season. The purpose of this paper is to provide decision makers with a stochastic model of winter precipitation that relies on the analysis of a minimal amount of readily available data and which can incorporate the effects of mountainous terrain on precipitation. The approach is based on describing rainfall as an intermittent stochastic process (event-based approach), as proposed by Todorovic and Yevjevich (1969) and Fogel and Duckstein (1969).

Earlier papers (Duckstein et al., 1972 and 1973) demonstrated the applicability of the event-based approach for modeling the short-duration, intense, localized convective storm. Using a rainfall-runoff relationship, probability distributions of precipitation obtained from the model were transformed into distributions of runoff. The intent of this effort is to develop a winter precipitation model that can be used as an input into a deterministic watershed model to produce synthetic sequences of streamflow. In turn, these simulated traces can be analyzed, for example, to determine the distribution of extreme events.

Used in conjunction with a watershed model, the combined models have the capability of forecasting water yields from snow-covered watersheds. Techniques currently used in the west are largely limited by the prediction of precipitation following the forecast data and by the form of that precipitation, rain or snow. Water yield forecasts generally consist of a regression analysis in which the independent variables are base flow, snow water equivalent on ground and fall and spring precipitation following forecast date (Soil Conservation Service, 1972).

A calibrated and verified watershed model should provide users with a more accurate forecast on the timing of snowmelt runoff than a statistical analysis. The timing of snowmelt runoff is highly dependent on the amount, timing and form of precipitation and on energy available to melt the snow, all of which can be incorporated into a watershed model. The combined precipitation-watershed model has the added capability of including the effects of elevation and topography on the accumulation and ablation of snow, an important consideration in forecasting water yields from mountainous watersheds.

In this paper, two probabilistic precipitation models are considered. The first model assumes that the arrival of winter storms is a Poisson process, which implies that the number of events in any time interval is independent of the number in any other interval of time. With the assumption that there is some persistence in the weather and that the occurrence of a particular event or sequence of events is somewhat dependent on past events, a second model is developed which employs a mixed distribution to describe the number of events in an interval of time.

SIMPLE POISSON PROCESS: MODEL I

With the assumption that winter storms arrive in an independent manner, the probabilistic model for such storms is similar in form to the previously-developed convective-storm model (Duckstein et al., 1972). In the case under consideration, an event is defined as a sequence of consecutive wet days for which each day a measurable (equal or greater than 0.01 inch) amount of precipitation is recorded. The test for such an assumption is whether the interarrival time for events can be described by an exponential distribution. The model is attempting to simulate a set of meteorologic events, each of which is assumed to be the aforementioned sequence of wet days.

For summer-type precipitation, Fogel and Duckstein (1969) derived a geometric distribution to describe point rainfall per event. A later paper, Fogel et al., (1971) showed that a negative binomial function could be used for the distribution of mean areal rainfall. In this study, it is suggested that for certain simulation purposes it may be more convenient to describe the distribution of precipitation amounts for each event as a negative binomial distribution, which is the discrete version of the two-parameter gamma.

Once again referring to earlier efforts by the authors in modeling thunderstorm rainfall, distributions of extreme values and total seasonal rainfall were derived under the assumption that events were independent identically distributed random variables. In a like manner, distributions for winter precipitation can be obtained from the basic distributions for the number of events per season or time interval and the amount of precipitation per event. For summer precipitation, storm duration was at least initially assumed to be small and constant, which justified the assumption that duration and amount were stochastically independent; in contrast, winter precipitation exhibits a wide range in terms of number of days per event, in which case it is hard to believe that duration and amount may be independent (Gupta, 1973). Any simulation, therefore, must include at least three random variables, namely, number of events per time interval N , amount of precipitation per event R and storm duration W . (See Figure 1). Furthermore, R and W should be defined in the form of a joint probability distribution. Crovelli (1971) proposed a bivariate gamma distribution to describe storm depths R and duration W . This distribution which was used for an event-based model of seasonal sediment yield by Smith et al., (1974), provides a basis for a simulation as shown below.

Let $T = W + D$ be the interarrival (renewal) time between events, which are separated by a dry time duration D (Figure 1). The most direct simulation consists in fitting a probability distribution to historical data on D , then a joint probability distribution to data on (R, W) such as the bivariate gamma of Crovelli (1971). Then sample values of D and joint sample values of (R, W) are generated by Monte-Carlo simulation. Such an approach was used to generate synthetic sequences of rainfall (recharge) input into a karstic aquifer (Duckstein and Simpson, 1975). The drawback of such an approach is that the distribution of D is purely empirical and is thus very strongly dependent on the sample on hand. In the case (frequent in continental climates) when the mean event duration \bar{W} is made smaller (say at least 5 times) than the mean dry duration of \bar{D} , the distribution of D may be

approximated by that of \underline{T} , i.e. an exponential (Gupta et al., 1973). The simulated intermittent series of precipitation events is generated as before, except that sample values of \underline{D} are now generated from an exponential (or geometric) distribution.

The rigorous formulation of this model will be considered as a special case of the development given next for model II.

MIXED DISTRIBUTION: MODEL II

The rationale for using the mixed distribution model is based on observations which note that under certain meteorological conditions, winter storms often come in sequences in which one storm follows another within a short time interval. At other times, a winter storm appears to arrive in an independent manner. Random variables used in this model are schematically shown in Figure 2, and are defined as follows:

Events. As in model I, consecutive days $j = 1, 2, \dots$, with precipitation amounts $R(j) > C$ constitute a rainfall event of magnitude \underline{R} (i.e., cumulative rainfall) and duration \underline{W} of wet spell. Threshold C is, for example, 0.1 cm.

Sequences. Events \underline{R} separated by a duration \underline{D}' of one, two, or three dry days constitute a rainfall sequence of duration \underline{V} . The number of events in a sequence is random variable \underline{N}_O .

Dry spell duration. Two sequences are separated by a dry spell $\underline{B} = 4, 5, 6, \dots$, days. The seasonal maximum of \underline{B} defines extreme droughts (Gupta and Duckstein, 1975).

Interarrival time. The time \underline{Z} between the beginning of one sequence and the beginning of the next one is the interarrival or renewal time: $\underline{Z} = \underline{V} + \underline{B}$.

Let the probability mass function (pmf) and probability generating function (GF) of the random variable \underline{X} be denoted as follows:

$$\text{pmf of } \underline{X}: f_{\underline{X}}(j), j = 0, 1, 2, \dots$$

$$\text{GF of } \underline{X}: X^*(s) = \sum_{j=0}^{\infty} s^j f_{\underline{X}}(j)$$

If X were a continuous random variable, then its probability density function (pdf) would be density $f_{\underline{X}}(\underline{x})$. Here, \underline{x} stands for any of the above defined random variables. In the case of two variates \underline{x} and \underline{y} , the joint pmf is $f_{\underline{x}, \underline{y}}(j, k)$ and the bivariate GF is $\phi^*(s_1, s_2)$. For this compound model, it will be assumed that the same dependence exists between event duration \underline{V} and amount \underline{R} as in model I. However, the complete stochastic description of such a process which necessitates the use of bivariate GF would be too lengthy. Thus, the duration process and the rainfall amount process are described separately, that is in terms of marginal pmf and DF. The dependence between \underline{W} and \underline{R} will be reintroduced in the simulation algorithm.

The duration of sequence is the sum of \underline{N}_0 events and $(\underline{N}_0 - 1)$ durations \underline{D}' .

$$\underline{V}(n) = \underline{W}(1) + \underline{D}'(1) + \underline{W}(2) + \underline{D}'(2) + \dots + \underline{D}'(n-1) + \underline{W}(n) \text{ for } \underline{N}_0 = n$$

or

$$\underline{V}(n) = \sum_{j=1}^{n-1} \underline{D}'(j) + \sum_{j=1}^n \underline{W}(j) \text{ for } \underline{N}_0 = n. \quad (1)$$

In terms of conditional GF, this equation is written

$$\underline{V}^*(s) = [\underline{D}'^*(s)]^{n-1} [\underline{W}^*(s)]^n \text{ for } \underline{N}_0 = n \quad (2)$$

and for the unconditional GF,

$$\underline{V}^*(s) = \frac{1}{\underline{D}'^*(s)} \sum_{n=1}^{\infty} [\underline{D}'^*(s) \underline{W}^*(s)]^n f_{\underline{N}_0}(n) \quad (3)$$

In general, then

$$\underline{V}^*(s) = \frac{1}{\underline{D}'^*(s)} \underline{N}_0^* [\underline{D}'^*(s) \underline{W}^*(s)] \quad (4)$$

For example, if

$$f_{\underline{N}_0}(n) = e^{-m} \frac{m^n}{n!} \text{ (Poisson), and } \underline{N}_0^*(s) = e^{-m+ms}, \quad (5)$$

then $\underline{V}^*(s)$ becomes

$$\underline{V}^*(s) = \frac{1}{\underline{D}'^*(s)} \exp \{-m+m[\underline{D}'^*(s) \underline{W}^*(s)]\} \quad (6)$$

Since $E(\underline{N}_0)$ is rather small, the GF, $\underline{V}^*(s)$ is expected to converge rapidly. In the case when only mean and variance of wet spell are desired, then

$$E(\underline{V}) = E(\underline{N}_0 - 1) E(\underline{D}') + E(\underline{N}_0) E(\underline{W}) = \left. \frac{d\underline{V}^*(s)}{ds} \right|_{s=1} \quad (7)$$

$$\text{VAR}(\underline{V}) = \left[\left. \frac{d^2 \underline{V}^*(s)}{ds^2} + \frac{d\underline{V}^*(s)}{ds} - \left[\frac{d\underline{V}^*(s)}{ds} \right]^2 \right] \right|_{s=1}$$

The dry well duration \underline{B} between two sequences has a truncated pmf since $\underline{B} \geq 4$ by hypothesis. The GF is thus

$$\underline{B}^*(s) = \sum_{j=4}^{\infty} s^j f_{\underline{B}}(j) \quad (8)$$

The GF, of $\underline{Z} = \underline{V} + \underline{B}$ is readily obtained from Equations (6) and (8)

$$\underline{Z}^*(s) = \underline{V}^*(s) \underline{B}^*(s) = \frac{\underline{B}^*(s)}{\underline{D}'^*(s)} [\underline{D}'^*(s) \underline{W}'^*(s)] \quad (9)$$

A renewal process has thus been defined (Feller, 1968), such that the probability $u(n)$ of a sequence starting on any given day n may be determined by the GF.

$$U^*(s) = \frac{1}{1 - \underline{Z}^*(s)} = \sum_{n=0}^{\infty} u(n) s^n \text{ with } u(0) = 1 \quad (10)$$

Let $\mu = E(\underline{Z})$ and $\sigma^2 = \text{VAR}(\underline{Z})$.

Over a sufficiently long period of time, the mean recurrence probability tends to

$$\lim_{n \rightarrow \infty} u(n) = \frac{1}{E(\underline{Z})} = \frac{1}{\mu} \quad (11)$$

The number $\underline{N}'(n)$ of occurrences of sequences over the n days (time units) is asymptotically normal (Feller, 1968, Vol. 1, p. 321) and given by:

$$P \{ \underline{N}'(n) \geq \underline{z} \} \rightarrow \phi(\underline{z}) \quad (12)$$

where $\phi(n)$ is the standard normal distribution and $\underline{N}'(n)$ is the standardized normal variate:

$$\underline{N}'(n) = (\mu \underline{N}'(n) - n) \sqrt{\frac{\mu}{\sigma^2 n}} \quad (13)$$

Equations (12) and (13) imply that

$$E(\underline{N}'(n)) \sim \frac{n}{\mu}, \text{ VAR}(\underline{N}'(n)) \sim \frac{n^2 \sigma^2}{\mu^3} \quad (14)$$

Whether or not 1 year is sufficient to reach asymptotic values is questionable. The precipitation amount process is characterized (in marginal terms) by the cumulative rainfall \underline{R}' per sequence:

$$\underline{R}' = \underline{R}(1) + \underline{R}(2) + \dots + \underline{R}(\underline{N}_0) \text{ the GF of which is}$$

$$\text{GF: } \underline{R}'^*(s) = \underline{N}_0^*(\underline{R}^*(s)) \quad (15)$$

The mean and variance of \underline{R} can be obtained directly (Benjamin and Cornell, 1970, p. 178).

$$E(\underline{R}') = E(\underline{N}_0) E(\underline{R})$$

$$\text{VAR}(\underline{R}') = E(\underline{N}_0) \text{VAR}(\underline{R}) + (E(\underline{R}))^2 \text{VAR}(\underline{N}_0) \quad (16)$$

Next, suppose the seasonal total rainfall $\underline{S}(n)$ is of interest. During one winter season of duration n days, there are $\underline{N}'(n)$ events, so that $\underline{S}(n)$ is the sum of a random number $\underline{N}'(n)$ of random variables \underline{R}' . However difficulties arise in evaluating $\underline{S}(n)$ because the number of events $\underline{N}'(n)$ and their duration \underline{V} are not independent; the theoretical treatment of such a case which is not simple, may be found in Gupta (1973).

If, on the other hand, $E(\underline{Z}) = \text{mean interarrival time} \gg E(\underline{V}) = \text{mean sequence duration}$, then we can get an approximation to the seasonal total $\underline{S}(n)$ by summing a random number $\underline{N}'(n)$ of i.i.d. variates $\underline{R}'(k)$ where \underline{N}' and the \underline{R}' are taken as independent.

$$\underline{S}(n) = \underline{R}'(1) + \underline{R}'(2) + \dots + \underline{R}'(\underline{N}'(n)) \quad (17)$$

The mean and variance of $\underline{S}(n)$ can be calculated by formula as in Eq. 16 into which asymptotic results of Eq. 14 may be incorporated.

$$E(\underline{S}(n)) = E(\underline{N}'(n)) E(\underline{R}') \cong \frac{n}{\mu} E(\underline{R}') \quad (18)$$

$$\text{VAR}(\underline{S}(n)) = E(\underline{N}'(n)) \text{VAR}(\underline{R}') + [E(\underline{R}')]^2 \text{VAR}(\underline{N}'(n))$$

$$\cong \frac{n}{N} \text{VAR}(\underline{R}') + \frac{n\sigma^2}{\mu\sigma^3} [E(\underline{R}')]^2 \quad (19)$$

In this case, the maximal distribution of \underline{R}' may also be ascertained as in Duckstein, et al., (1972).

Model II may be used to generate synthetic series of winter rainfall as follows:

(1) Generate i th renewal epoch (time).

(a) For $i = 1$, use one of several techniques to estimate the pmf of the start of the first event of the season (Feller, 1968).

- (b) For $i > 1$, draw a dry spell duration \underline{B} since the termination of the preceding sequence.
- (2) Generate a number \underline{N}_O for the i th sequence.
 - (3) Generate \underline{N}_O bivariate events $(\underline{N}, \underline{R})$.
 - (4) Generate $\underline{N}_O - 1$ dry spells.
 - (5) Calculate \underline{R}' , \underline{V} , and iterate.

As a check of internal consistency of the model, the pmf of the number of sequences per season may be compared to the pmf of \underline{N}' .

ELEVATION EFFECT

Assume that the common situation in which precipitation increases with elevation is to be modelled. In contrast with plain regression or correlation models, the event-based approach provides several phenomenological options to explain this behavior.

In Model I, the elevation effect may be caused by:

- (a) An increase of the rate of arrival of events $E(\underline{N})$ or equivalent decrease of expected interarrival time $E(\underline{T})$.
- (b) An increase of the mean rainfall per event $E(\underline{R})$ which in turn may originate from change in the event structure, namely, in $E(\underline{W})$ and the dependence between $(\underline{W}, \underline{R})$.
- (c) A combination of (a) and (b).

The discussion of such a model applied to summer-type precipitation is found in Duckstein, et al., (1973) where data from the Santa Catalina Mountains near Tucson, Arizona, are used to demonstrate the applicability of the method. In an unpublished study, Krummenacher of the University of Geneva stated that the model was applicable to the French Jura Mountains!

In Model II, the elevation effect may be accounted for as in Model I, with the following additional features specific to the definition of a sequence:

- (a) The mean number of events per sequence $E(\underline{N}_O)$ may increase.
- (b) The mean duration of sequences $E(\underline{V})$ may increase.
- (c) The mean dry spell duration between events in a sequence $E(\underline{D}')$ may change (presumably decrease).

In each case, it is suggested that a linear regression between the expected value of the variate considered \underline{X} and elevation h be tested: $E(\underline{X}|h) = a + bh$, with the null hypothesis $H_0: b = 0$. Then only the most significant relationships should be kept in the model.

DATA AND RESULTS

Daily precipitation data from San Antonio, Texas, were used in this study. For sake of comparison, the pmf of interarrival time between groups and between sequences has also been analyzed at Alpine, Arizona. Earlier studies (Kao, *et al.*, 1971; Fogel, *et al.*, 1973; Cary, *et al.*, 1974; and Yakowitz, *et al.*, 1974) used Arizona and California data in developing winter precipitation models. The idea in using Texas data is to demonstrate the robustness of the model in terms of applicability to different geographical and climatic regions. Certainly the mountainous effect cannot be studied in the immediate vicinity of San Antonio, but this analysis sets the stage for a study of winter mountainous rainfall in the same climatic range as that of San Antonio.

The empirical and fitted pmf are shown in Figs. 3 to 13. Figs. 3, 5 and 6 are in fact common to both modes: Figs. 4 and 7 refer specifically to Model I, then Figs. 8 to 13, to Model II. The analysis is performed along that subdivision, using some of the equations presented earlier to check the internal consistency of the model assumptions.

The winter season is taken from November 1 to March 31 or $n = 150$ days. All hypotheses are tested at the 0.95 level with a K-S test.

(a) Basic process: The pmf of the number of storms or events N per season is shown in Fig. 3; the mean $E(N) = 19.86$, with a variance $VAR(N) = 13.91$ (standard deviation $s(N) = 3.73$), and a sample size $K = 44$. The hypothesis of a Poisson pmf with $m = 19.86$ cannot be rejected; furthermore, a normal approximation to the Poisson seems to be adequate, as shown later in this section. Next, the pmf of rainfall per event R is shown in Fig. 6, with $E(R) = 0.35$ m, $VAR(R) = 0.080$, ($s(R) = .283$), and $K = 94$. As indicated in Yakowitz, *et al.*, (1974), a J-shaped gamma pdf gives a proper representation of $f_R(x)$; here, the discrete equivalent of the gamma, i.e., a negative binomial pmf may be chosen. Next, Fig. 5 shows the pmf of event duration W ; $E(W) = 1.68$, $VAR(W) = 1.416$, ($s(W) = 1.19$), $K = 98$. Again a negative binomial is a good representation; however, a good first approximation is a geometric pdf with parameter $p = .40$: $f_W(j) = (.6)(.4)^{j-1}$, $j = 1, 2, \dots$

(b) Model I only: The pmf of dry spell duration D , shown in Fig. 4, has a very high value for 1, 2, or 3 days, which may be considered as a statistical justification for developing and using Model II, in addition to the phenomenological reasons given earlier. One finds $E(D) = 5.83$, $VAR(D) = 43.2$ ($s(D) = 6.56$) for $K = 93$. A negative binomial may be fitted. The distribution of interarrival time T shown in Fig. 7 fits an exponential pmf: $E(T) = 7.51 = 150 E(N)^{-1}$, $VAR(T) = 43.3$ ($s(T) = 6.57$) with $K = 93$. Furthermore, note that

$$\begin{aligned} E(T) &= 7.51 = E(W) + E(D) = 1.68 + 5.83, \\ VAR(T) &= 43.3 = VAR(W) + VAR(D) = 1.42 + 43.2 \end{aligned}$$

The latter relationship seems to corroborate that W and D are independent, which was implied in the simulation algorithm. Also, it can be seen that D dominates W , especially in terms of variance.

(c) Model II only: The number of sequences per season N' follows a fairly peaked and symmetric pmf shown in Fig. 8; $E(N') = 13.09$, $VAR(N') = 4.57$ ($s(N') = 2.14$) for $K = 44$. The hypothesis of a normal approximation to a Poisson pmf with indicated mean as put forth in Eq. 12, cannot be rejected. Fig. 9 shows the pmf of number of events per sequence N_0 with a negative binomial fit corresponding to $E(N_0) = 2.15$, $VAR(N_0) = 1.86$, ($s(N_0) = 1.365$) for $K = 46$. The amount of precipitation per sequence R' also appears to follow a negative binomial pmf, as shown in Fig. 10, for $E(R') = .72$, $VAR(R') = .181$ ($s(R') = .424$), $K = 46$. At this point, Eq. 16 may be used for a verification:

$$E(R') = .72 \approx E(N_0) E(R) = 2.15 \times 0.35 = .750$$

$$VAR(R') = .181 \approx E(N_0) VAR(R) + VAR(N_0) (E(R))^2$$

$$= (2.15)(.08) + (1.86)(.35)^2 = 0.195$$

Duration D' between events in a sequence appears to be uniform with mean 2. The sample record is as follows:

Duration	1	2	4	4	5	6	...	13
Number of Points	19	14	18	7	4	3	...	4, Total 92

Still a negative binomial appears to give an acceptable representation of sequence duration V (Fig. 11), where $E(V) = 5.90$, $VAR(V) = 21.2$, ($s(V) = 4.78$) for $K = 41$. Note that the first relation in Eq. 7 holds approximately

$$E(N_0 - 1) E(D') + E(N_0) E(W) = (1.15)(2) + (2.15)(1.68) = 5.91 \approx E(V)$$

Fig. 12 shows the pmf of dry spell duration $B(>4)$; $E(B) = 10.63$, $VAR(B) = 56$ ($s(B) = 7.48$) with $n = 41$. Fig. 13 shows a widely scattered interarrival time; $E(Z) = 16.30$, $VAR(Z) = 59$ ($s(Z) = 7.64$) with $n = 41$. Both B and Z may be fitted to a negative binomial pmf. Also, the relationship $E(Z) = E(V) + E(B)$ holds but $VAR(Z) = 59 < VAR(V) + VAR(B) = 77.2$.

The asymptotic relationships of Eqs. 10 to 14 may now be used to check the validity of the Poisson hypothesis made on the renewal process of sequence starting epochs. With $\mu = E(Z)\sigma = 12.3$ (because $Z \geq 4$), $\sigma^2 = VAR(Z) = 59$, $n = 150$, Eq. 14 yields

$$E(N'(n)) \approx \frac{150}{12.3} = 12.2 \quad \text{compared to } 13.09$$

$$VAR(N'(n)) \approx \frac{150 \cdot 59}{(12.30)^3} = 5.88 \quad \text{compared to } 4.57$$

Remarkably enough, this model seems to approach its asymptotic form after only one season (150 days). In other works, for a climate similar to San Antonio's a synthetic series of events may be generated by the following approximation:

- (1) Define n , and estimate $\mu = E(\underline{Z})$, $\sigma^2 = \text{VAR}(\underline{Z})$ from the record.
- (2) Generate samples of $\underline{N}'(n)$ from the normal pdf defined by Eqs. 13 and 14.
- (3) Generate samples of $\underline{N}'(n)$ values of \underline{R}' and place them at random on the line $(0,n)$.

Clearly such an approximation would be readily acceptable for summer rainfall, since the duration \underline{V} would be very small compared to \underline{Z} (or B).

DISCUSSION AND CONCLUSIONS

This investigation is far from being all-inclusive; for example, the stochastic dependence between \underline{R}' and \underline{V} could be derived from that between \underline{R} and \underline{W} . Several hypotheses have been suggested concerning the elevation effect on either model, further data analysis will tell which hypothesis is acceptable. Also, the simplified synthetic series generation scheme proposed at the end of the preceding section requires further experimentation: it would have the great advantage of providing for a year-round rainfall event generator by simply adjusting the parameters seasonally. It thus turns out that the models possess considerable flexibility--one may choose the level of complexity matching the data and problem on hand. Model II which is based on both prior observation and experimental evidence, does not seem to possess substantially better features than the simpler Model I, at least for San Antonio data. In contrast, the comparison between Figs. 14 and 15, which correspond to east central Arizona data show that at that location interarrival time between sequences may be exponentially distributed (Figure 15) while interarrival time between groups do not seem to be so (Figure 14). The data analysis yields $E(\underline{T}) = 9.15$, $\text{VAR}(\underline{T}) = 66.3$ ($s(\underline{T}) = 8.14$, $K = 632$; data not shown in Figure 14 at 33(2), 35, 37, 40, 41, 43, 45, 57, 84, $E(\underline{Z}) = 12.22$, $\text{VAR}(\underline{Z}) = 73.45$ ($s(\underline{Z}) = 8.57$), $K = 392$; data not shown in Figure 15 at 33(3), 37, 40, 41, 43, 57, 94.

- (4) Either model may be used to generate synthetic series of rainfall.
- (5) Either model provides a framework for studying elevation effect in precipitation modeling.
- (6) Robustness of the models is such that an asymptotic normal process is reached after one season only (150 days) which leads to a simplified approximate generation scheme.
- (7) Internal consistency checks of the model tend to confirm that the assumptions may be reasonable and that data should be gathered along event-based lines rather than equispaced intervals.

ACKNOWLEDGEMENTS

The work upon which this paper is based was supported in part by funds provided by the United States Department of the Interior, Office of Water Resources Research, as authorized under the Water Resources Act of 1964, Project No. B-032AZ, entitled, "Decision Analysis for Watershed Management Alternatives", and by the National Science Foundation Grant ENG74-20462,

"Sensitivity of Decisions in Resources Engineering to Assumptions of Multivariate Models". The help of John Yu in retrieving and analyzing data is gratefully acknowledged.

REFERENCES

- Benjamin, J. R., and C. A. Cornell, Probability, Statistics, and Decision for Civil Engineers, McGraw-Hill, New York, 1970, p. 178.
- Cary, L., V. Gupta, and M. Fogel, A Stochastic Model of Snow Accumulation and Ablation, AGU National Meeting, Washington, D. C., April, 1974.
- Crovelli, R. A., Stochastic Models for Precipitation, Ph.D. dissertation, Colorado State University, F. Collins, Colorado, 1971.
- Duckstein, L., M. Fogel, and C. C. Kisiel, A Stochastic Model of Runoff-Producing Rainfall for Summer Type Storms, Water Resources Research, Vol. 8, No. 2, April, 1972, pp. 410-421.
- Duckstein, L., M. Fogel, and J. Thames, Elevation Effects on Rainfall: A Stochastic Model, Journal of Hydrology, Vol 18, December, 1973, pp. 21-35.
- Duckstein, L., E. Simpson, Uncertainties in Karstic Water Resources Systems, Yugoslavia, June, 1975.
- Feller, W., An Introduction to Probability Theory and Its Applications, Vol. 1, John Wiley, New York, 1968, p. 321.
- Fogel, M., and L. Duckstein, Point Rainfall Frequencies in Convective Storms, Water Resources Research, Vol. 5, No. 6, December, 1969, pp. 1129-1237.
- Fogel, M., L. Duckstein, and C. C. Kisiel, Space-time Validation of a Rainfall Model for Summer-type Precipitation, Water Resources Bulletin, Vol. 7, No. 2, March, 1971, pp. 309-316.
- Gupta, V. K., A Stochastic Approach to Space-time Modeling of Rainfall, Technical Report No. 18, Hydrology and Water Resources Interdisciplinary Program, University of Arizona, 1973.
- Gupta, V. K., and L. Duckstein, A Stochastic Analysis of Extreme Droughts, Water Resources Research, 1975.
- Kao, S., L. Duckstein, and M. Fogel, A Probabilistic Model for Winter Rainfall, AGU National Winter Meeting, San Francisco, California, December, 1971.
- Smith, J., M. Fogel, and L. Duckstein, Uncertainty in Sediment Yield From a Semiarid Watershed, Proceedings, 18th Annual Meeting, Arizona Academy of Sciences, Flagstaff, Arizona, April, 1974, pp. 258-268.
- Soil Conservation Service, Snow Survey and Water Supply Forecasting. U. S. Department of Agriculture, April, 1972.

Todorovic, P., and V. Yevjevich, Stochastic Process of Precipitation, Colorado State University, Ft. Collins, Colorado, Hydrology Paper No. 35, 1969.

Yakowitz, S., L. Duckstein, and C. C. Kisiel, Decision Analysis of a Gamma Hydrologic Variate, Water Resources Research, Vol. 10, No. 4, August, 1974, pp. 695-704.

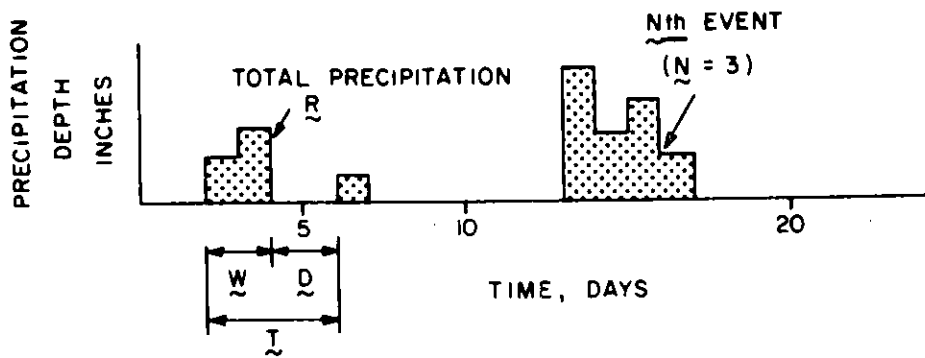


Figure 1. Definition sketch for Model I

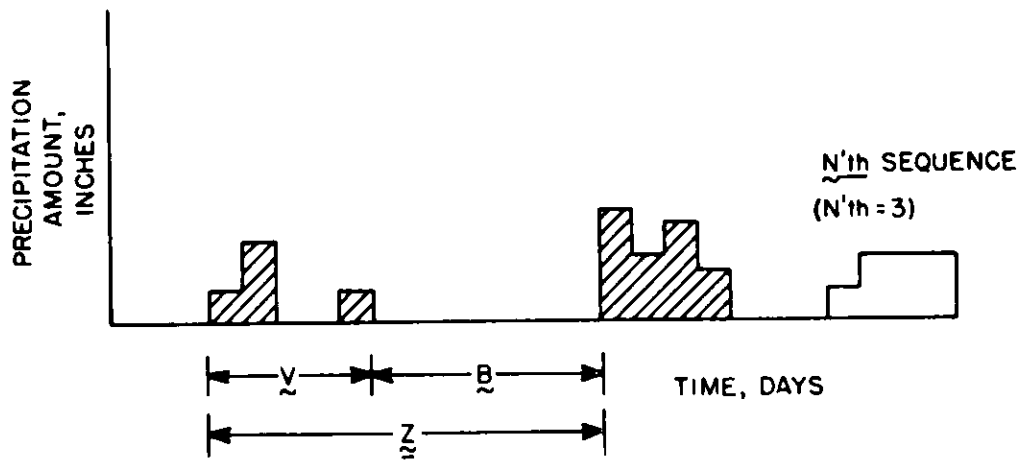


Figure 2. Definition sketch for Model II

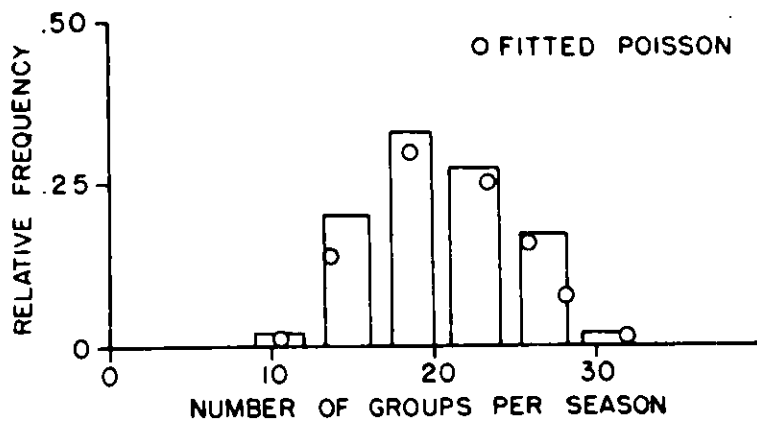


Figure 3. Number of events (groups) \underline{N} per season

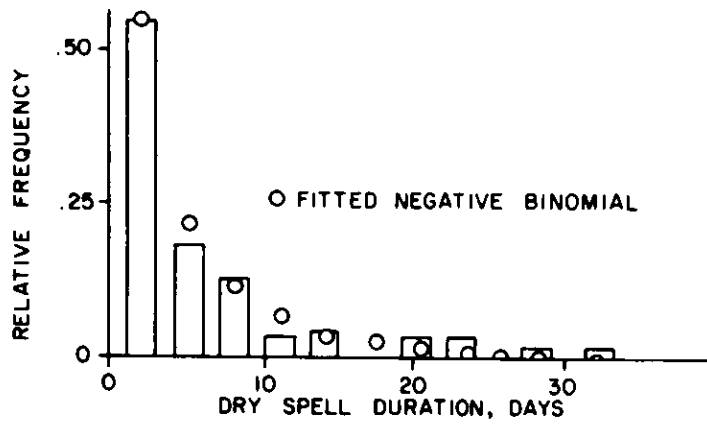


Figure 4. Duration of dry spell \underline{D} between events (groups for Model I)

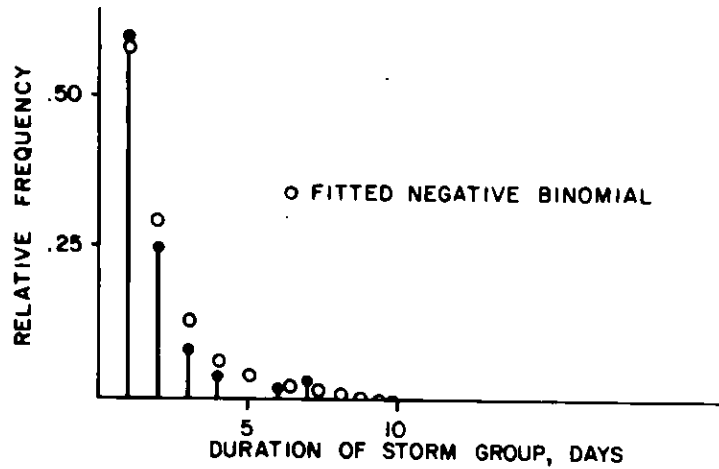


Figure 5. Duration of rainfall event (storm group) \underline{W}

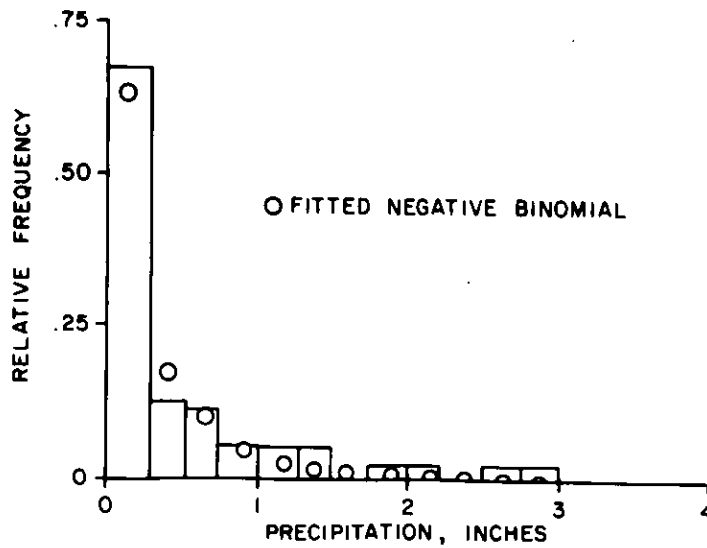


Figure 6. pmf of rainfall amount \underline{R} per event

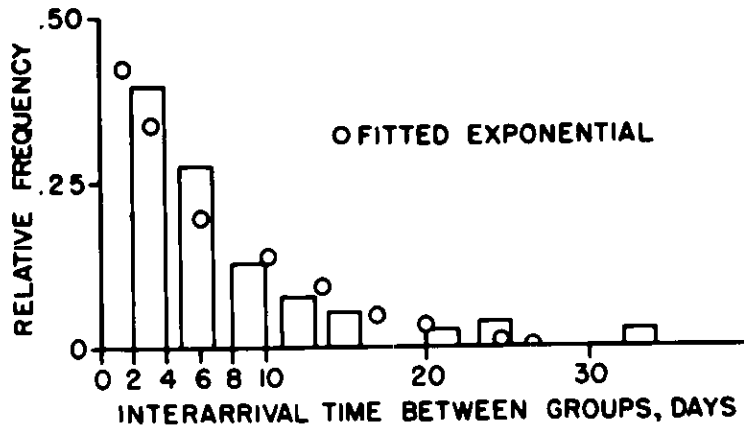


Figure 7. Interarrival (renewal) time \underline{T} between events (groups) for Model I

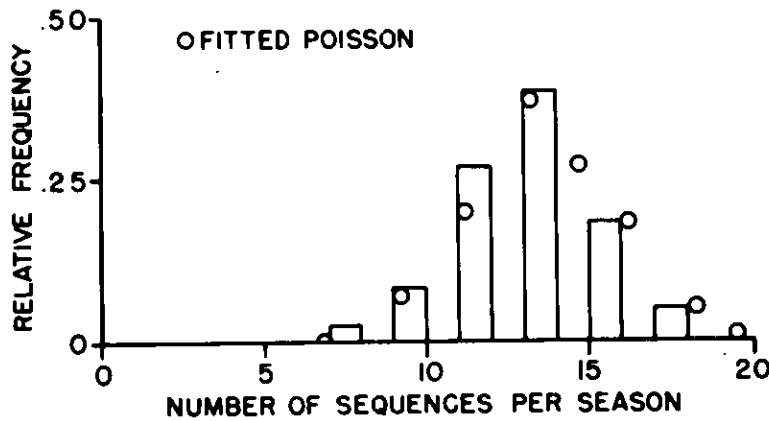


Figure 8. Number of sequences \underline{N} per season for Model II

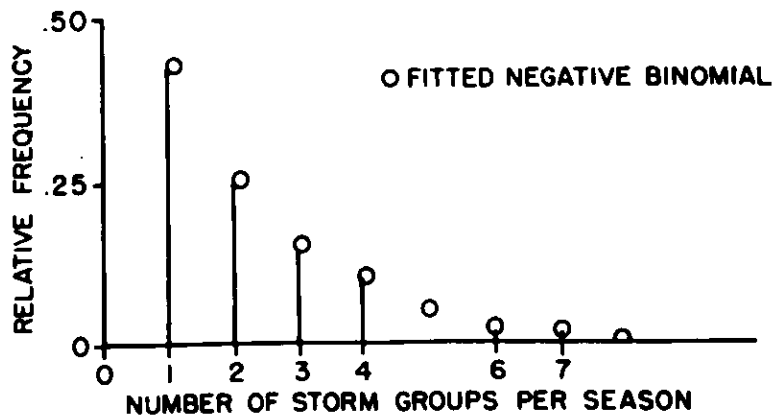


Figure 9. Number of events (groups) \underline{N}_0 per sequence for Model II

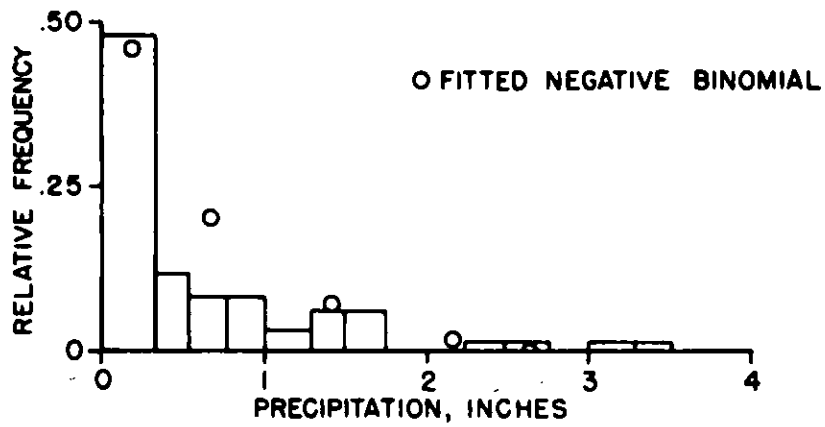


Figure 10. Amount of precipitation R' per sequence for Model II

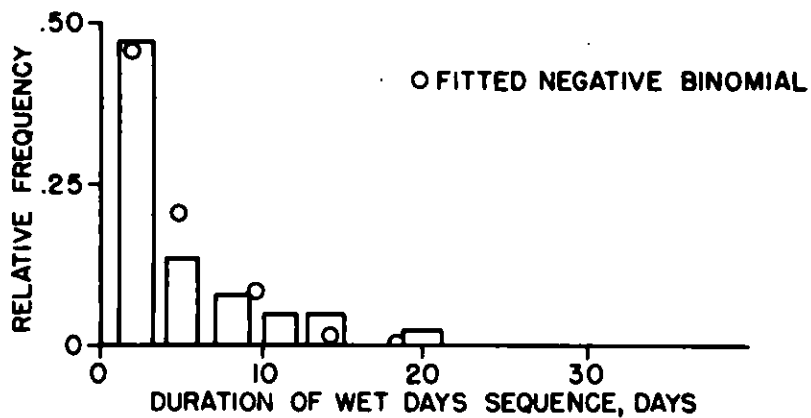


Figure 11. Duration of wet sequence Y for Model II

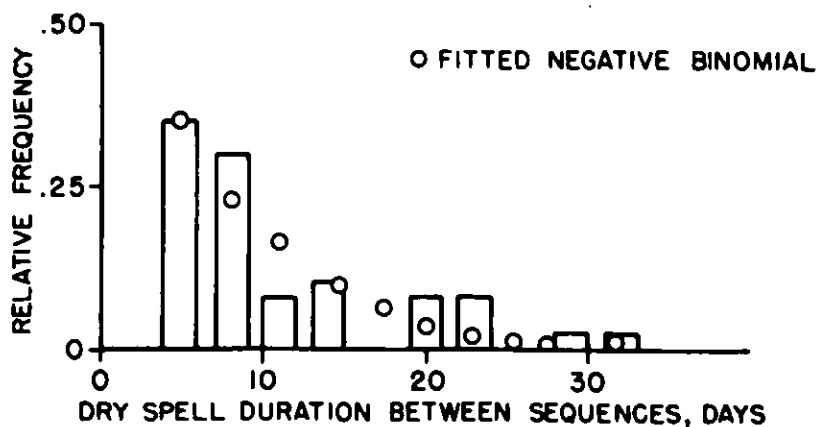


Figure 12. Duration of dry spell $B \geq 4$ between sequences for Model II

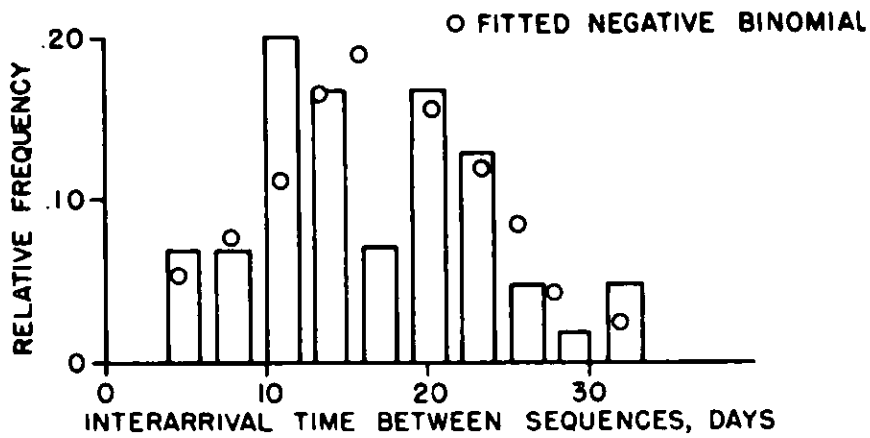


Figure 13. Interarrival (renewal) time \underline{z} between sequences for Model II

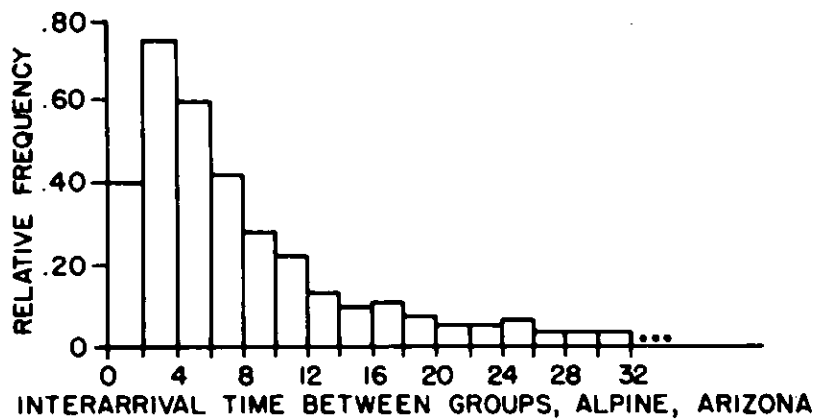


Figure 14. Interarrival time \underline{T} between groups, East Central Arizona

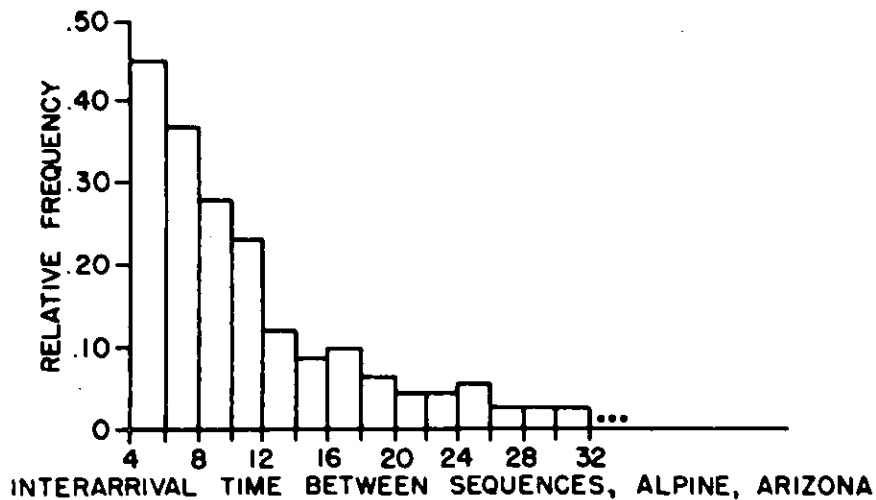


Figure 15. Interarrival time \underline{z} between sequences, East Central Arizona

GROUND-WATER MONITORING
AT SOLID WASTE DISPOSAL SITES -
TWO CASE STUDIES

by

PAUL H. ROUX, M.S. in Geohydrology
DAVID W. MILLER, M.S. in Geology

Geraghty & Miller, Inc.
Consulting Ground-Water Geologists and Hydrologists

INTRODUCTION

Many landfills in the eastern United States are located in marshes, abandoned gravel pits, along the banks of streams and in other areas where the water table is at or near land surface. The majority of landfill contamination studies reported in the literature are for sites with a deep water table. Ground-water flow patterns, however, and consequently the extent and severity of pollution from this type of site differs in many respects from landfills situated in shallow water table areas.

This paper describes some of the methods used and summarizes the results obtained for ground-water investigations at two landfills located in wetland areas. Investigative methods found useful include: drilled wells, hand driven well points, temperature and conductivity probing, and electrical earth resistivity surveys. The landfills described are the Croton Point landfill in Westchester County, New York, and the Milford landfill in Milford, Connecticut. The investigations were carried out by Geraghty & Miller, Inc. for Westchester County and the State of Connecticut, respectively. The field work described was carried out over the period 1972 through 1975.

CROTON POINT LANDFILL

Croton Point is a peninsula that extends into the Hudson River about 25 miles north of New York City. The land, owned by Westchester County, has for many years been used as a dump by local residents and for municipalities within the County. At present, the Croton Point landfill receives daily, 6 days per week, about 1,600 to 2,000 tons of refuse, including various types of non-chemical industrial waste. Located in a tidal marsh near the center of Croton Point, the landfill covers an area of about 70 acres and is as much as 80 feet thick. The location of the landfill is shown on Figure 1.

Well Installation

In order to obtain more detailed data on subsurface geology, the nature of the ground-water flow system, and physical and chemical characteristics of ground water at the Croton Point landfill, a well-drilling contractor was retained to construct small-diameter test wells. These were located, based on the analysis of the reconnaissance studies, at strategic points both in and around the landfill. Three borings penetrated the landfill itself and three were drilled in natural unconsolidated sediments off the landfill. The locations of the six wells (1 to 6) are shown on Figure 1. Two sets of casings and screens were set in each of the borings drilled on the landfill so that water levels and samples could be obtained at significantly different depths at the same site (shallower wells are designated 2A, 3A, and 4A). The completed wells range in depth from 39 to 131 feet below land surface and were left in place as permanent monitoring points.

The well drilling equipment consisted of an auger rig, capable of driving and pulling casing. On the landfill itself, a 4-inch hole was first augered through the refuse, and a 2-1/2-inch diameter steel casing was set in the hole. The casing was then driven to the desired depth. A water jet was used to remove sediments from the open casing, and a 2-foot long, 1-1/4-inch

screen was set opposite the zone to be monitored. The casing was then pulled back to expose the screen.

The second test well was lowered into the open hole next to the 2-1/2-inch casing and screened near the top of the water table. It consists of 1-1/2-inch diameter steel casing with a 1-1/4-inch, 2-foot long stainless steel well screen attached. The borehole was then backfilled with the material originally removed to prevent circulation of water within the hole. For each of the three test wells installed off the landfill, a single casing was used.

Geologic samples in the drilled wells were obtained either directly from the auger flights or by collecting sediment removed from the casing by the water jet. The actual depth to major changes in material types was determined by noting where the difficulty of drilling changed. At key locations, split spoon samples were obtained and used for geologic interpretation.

Fifteen small-diameter test wells (A to P on Figure 1) were hand driven in areas around the landfill where soft marsh sediments lay at and near the land surface or in sandy soils where the water table was at a shallow depth. This was accomplished by driving, using a 75 pound drive hammer, 1-1/4-inch diameter steel well casing with a 2-foot long, 1-1/4-inch well point attached. The process was fairly easy and a four man team was able to install, test pump, and sample about 5 wells per day.

As in the case of the drilled wells, all screens are stainless steel with a slot size opening of either 0.010 or 0.015 inches. The hand driven wells range in depth from 4.2 to 44 feet below land surface and were left in place for permanent monitoring. Approximate material cost for a 20-foot deep well as described above is \$75.00.

Water-level measurements were taken in all wells on a periodic basis throughout the study by means of a chalked tape and/or an electric probe device. Measuring points were established by level circuits and transit-traverse surveys of second-order accuracy. Water samples were collected by first blowing water out of the well casing by means of an air jet and then bailing the required quantity for analysis. Several rounds of sampling were carried out during the course of the investigation. Selected physical and chemical tests on water samples were conducted on site as the samples were collected. More detailed analyses were run by Olin Water Service Laboratory of New York.

Geologic Setting

Figure 2 is a generalized geologic cross-section drawn along the profile line A-A' on Figure 1. It is based mainly on the logs of Wells 3 and 4. Although geologic samples could not be obtained during the installation of the hand driven wells, an indication of the type of deposit being penetrated by the well point could be ascertained by the number of blows required to force the casing into the ground and by how easily the well would pump. Therefore, Wells A, G., H, and J are included on the cross section. Wells A and H encountered all bog deposits and Wells G and J were completed in sand.

The diagram shows the relationship between the various beds underlying the landfill, including the estimated position of the bedrock surface. As can be seen, the landfill is underlain by more than 60 feet of organic bog and silt and clay lacustrine deposits. These low permeability sediments were found to impede, but not to prevent, the downward and outward migration of water recharged through the landfill.

The areas surrounding the landfill are primarily fine sand and silt glacial outwash deposits overlying silt and clay lacustrine sediments. The bog deposits which underlie the landfill and marsh areas fill an eroded depression which once extended across the entire point. Bedrock was not encountered during drilling, so its depth is not accurately known. Seismic data indicates, however, that it is more than 150 feet below sea level.

Water Levels

Major emphasis during the investigation was given to the collection of water-level data in and around the landfill. Measurements were taken periodically in all wells in an effort to use the information to help develop an understanding of the movement of ground water beneath Croton Point.

Ground water is always in motion through geologic formations, following paths from areas of intake to areas of discharge. The land surface is the area of intake for water derived from precipitation. Rivers, bays, other surface waters, and wetlands, are the bodies into which ground water ultimately discharges. From its point of entry underground, any single drop of water follows a continuous path through the unconsolidated deposits and rock until it arrives at the nearest point of discharge.

Ground water seldom travels great distances, because in most places the bodies of surface water that serve as discharge areas are not very far apart. Water may travel in any direction with respect to hydraulic gradients or elevations. The actual path of water movement can be defined in terms of head of water. In other words, pressures and elevations do not in themselves determine which way ground water will move. The path followed by a drop of ground water is determined mainly by differences in the head of water in the ground-water system, and may be downward, horizontal, or upward, depending on the flow pattern.

Movement of ground water is most commonly portrayed by means of water-table maps, which indicate horizontal components of flow. Figure 3 shows the water table on Croton Point in the vicinity of the landfill. The contours have been drawn to connect points on the water table having an equal elevation above mean sea level. According to one basic law of ground-water flow, the direction of movement of any drop of ground water in an unconfined aquifer is at right angles to the water-table contours. Thus, a drop starting in the vicinity of Well 2, for example, will move almost due south toward Well 1. A drop starting at Well 3 would follow a line toward Well F.

The water-table map shows only the horizontal direction of flow and gives no indication of how deeply the drop of water descends along its path to the Bay or the River. Under some conditions, a drop of water may travel at fairly shallow depths from the place where it reaches the water table to the place where it leaves the ground-water system. Elsewhere, it may descend

rather steeply to invade deeper saturated zones. Thus, a proper evaluation of ground-water flow involves a knowledge of what is taking place in the vertical dimension as well as in the horizontal.

Figure 4 is an east-west section along profile A-A'. The arrows show the generalized pattern of ground-water flow. Water reaching the water table in the center of the peninsula first moves downward but eventually discharges either toward Croton Bay or Haverstraw Bay depending upon the position of a particular drop of ground water in relation to the ground-water divide.

The dashed lines on the illustration, which are similar in some respects to water-table contours except that they are oriented vertically, show heads of water in feet above sea level. These lines of equal head are called isopotential lines, because each of them traces out a region in the water-bearing deposits along which the potential or head of water is everywhere the same. The diagram shows that if you screen progressively deeper wells near the center of the landfill, the resulting water level each time would be progressively lower in elevation. The opposite holds true for a well drilled in the marsh area.

Both Figures 3 and 4 reveal a number of other important factors. The water table attains a maximum elevation of more than 14 feet above sea level near the center of the Point under the landfill. This mounding is probably the result of two factors: (1) the difference in permeability between the landfill and the underlying deposits, and (2) the high recharge rate through the flat, unvegetated and relatively permeable landfill surface. The mounding is the driving force that causes ground water to move away from the landfill in all directions. However, the shape of the contours on Figure 4 indicates that ground water moving through the landfill discharges rather quickly into the marsh area to the southeast compared with that flowing in a northwesterly direction toward the beach. This conforms to the water quality findings, which showed that ground water encountered in the shallow wells to the east of the landfill were the most highly contaminated.

The shape of the contours on Figure 4 also shows the effects of the geology of the sediments underlying the landfill on the movement of ground water. Because the beds were laid down horizontally, and thin beds of clay are interlain with thicker beds of sand, permeability in the horizontal direction is considerably greater than in the vertical direction. This results in the elongated shape of each trace of the equipotential surface and can be observed on the diagram in spite of the vertical scale exaggeration of approximately eight times. The diagram also reveals that some ground water is moving through the relatively fine-grained sediments and has penetrated vertically to the deeper well screens at the sites of Wells 3 and 4. The deep vertical migration of water that has been in contact with refuse, corroborates the temperature and chemical data determined for water samples obtained from the two wells.

Figures 3 and 4 also provide, together with the analysis of geologic samples obtained during drilling, some insight into the velocity of ground-water flow from the point of recharge to the ground-water system to the point of discharge. The velocity of ground-water flow is dependent on the permeability of the deposits and the hydraulic gradient in the ground-water body. Permeability is a measure of the ease with which water

can move through a given material. The hydraulic gradient is the loss of head that occurs along the path followed by the water; it is usually expressed in terms of the drop in head per-foot traveled. Clayey silt and bog deposits, for example, have low permeabilities and typical flow rates through these formations are normally measured in inches per day. Sand and gravel, on the other hand, have relatively high permeabilities and will transmit ground water at velocities of up to several feet per day. Using the hydraulic gradients developed in and around the Croton Point landfill and estimated permeabilities for the various geologic formations penetrated, it appears that under present conditions, ground water is moving on the average of about one-half to one foot per day.

Using all of the geologic and hydrologic information presently available, a broad estimate of total recharge and, thus the equivalent discharge, can be determined for the landfill. This can be approached in two ways: first by analyzing discharge based on cross-sectional areas, permeabilities, and gradients; and second by analyzing recharge based on infiltration areas, infiltration rates, and rainfall (rainfall averages about 45 inches per year). Both methods indicate average recharge and discharge in the range of approximately 100,000 gpd (gallons per day). This value, approximately one half of the total precipitation on the landfill surface, represents the rate of leachate generation for the Croton Point landfill.

Ground-Water Temperature

One key physical effect that decomposition of refuse has on water as it moves through the landfill is to raise its temperature. Because ground water loses heat very slowly as it passes through sediments, this characteristic can sometimes be used as an effective tracer of flow direction and movement of contaminated water away from a landfill. Consequently, vertical and horizontal temperature profiles were constructed for the ground waters of Croton Point based on readings taken in the drilled and driven wells and at a large number of temporary sampling points in the marsh and beach areas.

The temporary sampling points were measured by means of a specially designed temperature-conductivity probe. This device consisted of an aluminum tube, pointed at one end with a thermometer and specific conductance meter mounted at the other. Remote probes extended from the instruments to the pointed end which is perforated over a one-foot length. The perforations are covered by an aluminum sleeve which can be retracted to expose the openings. The probe is pushed into soft sediments to a depth of from 1 to 8 feet and the sleeve is retracted. Ground water seeps into the probe and its temperature and specific conductance is measured directly.

The temperature of ground water near the surface of the water table within the landfill itself exceeds 130°F. This is in sharp contrast to normal ground-water temperature, which should be about 53°F. This clearly shows that the landfill generates heat that affects ground-water temperatures. Figure 5 shows the distribution of ground-water temperature at the Croton Point landfill. During the collection of temperature data at the driven wells in the marsh, there appeared to be a close relationship between the permeability of the sediments opposite the well screen and the degree of temperature anomaly. Those wells that were the easiest to pump and consequently tapped the more permeable deposits consistently yielded water

with higher temperatures than those wells that were difficult to pump. Thus, ground water moving away from the landfill through these more permeable zones has a greater velocity. Because natural ground water in this area has a temperature of about 53°F, any encountered at shallow depth with a higher temperature probably has infiltrated through the landfill first before reaching the point of sampling.

The broad area east of the landfill where temperature are greater than 55°F may be indicative of the discharge into the shallow sediments underlying the marsh of deeper affected waters emanating from the landfill. Heated ground water is also discharging to the west of the landfill. On the other hand, water significantly affected by infiltration through the refuse has not moved very far from the landfill in the direction of Well 1 to the southwest, or Well 6 to the northeast.

Temperature data also can be useful in tracing vertical movement of ground water through and away from the landfill as illustrated in Figure 6. This diagram is a graph of the temperature recorded in each of the drilled wells versus elevation, referenced to mean sea level, of the sampling point. Wells 3 and 4, which are located in the landfill, again show very high temperature readings at the water table. These temperatures become progressively lower with depth but are anomalous even at an elevation of -45 feet, considerably below the bottom of the landfill. This indicates that ground water moving through the landfill has penetrated the underlying bog and silt and clay deposits. Well 2 also shows relatively high ground-water temperatures throughout the entire section sampled, but the shallow readings are not as extreme as Wells 3 and 4 because it is located on the edge of the landfill. Wells 1, 5, and 6 are located away from the landfill and show background conditions.

Ground-Water Quality

The results of chemical analyses of water samples from the drilled test wells are given in Table 1. The locations of the wells are shown in Figure 1. The analyses show the general character of the leachate being generated at the Croton Point landfill: high concentrations of dissolved solids such as chloride, calcium, magnesium, alkalinity; low nitrate and nitrite but fairly high ammonia; low concentrations of lead and aluminum; and an approxiamtely neutral pH.

The analyses of water from Wells G and H are included to show how the chemical data supports the flow diagram shown in Figure 4. Although Well G is located closer to the landfill, water from Well H is considerably more highly mineralized. This condition is related to the flow system that exists under the landfill. The degree of contamination in the water from each well is dependent upon the position of the well screen relative to ground-water heads rather than the comparative overland distance of each well from the toe of the landfill. Thus, in monitoring the landfill, depth of each well screen is as important as the areal distribution of the monitoring points.

Water quality at Wells A and J is indicative of leachate contamination. Well 5 is slightly affected, whereas water from Wells 1 and 6 is approximately background quality.

MILFORD LANDFILL

The Milford landfill is located on the shore of Long Island Sound in Milford, Connecticut. Figure 7 is a location map showing the landfill and surrounding area. The active landfill and the abandoned power plant fly-ash disposal site occupy an area of approximately 50 acres. The landfill is situated on a former tidal marsh adjacent to Long Island Sound. A part of the marsh is still evident and almost completely surrounds the landfill. Refuse is derived from the surrounding community and consists of common household wastes, construction rubble, brush, leaves and various types of solid and liquid wastes from many of the local industries. Recently, a volume-reduction plant was constructed at the site to shred a portion of the refuse prior to deposition in the landfill.

Well Installation

Test wells were installed by a well drilling contractor at the sites designated TW 1 through TW 9 on Figure 7. At selected locations, two wells (one deep and one shallow) were placed adjacent to each other in order to establish relationships of the ground-water system at different depths (the shallow well is indicated by an A). Altogether 14 wells were drilled. The drilling and construction methods used were as described for the Croton Point landfill. Ten wells penetrated the landfill itself, and four were located in the natural sediments. The wells ranged in depth from 12 to 96 feet below land surface.

Twenty-two hand driven shallow well points were installed to obtain additional data on water quality and water levels in the sediments around the landfill. Wells installed by hand have letter designations on Figure 7.

Geologic Setting

Almost the entire project site at one time was underlain by swamp deposits ranging from a few to tens of feet thick, covering an area approximately one mile by one-half mile. Directly beneath the landfill these deposits appear to have been compressed and mixed with fill materials so that a distinct layer can no longer be discerned. The landfill site was formerly a tidal marsh but has since been isolated from tidal effects except for one channel in the eastern section. In this latter area, streams discharge fresh water during the low tide cycle and contain salt water in at least a portion of their reach during high tide. Approximately half of the original marsh has been filled in to allow for construction of houses, roads, etc.

The marsh deposits are underlain by a 40- to 60-foot thick section of unconsolidated material consisting of glacial till and outwash sediments. The till extends into the site from the northwest. The outwash sediments are part of the Wepawaug River Valley formation, extending northeast to southwest through the area, and they include layers of fine sand, silt, and clay. Individual beds do not appear to be extensive.

The underlying bedrock is primarily schist with some gneiss. A bedrock valley extends from west to east across the northern portion of the landfill site. Figure 8 is a generalized geologic cross section through the landfill, designated A-A' on Figure 7. As can be seen, the bedrock slopes gently from

the center of the landfill toward the southeast. A bedrock outcrop is located northwest of the landfill site.

Water Levels

Figure 9 shows the water table at the Milford landfill site. These contours have been drawn to connect points on the water table having equal elevation above mean sea level. Data on which the map is based are water levels from the wells shown on Figure 7.

The water-table map is similar to the Croton Point example in that a ground-water mound has formed near the center of the landfill. One difference, however, is that in this case ground water is flowing from the high area to the northwest toward the landfill so that leachate flowing in this direction is deflected to the northeast and southwest.

Figure 10 is a northwest-southeast schematic diagram indicating the generalized ground-water flow pattern along the profile line A-A', as shown on Figure 7. The numbers adjacent to the well screens are the altitude of water levels in each well. The ground-water flow pattern is from zones of high head to those of low head. The arrows show the generalized pattern of ground-water flow.

The landfill itself is the recharge area. Some of the water reaching the water table directly under the landfill first moves downward and then starts to flow laterally toward a point of discharge. The principal discharge takes place toward Long Island Sound.

Both Figures 9 and 10 show that the water table has attained an elevation of over 8 feet above sea level under the landfill while the refuse itself extends down to sea level.

This is caused by increased recharge and permeability differences as explained in the Croton Point discussion. The 8-foot head is providing the force necessary to cause leachate to migrate downward and away from the landfill.

The shape of the contours on Figure 9 indicates that contaminated ground water is moving southeast directly toward Long Island Sound. Ground water moving to the west and southwest is discharging into standing surface-water bodies and surface streams draining the area. In some portions of the site, the water table has risen above land surface, and leachate ponds have formed.

The pattern of flow in Figure 10 indicates that some of the ground water that has been in contact with the refuse is moving vertically downward and has invaded the deeper zones of unconsolidated materials directly below the landfill. This flow of highly mineralized ground water is corroborated by the chemical analyses of water taken from the deep wells. That contaminated ground water reaching these deep zones is less highly mineralized than water which is still in contact with the refuse demonstrates the capacity of the fine-grained sediments to remove some of the dissolved solids from the ground water.

The highest portion of the water table is located near the center of the landfill. Before refuse was placed at this site, the water table must have extended from the Sound to the natural hill to the north of the site, with only a relatively slight rise in head. The landfill operation has caused a new artificial water-level high. Consequently, the water table in areas adjacent to the landfill has also risen above the prelandfill level.

One of the effects of the abnormal high water table is the stress placed on the vegetation surrounding the landfill. Remote sensing aerial photographs taken at the site reveal that trees and shrubs in high water table areas adjacent to the landfill are dying off.

The methods for calculating rates and volumes of leachate generated are the same as described for Croton Point. Using the hydraulic gradients observed in and around the landfill, and the permeabilities calculated for the various geologic formations penetrated, it appears that under present conditions ground water is moving at an average rate of about 0.10 to 0.25 foot per day. A broad estimate of total recharge and thus the equivalent discharge was determined for the active portion of the landfill and adjacent fly-ash dump, an area of about 55 acres. Both recharge and discharge calculations indicate average generation is approximately 80,000 gpd or 55 gpm (gallons per minute).

Ground-Water Temperatures

An attempt was made to map the areal extent of contaminated ground water at the Milford landfill site using temperature measurements. Unfortunately, two interrelated factors existed which greatly reduced the success of the temperature analysis as a means for tracing leachate flow. First, this type of survey is dependent on the temperature of the contaminated body of ground water being significantly different than that of the natural ground water. In the case of the Milford landfill, the highest temperatures recorded in the ground-water body, directly under the thickest portion of the landfill, were between 62°F and 67°F. The temperature of the natural ground water in this region is about 52°F at depths between 30 to 50 feet. This temperature difference is somewhat less than was anticipated prior to the commencement of the drilling. The comparatively low temperature differential is probably due both to the relatively thin unsaturated section of refuse and to the nature of the wastes that have been deposited. That much of the refuse was shredded prior to placement in the fill may have influenced the temperature pattern; however, this is not certain.

The second factor related to the temperature survey was the air temperature at the time of the investigation. Since the field work at the landfill was conducted during the summer months, the average temperature of the air and infiltrating rainfall was naturally quite high, and water in shallow zones had been warmed. For example, the temperature of the natural ground water 5 to 7 feet below land surface was 49.9°F in mid-May while the temperature at the same point in mid-August was 59.2°F, a rise of 9.3°F. Thus, the maximum temperature differential between the background and contaminated ground-water bodies was less than 10°F at the time of the survey (August), and an effective definition of the lateral spread of leachate from the landfill was not possible using temperature methods.

Temperature data was useful, however, in tracing vertical movement of ground water beneath the landfill. In this case temperature of ground water from deeper zones, not affected by seasonal changes in air temperature, are of interest. Figure 11 is a plot of temperature vs. depth in Wells 1 through 5. Wells 1, 2, and 3 are located in the landfill, Wells 4 and 5 are located off the landfill, and contain ground water of approximately background temperatures.

It should be noted that Wells 1, 2, and 3 have significantly higher temperatures at the water table (the shallowest depth shown for each graph) than Wells 4 and 5. Furthermore, although the water temperatures in the landfill wells become increasingly lower with depth, the temperature level is anomalous even at 89 feet in the case of Well 2. This indicates that the heated water from the base of the landfill has penetrated to this depth.

The temperature of the ground water in Wells 4 and 5 is high near land surface due to seasonal influences but attains background level at about 10 feet below land surface. It cannot be stated with certainty why the water temperature in Wells 4 and 5 increases slightly below the 15-foot level. The rate of increase is considerably greater than the thermal gradient that should be expected and may be related to the landfill. The sharp rise in temperature at the bottom of Wells 1, 2, and 4 is caused by the thermometer probe penetrating sediments in the well prior to taking the last reading.

Resistivity Survey

Seventeen vertical electrical resistivity profiles were conducted at the Milford landfill site, to determine, among other things, the areal limits of highly contaminated ground water in the vicinity of the landfill. The locations of these profiles, designated RP1 through RP17, are shown on Figure 12.

For this type of survey, a series of single depth electrical resistivity measurements are made at a depth sufficient to penetrate the water table. Since highly contaminated ground water has a significantly lower resistivity than natural, fresh ground water, the relative values of the measurements will give a general indication of the pattern of occurrence of highly mineralized ground water.

In an area where brackish or salt-water bodies border or underlie landfills, as in the case of Milford, the use of this type of survey is limited. Since the salt water has a very low resistivity, there is no sharp, clear-cut delineation between the salt water and highly mineralized leachate.

Figure 12 shows the results of selected single resistivity values from each of the vertical profiles run at the Milford site. Each value represents the resistivity of the total section to a depth of between 15 to 20 feet below the water table. The figure indicates three major environments that have been defined by this survey. The northernmost is an area where the upper saturated section contains natural, high-quality, fresh, ground water. This, in turn, is bordered to the south by ground water affected by leachate from the landfill. The portion of the site adjacent to Long Island Sound is underlain by brackish water. Table 2 shows typical chemical analyses of water obtained from wells located in the three environments.

Water Quality

A number of laboratory analyses were run on water obtained from the drilled and driven test wells. The results from selected wells are shown in Table 3.

The pH of all the water samples was determined. Most natural ground waters have pH values ranging from about 6.0 to 8.5. The only water sample to fall significantly out of this range was obtained from Well E, which had a pH of 3.8. This well is located at the edge of the fly-ash dump, which is probably leaching sulfuric acid into the ground-water system.

Relatively low levels of hardness and alkalinity were found in water from Wells A and P, which are located in the natural ground-water environment. On the other hand, high concentrations of these two constituents are found in water from the zone directly beneath the landfill. As contaminated ground water moves into deeper aquifer zones below the landfill, hardness and alkalinity are reduced, but concentrations are still significantly above background level. In areas of naturally occurring salt water, the location of Well 5 for example, the disproportion of the ratio of calcium hardness to total hardness indicates that leachate has affected the ground water.

Chemical oxygen demand (COD) was determined in most of the well-water samples, since high concentrations are typically associated with landfill leachate. The results of the analyses show high concentrations of COD in waters from the zone directly beneath the refuse. Water from wells screened at greater depths and those located off the landfill showed no distinct pattern.

Ammonia in high concentrations was found in the saturated refuse section of the landfill site. The presence of this constituent correlates well with the presence of leachate. Background levels of ammonia in the area northwest of the landfill are about 0.02 mg/l (milligrams per litre) and in the marsh area to the east (Well 5) about 0.06 mg/l. Those obtained in the saturated refuse range from 35 to 202 mg/l. In the deep zone below the landfill, ammonia concentrations range from only 0.045 to 0.60 mg/l, while concentrations in water from shallow wells south and southeast of the landfill range from 1.6 to 40 mg/l.

These data indicate that ground water contaminated by the landfill is moving both downward and laterally toward the south and southeast, away from the landfill, and that there is significant modification of leachate composition by the natural sediments. The ammonia concentrations, along with COD and others, indicate a highly contaminated zone of ground water directly beneath the landfill with significantly lower contaminant concentrations away from the refuse area.

Iron, manganese, copper and lead were determined for most of the water samples obtained from the wells. High concentrations of iron and manganese were invariably found in waters immediately associated with the refuse and fly-ash areas. However, copper and lead were rarely above trace concentrations, even in the saturated refuse zone.

SUMMARY

Some of the investigative methods employed in and the results obtained from the Croton Point and Milford landfill studies are generally applicable to other landfills in similar settings. With regard to the installation of monitoring wells, it was found that well depth is as important a factor as well location, and that two or more small diameter wells installed at different depths in a single borehole through the landfill provide much more valuable information than a single well. To determine ground-water quality and flow patterns beyond the landfill, small diameter well points were driven into the soft sediments by hand.

Temperature and conductivity were found to be the most useful indicators of the presence of leachate because they are invariably affected by contact of ground water with refuse and are easily measured in the field. Difficulties did arise, however, when air temperature was very high and when naturally occurring brackish water was present. Electrical earth resistivity was useful but its value was limited at both sites by inaccessible terrain and the presence of brackish water.

Ground-water mounds were found in both of the landfills investigated. These were apparently the result of increased recharge through the landfill surface and a permeability differential at its base. These mounds provide the force which causes the leachate generated within a landfill to flow away horizontally and to migrate downward into the deeper underlying sediments. Leachate generation at both of the landfills investigated was about one gallon per minute per acre, and the rate of movement of leachate away from the landfills ranged from 0.1 to 1 foot per day. The distance the leachate traveled prior to discharge to a surface-water body was relatively short. Long leachate plumes associated with some landfills in areas with deep water tables did not develop.

Chemical characteristics of the leachate from the primarily municipal refuse in the two landfills included high concentrations of chloride, calcium, magnesium, iron, alkalinity, and ammonia. The chemical oxygen demand was high and the pH was invariably close to neutral. Concentrations of lead, aluminum, nitrate, and nitrite were relatively low.

Organic bog deposits and layers of silt and clay were found to impede the movement and to reduce the concentration of contaminants in the ground water. However, highly contaminated ground water was found hundreds of feet beyond the landfill boundaries and at the deepest depths drilled to at both sites.

SELECTED BIBLIOGRAPHY

- Apgar, M.A., and D. Langmuir, 1971, Ground-Water Pollution Potential of a Landfill Above the Water Table, *Ground Water*, V. 9, No. 6.
- Geraghty & Miller, Inc., 1973, Investigation of Ground-Water Conditions, Croton Point, Westchester County, N.Y., Consultant's Report, Port Washington, N.Y., 40 p.

- Geraghty & Miller, Inc., 1975, Phase II Program of Hydrogeologic Investigations at the Croton Point Landfill Site, Westchester County, N.Y., Consultant's Report, Port Washington, N.Y., 61 p.
- Geraghty & Miller, Inc., 1973, Environmental Feasibility, Proposed Silver Sands State Park, Milford, Connecticut, Consultant's Report, Port Washington, N.Y., 40 p.
- Hughes, G.M., R.A. Landon, and R.N. Farvolden, 1971, Hydrogeology of Solid Waste Disposal Sites in Northeastern Illinois, U.S. Environmental Protection Agency, Washington, D.C., 154 p.
- Kimmel, G.E., and O.C. Braids, 1975, Preliminary Findings of a Leachate Study on Two Landfills in Suffolk County, New York, Journal of Research, U.S. Geological Survey, Vol. 3, No. 3, p. 273-280.

Table 1. Chemical analyses of selected observation wells, Croton Point landfill, Westchester County, New York.

	Well 1	Well 2	Well 2A	Well 3	Well 3A	Well 4	Well 4A
Depth	96	124	58	131	59	117	44
pH	7.5	7.2	-	7.3	-	7.0	-
Specific Conductivity, (MMHOS)	700	1,300	-	6,400	-	10,250	-
Total Dissolved Solids	235	790	-	2,880	-	4,840	-
Chloride (Cl)	48	122	110	1,875	2,450	2,375	1,250
Total Hardness (CaCO ₃)	176	406	640	660	650	880	260
Alkalinity (CaCO ₃)	144	352	504	628	3,320	708	1,760
Aluminum (Al)	0.5	0.5	0.5	0.5	0.5	0.5	0.5
Lead (Pb)	0.1	0.1	0.1	0.1	0.2	0.1	0.1
Magnesium (CaCO ₃)	82	303	307	533	710	779	188
Calcium (CaCO ₃)	125	80	235	124	157	190	140
Fluoride (F)	0.1	0.1	-	0.1	-	0.1	-
Nitrate (NO ₃)	1.5	1.3	-	1.4	-	1.5	-
Nitrite (N)	0.009	0.009	-	0.01	-	0.005	-
Ammonia (N)	0.7	11.9	-	14.7	-	27.7	-
Phosphate, total (PO ₄)	0.7	0.5	-	2.0	-	2.0	-
Ortho Phosphate (PO ₄)	0.5	0.5	-	0.5	-	0.7	-
Sulfate (SO ₄)	32	11	-	3	-	3	-

Table 1. (Continued)

	Well 5	Well 6	Well A	Well G	Well H	Well J
Depth	39	48	30	7	22	7
pH	7.7	7.7	-	6.7	-	7.1
Specific Conductivity, (MMHOS)	1,600	900	-	5,750	-	1,250
Total Dissolved Solids	500	280	-	3,160	-	1,085
Chloride (Cl)	80	45	2,550	1,625	3,000	175
Total Hardness (CaCO ₃)	208	120	1,600	620	1,660	519
Alkalinity (CaCO ₃)	180	80	2,040	340	1,720	160
Aluminum (Al)	0.5	0.5	0.5	0.5	0.5	0.5
Lead (Pb)	0.1	0.1	0.1	0.1	0.1	0.1
Magnesium (CaCO ₃)	79	41	1,435	459	1,435	184
Calcium (CaCO ₃)	122	73	225	135	312	275
Fluoride (F)	0.4	0.1	-	0.1	-	0.2
Nitrate (NO ₃)	0.4	1.0	-	31.5	-	2.6
Nitrite (N)	0.009	0.008	-	0.034	-	0.85
Ammonia (N)	0.07	0.07	-	2.1	-	0.07
Phosphate, total (PO ₄)	0.5	1.7	-	3.2	-	0.5
Ortho Phosphate (PO ₄)	0.5	0.5	-	0.5	-	0.5
Sulfate (SO ₄)	22	23	-	6	-	168

Table 2. Chemical analyses in three major ground-water environments, Milford, Connecticut. (Results expressed in mg/l, where applicable.)

	Natural Well A	Contaminated		Brackish Well 5A
		Landfill Area Well 3A	Fly-Ash Area Well E	
pH	5.9	5.8	3.8	6.5
Alkalinity (CaCO ₃)	8.0	1,700	3,885 (total acidity)	32
Total Hardness (CaCO ₃)	64	2,240	540	7,000
Calcium Hardness (CaCO ₃)	28	1,300	80	1,000
Specific Conductance (micromhos/cm)	142	5,990	4,610	36,300
Chemical Oxygen Demand (COD)	34	12,400	227	924
Ammonia (N)	0.018	103	6.0	7.0
Chloride (Cl)	7.0	650	40	18,400
Iron (Fe)	0.25	63	252	0.05
Manganese (Mn)	0.08	12	6.25	1.54
Copper (Cu)	0.06	0.00	0.75	-
Lead (Pb)	0.05	-	0.05	-

Table 3. Chemical analyses of ground water, Milford, Connecticut.
(Results expressed in mg/l, where applicable.)

	Well 1	Well 1A	Well 2	Well 2A	Well 3	Well 3A
Depth (feet)	66	30	99	35	79	26
Color	-	-	-	-	-	-
Turbidity	-	-	-	-	-	-
pH	7.5	6.8	6.4	6.65	5.3	5.8
Alkalinity (CaCO ₃)	142	980	80	1,720	10	1,700
Total Hardness (CaCO ₃)	184	490	370	700	500	2,440
Calcium Hardness (CaCO ₃)	84	110	200	300	230	1,300
Conductivity (micromhos/cm)	879	3,740	1,169	6,660	2,350	5,990
Chemical Oxygen Demand	40	991	57.6	2,050	92	12,400
Ammonia (N)	0.045	113	0.21	242	0.60	103
Calcium (Ca)	-	44	-	-	92	520
Magnesium (Mg)	-	91	-	-	65	226
Sodium (Na)	140	330	135	630	300	500
Chloride (Cl)	175	550	255	1,500	550	650
Iron (Fe)	0.14	63	0.23	55	41	63
Manganese (Mn)	0.94	8.3	0.00	130	6.4	12
Copper (Cu)	0.00	0.00	0.00	0.00	0.00	0.00
Lead (Pb)	-	-	0.05	0.10	-	-

Table 3. (Continued)

	Well 4	Well 4A	Well 5	Well 5A	Well 6	Well 7
Depth (feet)	58	12	63	13	24	23
Color	-	-	-	-	-	-
Turbidity	-	-	-	-	-	-
pH	6.8	6.8	7.1	6.5	7.0	7.2
Alkalinity (CaCO ₃)	164	716	172	32	1,030	524
Total Hardness (CaCO ₃)	2,980	480	4,300	7,000	600	350
Calcium Hardness (CaCO ₃)	880	200	1,000	1,000	180	130
Conductivity (micromhos/cm)	18,500	2,130	25,800	36,300	4,240	2,070
Chemical Oxygen Demand	168	1,190	620	924	2,080	240
Ammonia (N)	0.15	40	0.68	7.0	122	35
Calcium (Ca)	352	80	400	400	72	52
Magnesium (Mg)	504	67	792	1,440	101	53
Sodium (Na)	4,000	170	5,900	8,700	360	190
Chloride (Cl)	7,400	250	11,700	18,400	600	400
Iron (Fe)	0.73	42	2.4	0.05	52	3.2
Manganese (Mn)	10.5	0.84	3.4	1.54	4.9	7.0
Copper (Cu)	0.00	0.00	0.00	0.00	0.00	0.00
Lead (Pb)	-	-	-	-	-	-

Table 3. (Continued)

	Well 8	Well 9	Well A	Well E	Well F	Well P	Well S
Depth (feet)	29	16	6	6	16	5	4
Color	-	-	120	2,500	-	-	-
Turbidity	-	-	150	180	-	-	-
pH	6.9	6.4	5.95	3.8	6.7	7.8	7.5
Alkalinity (CaCO ₃)	1,350	340	8	3,885	280	48	52
Total Hardness (CaCO ₃)	840	360	64	540	1,320	84	550
Calcium Hardness (CaCO ₃)	200	110	28	80	410	40	90
Conductivity (micromhos/cm)	4,080	1,330	142	4,610	10,450	304	7,020
Chemical Oxygen Demand	1,480	365	34	227	128	-	170
Ammonia (N)	71	1.70	0.018	6.0	1.6	-	0.06
Calcium (Ca)	80	44	-	-	164	16	36
Magnesium (Mg)	154	60	-	-	218	16.3	110
Sodium (Na)	480	160	-	-	1,800	40	1,500
Chloride (Cl)	550	250	7	40	3,900	24	2,380
Iron (Fe)	51	32	0.25	252	45	0.11	36
Manganese (Mn)	2.4	2.5	0.08	6.25	7.6	0.02	0.24
Copper (Cu)	0.02	0.00	0.06	0.75	0.00	0.02	0.01
Lead (Pb)	-	-	0.05	0.05	-	0.05	0.05

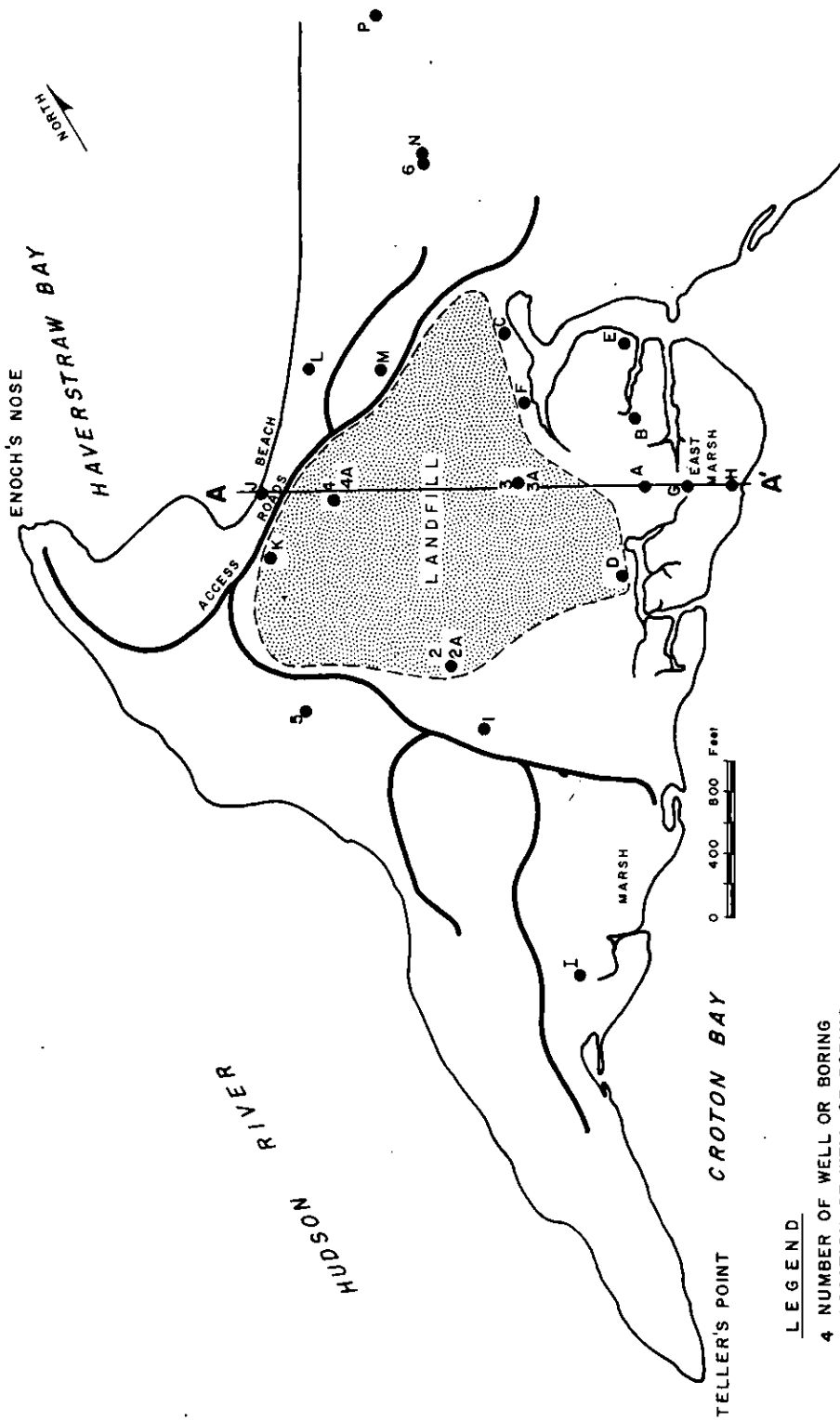


FIGURE 1
 Location Map
 Croton Point Landfill

LEGEND

- 4 NUMBER OF WELL OR BORING
- LOCATION OF WELL OR BORING

NOTE:
 CROSS SECTION A-A' SHOWN
 ON FIGURE 2

NOTE:
 LOCATION OF CROSS SECTION
 SHOWN ON FIGURE 1
 VERTICAL EXAGGERATION IS
 APPROXIMATELY 8 TIMES

NW
 A

SE
 A'

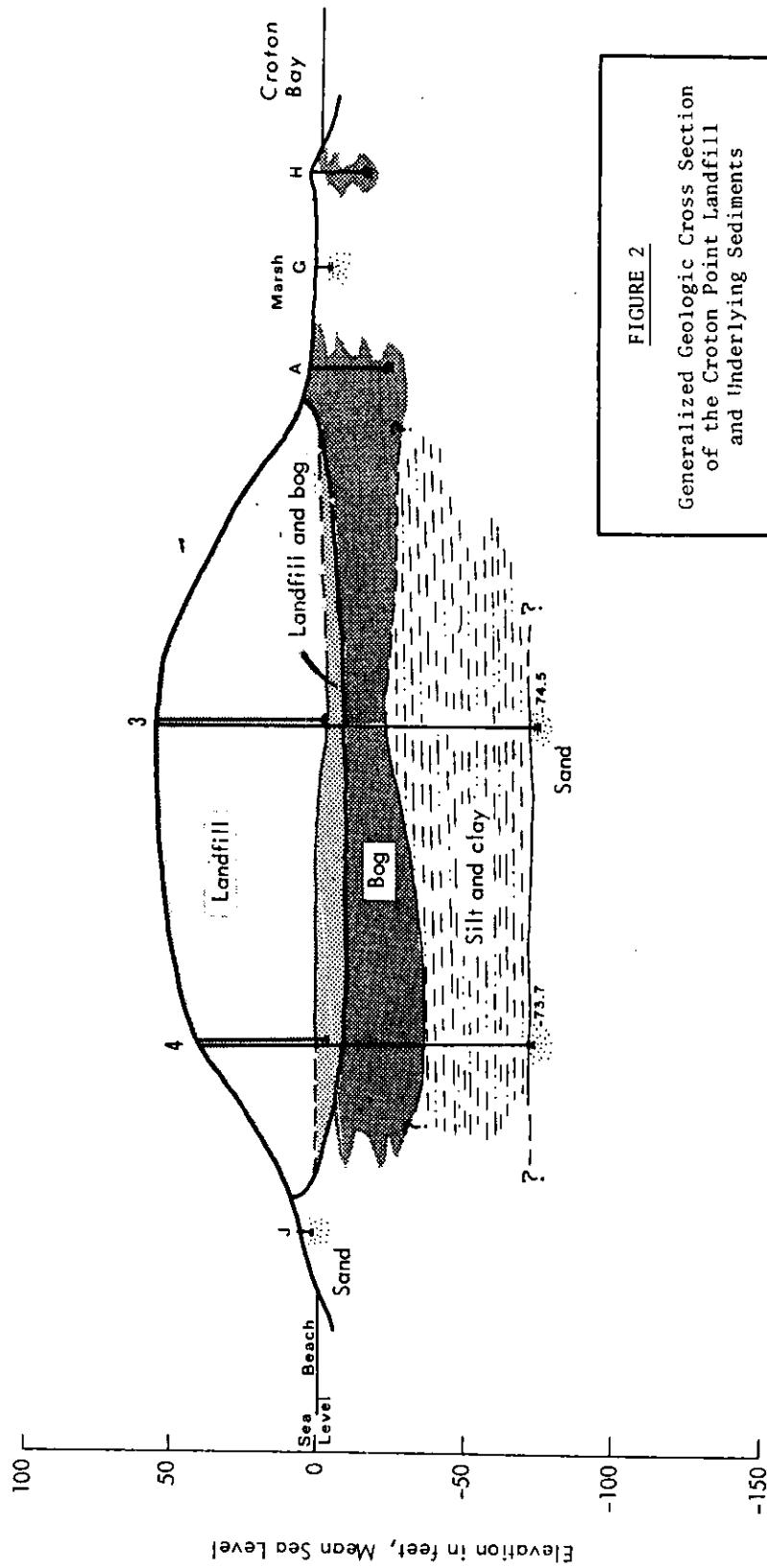
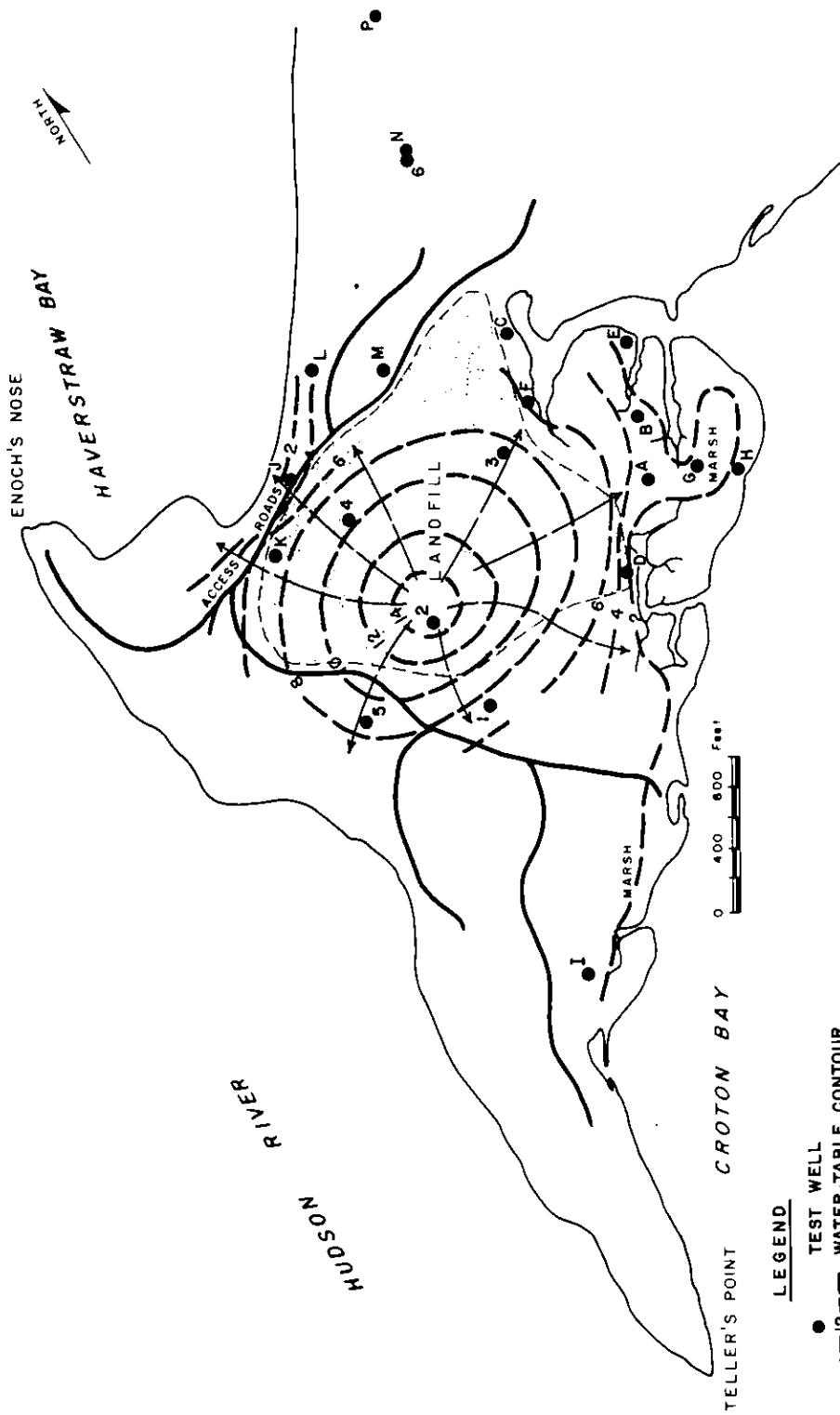


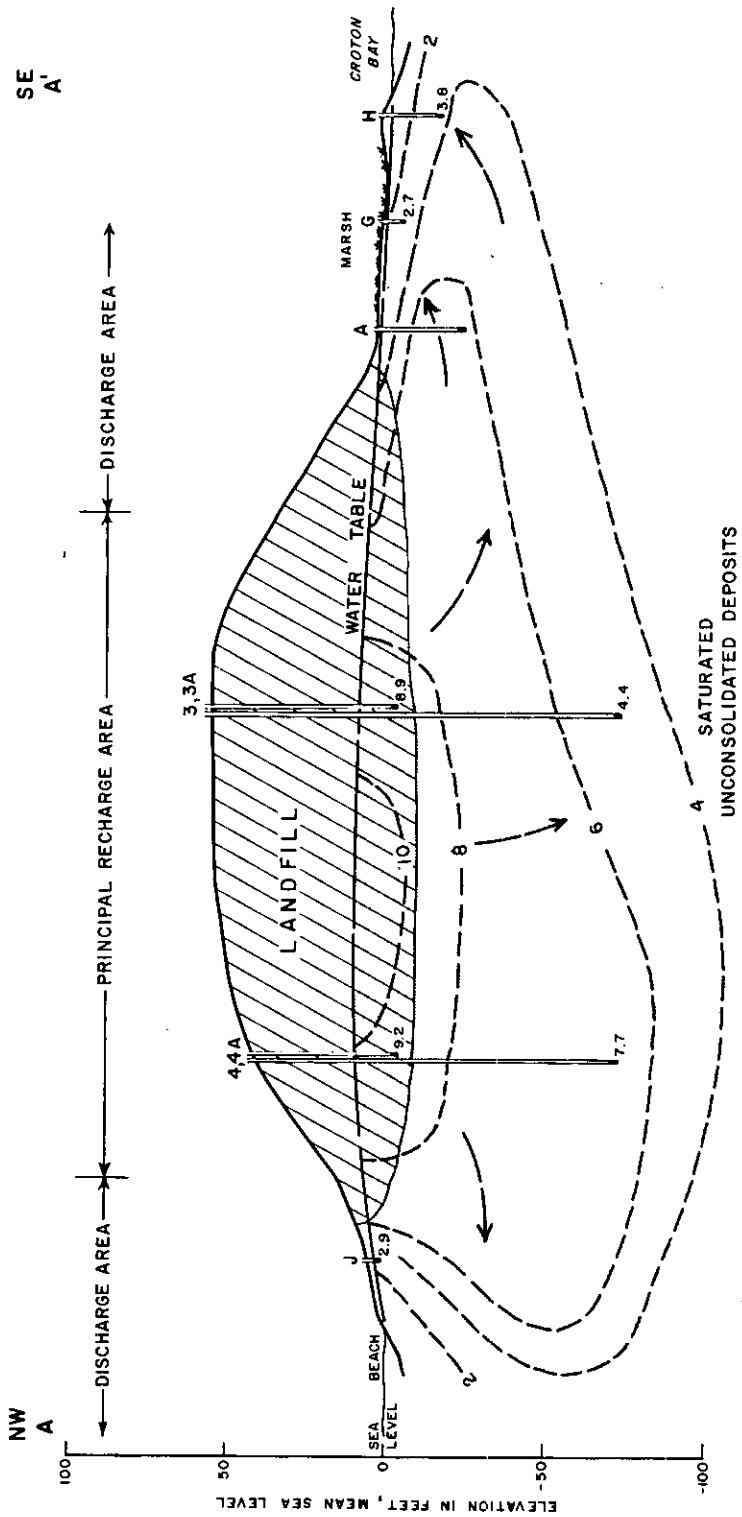
FIGURE 2
 Generalized Geologic Cross Section
 of the Croton Point Landfill
 and Underlying Sediments



LEGEND

- TEST WELL
- WATER-TABLE CONTOUR
- DIRECTION OF GROUND-WATER FLOW
- CONTOUR INTERVAL 2 FEET : DATUM IS MEAN SEA LEVEL
- EXTENT OF LANDFILL

FIGURE 3
 Water Table Configuration and Directions
 of Ground-Water Flow, Croton Point Landfill



- LEGEND**
- 6 -- TRACE OF EQUIPOTENTIAL SURFACE ON PLANE OF SECTION
 - ← 4 → GROUND-WATER FLOW
 - 4 WELL NUMBER
 - || 7.7 WELL SCREEN AND WATER LEVEL IN FEET ABOVE MEAN SEA LEVEL

NOTE: SEE FIGURE 1 FOR CROSS-SECTION LOCATION
 VERTICAL EXAGGERATION IS APPROXIMATELY 8 TIMES

FIGURE 4
 Schematic Hydrologic Cross Section Showing the Potentiometric Head Distribution Beneath the Croton Point Landfill

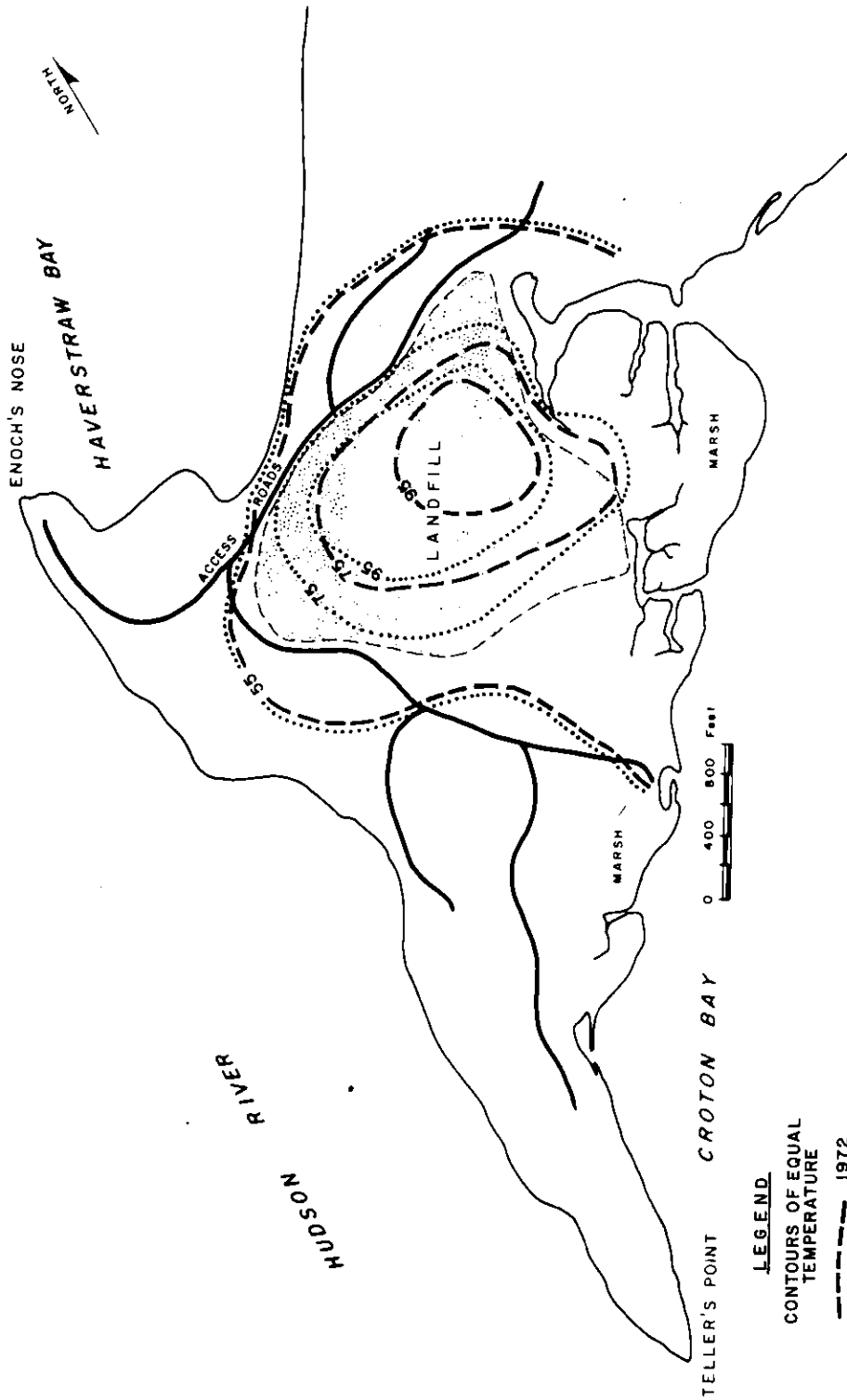


FIGURE 5
 Ground-Water Temperature Configuration
 At Croton Point
 During the Period 1972 to 1974

LEGEND
 CONTOURS OF EQUAL TEMPERATURE
 - - - - - 1972
 1974
 CONTOUR INTERVAL 20°F
 [Stippled Area] EXTENT OF LANDFILL

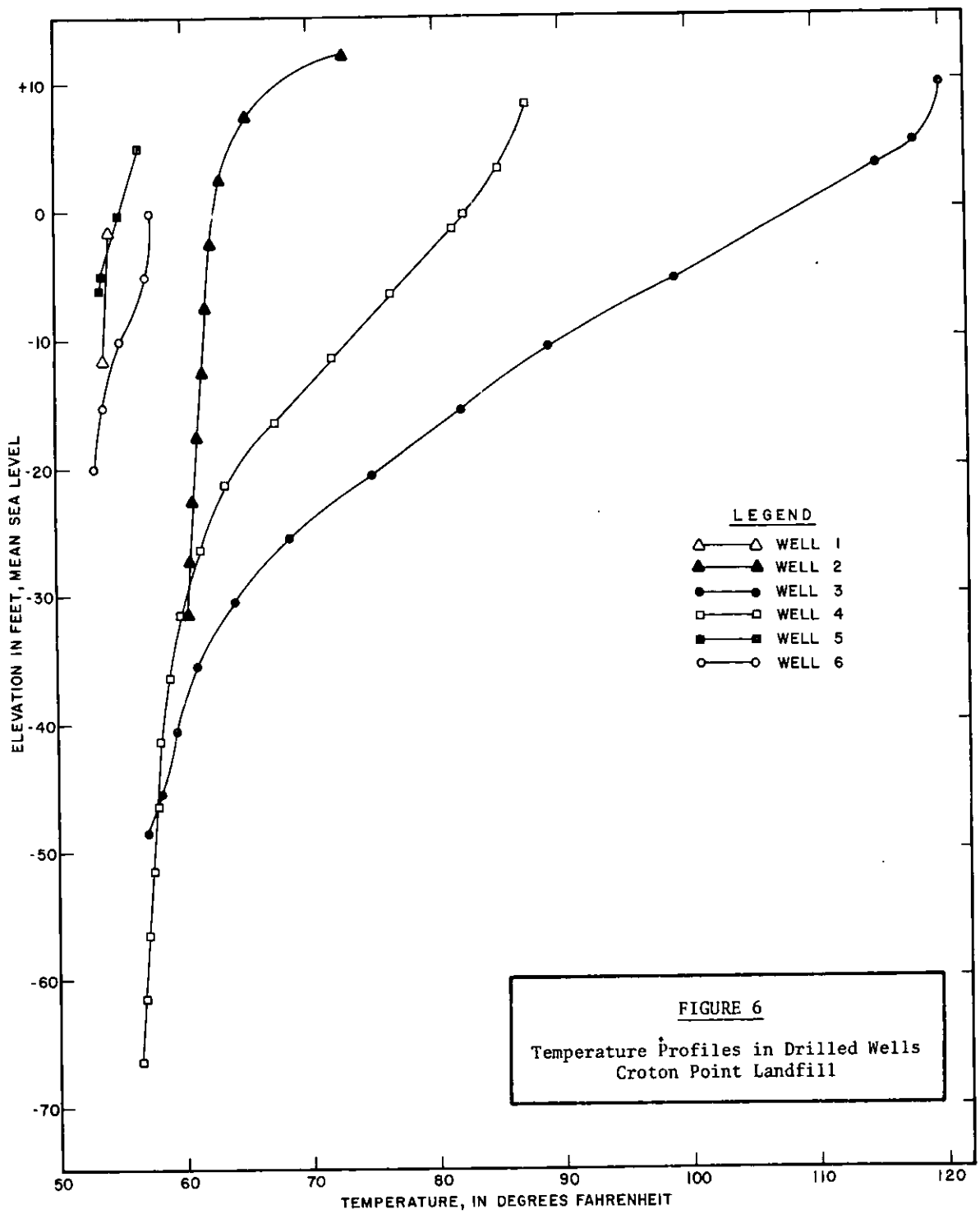


FIGURE 6
 Temperature Profiles in Drilled Wells
 Croton Point Landfill

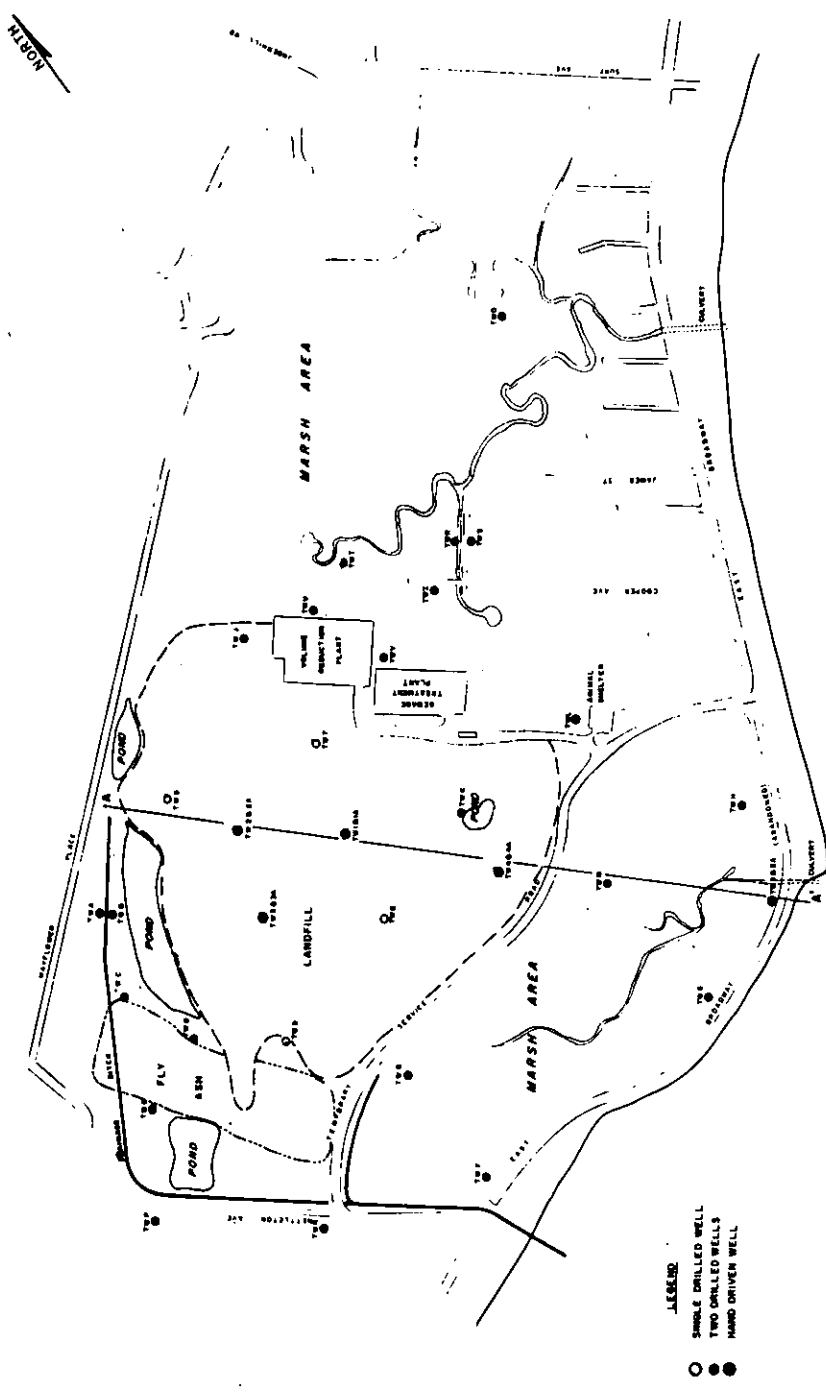
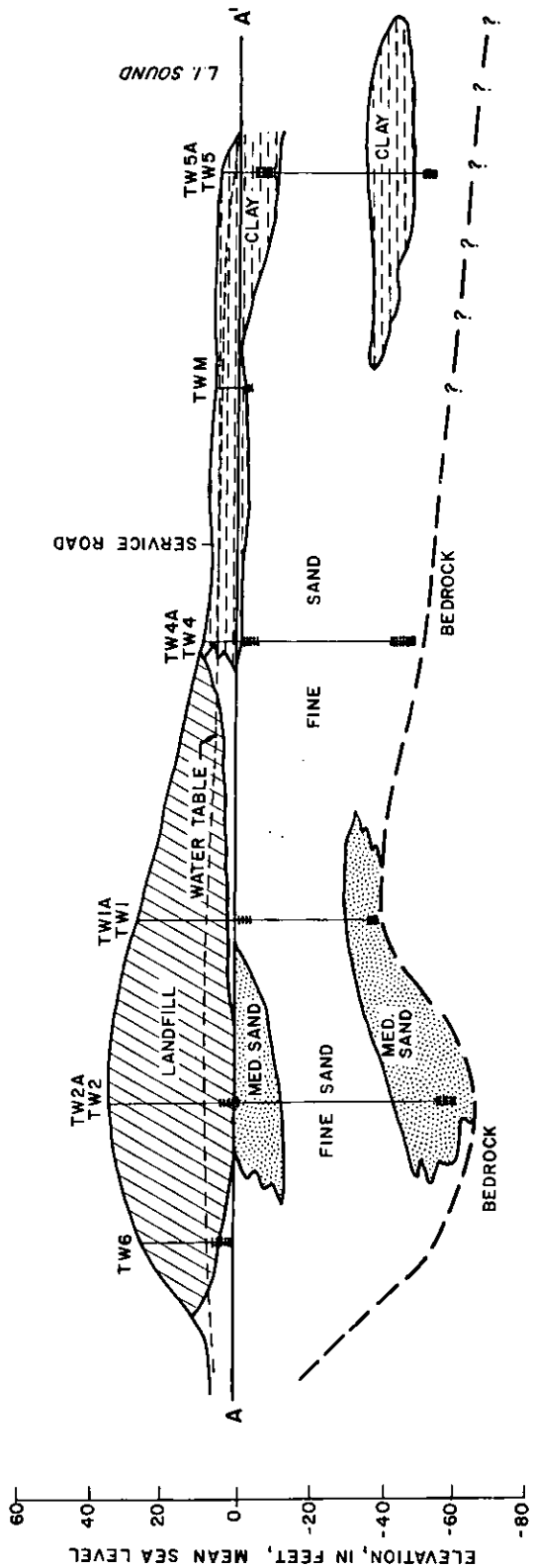
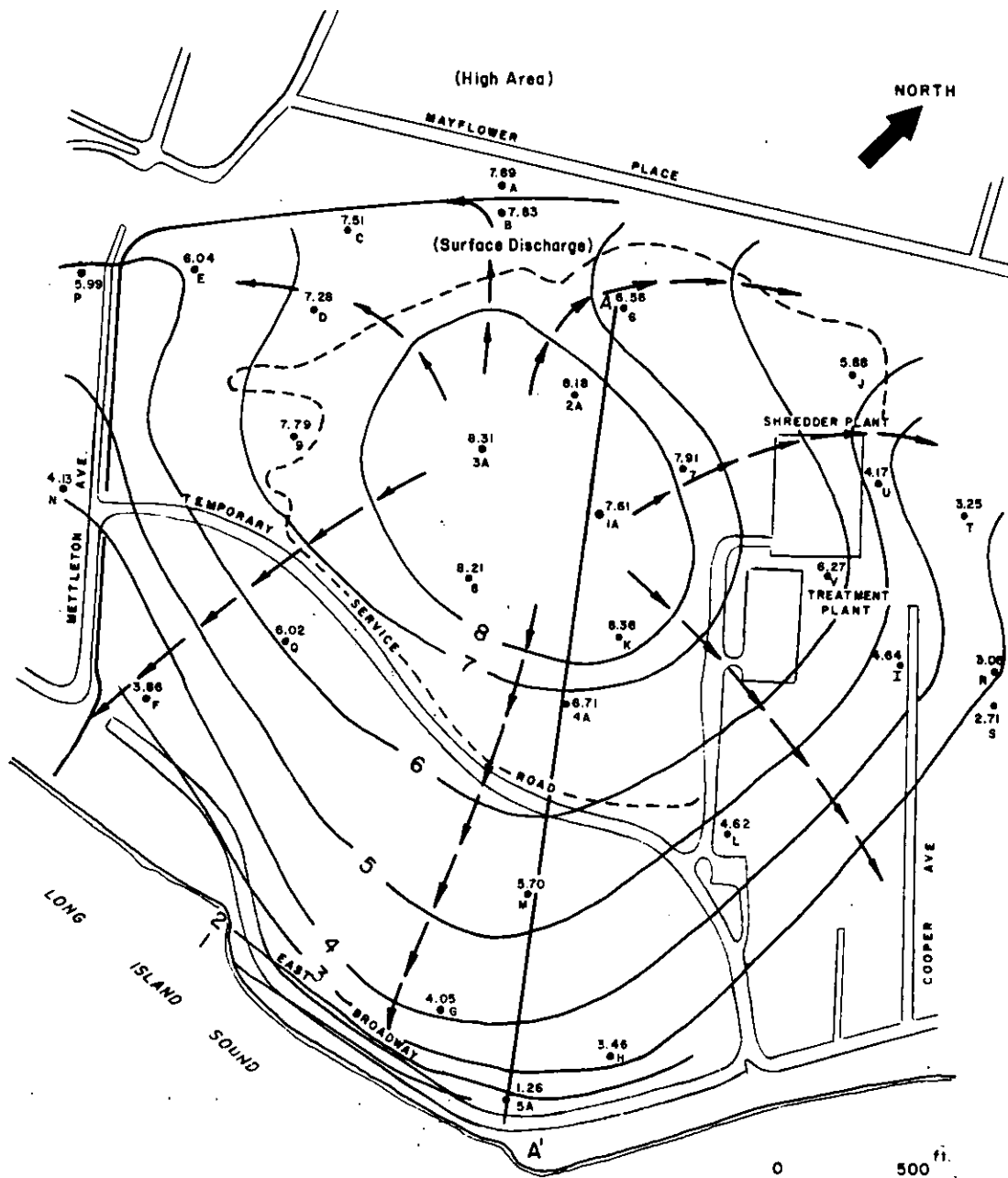


FIGURE 7
 Location Map
 Milford Landfill



NOTE:
VERTICAL EXAGGERATION 10 TIMES
FOR LOCATION OF SECTION SEE FIGURE 1

FIGURE 8
Generalized Geologic Cross Section A-A'
Milford Landfill



LEGEND

- 4.62
L Location of observation well with altitude of water in feet above mean sea level, and well number.
- Leachate flow direction
- 5 — Line of equal head
- - - - Limit of existing landfill

FIGURE 9
Water Table Configuration and Directions of Ground-Water Flow Milford Landfill

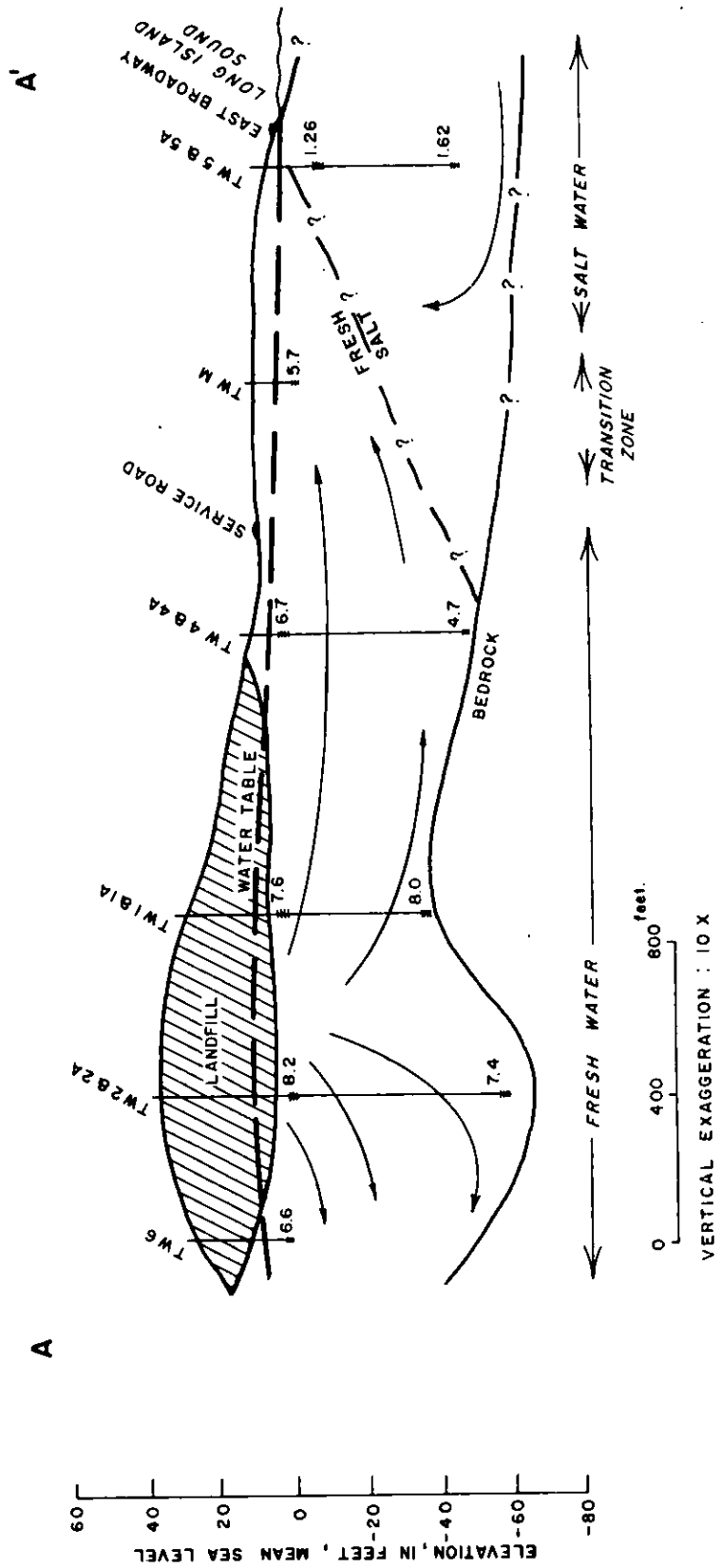


FIGURE 10
 Schematic Hydraulic Profile
 Along Section A-A'
 Milford Landfill

Legend

- 8— Trace of equipotential surface on plane of section
- Ground-water flow
- TW 6 Well number
- ± 7.4 Well screen, and head in feet above sea level.
- Approximate location of interface

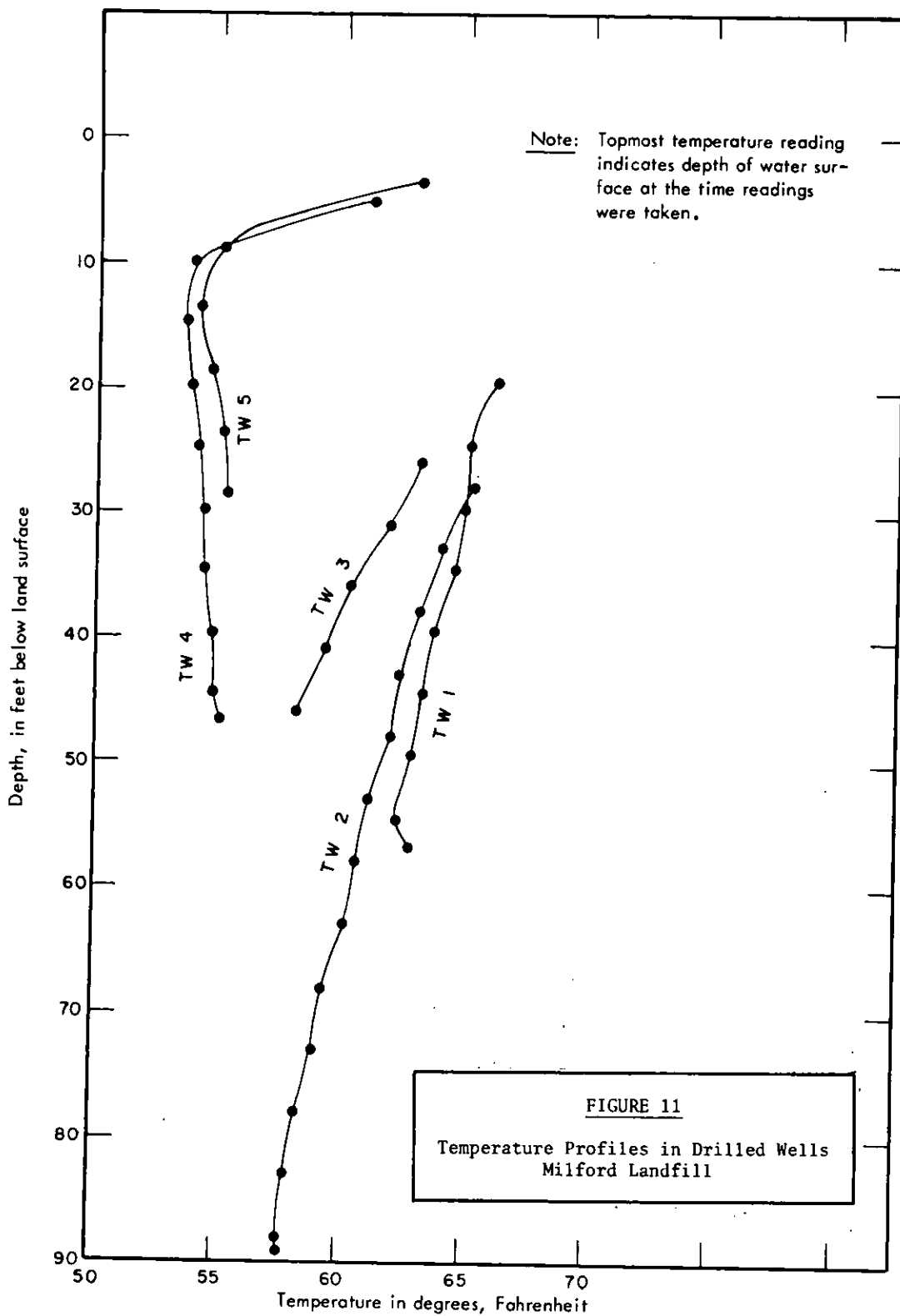
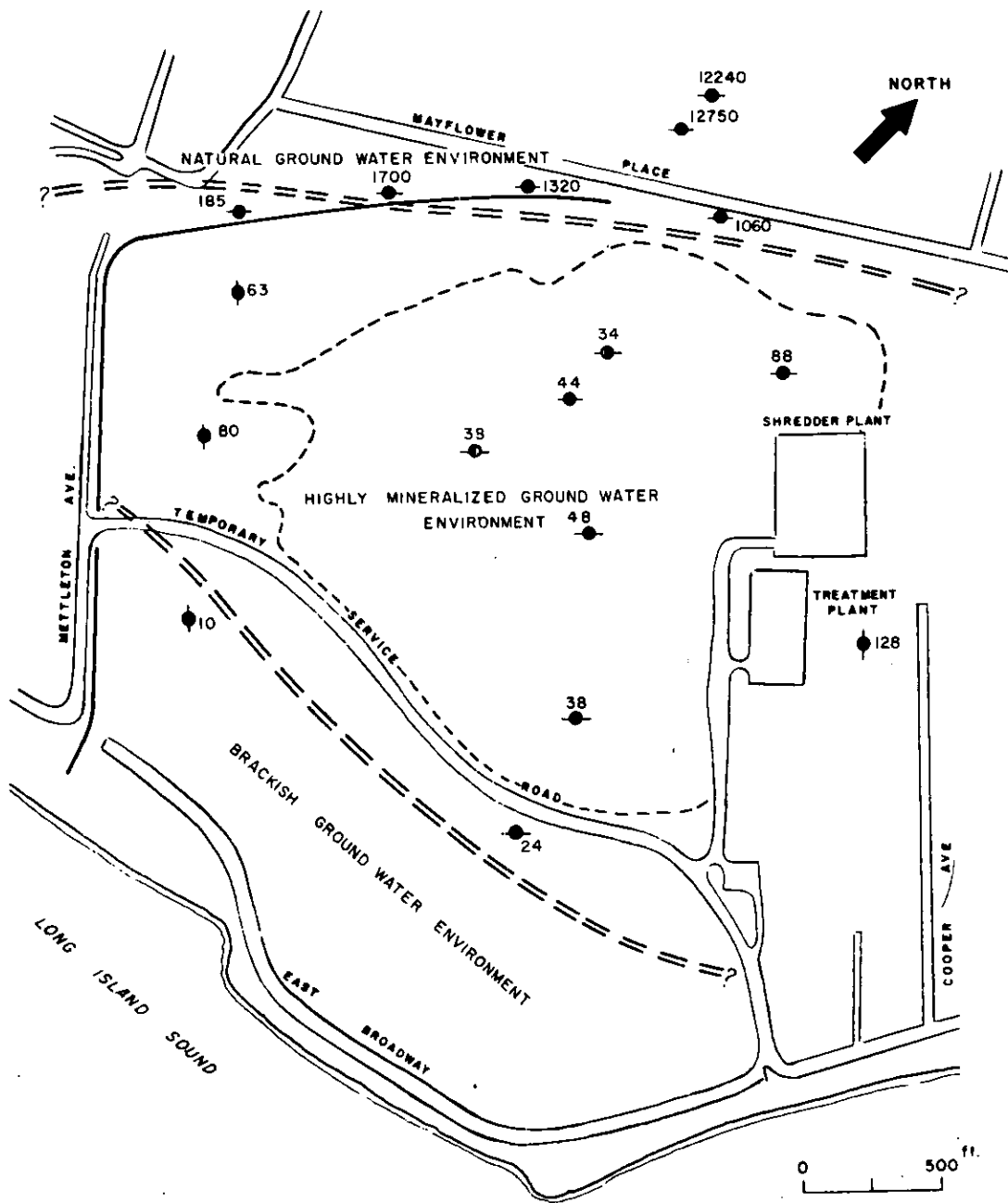


FIGURE 11
Temperature Profiles in Drilled Wells
Milford Landfill



LEGEND

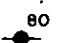
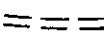
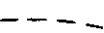
- 
 Resistivity station with apparent resistivity value in ohm-ft at a single selected depth.
- 
 Approximate limit of environment
- 
 Limit of existing landfill

FIGURE 12
 Three Major Ground-Water Environments
 As Delineated By Interpretation of
 Resistivity Data 15 to 20 feet
 Below Water Table
 Milford Landfill

SOME EFFECTS OF NOISE POLLUTION ON
BIOACOUSTICS IN THE SEA

by

GERALD W. ROBIN, M.S.

Columbia University Seminar on Pollution
and Water Resources

INTRODUCTION

Interest in underwater sound increased during the Second World War in connection with the application of underwater acoustical direction finding equipment to anti-submarine warfare. It was found however, that ambient noise affected the reception of signals to such an extent that their meaning or significance were often masked. Many different sounds with changing intensity were recorded. These sounds turned out to be so perplexing and unintelligible in nature that tactical requirements, if not scientific curiosity required that their source, spectral composition, and pressure intensity be recorded and studied.

Only a small fraction of all the sounds heard in the sea have ever been directly identified with their source. One of the major problems in identification of these sources is that, in most cases, it remains invisible to the observer. At best an observer has only limited vision in his immediate vicinity, where as underwater sound transmission may be promulgated over long distances. For example, noise made by snapping shrimp has been recorded by underwater sound detectors at a distance of one kilometer from the source.

Most of the literature regarding marine animal sounds has been concerned with the description of individual sounds and the mechanisms which produce them. A large body of this information, mostly pertaining to fishes, was accumulated during the last half of the 19th century and the early decades of the 20th century.^{1,2,3} A reference file of biological underwater sounds has been prepared. Sounds of various species of fish and animals, materials and methods of collecting sound data and types of equipment used are examined.

In the case of those fish species which have been identified as noise makers, most have been identified with their characteristic sounds because they make them while being removed from a hook or net. Some times the sound is matched to the source by an often lengthy correlative process (presence of animal, presence of sound, absence of animal, absence of sound;) and if the animal is adaptable to aquarium life, the hypothesis may be tested there, although normally noisy species may be less so or even totally quiet in captivity.^{5,6}

Figure 1 is a composite of ambient-noise spectra. In general the ambient-noise levels decrease with increasing frequency, falling between the limits indicated by the heavy top and bottom curves. The overall range in level is about 120 dB and at a given frequency the spread is 40 to 50 dB, where the sound pressure spectrum level is referenced to 0.002 dyne/cm² (or overall range in level is about +46 dB where the sound pressure spectrum level is referenced to 1 dyne/cm².) Of special interest to this discussion is the large bandwidth given the key "BIOLOGICS", that is, from less than 10 Hertz to more than 100,000 Hertz.

The main object of this report will be to identify some of the marine life contributors with ambient noise, and to define a few of the characteristics associated with the noise they generate.²³ It is felt that these exhibits can then be utilized in the development of economic resources studies of fisheries and ASW maps of noise in the ocean.

SOUND PRODUCING ORGANISMS

CRUSTACEANS

Characteristics

The most studied of the marine sound producing animals are the crustaceans which are a major source of sustained noise. Three types of crustaceans, the snapping or pistol shrimp, the spiny lobster or Langouste, the mussel are discussed here. Characteristics are shown in Table III.

The pistol shrimp produces a loud snapping sound with its large claw; the large colony produces a continuous crackling noise resembling frying fat. This shrimp noise ranges in frequency from less than 1 Hertz to about 50 kiloHertz; with principal components between 2 Hertz and 20 kHz. Shrimp crackle dominates water noise above 2 kHz and exerts a strong masking effect on acoustic signals. The chorus can increase the ambient noise level by more than 50 dB above one microbar.⁸

Typical peak pressures for single snaps of snapping shrimp (Alpheus, also known as Crangon and Synalpheus) are about 200 dynes per square centimeter. This pressure intensity is sufficient to shatter the glass of laboratory aquarium tanks. Albers has detected pressure levels as high as 40 dB above 1 microbar at a distance of about 1 kilometer from a shrimp bed.

Figure 2 shows how the shrimp noise affects the ambient-noise levels (measured by a hydrophone suspended over a shrimp bed.) Below 1 kHz, the shrimp noise is negligible in comparison with normal ambient noise; but, above 2 kHz, the shrimp noise dominates the ambient noise. At 10 kHz and 20 kHz, the shrimp noise is about 25 dB above the ambient noise in a No. 1 sea state. Above 24 kHz, ⁹ extrapolation based on the assumption of a decreased level with increasing frequency of 5 dB per octave, gives a value of about -45 dB relative to 1 dyne per cm² at 100 kHz.

When we compare this noise level with the noise created by sea state No. 6, a high sea with wind speeds of 32 to 54 miles per hour and wave heights of 12 to 20 feet, we note that it does not compare to the overall level of noise generated by shrimp beds.

In regions where characteristics of shrimp noise have been studied, no seasonal variations have been noted. However, slight diurnal variations have been reported, the night time level being about 2 to 5 dB higher than the day time level. A slight peak in noise occurs just after sunset and just before sunrise.

An unusual component of ambient sea noise field off costal New Zealand waters has been recognized for some years. The phenomenon involves an increase in noise level at sunset and sunrise, predominantly in the range of 1-2 kHz, with seasonal trends varying the pattern. The effect was first reported in 1962 and tentatively attributed to the sea urchin Evechinus chloroticus. A continuous study in the shallow waters of the Hauraki Gulf throughout 1973 has confirmed this hypothesis.¹⁰

Another sonic crustacean is the spiny lobster or Langouste. This animal makes a rasping or rattling sound by rubbing its long antennae against a ridged area of its shell. Spiny lobsters tend to increase their production of sound when gathered together in groups. Thus the combined output of many lobsters may result in significant increase in overall ambient noise level in certain localities.

A recent investigation¹¹ concerning sound production by the edible mussel (Mytilus edulis) indicates that mussel noise due to mussel "hair" stridulation may be a major component of ambient noise in temperate coastal waters. Although the black mussel lacks as obvious a sonic mechanism as the plunger-apparatus of the shrimp, Crangon, low intensity snaps resembling these sounds are induced manually by breaking the individual byssal threads by which these animals attach themselves to pilings, submerged objects and each other.

Distribution

Shrimp are present in greatest numbers in and around kelp, coral, rock, sponge beds, shell bottom and other locations that afford cover and concealment. Heaviest concentrations are found in depths less than 300 feet and in tropical and subtropical waters. However, snapping shrimp have been recovered from depths greater than 900 feet.

In the Western North Atlantic (Figure 3), snapping shrimp are common along the coast of southeastern United States and throughout the West Indies. Spiny lobsters are abundant off southern Florida, Yucatan and the Bahama Islands. Mussels occur attached to hard surfaces in shoal waters from Newfoundland to Virginia, with a center of abundance in New England.

Noise has also been encountered off the Coast of California at Point Loma, San Diego Harbor, La Jolla, Oceanside and Cape Mendocino. North of California only minor or negligible noise interference by these animals is found.

FISH

Characteristics

Judging from available evidence¹² hundreds of species of marine fish are capable of producing sounds, either by by-products of feeding and other activities (mechanical) or through use of organs apparently especially adapted to the production of sound (biological). Table I lists the variety of methods of acoustical production.

Sonic fish, if present in large numbers, are capable of contributing considerable background noise to sound ranging operations. Individual noise making fish may produce sound sufficiently intense to interfere with the proper functioning of underwater acoustic mechanisms; schools of sonic fish can mask ranging completely.

The principal sound producing fish are bottom-dwelling coastal forms and tropical reef inhabitants. Most of these fish are gregarious; such as the cod, hake, croaker, catfish and jack, form sizable schools. The grunts,

triggerfish, squirrelfish and young groupers swim about the reefs in small groups. Among the sonic fish that occur singly or as widely dispersed populations are the toadfish, sculpin, sea robin, and adult grouper.

Fish noises fall principally in the frequency range of 0.2 to 2.0 kHz with a sound level ranging from -30 to -40 dB above 1 dyne per square centimeter. Thus, these noises are not only in the audible range, but can be of sufficient intensity to be detected readily by most sonic equipment.

Of the "biological" sound producers having principal frequencies between 75 and 300 Hz; none exhibit sounds lower than 20 Hz, several produced sounds higher than 1600 Hz; stridulatory sounds of trigger-fish, filefish and burrfish reached 2400-4800 Hz octave. Noise of "mechanical origin" is noted for several additional species.

In view of the variety of mechanisms producing sounds among fish, perhaps it is not surprising that each species produces sounds of characteristic frequency and intensity patterns. Although predominant intensities may vary from one part of the year to another, presumably due to age difference within a population, the pictures obtained on vibration frequency analysis of specific sounds are characteristic of species studied, and comparisons of such sound spectrograms can assist in the identification of sounds heard in the sea.

Distribution

The distribution and relative abundance of the principal sonic fish is shown in Figure 4. The chart indicates that sound producing fish are most abundant in coastal waters, particularly those of the tropical and sub-tropical islands where there are reef habitants. Figure 4 shows possible limits of fish activity during the spring.

The sound producing fish of cold waters such as cod, hake, sculpin and sea robin exhibit an annual migration pattern. They are found in fairly shoal waters during the warm months but move to deeper offshore grounds in late autumn, remaining there until spring.

In the warm temperate part of the Atlantic, the major sonic fish are several species of croaker, the toadfish, marine catfish, and southern sea robin. Seasonal fluctuations in abundance of these fish are not pronounced, but there is some decrease in coastal populations during winter.

Noisy reef dwellers of the tropical and subtropical western Atlantic include various species of grouper, grunt, triggerfish, squirrelfish and jackfish. These fish are abundant throughout the year in their reef habitats.

Several species of croaker family, highly sonic fish, are abundant in waters from Baja California to Point Conception, California.¹³ North of Point Conception these fish become progressively scarce.

Some of these fish, (Figure 4), are present throughout the year. Other species attain maximum populations in the spring, summer and autumn. Croakers prefer shallow inshore waters with sandy bottoms where they usually

occur in small, dense schools. Sonic investigations⁶ have shown that "croaker choruses" are more intense after dark.

MAMMALS

Characteristics

Most marine mammals are capable of producing sound and may be expected to contribute significantly to background noise wherever they appear in large numbers. Whales are divided into two suborders, the baleen (whalebone) and toothed whales. Of the baleen whales only the humpback and fin whale are known to produce underwater sounds. The toothed whales, which include the sperm whale, killer whale, pilot whale, and the porpoises, are the most consistent sound producers.

Most recently, evidence that a captive humpback whale does not use sonar was obtained by temporarily blindfolding the whale and allowing it to swim through a maze of aluminum poles. No evidence of echolocation was obtained. These experiments were designed to study whether a baleen whale like many species of toothed whales is able to echolocate targets.¹⁴

Recently more has been published on the sound spectra of cetaceans.^{15,16,17} A wide variety of sound emitted by toothed whales have been recorded¹⁸ and analyzed, proving that these mammals have highly versatile acoustic capabilities.

Although the number of mammals capable of sound production is smaller than the number of sound-producing fish, marine mammals may contribute more to the ground state of background noise in some parts of the ocean and at certain seasons of the year than do fish.

Even though some representations of these mammal groups which include seals, sea lions, porpoises and whales, have proved to be sonic, the sonic potential for many common species still awaits study. Many whales are assumed to be sonic either because of their relationship to known sonic species or because of the presence of certain anatomical features usually associated with sound production.¹⁴

Methods of sound production by mammals are of two general types based on the origin of the sound. Sound may be produced by vocal cords or various structures within the animal (internal) or by swimming movements (external).

Internally produced sounds may be uttered in air, while the animal swims at the surface or lies on ice or rocks, or underwater. Sounds produced in either place contribute to the overall background noise levels; however, those which originate underwater are more important.

Table II is a list of some types of sounds produced by aquatic mammals and the more important frequencies associated with them.

Although toothed and baleen whales may produce some external sounds, most of which originate with swimming movements, some are noisier than others. For example, toothed whales (such as porpoises, pilot and sperm whales)

produce more sound than whalebone whales (such as blue, humpback, and right whales.)

The frequencies of sounds produced by marine mammals vary considerably more than those of either fish or crustaceans. Some species produce sounds with frequencies at least as low as 70 Hz and perhaps as high as 200 kHz. However, most frequencies produced lie within the audible range.

Sperm whales (Physeter catodon) produce several types of sounds. Sometimes they make a muffled, smashing noise, suggesting hammering, with impulses one-half second apart increasing in intensity toward the end of a series. At other times they produce low-pitched groans lasting as long as five seconds and sounding very much like a rusty hinge creaking. The most common type of sound produced by sperm whales is a series of short clicks, the individual clicks uttered about every 1/2 second but sometimes as frequently as 5 per second. These whales may produce as many as 70 consecutive clicks, but usually they utter only about 20 per series. Since one sperm whale may click immediately after another, the series of clicks may seem unbroken. The upper frequency limit for these whales has not been established but equipment has registered frequencies between 10 and 17 kHz sounds produced by them.

Sounds produced by the beluga (Delphinapterus leucas) have been described as high-pitched resonant whistles and squeaks, like children shouting in the distance. These are the sounds most commonly heard. Other descriptions liken their sounds to violent agitation of a tin plate, grating sounds, put-put- of a motor boat, piglike grunts, moans and bellows.¹⁹

Carefully controlled experiments have shown that the bottlenose porpoise (Tursiops) uses high frequency clicks to locate food and to avoid obstacles in murky waters. Other sounds, such as whistles and squeals, are thought to have a communicative function. The "whistles" are between 7 and 15 kHz, but the "clicks" have components as high as 120 kHz. Analyses of the sound spectrographs of pothead or pilot whales (Globicephala), indicates a series of clicks below 2 kHz and squeals as high as 7.5 kHz. Sound spectrographs show energy present near the upper limit of the record at 8.8 kHz. Sound pressure levels for unidentified porpoises at an unspecified distance from the hydrophone of from -4 to about +16 dB (re: 1 dyne per cm²) have been recorded (one-Hertz bands over the range from about 100 Hz to about 3 kHz).

Certain characteristics related to the size and behavior of marine mammals and their sonic capabilities are presented in Tables V and VI.

Distribution

In winter, marine mammals are most common in the Gulf of St. Lawrence, where seals congregate to breed, and on the rich fishing banks off Nova Scotia and New Foundland, where seals and pilot whales find large schools of fish to prey upon. During this season sperm whales are common in the north-eastern Gulf of Mexico and off eastern Florida, and whales and porpoises are scattered throughout the Caribbean region, with a concentration of pilot whales and humpback whales in the vicinity of the Windward and Leeward Antilles.

In summer, marine mammals are present in maximum numbers in the northern part of the North Atlantic. Gray seals, pilot whales, and fin whales are observed in the Gulf of St. Lawrence and off Nova Scotia at this time. In the coastal waters of the southeastern United States, the bottlenose porpoise is common in summer.

In autumn, pilot whales and seals continue to be numerous in northern waters, while baleen whales become scarce. The smaller toothed whales are present in considerable numbers off the east coast of the United States during this season. Sperm whales are reported in Atlantic waters between Cape Cod and the Bahama Islands from October to early January.

CONCLUSION

Sound producing animals occur throughout the oceans, but are most abundant in shoal waters of the lower latitudes. Maps of some noisy marine animals are depicted in Figures 3 and 4.

A pictorial display of the noise levels due to the bioacoustic distribution of sound levels in the ocean creates a pattern called a "marine clamorgraph", shown in Figure 5, which apportions unique zones to various parts of the ocean. The zones with the largest numbers are indicative of the highest levels of noise. The curves enclosing the areas show their approximate limits. The model that has been employed here indicates that the areas with the greatest animal activity denote the highest levels of bioacoustic animation. These areas are usually close to continental shelves where there is an abundance of available food and light and as a result the predators follow in accordance with the ecological cycle. The immense fisheries off the Peruvian coast in the Humboldt Current are indicative of these phenomena, but this investigator was not able to obtain any bioacoustical data for that area.

It is felt that "Marine Clamorgraphs" such as depicted here can possibly be used to help in the future development of marine fisheries and harvesting as well as be an aid in the ASW effort by providing a ready reference for the recognition of underwater noise.

REFERENCES

1. Dufosse, A. 1874. Recherches sur les bruits et les sons que font entendre les poissons d'Europe et sur les organes, etc. Ann. Sci. Nat. ser. 5, 19, 1-53; ser. 5, 20, 1-134.
2. Sorensen. W. E. 1884. Om lydorganer hos fiske. En phsiologisk og comparative-anatonnisk undersogelse; Thanning and Appels, Copenhagen.
3. Smith. H. M. 1905. The drumming of the drumfish. Science, 22, 376-378.
4. Fish, M. P. and Mowbray, W. H. 1970. Sounds of Western North Atlantic Fisheries. The Johns Hopkins Press, Baltimore, 224 p.
5. Dobrin, M. B. 1947. Measurements of underwater noise produced by marine life; Sience 105, 19-23.

6. Fish, M. P. 1948. Sonic fish of the Pacific; Pacif. Ocean. Biol Proj., Tech. Rept. 2, 1-144, W.H.O.I.
7. Wenz, G. M. 1962. Acoustic Ambient Noise in the Ocean. J. Acoust Soc. Am. Vol. 34, No. 12, p. 1952.
8. Tavolga, W. M. 1965. Review of Marine Bio-Acoustics; Department of Animal Behavior, American Museum of Natural History, New York, N. Y.
9. Albers, V. M. 1965. Underwater Acoustics Handbook II. Penn State Univ. Press. P. 221-227.
10. Castle, M. J. and Kibblewhite, A. C. 1975. The contribution of the Sea Urchin to Ambient Sea Noise. J. Acoust. Soc. Am. (Supp. 1): S112, Fall.
11. Fish, M. P. 1964. Biological Sources of Sustained Ambient Sea Noise, In "Marine Bio-Acoustics", Vol. 1, Pergamon Press, New York, p. 178.
12. Naragansett Marine Laboratory Reference File of Biological Underwater Sounds, 1968. Kingston, Rhode Island.
13. Sverdrup, H. U., and Fleming, R. H. 1937. The waters off the Coast of Southern California, March to July, 1937. Calif. Univ. Scripps Inst. of Oceanog., La Jolla, Bull., Tech., Series Vol. 4, 261-278, 1936-41.
14. Beamish, Peter. 1978. Evidence that a Captive Humpback Whale (*Megaptera novaeangliae*) Does Not Use Sonar. Depp-Sea Res. 25(5): 469-472 pp. Pergamon Press.
15. Watkins, W. A., Schevill, W. E., Ray, C. 1971. Underwater Sounds of Monodon (Narwhal). J. Acoust Soc. Am. 49(2): 595-599, Feb.
16. Cummings, W. C., Fish, J. F., Thompson, P. O., and Jehl, J. R., Jr. 1971. Bioacoustics of Marine Animals off Argentina; R/V Hero Cruise 71-3. Antarctic Jour. of the United States, 6(6): 266-268, Nov. - Dec.
17. Caldwell, M. C., Caldwell, D. K., and Turner, R. H. 1970. Statistical Analysis of the Signature Whistle of an Atlantic Bottlenosed Dolphin with Correlations Between Vocal Changes and Level of Arousel. U.S. Natl tech.infor. ser., U. S. Govt res. and dev. Rept 70(17): 78-79, Sept.
18. Schevill, W. E. and W. A. Watkins, 1962. Whale and Porpoise voices, Woods Hole Oceanographic Inst., Woods Hole, Mass. pp 1-24 and phonograph disc.
19. Robin, G. W. 1968. Personal recording of Beluga Whales at N.Y Aquarium, Coney Island, N. Y.
20. Kellog, W. N., R. Kohler, and H. N. Norris, 1953. Porpoise sounds as sonar signals, Science 117, 239-243.
21. Hersey, J. B. 1957. Electronics in Oceanography, Adv. Electronics & Electron Phys. 9, 239-295.

22. Knudsen, V. O., R. S. Alford, and J. W. Emling, 1948. Jour. Marine Research 7, 410.
23. Robin, G. W. 1973. Noise is Pollution. Proc. Univ. Sem. Pollut. Water Resour., Columbia Univ., Vol. VII, G. J. Halasi-Kun and K. Widmer, Eds., pp. 47-63.

TABLE I

SOME METHODS OF SOUND PRODUCTION AMONG VARIOUS FISHES

<u>Method</u>	<u>Description</u>	<u>Predominant Frequencies (Hz)</u>
<u>Stridulatory Sounds</u> Sounds produced by the grating of pharyngeal denticles, jaw teeth, fin rays, or bones are essentially non-harmonic in structure. There are two general categories: High frequency stridulation produced by the gnashing of teeth and the pharyngeal denticles during feeding, low frequency stridulation produced by the swim bladder to some extent.	Rasps, scratches, clicks, chirps, scrapes	<u>High Frequency:</u> Range: 100 to 8000 + Predominance: 1000 to 4000 Duration: Extremely variable <u>Low Frequency:</u> Range: 100 to 8000 Predominance: below 1000 Duration: Extremely variable Description of Sounds: grunts, croaks, thumps, knocks
<u>Swim Bladder Sounds</u> Sounds produced by the vibration of muscles around or attached to the swim bladder. Are usually recognized by their harmonic structure.	Vibrant and tonal, boat whistle, Whistles, hissing, clicks	Range: 40 to 1200 Predominance: 40 to 200 fundamentals Duration: pulses 20 to 500 m sec ea. Harmonics: to 3000
<u>Hydrodynamic and swimming sounds</u> Sounds produced by the motion of swimming animals through the water. Sounds are mostly non-harmonic. Individual and schooling fish produce sound due to rapid change in direction or speed. Usually short range phenomena, need high intensity to be detected.	Low roar, some times like a mallet striking a full barrel or side of boat.	Range: up to 500 Dominance: less than 100
<u>Miscellaneous Sounds</u> Acoustical signals resembling hydrodynamic pulses. Possibly due to explosive jet of water through gill slits. Also doubtful low frequency grunts due to electrical discharges of elasmobranch.	Low frequency thumps and grunts	Range: below 100

TABLE II

SOME TYPES OF SOUNDS PRODUCED BY AQUATIC MAMMALS

Types	Description	Important Frequencies (Hz)
1st Class: produced mainly by toothed whales (Odontocetes) which include porpoise.	High-pitched whistles. Mewing and squeals are probably a variation of whistles, with rapid modulation.	1000 to 15000, avg. duration 0.5 sec. 1000 to 15000, avg. duration up to 3 sec. Dominant freq.: 1000, 2000, 5000 Hz. Intensity unverified
2nd Class: explosive Echo location clicks produced by toothed whales. Rep rates increase rapidly as object is approached.	Variable rep rate from low buzzy to rising creaking sound. Each click is believed to be a pulse of white noise exhibiting a sharp front with a continuous frequency spectrum. Most energy in sonic range (below 20K Hz) strong ultrasonic components up to 170K Hz.	Up to 40,000 duration up to 20 m sec. Pulse or ping rate about 5 to 500/sec. Pulses or click, produced singularly or in trains. Described as: rusty hinge, creaks, quacks, squawks, beats. Harmonics: up to 120K and 170K Hz. Intensity: no specific data other than considered quite powerful.
Other miscellaneous sounds produced by toothed whales	Yelps-heard during the mating spring mating season. Clap - of jaws violently when angered Crack - associated with a fright response in captive porpoises.	Data not available
Sounds produced by Baleen whales (Mysticeti) There are no verified records of explosive clicks.	Low-pitched cries: groans, growls, moos, moans and wails. Screams: occasional raising in pitch to about 1000 Hz.	Harmonic in structure - up to 6000 Hz. Dominant freq: 20, 40, 100 and 200 Hz. Duration: 0.1 to 0.3 sec. Max. Energy Spectrum: 80 to 300 Hz. at over 70 db (re 1 ub at 1 meter)
Sounds produced by seals. (Phocidae) and sea lions (Pinnipeds).	Click type sounds and barks. Possible use in echo location.	Short impulse type, faint in seals (Phocidae).

TABLE III. CHARACTERISTICS OF SOUND - PRODUCING CHEUSTACEANS

Common Name	Principle Genus	Habitat	Seasonal Variations in Abundance	Represent. Genus for which Data is Available	Freq. Range Hz.	Principle Freq. Hz.	Max. Overall Pressure dB RE 1 dyne/cm^2	Description of Sounds
Snapping Shrimp	Alpheus Synalpheus	Bottom dwellers in shoal waters, less than 180 ft. common rock, gravel, shell, coral; may inhabit mud bottom among seaweed and sponges	None	Alpheus	500-50K	2K - 20K	-29 over shrimp bed; 54 for individual shrimp snap	Continuous background crackling noise over beds, with occasional loud snaps or cracks resembling burning twigs.
Spiky Lobster	Panulirus	Inhabits coastal waters where rough bottom types prevail; also lives offshore in considerable depths	common off Southern Florida from Feb. to Mid-June	Panulirus	40-9K	600, 800, 2500-4700	n.a.	Slow, low-pitched rattle; sharp rasp or crackling noise

TABLE IV CHARACTERISTICS OF SOUND - PRODUCING FISHES

Common Name	Principle Genus	Habitat	Seasonal Variations in abundance	Represent. Genus for which Data is Available	Freq. Range Hz.	Principle Freq. Hz.	Max. Overall Pressure dB RE. 1 dyne/cm ²	Description of Sounds
Croaker	Cynoscion } W. No. Atlan. Microstegus } Atlan. Sciaenops } E. No. Atlan. Sciaenops } Atlan. Umbra } Atlan. Johnius }	Inshore fishes frequent sandy bay and estuaries warm temperate waters. Along coast Spain & Portugal in autumn & winter. In spring along Africa coast.	Spring-African coast & island summer-Cape Cod to Ga. Autumn & Winter-Spain & Portugal & Gulf of Mexico	Cynoscion	20-1200	50-100 325	36	Croaks, clucks, rapid drum rolls
Searobin	Prionotus Bellator	Bottom fishes inhabiting depths between 30 & 500 ft., chiefly over smooth hard body.	Common inshore from Maine to Va. in summer moves offshore in winter.	Prionotus	40-2400	150, 300, 450, 600	44 (85.0 db with* 10 $\frac{1}{2}$ specimen)	Single squawk or series of rapid clucks. Sometimes grunting sound (air bladder/muscles).
Toadfish	Opsanus } W. No. Forchthys) Atlan. Batrachoides } E. No. Atlantic	Bottom fishes frequenting shallow waters on mud or sand bottom, often hiding in weed beds. Shore fishes of warm regions	Cape Cod-Cape Lookout in summer, Bahamas in Dec.-Jan.; Eastern N. Atlantic spring to autumn, offshore in winter. Prespawning activities R.I. waters.	Opsanus	< 50 > 800 > 2000 < 340 - 3950	60, 100, 140, 200, 240-300, 250, 325, 350, 8" 625, 700, 1020	48 (150 db with* 8" specimen)	Female: Hoots like a boat-whistle Male: Coarse grunting sound, loud intermittent, blasts, (air bladder/muscles).
Cat fish	Galeichthys Bagre	Schooling fishes of shallow bays and estuaries.	Abundant along U.S. coast of Gulf of Mexico in May and June	Bagre	150-1400	350, 700	n.a.	Long, sob like sounds; short yelps; rhythmic drumming.
Grouper	Mycteroperca Epinephelus Centropristis	Bottom dwellers frequenting reefs and rocky places in depths from 30 to 500 ft. Daylight feeders.	Common from Cape Lookout to S. Florida from Feb. to Mid-July, also common in Eastern N. Atlantic in shallow, Bahamas & Bermuda (Bassau Grouper)	Epinephelus	< 50-2000	50-100, 75-150, 4000	37	Vibrant prolonged grunts, growls, grinding noises.

* Source within 2 ft of hydrophone

TABLE IV (Cont'd.) CHARACTERISTICS OF SOUND - PRODUCING FISHES

Common Name	Principle Genus	Habitat	Seasonal Variations in abundance	Represent Genus for which Date is Available	Freq. Range Hz	Principle Freq. Hz	Max. Overall Pressure dB RE. 1 dyne/cm ²	Description of Sounds
Gurnard	Trigla	Bottom fish; most common on rock or gravel between 30-600 feet, East N. Atlantic	Spawn near surface in summer; move offshore in late autumn, returning to shoal water in spring	Prionotus	40-2400	300, 150, 450 600	44	Single squawk or series of rapid clucks, or staccato call - 2 1/2 minute duration communication call during breeding season
Herring	Clupea	Fish of open water, travels in schools of 100 to 1000's; surfaces at night; spawn over gravel bottoms in 12 to 180 feet or more.	Spawning off S.W. Norway and the Falmores & Shetlands in winter, off E. England in early autumn	Clupea	No measurements of biological noise appears to be available, but mechanical (swimming) noise has been noted			Water noise produced by sudden violent movement of immense shoals of herring during feeding or escape maneuvers.
Black Angelfish	Pomacanthus arcuatus		Bahamas		450-600	50-100 75-150	64	Short, percussive grunts during swimming and feeding. Emits considerably longer bursts of sound of pattern upon meeting its species. Appears to be a communication of recognition.
Black Drumfish	Pogonias cromis		Off coast of Western N. Atlantic					Male: Drumsing Female: Soft drumming
Weak Fish (Squeteague)	Cynoscion regalis	Move in schools, near surface, less than 30 ft during summer. Frequent sandy shores, not rocks, winter offshore on continental ledge or southward.	Off coast of W. North Atlantic. Spawning migration W. South Atlantic and Gulf Coast, Mass. to Fla. spawning May-June depths to 30 ft.		20-1200	50-100 250-325	61	One of the most important sound procedures. Sound increases during spawning migration.
Stripped Bass	Rococcus lineatus	Frequent shallow, weedy estuaries, surf or sandy beaches, rocky headlands, scattered schools in spring and fall.	Gulf of St. Lawrence to Gulf of Mexico, most abundant Cape Cod to Cape May, resident within 2 miles offshore.		< 50-1200	75-150 or 150-300 variation	66 (within 6 feet) specimen 36'	Low "unk" with tom-tom quality. Singly or in bursts of 3 or 4 when alarmed.

TABLE IV (Cont.'A.) CHARACTERISTICS OF SOUND - PRODUCING FISHES

Common Name	Principle Genus	Habitat	Seasonal Variations in abundance	Represent. Genus for which Data is Available	Freq. Range Hz.	Principle Freq. Hz.	Max. Overall Pressure dB Re. 1 dyne/cm ²	Description of Sounds
Grunt	Haemulon } W. No. Barbystomus } Atlantic Orthopristis) Pomadasys } E. No. Parapristipoma } Atlantic	Inshore fishes frequenting a variety of habitats including coral reefs, rocky regions, sandy slopes, and estuaries.	Present all year in tropical waters, no apparent seasonal fluctuations in abundance, spawning late spring and summer in E. N. Atlan.	Haemulon	<50> 4800-8000	50-100, 200-400, 800-1600	35	Single, low-pitched grunts; prolonged series of grunts; rasping noises, snoring sounds.
Triggerfish	Ballistes Canthidermis	Sluggish fishes of reef or rocky regions, sometimes living among weeds.	"	Ballistes	50-8K	700-1800, 2400-4800	26	Metallic scratching; humming and drumming sounds.
Squirrel fish	Holocentrus Myripristis	Active swimmers around coral reefs and rocks. Night time feeders.	" Bahamas & Bermuda Banks	Holocentrus	50-1200	50-100 150-300		Isolated grunts; rapid series of grunts, volleys of thrump like sounds.
Jack	Caranx Trachurus Seriola Alecthis	Strong swimmers frequenting upper water levels of open sea and coastal waters, often forming sizeable schools	Abundant off New England in summer; common in tropics all year	Alecthis	50-4800	400-800	24	Scratchy bursts and sharp barking sounds.
Cod	Gadus	Primarily bottom fish over rough and mud bottoms, down to 1200 feet or more.	Spawning concentrates gather off Nova Scotia in winter and early spring.	Gadus	< 50 + very narrow upper limit	< 50	18	Grunts
Hake	Merluccius	Strong swimmers at all depths from tide line to depths of 1200 feet or more.	Spawning concentrations occur off Nova Scotia in July and Aug.	Merluccius	80-875	300	n.a.	Single weak knock; boot, raps
Sculpin	Myoxocephalus Gymnocephalus Triglopa	Bottom fishes living over various bottom types and rocks, occurring down to 600 feet or more.	Common from Cape Cod to New Jersey from Sept. to Mid-May; prevalent north of Cape Cod all year.	Myoxocephalus	20-650	50-100 100-200 200-400	30	Low drumming like generator hum; grunts, spontaneous and under duress.

TABLE V. CHARACTERISTICS OF CERTAIN SOUND - PRODUCING & SOUND - REFLECTING MARINE MAMMALS

COMMON NAME (SCIENTIFIC)	SIZE (Feet)	GROUPING HABITS	GENERAL OCCURRENCE	SWIMMING CHARACTERISTICS*		SONIC CHARACTERISTICS**	
				SPEED (KNOTS)	SURFACING & DIVING BEHAVIOR	DESCRIPTION OF SOUNDS	FREQUENCIES (KHz)
WHALEBONE WHALES							
Blue (<i>Sibbaldius musculus</i>)	75-85	Singly or in pairs, less frequently in groups to 10.	Oceanic	14-15 normal > 20 for 10 min. > 30 in spurts	After surfacing from deep dive, generally makes 12 or more shallow dives of 12-15 sec duration; deep dives last 10-20 min., max. 50***	n.a.	n.a.
Finback (<i>Balaenoptera physalus</i>)	60-80	Singly or in pairs, but more often in schools of several to 200 or more.	Throughout Atlantic, chiefly of New England in summer. Oceanic & Coastal.	10 to 12 normal 15 to 12 max.	Takes 3 to 15 breaths before diving 8 to 15 minutes*** Maximum dive 30 min.	Said to produce a flute like tone lasting about 1 second; repeated at irregular intervals.	Mostly below .2
North Atlantic Right (<i>Eubalaena glacialis</i>)	45-60	Singly & in small groups.	Oceanic & Coastal.	5 surface maximum	Duration of dives 15-20 min. Max. dive 60 min. Rarely submerge deeper than 300 ft.		
Sei (<i>Balaenoptera borealis</i>)	40-55	In small groups occasionally in large schools.	Oceanic & Coastal.	30 in spurts of less than 1/2 mile.	Takes a few breaths before diving 5-10 min. Rarely submerge deeper than 300 ft.		
HUMPBACK (<i>Megaptera novaeangliae</i>)	40-50	Small groups of 4 to 8, sometimes to 20.	Throughout Atlantic, rare in Gulf of Mexico & Western Caribbean, Oceanic & Coastal.	2.5 > 4.5 > 6.5	1 to 18 shallow dives before deep dive of 15 to 20 minutes.***	A variety of low-pitched sounds resembling whistles, roars, squeals, and yeeps.	Yeip like sounds range to about 1.2.
Bryde's (<i>Balaenoptera brydei</i>)	35-50	n.a.	Oceanic & Coastal	n.a.	n.a.	Spout accompanied by metallic whistle, audible to < 1 mile.	n.a.
Minke (<i>Balaenoptera acutorostrata</i>)	20-30	Singly or in small groups; schools 10 to 50 or more.	Common in N. Atlantic in summer, rare in tropical waters. Coastal.	Capable of 14 to 18	Takes 5 to 8 breaths before diving 6 to 7 minutes.*** Rarely submerge deeper than 300 ft.		n.a.

*** Whalebone whales rarely submerge deeper than 300 feet.

TABLE VI. CHARACTERISTICS OF CERTAIN SOUND - PRODUCING & SOUND - REFLECTING MARINE MAMMALS

COMMON NAME (SCIENTIFIC)	SIZE (Feet)	GROUPING HABITS	GENERAL OCCURRENCE	SWIMMING CHARACTERISTICS*		SONIC CHARACTERISTICS**	
				SPEED (KNOTS)	SURFACING & DIVING BEHAVIOR	DESCRIPTION OF SOUNDS	FREQUENCIES (KHz.)
TOOTHED WHALES & PORPOISES:							
Sperm Whale (<i>Physeter catodon</i>)	30-60	Singly or in small groups; schools 40 to several 100	Throughout Atlantic, chiefly oceanic.	3 to 4 average 10 to 12 maximum 20 spurts	Blows 30 to 60 times for 10 to 11 minutes; like rusty hinges, more for 40 to 75 minutes	Muffled noise like hammering, low groans trains of short clicks 15 > 40 per sec, 20-75 in sequence.	2 > 5 > 32 Maximum intensity at 5.
Bottlenose Whale (<i>Hyperoodon ampullatus</i>)	20-30	Groups of 4-12	Oceanic & Coastal	n.a.	Normally surfaces every 10 to 20 minutes; may remain submerged < 60 minutes.	n.a.	n.a.
Killer Whale (<i>Grampus orca</i>)	15-35	Groups of 3 to 40	Throughout Atlantic, common north of New Jersey, oceanic & coastal.	15 > 20 > 30	Normally surfaces every 30 to 45 seconds; may submerge for 3 to 7 minutes.	Clicks & Whistles	n.a.
Goose-Beaked Whale (<i>Ziphius cavirostris</i>)	18-28	Travel in tight schools of 30 to 40.	Throughout Atlantic, chiefly oceanic.	n.a.	Spouts on surface for 10 minutes; dives for 30 minutes or more.	n.a.	n.a.
Pilot Whale (<i>Globicephala melaleuca</i> & <i>G. macrorhyncha</i>)	15-25	Large groups of 1000 or more.	Throughout Atlantic, oceanic and coastal.	To 20 or more.	n.a.	Clicking, creaking, or buzzing sounds; bleating, crying sounds; squeals and whistles. Slow ones like knocks, quickest like grunts or groans.	Rep. rate < 10 to > 400. < 1.5 Broad spectrum < 12
False Killer Whale (<i>Pseudorca crassidens</i>)	12-18	Schools of 10 to 300.	Throughout Atlantic, chiefly oceanic.	To 14 or more	n.a.	Drawn-out high squeak of constant pitch; continuous squeaking reported from a school of 300	.3

TABLE VI. CHARACTERISTICS OF CERTAIN SOUND - PRODUCING & SOUND - REFLECTING MARINE MAMMALS
Continued

COMMON NAME (SCIENTIFIC)	SIZE (Feet)	GROUPING HABITS	GENERAL OCCURRENCE	SWIMMING CHARACTERISTICS*		SONIC CHARACTERISTICS**	
				SPEED (KNOTS)	SURFACING & DIVING BEHAVIOR	DESCRIPTION OF SOUNDS	FREQUENCIES (KHz)
SEALS							
Gray (<i>Halichoerus grypus</i>)	to 8	Herds of less than 50 to 2000 or more.	Coastal water off eastern Canada	n.a.	May dive 400 to 500 ft; maximum duration 20 min.	Fast clicks up to 60 per min.	6 to 12 predominant in some clicks, 30 in others
Monk Seal (<i>Monachus monachus</i>)	to 7	Small herds usually less than 20.	Coastal	n.a.	n.a.	Barking sounds in air; pig like grunting and chattering reported as typical underwater noises.	n.a.
Harbor (<i>Phoca vitulina</i>)	4 to 6	Herds of less than 50 to 1000 or more.	Coastal waters north of New Jersey; common in Gulf of St. Lawrence	n.a.	Maximum dive about 20 min.	Weak clicks	Major component near 12; some pulses emphasized 6 to 8
Harp (<i>Pagophilus groenlandicus</i>)	4 to 5.5	Large herds	Gulf of St. Lawrence	n.a.	May dive 600 to 900 ft.	Weak clicks up to about 130 per second	Major component near 2.
Ringed (<i>Pusa hispida</i>)	4-5	Herds of less than 50 to several hundred	Coastal	n.a.	Maximum dive about 20 min.		
Ross (Thompson, 1968)			Coastal in Ross Sea, Antarctic				Guttural thumping, high pitched combinations of whistling noises similar to hi-freq. sounds recorded underwater from other seals

n.a. Data not available

* No applicable

** Swimming characteristics will vary if the animal is disturbed.

All whales are presumed to produce swimming noises by beating action of their tail flukes at the surface; submerged fluke beats are reported to be relatively noiseless.

TABLE VI. CHARACTERISTICS OF CERTAIN SOUND - PRODUCING & SOUND - REFLECTING MARINE MAMMALS

Continued

COMMON NAME (SCIENTIFIC)	SIZE (Feet)	GROUPING HABITS	GENERAL OCCURRENCE	SWIMMING CHARACTERISTICS*		SONIC CHARACTERISTICS**	
				SPED (KNOTS)	SURFACING & DIVING BEHAVIOR	DESCRIPTION OF SOUNDS	FREQUENCIES (MHz)
TOOTHED WHALES & PORPOISES (Cont'd.)							
Beluga (<i>Delphinapterus leucas</i>)	12-14	Singly or in groups of 10-30, occasionally in schools of 100 or more.	Coastal	6 > 8 > 10 in spurts	Normally surfaces every 10-15 seconds; may re-main submerged 15 min. or more.		
Grampus, Risso's Dolphin (<i>Grampidephus griseus</i>)	10-13	Singly or in small groups less than 12.	Oceanic & Coastal	n.a.	n.a.	Drawn-out high squeak of constant pitch; constant squeaking reported from school of 300.	n.a.
Pigmy Sperm Whale (<i>Meia brevicaeps</i>)	9-13	Small groups or sizeable schools	Cape Cod to Florida, chiefly oceanic.	Slow swimmer.	Often basks on surface.		n.a.
Bottlenose Porpoise (<i>ursiops truncatus</i>)	10-12	Singly or in schools to 100 or more.	Coastal waters from Cape Hatteras to Texas.	10 to 12 normal 20 spurts	Normally surfaces every 15 to 30 seconds; maximum dive about 10 minutes.	Clicking, creaking, rep. rate: <10 to >400. buzzing; bleating, 1.5, slowest one's like knocks, crying; squeals and whistling sounds.	
White Beaked Porpoise (<i>Lagenorhynchus albirostris</i>)	8-10	Schools to 1500 or more.	Oceanic & Coastal	to 15 or more	n.a.		
White Sided Porpoise (<i>Lagenorhynchus acutus</i>)	7-9	Schools to 1000 or more.	Oceanic & Coastal	to 15 or more	n.a.		
Common Dolphin (<i>Delphinus delphis</i>)	6-8	Schools to several hundred.	Throughout Atlantic, chiefly oceanic and coastal	25 maximum	Dives for 1.5 to 3 min.	Series of short clicks whistles	4 to 14 + 8 to 13 +
Spotted Dolphin (<i>Stenella plagiodon</i>)	6-8	Small groups of 2 to 6; schools of 50 or more.	Gulf of Mexico & off east coast of Florida, chiefly oceanic.	12 to 15 + maximum	Blows every 5 to 10 seconds when moving rapidly.	Whistles and barks	4 > 6 > 10
Harbor Porpoise (<i>Phocoena phocoena</i>)	4-6	Small groups or schools 100 or more.	Coastal waters north of New Jersey	10 to 15 normal 20 spurts	Surfaces 3 to 4 times a minute.	Clicks & grating sounds.	1 > 6 > 30 Maximum energy 1 to 6 Major component near 6

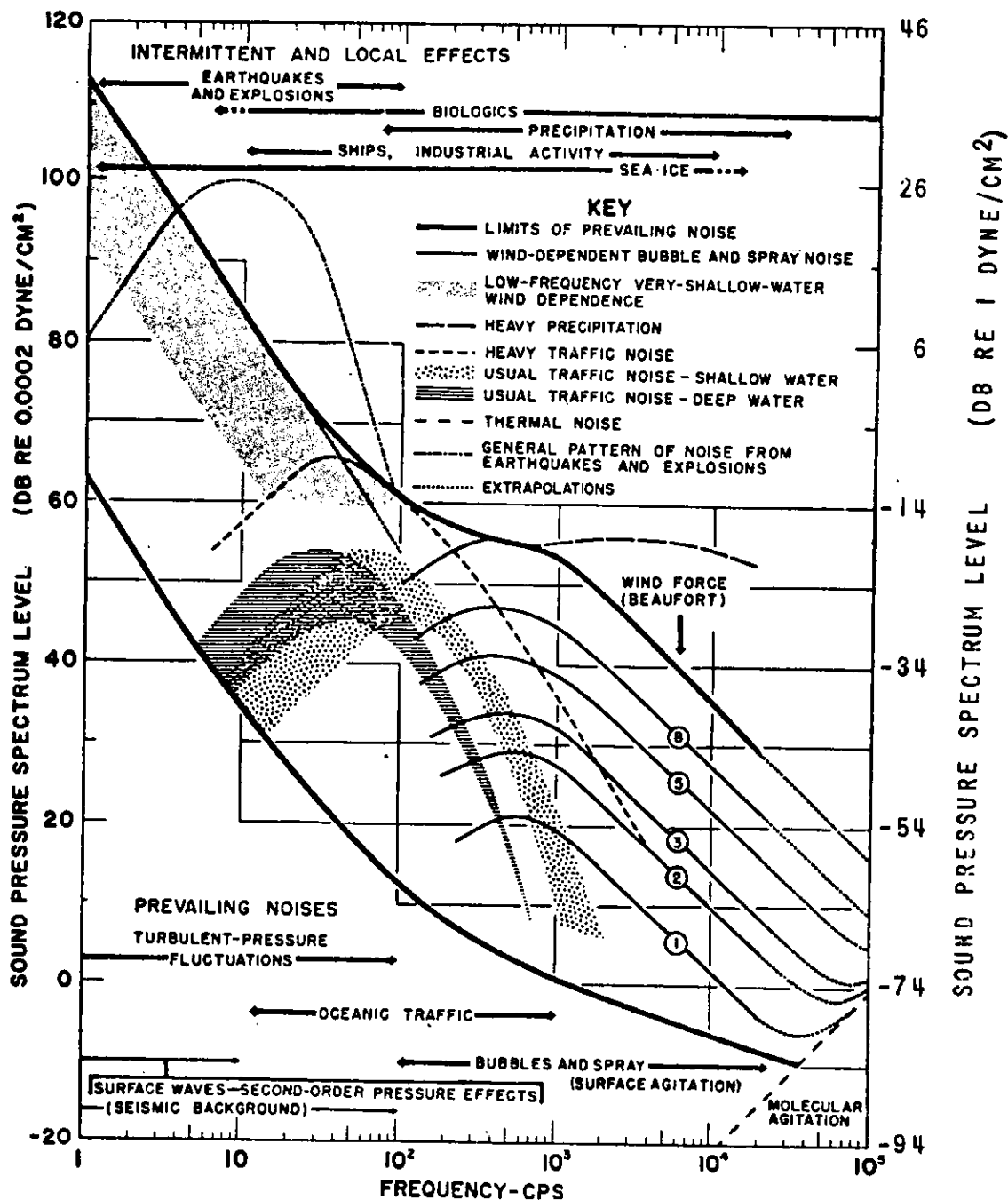
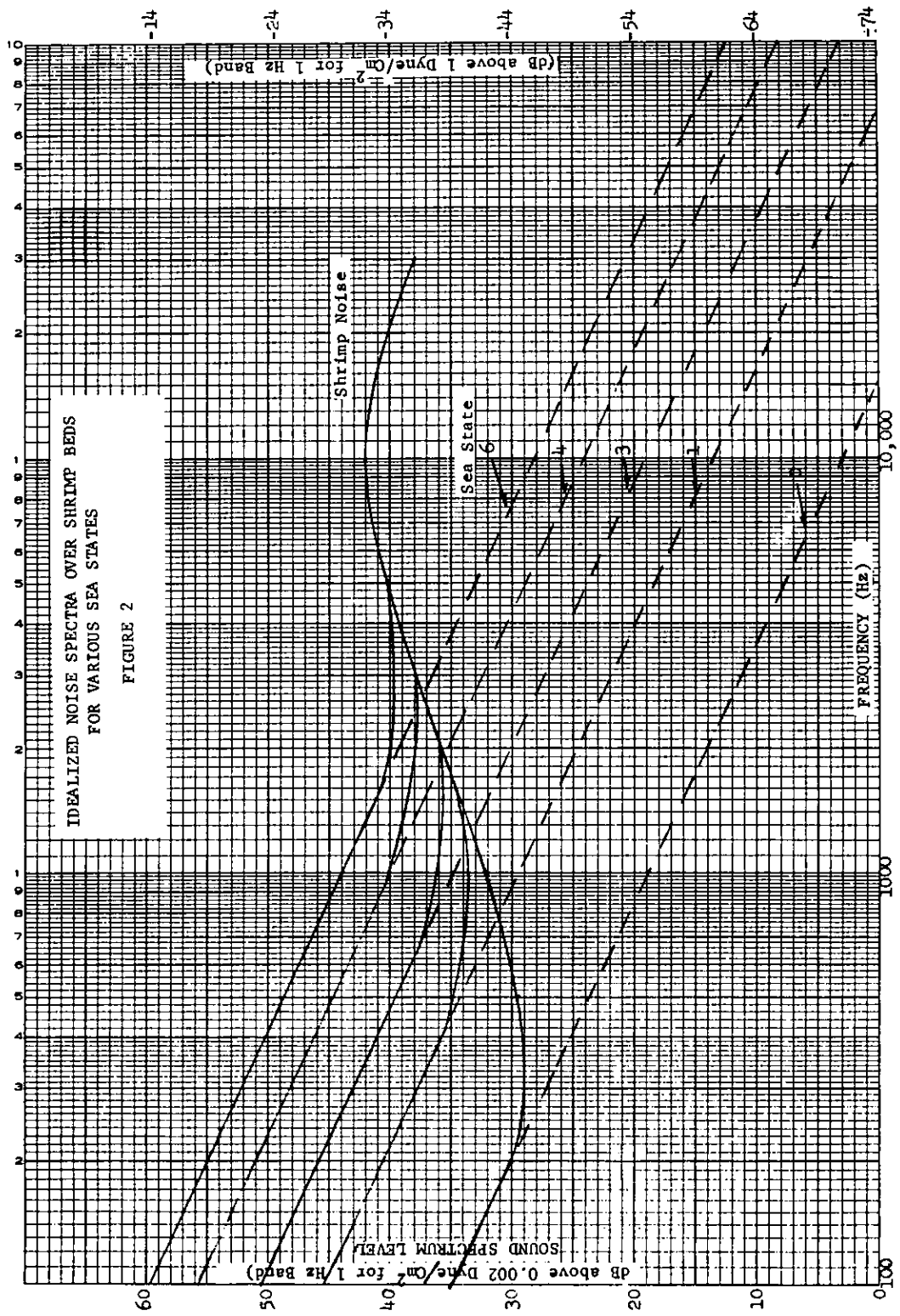


FIG. 1 A composite of ambient-noise spectra, summarizing results and conclusions concerning spectrum shape and level, and probable sources and mechanisms of the ambient noise in various parts of the spectrum between 1 cps and 100 kcps. The key identifies component spectra. Horizontal arrows show the approximate frequency band of influence of the various sources (after Wenz, 1962).



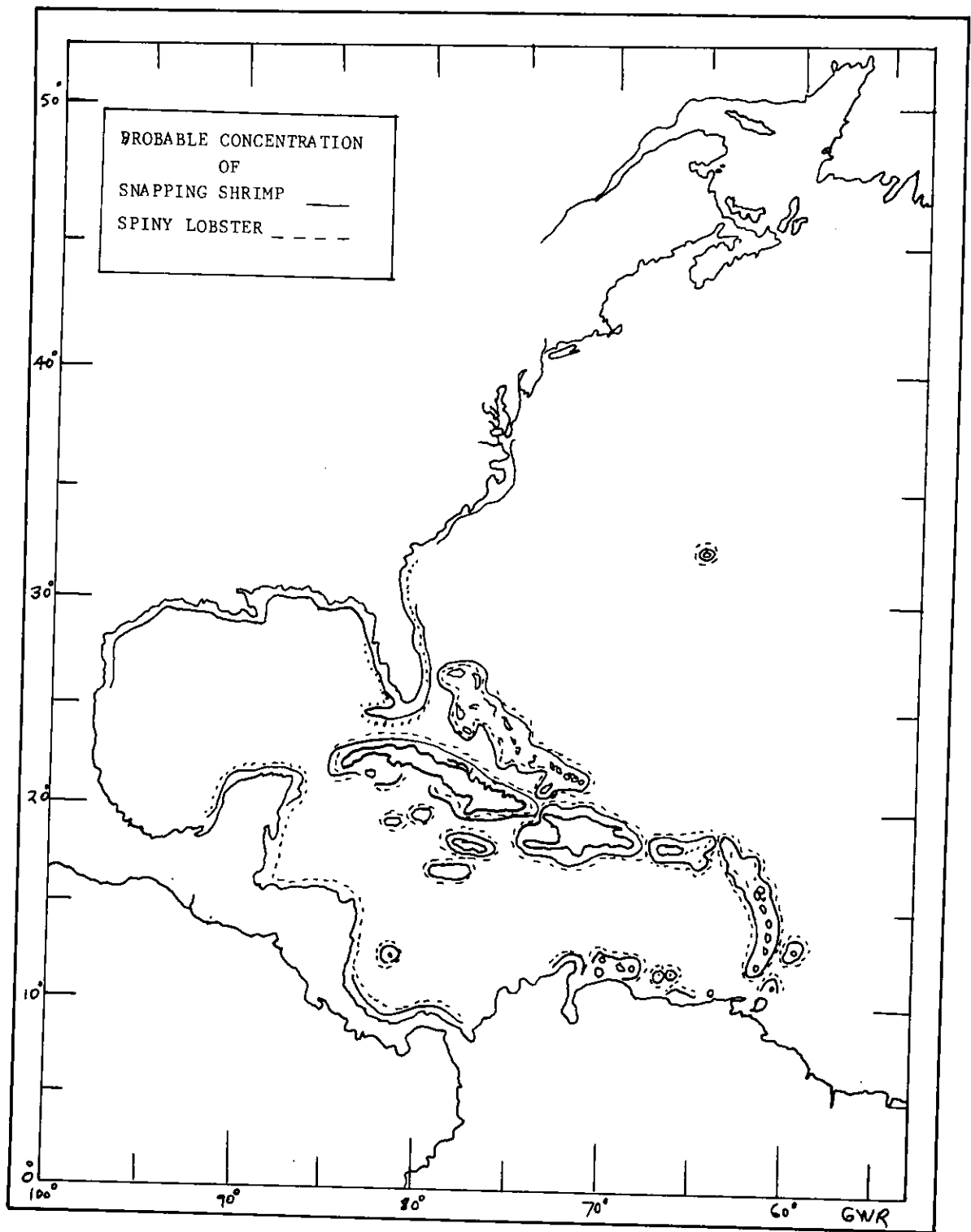


FIGURE 3

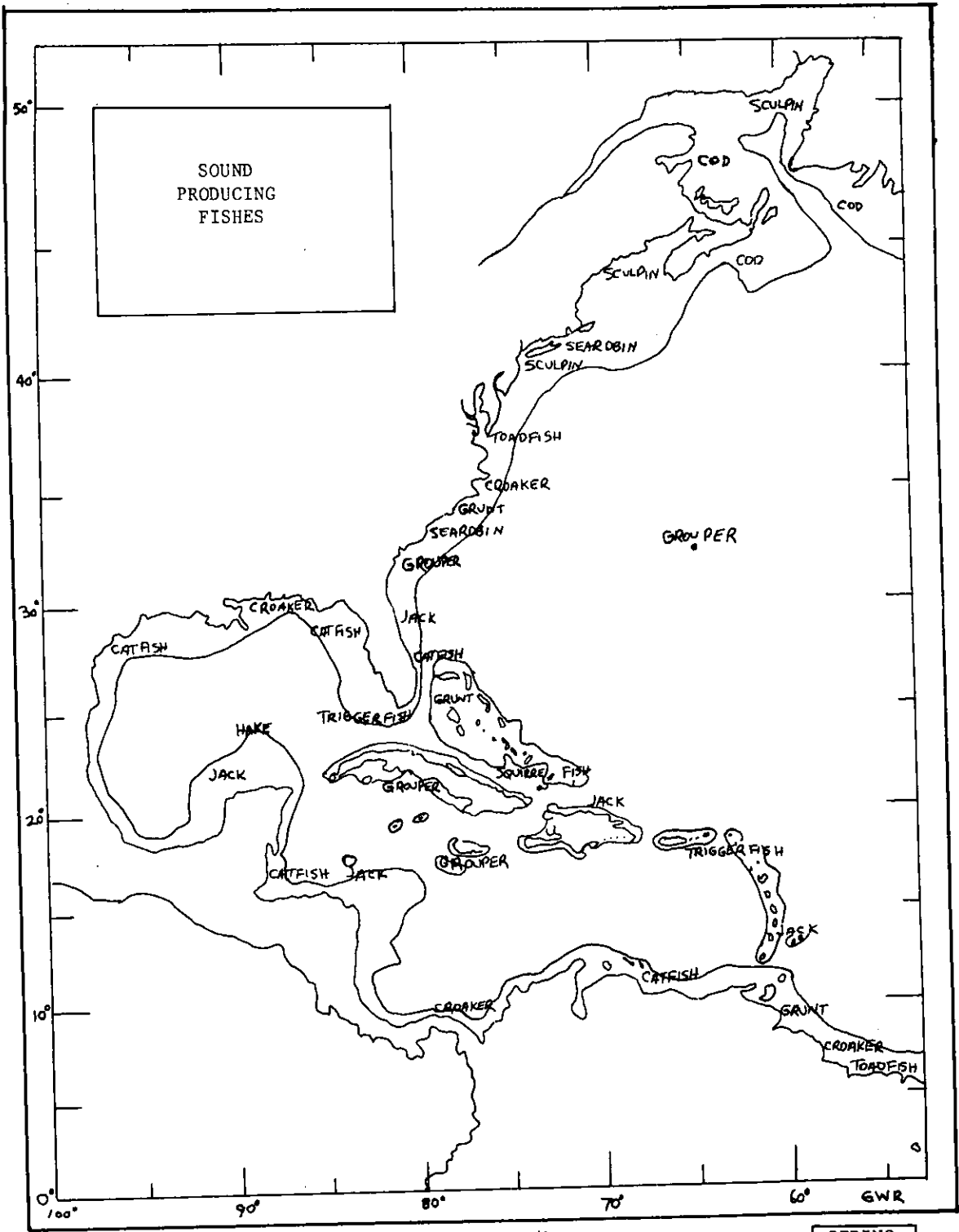
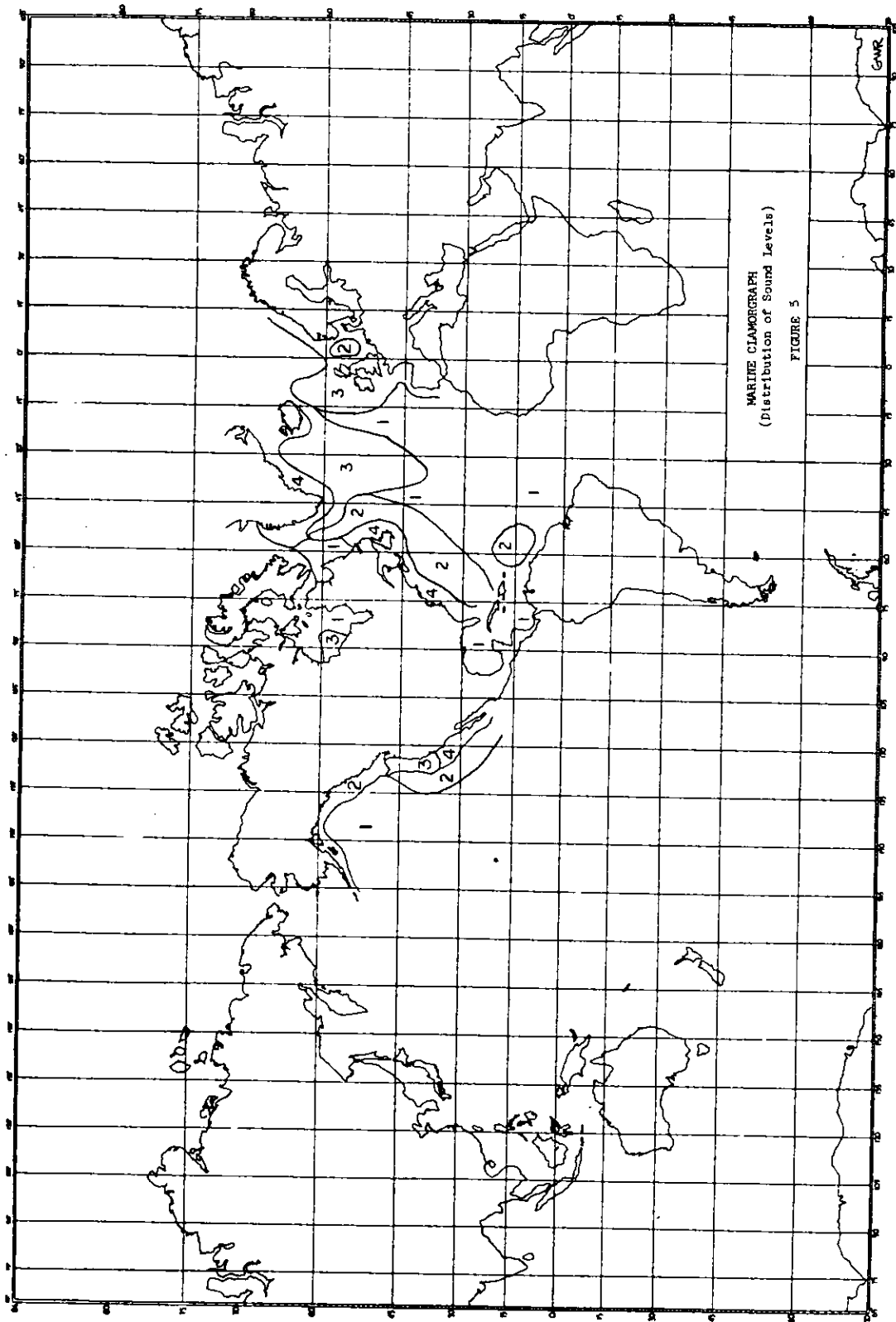


FIGURE 4

SPRING



APPENDIX

MEMBERS OF THE SEMINAR, 1975-1978

Chairman of the Seminar

George J. Halasi-Kun
Hydrologist
Columbia University

Steering Committee:

Charles H. Behre, Jr.
Professor Emeritus of Geology
Columbia University

George Claus
Rutgers University, Medical School

Courtney C. Brown
Professor Emeritus of Business
Columbia University

Kemble Widmer
State Geologist of New Jersey
Trenton, N. J.

Members:

Thad P. Alton
International Financial Research
633 W. 115 St., New York City

Stephen K. Breslauer
NUS Corp. Environmental Safeguard Div.
Rockville, Md. 20850

Conrad M. Arsenberg
Professor of Anthropology
Columbia University

Wallace S. Broecker
Professor of Geology
Columbia University

Armando Ballofet, Consultant
Tippetts-Abbett-McCarthy-Stratton
Engineers & Architects, N. Y.

Joseph H. Butler
Professor of Geology
State University of New York at
Binghamton

Jeanette A. Behre
Retired Asst. Professor of
Biochemistry
Columbia University

William S. Butcher
National Science Foundation,
Washington, D. C.

Chaba Benedek,* Chief Engineer
Swindell-Dressler Pan American Co.
Washington, D. C.

David L. Campbell
Asst. Professor of Mining
Columbia University

Macieg P. Bieniek
Professor of Civil Engineering
Columbia University

Bertrand H. Chatel
United Nations
New York City

Paul Bock
Professor of Hydrology
University of Connecticut

Joseph S. Cragwall, Jr.
Chief Hydrologist
U.S. Dept. of Interior
Geological Survey, Reston, Va.

* died while engaged in a governmental project in VENEZUELA in 1976

Laszlo Czirjak
Consultant Greenwich, Conn.

Donald V. Dunlap
State Meteorologist of N. J.
New Brunswick

Augustine O. Esogbue
Professor of Industrial & Systems
Engineering
Georgia Institute of Technology

John Fabianek
Professor of Life Sciences
N.Y. Institute of Technology

Rhodes W. Fairbridge
Professor of Geology
Columbia University

James J. Geraghty
Groundwater Geologist
Port Washington, N. Y.

Robert D. Gerard
Research Associate in Physical
Oceanography
Columbia University

Alvin S. Goodman
Professor of Civil Engineering
Polytechnic Institute of N. Y.

Richard W. Goodwin
Manager
Research-Cottrell, Bound Brook, N. J.

Isadore S. Grossman
Board of Water Supply of
New York City

William A. Hance
Professor of Geography
Columbia University

Steve Hartman
Biologist Consultant
Sea Cliff, N. Y.

Robert Hordon
Professor of Geography
Rutgers University

Colin High
Asst. Professor of Geography
Columbia University

Allan Hirsch
U.S. Dept. of the Interior
Fish & Wildlife Service
Washington, D.C.

Raphael Hurwitz
Board of Water Supply of
New York City

William Jamieson
Consultant
Amityville, N. Y.

John A. Jones
Professor of Earth Sciences
Miami-Dade Junior College

William C. Kennard, Director,
Institute of Water Resources
University of Connecticut

Walter Kiechel, Jr.
Deputy Asst. Attorney General
Land & Natural Resources Div.
U.S. Dept. of Justice
Washington, D. C.

Adolfo Korn
Mining & Mechanical Engineer
United Nations, New York City

Gregory Lazarcik
Professor of Economics
State University of New York
at Genesee

Richard LoPinto
Director, Marine Biology Program
Fairleigh Dickinson University

Daniel P. Loucks
Professor of Water Resources Eng.
Cornell University

Ulrich A. Maniak
Tech. University of Brunswick
F.R. Germany

Vincent E. McKelvey
Former Director
US Geological Survey
Washington, D. C.

H. William Menard
Director of U.S. Geological Survey
U.S. Dept. of the Interior (1978-)
Washington, D. C.

James Miller
Professor of Oceanography
Rutgers University

David Miller
Groundwater Geologist
Port Washington, N. Y.

Francis C. Monastero, Oceanographer
U.S. Dept. of the Interior
Bureau of Land Management
Washington, D. C.

Alfred A. Porro, Jr.
Tidal Water Law Expert,
Lyndhurst, N. J.

Norbert Psuty
Director Marine Sciences Center
Rutgers University

Habib S. Rahme
Consultant
Syosset, N. Y.

George Redey
Civil Engineer
Englewood, N. J.

Peter P. Remec
Professor of Political Sciences
Fordham University

Hugh B. Ripman, Dir. of Administration
International Bank for Reconstruction
& Development
Washington, D. C.

Gerald W. Robin
State University of New York
Stony Brook, N. Y.

H. James Simpson
Asst. Professor of Geology
Columbia University

Richard Skalak
Professor of Civil Engineering
Columbia University

Victor T. Stringfield
USGS Water Resources Div.
U.S. Dept of the Interior
Washington, D. C.

Emil Szebeny
Professor of Biology
Fairleigh Dickinson University
Rutherford, N. J.

Martin S. Tanzer
Manager, Business Development
Edgerton, Germeshausen & Grier Co.
Waltham, Mass

Grant F. Walton
Professor of Environmental Sciences
Rutgers University

James P. Weidener
Director of Survey
Pandullo & Quirk Assoc.
Wayne, N. J.

George W. Whetstone
Asst. Chief Hydrologist
U.S. Dept. of the Interior
Geological Survey
Reston, Va.

Guirquis Yassa
Director
Robinson Aerial Survey Inc.
Newton, N. J.

Warren E. Yasso
Professor of Natural Sciences
Columbia University

Leonard B. Zobler
Professor of Geology and Geography
Columbia University

RECORDING MEMBER:

Elisabeth Sorad H.-K. Consultant
Pennington, N. J.

Guest Members:

Frank Basile
Bureau of Land Management of U.S.
Dept. of the Interior
New York City

E. L. Bourodimos
Professor of Civil Engineering
Rugters University

Kareen Bolander Claus
Consultant
Sommerville, N. J.

Nicholas de Kun
Consultant
Bruxellers, Belgium

M. Grant Gross
Professor of Oceanography
The Johns Hopkins University

Michael Hermel
Director
Broadway Medical Lab., New York City

Gerald R. Iwan
Sect. Leader of Field Studies
Union Carbide Env. Services

Martin Lang
Former First Deputy Administrator
Environmental Protection Agency
New York City

Peter P. Madri
Chief Chemical Lab.
New Brunswick Memorial Hospital,
Amityville, N. J.

Jules Markofsky
Researcher
Goldwater Memorial Hospital,
New York City

Michael J. Passow
Professor of Natural Sciences
Horace Man HS, New York City

George Pinder
Professor of Civil Engineering
Princeton University

Edith B. Weiss
Asst. Professor of Civil Engrng.
& Political Sciences
Princeton University

Junior Members:

from Columbia University

David Harper

Yeshwant K. Purandare
(also State University of New
York)

Frances Pecenka (also New York
University)

Charles Szilagyi

from City University of New York

Richard Krauser (Queens College)

from Princeton University

Deborah Konopko

from Rutgers University

Vladimir Michna